Autogenerative High Pressure Digestion

Biogas production and upgrading in a single step

Ralph E.F. Lindeboom

Thesis committee

Promotor

Prof. Dr J.B. van Lier

Professor of Anaerobic Wastewater Treatment for Reuse and Irrigation

Wageningen University

Co-promotors

Dr J. Weijma

Researcher, Subdepartment of Environmental Technology

Wageningen University

Dr C.M. Plugge

Assistant professor, Laboratory of Microbiology

Wageningen University

Other members

Prof. Dr A.J.M. Stams, Wageningen University

Prof. Dr R.N.J. Comans, Wageningen University

Prof. Dr L.A.M. van de Wielen, Delft University of Technology

Prof. Dr K. Rabaey, Ghent University, Belgium

This research was conducted under the auspices of the Graduate School SENSE (Socio-Economic and Natural Sciences of the Environment)

Autogenerative High Pressure Digestion

Biogass production and upgrading in a single step

Ralph Erwin Franciscus Lindeboom

Thesis
submitted in fulfilment of the requirements for the degree of doctor
at Wageningen University
by the authority of the Rector Magnificus
Prof. Dr M.J. Kropff,
in the presence of the
Thesis Committee appointed by the Academic Board
to be defended in public
on Thursday 27 February 2014
at 11 a.m. in the Aula.

Ralph E.F. Lindeboom

Autogenerative High Pressure Digestion: Biogas production and upgrading in a single step

208 pages.

PhD thesis, Wageningen University, Wageningen, NL (2014)

With references, with summaries in Dutch and English

ISBN 978-94-6173-860-8

Table of Contents

Chapter 1

General Introduction

1 General Introduction

1.1 Background and problem analysis

Although earliest records date back to ancient Assyrians heating their baths with biogas [1], the worldwide (re-)interest in anaerobic conversion processes has only been rapidly growing since the last decades, due to the growing concerns on energy scarcity and greenhouse gas emissions. Anaerobic digestion combines waste-(water) treatment and energy production by converting the chemically bound energy in organic waste constituents into energy-rich biogas, a mixture mainly consisting of the most reduced and most oxidised forms of carbon, i.e. CH_4 and CO_2. For example, in the Netherlands, about 500 kton per year of organic sanitary waste (faecal matter and urine) is conveyed through its sewer system. Assuming 50% of this waste can be anaerobically digested to methane, it has a primary energy content of 4-5 PJ ($1.3 * 10^9$ kWh). A maximum primary energy potential of 50-60 PJ is estimated annually if also garden waste, livestock manure, slaughterhouse and food industry residues are considered. Although this seems marginal compared to the current total natural gas consumption of about 1500 PJ $year^{-1}$, it could provide almost 1 million Dutch households with their annual gas supply when assuming an average gas consumption of 1800 Nm^3 $household^{-1}$ y^{-1} and a calorific value of 36 MJ Nm^{-3} [2]. Because energy from biogas may also represent a crucial component of future renewable energy mixes [2], cost-effective technologies are needed to convert this potential into actual energy.

The characteristics of biogas produced by anaerobic digestion do not meet the requirements for injection in existing gas distribution systems and other applications [3, 4] as is shown in Table 1-1. For all applications, it should be considered that the pressure of the produced gas must exceed the pressure requirement of the appliances or the local grid. Thus, feed-in gas pressures in the order of 25 hPa are already sufficient for gas stoves and stationary engines [4], whereas for regional gas grids a pressure of at least 0.8 MPa is required. In addition, pressures as high as 20 MPa are required to facilitate the desired reduction in storage volume for vehicle fuel.

Table 1 1: Overview of required gas upgrading for different applications [3-10]

Application	Pressure (MPa)	CH_4 (%)	CO_2 (%)	H_2O Dew point (^oC)	H_2S/ Total S	NH_3	Additional remarks Trace compounds ****
Biogas	0.1	55-70%	30-45%	Saturated 30^oC	50-5000 ppm	0-300 ppm	Source dependent
Natural gas	10-30	70-92	0-8%	Saturated	0-5%	-	Low
Boiler-gas heater and kitchen stove	0.1025	Preferably >96%	-	>150^oC to prevent corrosion from H_2SO_4	1000 ppm	-	Risk of damaging equipment
Stationary engine	0.1025	Preferably >96%	-		500 ppm	100 mg Nm^{-3}	High risk of corrosion
Regional Natural gas grid*	0.8	80-90%	< 6% in NL < 2% **	-10^oC at 0.8 MPa	< 5 mg Nm^{-3} / 45 mg Nm^{-3} 4ppm	3 mg Nm^{-3} or 0.167 mmol Nm^{-3}	Risk of corrosion and or silica deposition
Vehicle fuel	20	>96	3%	40^oC	23 ppm 15mg Nm^{-3}	25-50 mg Nm^{-3}	High risk of corrosion
Fuel Cell***	Wide variation possible				<1 ppm***	No data	No data

*all requirement values vary per country, minimal values shown ** in Sweden, Austria and Switzerland *** quality consideration highly dependent on fuel cell type **** amongst others siloxanes and halogenated hydrocarbons

With an increasing CO_2/CH_4 ratio in the biogas the calorific value decreases, and thus removing CO_2 seems to be beneficial for all applications. To maintain a constant calorific value of the natural gas in the national gas grid as well as in vehicle fuel, upper limits of 3-6% CO_2 are set. Furthermore, CO_2 can pose a risk of corrosion when associated with condensation of water due to the formation of carbonic acid. Because of the formation of the even more corrosive sulphuric acid, limits for H_2S and total S are much lower, especially for storage and underground piping systems [4]. Another reason to remove H_2S is its toxicity for humans and the potential risk of exposure in the case of a leakage in a piping or storage system [11].

Furthermore, condensation of water adds to the risk of corrosion and causes pressure fluctuations in the piping systems and should thus also be prevented. In general this is achieved by removing the water to levels below the condensation point, at the minimum temperature to which the gas could be exposed. A short introduction is given on basic calculations related to saturated water vapour pressures in paragraph 1.4.

The main reason to set restrictions on ammonia concentrations is to prevent the formation of NO_x upon combustion. Furthermore, the presence of ammonia in the fuel gas results in a shorter lifespan of engine oil. And finally, siloxanes, halogenated hydrocarbons and phosphines are man-made (toxic) compounds that can end up in the biogas via their presence in the organic waste, but in most situations they are only present in landfill gas [5, 6]. Although present in trace concentrations siloxanes and halogenated compounds could damage combustion equipment due to deposition and corrosion, respectively.

Thus, biogas upgrading units are necessary for injection into the natural gas grid and other high-grade applications. External (or downstream) upgrading technologies, like membranes, pressure swing adsorption and water scrubbing, require external compressors and thus demand external energy input [4], which make them only economically feasible at biogas flows > 100 $m^3 h^{-1}$. Consequently, lower biogas flows are so far disregarded for biogas upgrading techniques and its potential for high-grade use is generally lost. Often this even results in flaring of biogas, losing a useful energy

resource. For example, biogas generation from small-scale digesters, mounted in the so-called Decentralised Sanitation and Reuse (DeSaR) systems, does not exceed 10 m^3 biogas $person^{-1}$ y^{-1}. The handling and upgrading of this low amount is a main constraint for further development of DeSaR systems [12].

In this chapter we propose a novel anaerobic digestion concept for the production of high-grade biogas from slurries and waste water in just a single step: Autogenerative High Pressure Digestion (AHPD). The objective is to digest organic matter under autogenerated high pressure to CH_4 and CO_2 [13, 14]. Henry's constants for CH_4, CO_2, H_2S, and NH_3 in water are 0.016, 0.318, 1.150 and 620 mol L^{-1} MPa^{-1}, respectively [15]. From these theoretical constants it can be concluded that CO_2 dissolves relatively better than CH_4 in water at increasing pressures.

Moreover, it is aimed to produce AHPD-biogas directly at a suitable pressure for high-grade use. AHPD eventually aims to generate biogas that also meets the quality demands for Synthetic Natural Gas (SNG), or in popular words "green gas". Ideally, no additional upgrading technology would be required. Although investments are needed to operate anaerobic digestion at high pressure, we expect that with AHPD we can develop a cost-effective small-scale technology suitable for decentralised biogas production from organic waste. This research explores pressurised digestion systems in which the biological autogeneration of pressure is brought about by trapping the produced biogas inside the bioreactor.

In the past some papers, although not many, have been published describing the autogeneration of biogas pressure and the in-situ upgrading of biogas. The idea of differential solubility at increasing pressure between CH_4 and CO_2 was for example already described in 1991 by Richards and co-workers for energy crop and manure digestion. An overview of other relevant references can be found in Table 1-2.

Table 1-2: Overview of earlier work on pressurised anaerobic digestion and relevant bioreactor operation

Digestion conditions	Process performance	Reference
pCO_2 = 0.00 -0.10 MPa T = 55-70 ºC Substrate: VFA Batch-fed reactor	Acetoclastic methanogenesis inhibition with increasing pCO_2 (0.00, 0.03, 0.06 and 0.10 MPa) and T (55, 60, 65 and 70 ºC)	[16]
P = 0.1 - 0.3 MPa T = 35 ºC HRT = 3 days Substrate = glucose, VFA Fixed-film reactor (with CO_2 stripping)	With glucose: CH_4 = 54.1 %; $COD_{removal}$ = 93.7 % (0.10 MPa) CH_4 = 59.4 %; $COD_{removal}$ = 89.6 % (0.30 MPa) With VFA: CH_4 = 81.0 %; $COD_{removal}$ = 97.3 % (0.10 MPa) CH_4 = 93.2 %; $COD_{removal}$ = 97.3 % (0.30 MPa)	[17]
P = 0.1- 0.4 MPa T = 35-55 ºC HRT = 50-20 days Substrate = sludge	At 55 ºC: Decreased NH_3 inhibition CH_4 = 58-65 %; $OM_{removal}$ = 57 % (0.25- 0.30 MPa) SGP = 0.46 m^3 kg_{VSadd}^{-1} (0.25- 0.30 MPa) At 35 ºC: > Instability (0.30- 0.40 MPa)	[18]
P_{max} = 0.114 MPa T = 39 ºC HRT = 15 days Substrate = swine slurry	CH_4 = 60.9 % GPR = 0.85 m^3 m^{-3} d^{-1}	[19]
P = 0.1 - 0.3 MPa Theoretical model	Decreased NH_3 inhibition (0.30 MPa)	[20]
Using alkalinity recycling loop to produce high quality biogas from energy crops	>98% CH_4	[21]
Pressure temperature relationships biological growth in a pressurised bioreactor	Cultivation of marine piezophilic bacteria	[22]

Note: AHPD: Autogenerative High Pressure Digestion, GPR: gas production rate, HRT: Hydraulic residence time, OM: organic matter, P: Pressure, SGP: Specific gas production, T: Temperature, VFA: Volatile fatty acids

1.2 Anaerobic digestion at atmospheric pressure

Because of the relative small amount of data covered in articles on this specific topic, the literature overview in this chapter describes basic concepts and theory regarding anaerobic digestion, Henry's law and gas-liquid equilibria, mineral weathering and

general pressure effects applied to organisms involved in the anaerobic digestion process.

Generally, anaerobic digestion is regarded as 4 separate microbiological processes; hydrolysis, acidogenesis, acetogenesis and methanogenesis. Figure 1-1 shows a simplified overview of these stages. Complex organic matter is disintegrated, (enzymatically) dissolved and then hydrolyzed to amino acids, sugars and free long chain fatty acids by different enzymes excreted by the micro-organisms [23], as is depicted in the lower part of Figure 1-1.

In the next stage these intermediates like amino acids and glucose are converted into organic acids, alcohols and hydrogen and CO_2. From these organic intermediates acetogenic bacteria produce acetate, carbon dioxide and H_2. These are subsequently converted into H_2O, CH_4 and CO_2 by methanogens [24]. It is noteworthy that the digestion of proteins results in the formation of additional NH_3 and H_2S.

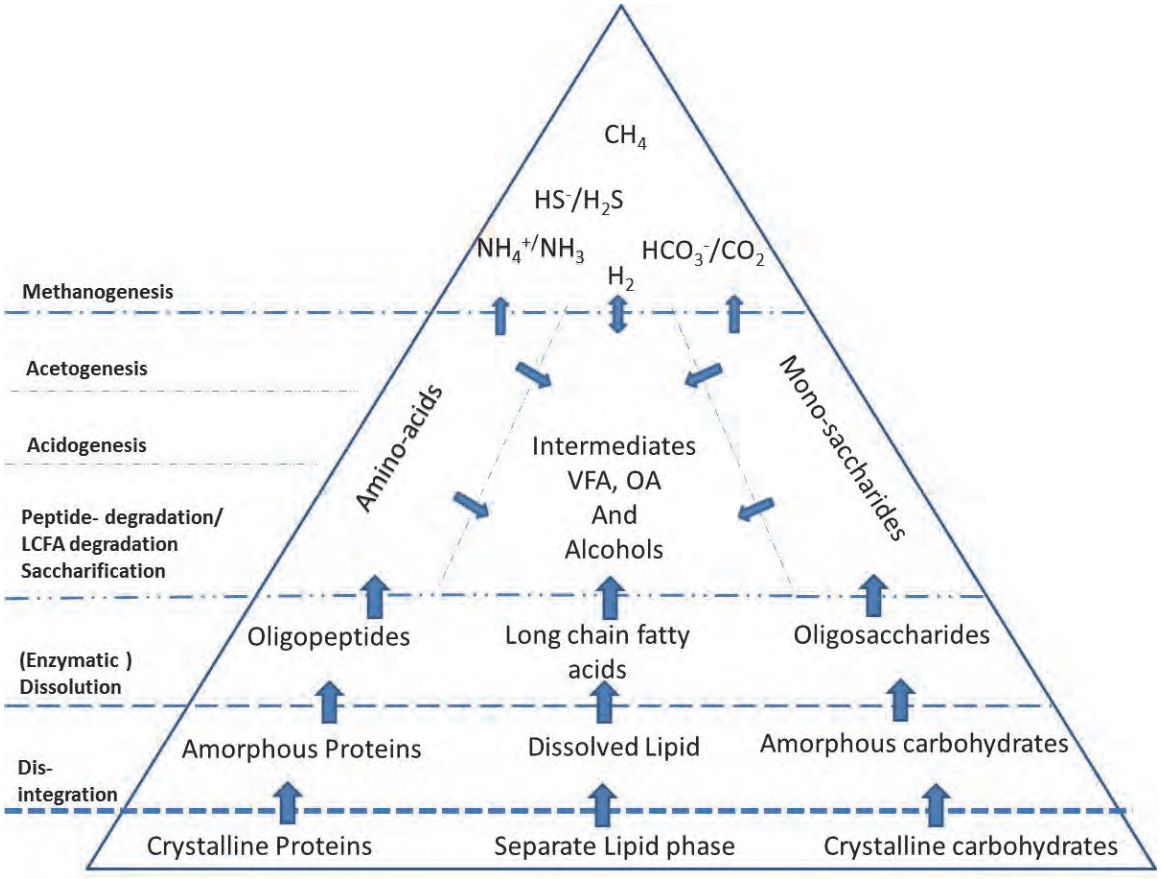

Figure 1-1: Schematic overview of anaerobic digestion in which the dotted lines represent the different stages and the arrows indicate the direction of the (bio)chemical conversion

All these steps have been thoroughly investigated over the years at atmospheric pressure, using a wide range of substrates, ion activities and temperatures. As a result many different systems have been developed for the full-scale treatment of waste water and organic waste streams, like the Upflow Anaerobic Sludge Blanket (UASB), fixed bed and fluidised bed reactor types [25, 26].

In these systems bioconversions follow thermodynamic equilibria i.e. the Gibbs free energy change of a biochemical reaction[27]. The following equations show several reactions for methanogenesis, homo-acetogenesis, acetogenesis and acidogenesis of carbohydrate based digestion under standard condition (298K, pH 7, 1M reactants, 100 kPa gas pressure)[27]. $\Delta G^{0'}$ is used to denote the Gibbs free energy potential at above mentioned standard conditions. Glucose is an easily degradable compound for many organisms and its conversion products (a.o. lactate, ethanol and acetate) are highly dependent on the type of organism and the prevailing conditions [28]. The chosen representation is a simplified reaction generally used for glycolysis in anaerobic digestion.

Aceticlastic methanogenesis **(Eq. 1-1)**

$CH_3COO^- + H_2O \rightarrow CH_4 + HCO_3^-$ $\Delta G^{0'} = -31$ kJ reaction^{-1}

Hydrogenotrophic methanogenesis **(Eq. 1-2)**

$4H_2 + HCO_3^- + H^+ \rightarrow CH_4 + 3\,H_2O$ $\Delta G^{0'} = -135$ kJ reaction^{-1}

Homo-acetogenesis **(Eq. 1-3)**

$4H_2 + HCO_3^- + H^+ \rightarrow CH_3COO^- + 4H_2O$ $\Delta G^{0'} = -104.6$ kJ reaction^{-1}

Propionate oxidation **(Eq. 1-4)**

$CH_3CH_2COO^- + 3H_2O \rightarrow CH_3COO^- + HCO_3^- + H^+ + 3H_2$ $\Delta G^{0'} = +76.1$ kJ reaction^{-1}

Glycolysis **(Eq. 1-5)**

$C_6H_{12}O_6 + 4H_2O \rightarrow 2CH_3COO^- + 4H^+ + 2HCO_3^- + 4H_2$ $\Delta G^{0'} = -216$ kJ reaction^{-1}

Gibbs free energy calculations can however also be used to predict the feasibility of a specific biochemical reaction under non-standard environmental conditions, such as a pressurised environment. When taking aceticlastic methanogenesis as an example, the Gibbs free energy change under actual conditions (ΔG') would be defined as:

$$\Delta G' = \Delta G^{0,} + RT\ ln\ \left(\frac{pCH_4 * [HCO_3^-]}{[Ac^-] * [H_2O]}\right) \quad \textbf{(Eq. 1-6)}$$

In which $\Delta G^{0,}$ = the Gibbs free energy under standard conditions (298K, pH 7, 1M reactants, 0.1 MPa gas pressure), R = gas constant 8.3145 J $K^{-1}mol^{-1}$, T= temperature in Kelvin (K), pCH_4 = gas pressure of CH_4, $[HCO_3^-]$, $[Ac^-]$ and $[H_2O]$ are the molar concentrations of bicarbonate, acetate and water.

In principle CH_4 can be oxidised by Anaerobic Methane Oxidising Bacteria (AMOB), potentially impacting the solubilised CH_4/CO_2 ratio [28]. Specific growth rates of AMOB are however very low, whereas owing to the relatively low solubility of CH_4, there will be a continuous migration of the produced CH_4 under atmospheric pressure to the gas phase. CH_4 can therefore be considered relatively "inert", but CO_2 is used by a wide variety of micro-organisms for both catabolic and anabolic reactions. Moreover, CO_2 can be present in many different forms, i.e. CO_2(gas), CO_2(aq), H_2CO_3, HCO_3^- and CO_3^{2-} in the liquid phase, or fixed as CO_3^{2-} in inorganic precipitates like $CaCO_3$. In addition, CO_2 also affects the reactor broth pH which subsequently affects microbiological growth and activity.

Hydrolysis of complex organic matter is considered the slowest step at ambient temperature conditions [29]. Pressure can theoretically influence the disintegration and/or the (enzymatic) dissolution of organic solid matter and the formation of monomers via parameters, like temperature, pH and ion activity [30]. At extreme pressures, changes in hydrolysis rates should therefore be anticipated. Additionally, accumulation of pCO_2 has a direct effect on liquid acidity and thus also affects the conditions under which hydrolysis takes place.

1.3 Henry's law, the carbonate equilibrium and acid neutralising capacity

From the reaction stoichiometry in equations 1-1 and 1-2 the final total pressure in batch digestion can be estimated using the ideal gas law, like it is used to calculate the

specific methanogenic activity (SMA) in batch assays as described by Cho et al. (2005). Because water is assumed to be non-compressible under the proposed reactor conditions the gas volume (V_g) is determined by the liquid volume (V_l) , the total reactor volume (V_{tot}) and the temperature (T). Because under pressurised conditions gases will dissolve, as described by Henry's law, only the non-dissolved gases should be included to calculate the final pressure.

$$P = \alpha_r(nCH_4 + nCO_2) * R * T * \frac{V_l}{(V_t - V_l)} \quad \textbf{(Eq. 1-7)}$$

In which P= pressure in 0.1 MPa, α_r = % of non-dissolved biogas, nCH_4 = CH_4 (mol), nCO_2 = CO_2 (mol), R = 8.3145 J $K^{-1}mol^{-1}$, T = temperature in K.

Henry´s law describes the solubility of gases in dependence to the partial pressure of the respective gas. For example, the amount of dissolved CO_2 (mol L^{-1}) at a given partial pressure is given by

$$[H_2CO_3] = K_{HCO_2} * pCO_2 \quad \textbf{(Eq. 1-8)}$$

For CO_2 this constant ($K_{H,C02}$) at 298 K is 0.318 mol L^{-1} MPa^{-1} and for CH_4 ($K_{H,CH4}$) this value is 0.016 mol L^{-1} MPa^{-1} [15]. So, Henry's law dictates that when dissolving both gases at a similar partial pressure into water, almost 20 times more CO_2 will dissolve.

In addition, CH_4 behaves "inert" while CO_2 reacts with water according to the carbonate equilibrium [31]. When dissolved CO_2 reacts with water carbonic acid is formed. In most cases dissolved CO_2 and H_2CO_3 are taken together and the relation with bicarbonate is described by the apparent dissociation constant $K_1 = 10^{-6.3}$ (Eq. 1-9), whereas (Eq. 1-10) describes the dissociation ($K = 10^{-10.25}$) of bicarbonate to carbonate. And finally, carbonate may be removed from the liquid by the formation of CaCO3 of which the solubility product (K_s) determines the precipitation of $CaCO_3$ (Eq. 1-11). Although not a topic of this thesis, both H_2S and NH_3 will dissolve and react with water, like CO_2.

$$K_1 = \frac{[H^+]*[HCO_3^-]}{[H_2CO_3^*]} \quad \textbf{(Eq. 1-9)}$$

$$K_2 = \frac{[H^+]*[CO_3^{2-}]}{[HCO_3^-]} \quad \textbf{(Eq. 1-10)}$$

$$K_2 = [Ca^{2+}] * [CO_3^{2-}] \quad \textbf{(Eq. 1-11)}$$

$$K_w = [H^+] * [OH^-] \quad \textbf{(Eq. 1-12)}$$

All given reactions determine the overall reactor acidity via equation 1-9, 1-10, 1-11 and 1-12. The excess of cations in relation to the concentration of strong anions is known as the alkalinity or acid neutralizing capacity (ANC) of the water [31, 32].

$$Alk = [Na^+] + [K^+] + 2[Ca^{2+}] + 2[Mg^{2+}] + [NH_4^+]$$

$$-[Cl^-] - 2[SO_4^{2-}] - 3[PO_4^{3-}] \quad \textbf{(Eq. 1-13)}$$

$$10^{-pH} = [Alk] - [OH^-] - 2[CO_3^{2-}] - 2[HCO_3^-] - [VFA^-] \quad \textbf{(Eq. 1-14)}$$

These equations will be used to derive a relationship between the alkalinity, pH and pressure under AHPD conditions. In these calculations pH should be kept circumneutral as a boundary condition for effective methanogenesis [25].

From equation 1-13 and 1-14 it can be derived that carbon dioxide accumulation will inevitably result in undesired reactor broth acidification, potentially inhibiting the methanogens. In order to remove CO_2 and $[H^+]$ while continuing the biological digestion process, the addition of minerals used for aqueous carbon sequestration, like wollastonite ($CaSiO_3$) and olivine $(Mg, Fe)_2SiO_4$) were studied in this thesis [33]. These minerals have the capacity to scavenge CO_2 and $[H^+]$ according to equations 1-15 and 1-16 [34, 35].

$$CaSiO_3\ (s) + 2\ H^+\ (aq) \rightarrow Ca^{2+}\ (aq) + SiO_2\ (s) + H_2O\ (l) \quad \textbf{(Eq. 1-15)}$$

$$Ca^{2+}\ (aq) + CO_3^{2-}\ (aq) \rightarrow CaCO_3\ (s) \quad \textbf{(Eq. 1-16)}$$

1.4 Water vapour and potential work load

The water vapour equilibrium inside the biogas in AHPD is only temperature dependent. In order to calculate the specific saturation water vapour pressure the Clausius Clapeyron equation (Equation 1-17) can be used [36].

$$ln\frac{e_s}{e_{s0}} = \frac{L}{R_v}\left(\frac{1}{T_0} - \frac{1}{T}\right) \quad \textbf{(Eq. 1-17)}$$

In which T is the temperature in K, T_o is 273K, e_s is the saturation water vapour pressure in hPa e_{so} is the saturation water vapour pressure at temperature T_o (6.11 hPa), L is the latent heat of vapourisation (2.453×10^6 J kg^{-1}), and R_v is the water vapour gas constant (461 J kg^{-1} K^{-1}).

To determine the water vapour pressure of the AHPD biogas, it is assumed that biogas is 100% saturated at the temperature of the bioreactor. According to the ideal gas law, pressure times volume before decompression equals pressure times volume after decompression at constant temperature [37], according to Equation 1-18.

$$\frac{P_1V_1}{T_1} = \frac{P_2V_2}{T_2} \quad \textbf{(Eq. 1-18)}$$

In which P = pressure in MPa, V = volume in m^3 and T = Temperature in K

So, when assuming isothermal[1] expansion without the biogas being in contact with the water phase, the total water vapour in the biogas remains constant, but the total volume increases linearly with decreasing pressure. Hence, the water vapour initially contained in the pressurised volume is now diluted over a larger atmospheric volume. Therefore the water vapour pressure of the decompressed biogas ($e_{sbiogas}$) at atmospheric pressure equals the water vapour pressure of biogas when produced at atmospheric pressure (e_{s0}) divided by the volume after decompression of the AHPD biogas (V_{final}). Rewriting, this results in Equation 1-19.

$$e_{sbiogas} = \frac{e_{so}\, e^{\frac{L}{R_v}\left(\frac{1}{T_0}-\frac{1}{T}\right)}}{V_{final}} \quad \textbf{(Eq. 1-19)}$$

[1] Isothermal = at constant temperature

For predicting the potential energy (in J) released by decompression of biogas from a batch system, isothermal expansion from a finite reactor gas volume into an infinite open atmosphere gas volume is considered. This energy can be converted into work (Equation 1-20) by assuming that the potential energy is converted into an increase of volume.

By integration of Equation 1-20 and substituting the pressure term for the ideal gas law equation 1-21 is obtained:

$$W = \int P \ dV \qquad \textbf{(Eq. 1-20)}$$

$$W = n * R * T * ln\left(\frac{V_f}{V_i}\right) \qquad \textbf{(Eq. 1-21)}$$

In which V_i and V_f are the volume (in L) prior to and after expansion, respectively

The gas molar quantity (n) is considered stabilised when all substrate has been converted and gas liquid equilibrium is reached. Then V_f and V_i can be substituted for P_i and P_f by using Equation 1-18. Now, the potential decompression energy (in J) can be calculated from the expanding biogas volume resulting from depressurising the compressed biogas using the universal gas constant (R), according to Equation 1-22.

$$W = n * R * T * ln\left(\frac{P_i}{P_f}\right) \qquad \textbf{(Eq. 1-22)}$$

In which P_i = operational pressure in MPa Pa, P_f = final or atmospheric pressure in MPa.

R is the universal gas constant, 8.3145 J K^{-1} mol^{-1}, n= molar amount of biogas

1.5 Pressure as selection mechanism for micro-organisms

To be able to classify the micro-organisms according to pressure a P,T,μ-diagram can be used in which both pressure and temperature are related to the organism's growth rate [38]. Based on P and T variations in experiments μ_{max} is derived. The temperature and pressure domain in which an organism shows a maximum growth rate determines whether an organism can be classified as piezophilic, piezo-tolerant or piezo-sensitive.

Piezophilic refers to the micro-organisms that show optimal growth at pressures exceeding 50 MPa at various temperatures. Piezo-tolerant micro-organisms grow relatively well at pressures up to 50 MPa, but their growth rate is decreasing with further increasing pressures. Piezo-sensitive organisms have highest growth rates at low pressures and die or are completely inactivated if pressure exceeds a certain maximum. Figure 1-2 graphically presents the various ranges for optimal growth for the mentioned bacterial groups.

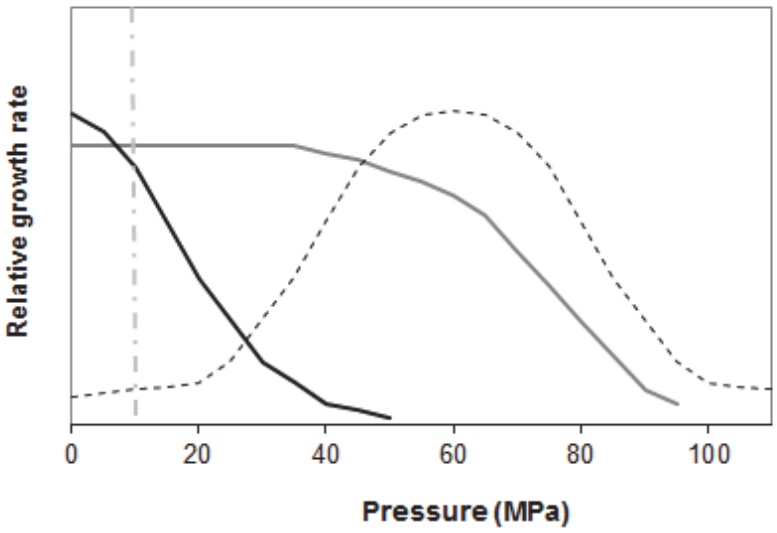

Figure 1-2: Classification of piezosensitive (black line), piezo-tolerant (grey line) and piezophilic (dotted line) micro-organisms (figure adapted from [39]). 'piezo' is the substitution for 'baro'. The vertical line indicates the maximum pressure reached in this study.

Although piezo-tolerance is not widely studied, different organisms also involved in anaerobic digestion, have been isolated from deep sea trenches up to a depth of 11000 m, which equals a pressure of 110 MPa [40, 41][2]. The same authors also described an experiment in which they isolated *Methonopyrus kandleri* from a black-smoker at a depth of 2000 m, which equals a hydrostatic pressure of 200 bar or 20 MPa. They have measured significant methane production from H_2 and $CO_{2,}$ as well as from formate addition in a cultivated high pressure batch reactor.

[2] Given the fact that the Mariana Trench is the deepest point of the ocean, the piezophilic limit of life on earth is set at 110 MPa.

The deepest isolation depth of 3000 meter, listed in the table below, corresponds to a pressure of 30 MPa and therefore there is not a pressure barrier for hydrogenotrophic methanogens up to these levels.

Table 1-3: Deep sea methanogens

	Depth	Characteristics (optimum in brackets)			Reference
		Substrate	T (°C)	pH	
Methanocaldococcus fervens	2003 m	H_2+CO_2	48-92 (85)	5.5-7.6 (6.5)	[42, 43]
Methanocaldococcus indicus	2420 m	H_2+CO_2	50-86 (85)	5.5-6.7 (6.5)	[44]
Methanocaldococcus infernus	3000 m	H_2+CO_2	55-91 (85)	5.25-7.0 (6.5)	[45]
Methanocaldococcus jannaschii	2600 m	H_2+CO_2	50-85 (85)	5.2-7.0 (6.0)	[46]
Methanocaldococcus vulcanius	2600 m	H_2+CO_2	49-89 (80)	5.25-7.0 (6.5)	[47]
Methanothermococcus okinawensis	972 m	H_2+CO_2, formate	40-75 (60–65)	4.5-8.5 (6-7)	[48]
Methanothermococcus thermolithotrophicus	0.5 m	H_2+CO_2, formate	30-70 (65)	6-8 (7)	[49]
Methanotorris Igneus	106 m	H_2+CO_2	45-91 (88)	5-7.5 (5.7)	[50]
Methanotorris Formicicus	2421 m	H_2+CO_2, formate	55–83 (75)	6.0–8.5 (6.7)	[40]

In our study on AHPD we studied the piezo-tolerance of inocula originating from atmospheric bioreactors. Although hydrogenotrophic methanogenic archaea are responsible for methane production [28, 51], for the complete conversion of complex organic matter a complex consortium of anaerobic micro-organisms is required. Aceticlastic methanogens have a very narrow substrate spectrum and are therefore dependent on fermentative and (homo)acetogenic bacteria for the production of methanogenic substrates like acetate, formate, methanol and hydrogen from complex organic matter [28], as also shown in Figure 1-1. Obviously, the AHPD process can

only function if these aceticlastic methanogens, fermentative and acetogenic bacteria are similarly piezo-tolerant.

No references have been found describing the piezo-tolerance of specific AD-related fermentative and acetogenic bacteria. Still, because also deep-sea methanogens rely on the activity of such micro-organisms, they doubtlessly form part of the food chain in the deep sea. Nonetheless, survival rates of human enteric bacteria in simulated deep sea conditions with regard to high pressures have been described. *Clostridium perfringens* for example, only showed significant sensitivity for pressures exceeding 25 MPa, whereas *Streptococcus faecali* was insensitive to pressure swings of up to 100 MPa [52]. Additionally, piezo-tolerant mutants of *Lactobacillus sanfranciscensis*, a species of lactic acid bacterium that gives sourdough bread its characteristic taste, could be grown after 100 generations of pressure treatment at 50 MPa or 500 bar [53]. Moreover, the extensive studies on inactivation by pressure swings of micro-organisms in food products have provided us with an overview of parameters affecting pressure tolerance of micro-organisms. The type of organisms is of main importance, but it also shows that environmental parameters like temperature, pH, water activity, nutrient level etc. influence the adaptability of micro-organisms to pressure. Based on this, it is hypothesised that next to methanogens fermentative and acetogenic bacteria will likely survive under AHPD conditions.

Table 1-4 lists the effects of pressure on individual organisms. However, the anaerobic community is much more than a random collection of individually operating organisms [28]. The syntrophic interactions between archaea and bacteria in anaerobic digestion are so closely intertwined that Martin and Müller [56] hypothesised that the first eukaryote cell evolved from these interactions. Therefore, the pressure-dependent response of every single organism, could potentially influence the whole population. For example, at the minimum pH_2 of 1 Pa that the methanogens can maintain under atmospheric conditions, the energetically most difficult biochemical step in propionate conversion, i.e. the oxidation of succinate to fumarate, is still endergonic and a mechanism of reverse electron transport (RET) is required to provide the required metabolic energy [28]. Based on the sensitivity of interspecies electron transfer at

atmospheric pressure it is speculated that the accumulation of gases (like H_2, CO_2, and even CH_4) in the liquid phase due to Henry's law will decrease the energetic feasibility further and will emphasize the role of interspecies electron transfer mechanisms for maintaining a balanced degradation. Therefore, in order to assess the potential effects of AHPD conditions on the overall degradation of more complex substrates, it is very important to study the population dynamics in relation to conversion of intermediate compounds.

Table 1-4: Parameters affecting inactivation of micro-organisms under high pressure conditions (summary from [54]and [55])

Type factor	Factor	Description
Microbial	Type of organism	Major differences exist between different phyla, but also between different species. Physical properties of the cell wall structure, type of active enzymes and shape determine their pressure resistance.
	Growth stage	Organisms in the exponential growth phase are more sensitive to pressure then organisms in the stationary growth phase.
	Temperature	Growth at non-optimal temperature can improve pressure tolerance.
Environmental	Water activity	A low water activity induces changes inside the organism influencing pressure resistance
	pH	At optimal pH, organisms are more resistant to high pressures.
	Nutrients	Availability of nutrients results in a better piezotolerance.
	Toxic compounds	When exposed to pressure cells are more sensitive to toxic compounds like antibiotics and organic acids.
	Other stressful conditions	Non-optimal pH, oxidative stress, starvation could result micro-organisms to slow down metabolism and switch to a protective mode also increasing piezo-tolerance.

1.6 Scope of this thesis

Chapter 2 demonstrates the feasibility of the AHPD concept, focussing on the limits of autogenerative pressure build up and a screening of the impact of elevated pressures on methanogenic activity. Standard batch operating procedures are tested in AHPD reactors.

Chapter 3 goes into more detail on the prediction of pressure production and gas composition using an equilibrium model, based on Henry's law and the carbonate equilibrium, and verifying this with biological fed-batch AHPD experiments.

In chapter 4 liquid acidity in AHPD reactors is managed by adding silicate mineral to the reactor broth as an alternative to NaOH. Depending on the liquid composition, CO_2 can be scavenged inside the reactor either as [CO_3^{2-}/ HCO_3^-] or as CO_2 (aq).

Chapter 5 evaluates the effects on the conversion rates of acetate, propionate and butyrate, under conditions where HCO_3^- is formed as dominant CO_2-species.

Chapter 6 discusses the effects of increased pCO_2 and CO_2(aq) on kinetics of glucose conversion and population dynamics in a long term experiment with a constant HCO_3^-.

When using complex organic matter at ambient temperature, hydrolysis generally limits the rate of monomer degradation and thus the formation of acidifying intermediates. Therefore, in chapter 7 we describe the influence of autogenerated pressure on the hydrolysis of starch and more importantly on the overall expected methane production rates.

Aim of the synthesis in chapter 8 is to combine concepts and discussion points of chapters 2-7 and focus on practical application of AHPD technology and derive ideas for future research. Chapter 9 concerns the Dutch summary.

Chapter 2

Proof-of-Principle

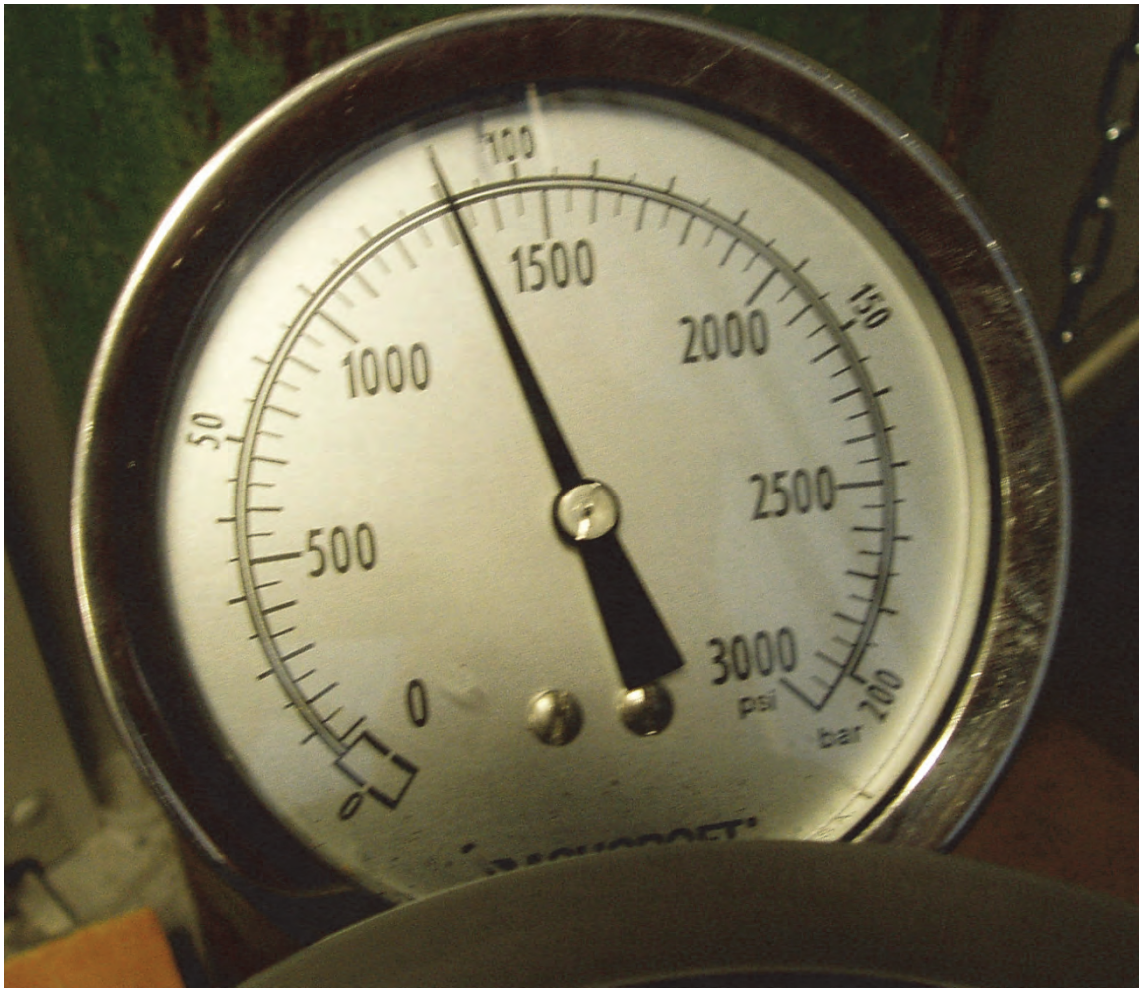

2 Feasibility of autogeneration of biogas pressure

Abstract

Conventional anaerobic digestion is a widely applied technology to produce biogas from organic wastes and residues. The biogas calorific value depends on the CH_4 content which generally ranges between 55 and 65%. Biogas upgrading to so-called 'green gas' with natural gas quality generally proceeds with add-on technologies, applicable only for biogas flows > 100 m^3 h^{-1}. In the concept of Autogenerative High Pressure Digestion (AHPD), methanogenic biomass builds up biogas pressure inside the reactor. Since CO_2 has a higher solubility than CH_4, it will proportion more to the liquid phase at higher pressures. Therefore, AHPD biogas is characterised by a measured CH_4 content reaching equilibrium values between 90-95% at a pressure of 0.30-9.00 MPa. Moreover, the biogas is calculated to have a dew point <-10^oC after expansion to atmospheric conditions. Ideally, high-quality biogas can be directly used for electricity and heat generation or injected in a local natural gas distribution net. In the present study, using sodium acetate as substrate and anaerobic granular sludge as inoculum, batch-fed reactors showed a pressure increase up to 9.00 MPa; the maximum allowable value for our used reactors. However, the specific methanogenic activity (SMA) of the sludge decreased on average by 30% compared to digestion at ambient pressure (0.1 MPa). These first AHPD findings show that it is a highly promising technology for anaerobic digestion and biogas upgrading in a single step reactor system.

Keywords

High-pressure; anaerobic digestion; CO_2 solubility; biogas upgrading.

This chapter is based on

Lindeboom, R.E.F., Fermoso, F.G., Weijma, J., Zagt, K. & Van Lier, J.B. Autogenerative high pressure digestion: Anaerobic digestion and biogas upgrading in a single step reactor system. Water Science and Technology **64**, 647-653 (2011).

2.1 Introduction

In this chapter the feasibility of a novel anaerobic digestion concept for production of high-grade biogas in a single step: Autogenerative High Pressure Digestion (AHPD) is tested. The objective is to digest organic matter under autogenerated high pressure to CH_4 and CO_2 [13]. Henry's constants for CH_4, CO_2, H_2S, and NH_3 in water are 0.016, 0.318, 1.15, and 620 mol L^{-1} MPa^{-1}, respectively [15]. With a higher constant more gas dissolves into the liquid phase. Consequently, the CH_4 content is expected to increase to values comparable to natural gas. Moreover, the biogas should already be at a suitable pressure for high-grade use. AHPD eventually aims to generate biogas that meets the demands for Synthetic Natural Gas (SNG), or in popular words "green gas". Then, no additional upgrading technology would be required. Although investments are needed to operate anaerobic digestion at high pressure, we expect that AHPD is cost-effective at small-scales and therefore suitable for decentralised biogas production from organic waste. The aim of the work described here is to demonstrate the feasibility of this concept focussing on autogenerative pressure build-up and the impact of high pressures on methanogenic activity.

2.2 Methods

2.2.1 Reactor set-up

All experiments were conducted in batch-fed high pressure reactors using different working volumes, i.e. 13.5 L, 1.7 L and 0.6 L (Figure 2-1). Safe range of operation for the reactors is 0.0-10.0 MPa and 4-125 ^{o}C. The 13.5 L reactor was equipped with a pH sensor (Bűchi high pressure probe), a pressure sensor (Parker PTD & PTX) and temperature sensor (PT100). The 13.5 L reactor set-up is shown in Figure 2-1. The 1.7 L and 0.6 L reactors were equipped with a pressure sensor. The temperature in these reactors was controlled by a water bath.

Online monitoring provided data for all experiments on total pressure, pH and temperature. A field point module functioned as receiver of data. Data was logged in Labview 7.1 (National Instruments). Stirring was provided a magnetically induced impeller at 60-500 rpm for the 13.5 L reactor.

(a) (b)

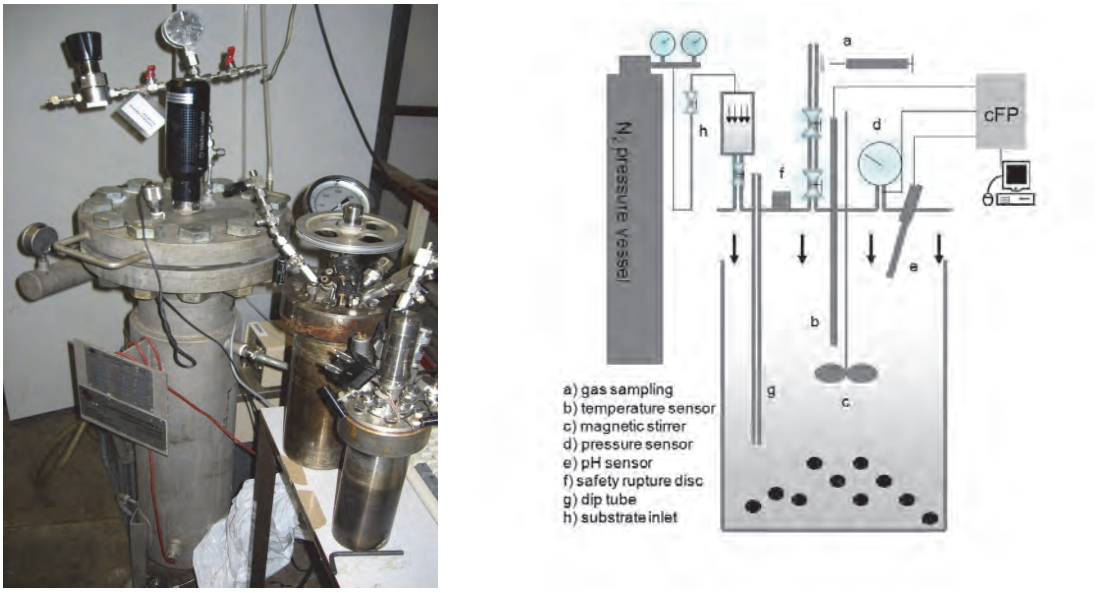

Figure 2-1: (a) Photo of the used reactors (b) Schematic view of high pressure reactors. The pH sensor was not included in chapter 2.

2.2.2 Reactor operation

The reactor experiments were performed at different liquid to gas ratios, ranging from 14:1 to 200:1. These ratios were chosen based on the stoichiometric conversion of substrate into biogas and an estimation of the final pressure based on the added amount of substrate and the ideal gas law. The reactors were inoculated with different concentrations of methanogenic granular sludge obtained from a full-scale UASB reactor treating paper mill waste water (pH 7.0, 30°C) at Industriewater Eerbeek (Eerbeek, The Netherlands). Macronutrient stock solution (6mL L^{-1}) and trace elements stock solution (0.6 mL L^{-1}) were added to the liquid medium (Table 2-1).

Furthermore, different concentrations of sodium acetate trihydrate ($NaCH_3COO.3H_2O$) were added as substrate. An overview of all experiments is shown in Table 2-2.

Table 2-1: **Macronutrient stock and trace element stock solution**

Macronutrients (6ml L^{-1})		Trace elements (0.6 ml L^{-1})	
Compound	**Concentration ($g\ L^{-1}$)**	**Compound**	**Concentration ($g\ L^{-1}$)**
$NaKHPO_4$	27	$FeCl_3 \cdot 4\ H_2O$	2
$MgSO_4 \cdot 7\ H_2O$	9	$MnCl_2 \cdot 4\ H_2O$	0.5
NH_4Cl	170	$ZnCl_2$	50
$CaCl_2 \cdot 2\ H_2O$	8	$(NH_4)_6Mo_7O_{24} \cdot 4\ H_2O$	90
		$NiCl_2 \cdot 6\ H_2O$	50
		$CoCl_2 \cdot 6\ H_2O$	2
		$CuCl_2 \cdot 2$ H2O	30
		HBO_3	50
		$Na_2SeO_3 \cdot 5\ H_2O$	100
		EDTA	1

*additionally 0.1 g L^{-1} yeast was added

2.2.3 Analyses

Total Suspended Solids (TSS) and Volatile Suspended Solids (VSS) were determined according to Standard Methods [57], prior to bioreactor inoculation.

Gas composition was determined by taking biogas samples at the end of each run. A two valve system, with a sampling port in between, connected to the high pressure reactor was used to decompress the biogas during sampling. The two valve system was flushed and 100µl gas samples were taken perpendicular to the flow direction by means of a gas syringe with sample-lock. Afterwards biogas was analysed at atmospheric pressure by means of gas chromatography (Fisons Instruments GC 8430). The gas sample was directed over two different columns. One was equipped with Molsieve (Alltech 13940) 30m, having a diameter of 0.53mm and the other with PoraBond Q (Varian 7354) 25m, having a diameter of 0.53mm. In the columns the gases were separated, using 0.4 MPa of helium pressure as the carrier gas.

Detection took place by a thermal conductivity detector. Furthermore, the oven, injection port and detector were operated at 53, 110 and 99^{o}C, respectively.

The specific methanogenic activity (SMA) was determined by pressure increase following the protocol of Zandvoort, Osuna, Geerts, Lettinga and Lens [58]. The online pressure sensor in the high pressure reactor allowed us to record pressure build-up continuously. Based on the total pressure and the gas composition, the partial pressures for CH_4 and CO_2 were derived. By using the ideal gas law, the total molar production of CH_4 was calculated.

To perform the SMA tests at atmospheric pressure, 1 L batch bottles were filled with 500 mL of liquid medium. The liquid medium contained 1 g COD L^{-1} and similar concentrations of macronutrients and trace elements solution as described above. Inoculum (2g VSS L^{-1}) was taken from the high pressure reactors after decompression. The gas phase was flushed with N_2 prior to the start of the experiments. Subsequently, the bottles were connected to an online pressure transducer and monitor (Pressdaq 2.0 and Pressdaq 2.0 software). Total gas phase of the bottle was determined by subtracting the liquid volume from the total volume of the bottle. Then like for the high pressure experiments molar CH_4 production was calculated using the ideal gas law and the data on pressure increase.

Liquid samples were taken from the reactor medium after each experiment. Sampling during operation was not possible without interfering in the on-going experiment. Samples were centrifuged at 10,000 rpm for 5 minutes and subsequently diluted by adding 0.5 ml 3% of formic acid to the 0.5 mL centrifuged sample. VFA was afterwards determined by a gas chromotograph (Hewlet Packard 5890 series II) with a flame ionisation detector (FID). A glass column (2m x 6mm x 2mm) with a 10% Fluorad 431 coating on Supelco-port (mesh 100-120) was used. Further operating conditions were the FID was operated at 280 ^{o}C; Oven temperature was 130 ^{0}C and injection temperature was 200 ^{o}C. The carrier gas was nitrogen saturated with formic acid.

2.3 Results

2.3.1 Autogenerative High Microbiological Pressure Production

Microbiological pressure generation was achieved in 9 fed-batch experiments using various gas and liquid volumes. In 8 out of 9 reactor experiments more pressure build-up was achieved than the 0.8 MPa which is required for injection in the natural gas grid (Table 2-2).

Table 2-2: Overview of proof-of-principle experiments

Exp. Nr.	Reactor volume (L)	Gas Volume (L)	Acetate (g COD L^{-1})	P range Initial (MPa)	Final	Final gas composition * %CH_4	%CO_2	%N_2	Time (h)
1	0.55	0.04	1	0.3	0.8	91	1	8	30
2	0.55	0.04	1	3.2	3.6	94	1	4	35
3	0.55	0.04	1	1.2	1.4	Leakage			25
4	1.68	0.04	3	0.0	2.33	94	3	2	160
5	1.68	0.04	5	0.0	2.2	89	6	2	60
6	1.68	0.01	14	0.0	5.8	96	2	1	96
7	1.68	0.01	14	0.0	9.0	n.a.			170
8	13.5	0.10	7	0.0	2.6	94	3	2	40
9	13.5	0.10	14	0.0	2.4	n.a.			40

*** all gas measurements have a 2% error margin**

In experiment 7, pressure build-up even continued up to 9.0 MPa (Figure 2-2). The final pressure is obviously determined by the amount of added substrate, the degree of stoichiometric conversion, and the chosen head space gas volume (liquid to gas ratio). The time required to reach the final pressure was less than a week in all experiments. The produced biogas in the head space reached CH_4 concentrations between 89 and 96%. The CO_2-content was below 6% in all experiments.

A linear increase in pressure between 0.0 and 9.0 MPa was observed in experiment 7 (Table 2-2 and Figure 2-2) over a period of one week. Afterwards the experiment had to be terminated to ensure biological pressure production would not damage the

equipment. Clearly, a 100-fold increase in pressure seemed not to have detrimentally harmed the methanogenic inoculum cultivated in an atmospheric UASB reactor for waste water treatment. Likely, the biomass can resist even higher pressures, because biogas production did not significantly level off near 9.0 MPa.

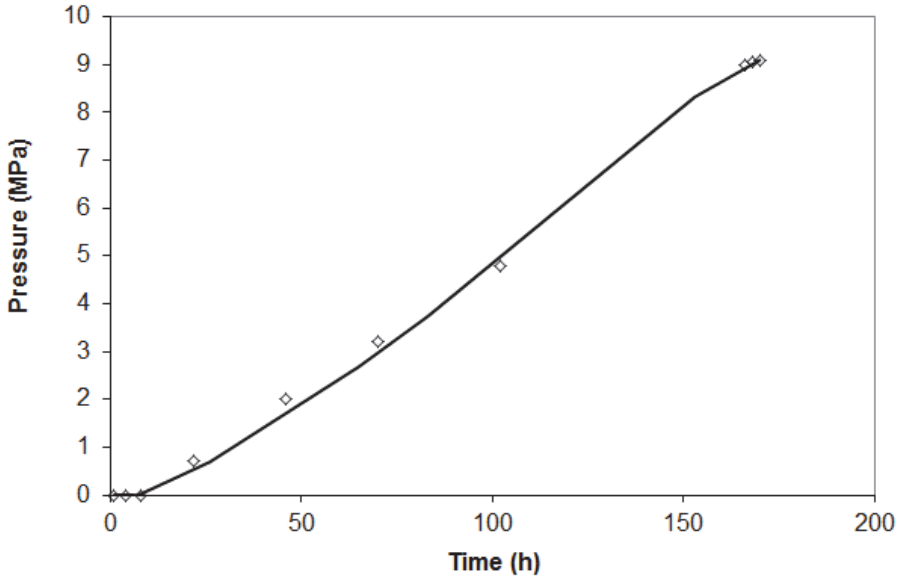

Figure 2-2: Gradual pressure build-up in experiment 7 up to 9 MPa

2.3.2 SMA under high pressure conditions

SMA tests done with the granular sludge inoculum revealed an SMA of 0.6 gCOD-CH_4 g^{-1} VSS d^{-1} at atmospheric pressure (Figure 2-3a). When the SMA was measured with an initial pressure of 0.3 MPa by adding a mixture of CO_2 5% and CH_4 95% to the head space, a moderate decrease in SMA to about 0.4 gCOD-CH_4 g^{-1} VSS was observed (Figure 2-3b). A third experiment was performed in which the reactor was pressurised up to 3.2MPa, using a similar gas composition (CO_2 5% and CH_4 95%). The observed SMA at 3.2MPa was in the same range as the SMA performed at 0.3 MPa (Figure 2-3b,c).

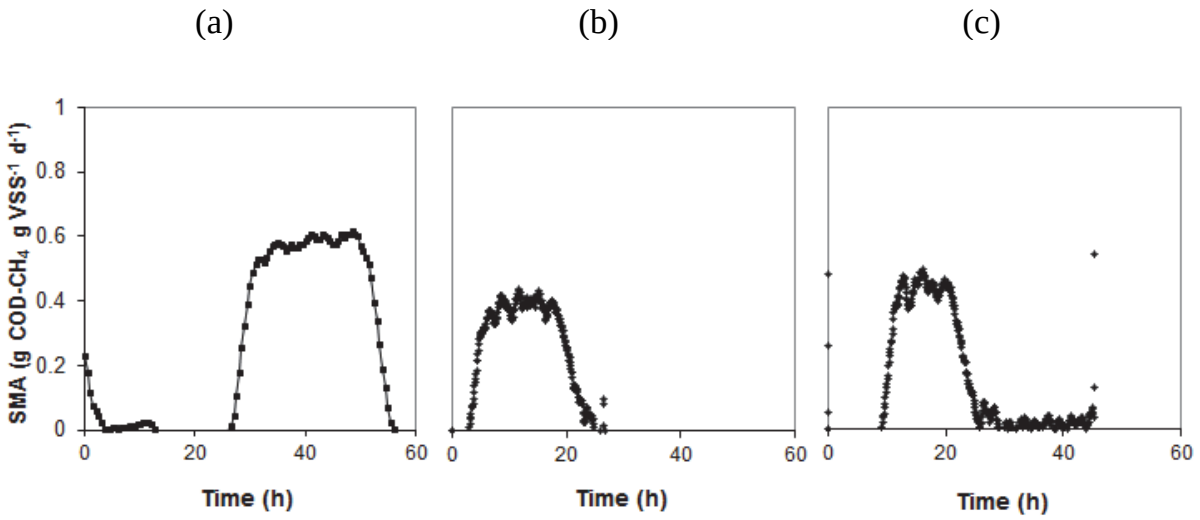

Figure 2-3: Overview of methanogenic activity at pressures (a) atmospheric, (b) 0.3 MPa and (c) 3.2 MPa

2.3.3 The influence of pressure and/or decompression

The impact of high pressures on the standardised SMA at atmospheric pressure was determined by assessing the standardised SMA after sludge exposure to high pressures. Results showed that an exposure to 1.6 MPa at 303K for 4 days, apparently had no effect since SMA test values of the inoculum and the SMA values after pressurised conditions were equal (Figure 2-3a and Figure 2-4a). The SMA value with the inoculum exposed to 5.8 MPa showed an unexpectedly high biogas yield in an SMA performed after decompression. More biogas was generated than expected based on the stoichiometric conversion of the added substrate (Figure 2-4b). Interestingly, in the liquid phase of the reactor at 5.8 MPa, propionate, butyrate and valerate were measured with values of 272 mg L^{-1}, 280 mg L^{-1} and 163 mg L^{-1}, respectively. Possibly, the increased soluble COD / VFAs was the result of lysis of bacterial and/or archaeal cells resulting from the sudden compression and decompression, but this could not be confirmed. Similar results have been obtained with sludge exposed to 9.0 MPa (data not shown). After being exposed to the high pressures, the granular structure was completely disrupted and visually, the sludge made an emulsified impression. Sludge exposed to 5.8 and 9.0 MPa appeared more viscous than sludge exposed to lower pressure, i.e. 0.8 and 1.6 MPa.

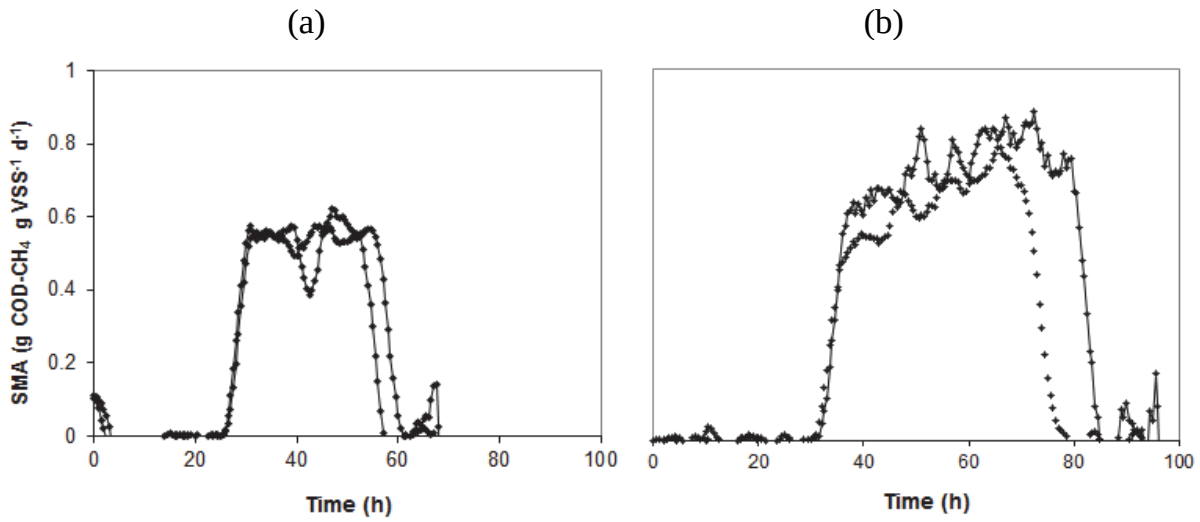

Figure 2-4: Overview of the specific methanogenic activity assays at atmospheric pressure (in g COD-CH_4 g^{-1} VSS day^{-1}) of sludge exposed to (a) 1.6 MPa, (b) 5.8 MPa (both presented in duplicate).

2.4 Discussion

To our knowledge no experiments have been reported in which the anaerobic digestion was used for the autogeneration of up to 9.0 MPa of pressure. The results presented in this study demonstrate that anaerobic granular sludge from a conventional waste water treatment plant can autogenerate a higher pressure than required for injecting biogas into the regional or local gas grid. This additional pressure could be used for direct mechanical work, e.g. in the AHPD process (pumping, membrane pressure, etc.) without the need for electrical equipment and electricity supply. It can be expected that use of the pressure for mechanical work is more efficient than via methane conversion into electrical energy and then back into mechanical energy, which only has an overall efficiency of 25-35%.

When comparing the gas composition results to the requirements for gas grid injection, it has been demonstrated that in-situ biogas upgrading is technically feasible, because the CO_2-content of the biogas was suitable for injection into the Dutch regional gas grid (<6% CO_2 required). The organic substrate in our experiments neither contained nitrogen nor sulphur. In practice, complex waste water may contain a high content of these elements, resulting in H_2S an NH_3 in the biogas, although levels are generally much lower than for CO_2. Based on the higher Henry's constants for both H_2S and NH_3 the in-situ biogas upgrading mechanism is expected to reduce the gas

concentration of both gases proportionally more than for CO_2. Further study is needed to find out if the strict limitations for these gases, which are -much lower than for CO_2, can be achieved at high autogenerated biogas pressure.

Based on the headspace composition and the total pressure a COD_{CH4} balance was made. The COD_{CH4} retrieved in all high pressure experiments (Table 2-2) was only between 60-80% of the COD added as acetate. In experiments 6 and 7, 14g COD L^{-1} was added and a similar final pressure was expected. Experiment 6 however resulted in an end-value of 5.8 MPa, whereas experiment 7 ended at 9.0 MPa when the experiment was terminated for safety reasons. In several experiments CH_4 was detected outside of the reactor, indicating that at higher pressures reactors started leaking and the procedure for sealing the reactor was not sufficiently effective. Based on the Henry's constant of CH_4, it is hypothesised that significant quantities of the produced CH_4 were dissolved in the liquid.

Pressure sensitivity of bacteria involved in the anaerobic digestion process and the impact of increased pressure and pressure swings on the methanogenic activity have hardly been reported in literature. Still, methanogens have been studied and isolated from deep sea trenches where the pressure can be as high as 110 MPa [40, 41]. Takai et al.[40] isolated and cultivated the thermophilic piezophilic *Methanopyrus kandleri.* in a batch reactor at 40.0 MPa. However, it concerned hydrogenotrophic methanogens while aceticlastic methanogens were not studied. Based on these results it is concluded that increased pressure has no detrimental effect on the SMA of acetotrophic methanogenic sludge. To our best knowledge that has not been shown previously.

The observed disrupted granular structures and the emulsified liquid broth, combined with the increased level of propionate, butyrate and valerate gave rise to an analogy with the presence of toxic compounds and/or sudden temperature increases beyond the respective range, which also resulted in increased levels of VFA in the liquid medium [59, 60].

Physical pressure was not the only possible stress factor for the biomass. With pressure also gaseous and dissolved CO_2 accumulated. The total inorganic carbon in the 1.68L

reactor was for instance estimated to be 0.36 mol. Additionally, a relatively high concentration of 5g Na^+ L^{-1} was present and the stirring mechanism required for CSTR conditions induced a high shear in the 13.5 L reactor. Notably, in the 5.8 MPa experiment the sludge was in the system for 96 hours. After being released from the system, the granule structure was completely disrupted. It is yet unclear to what extent the increased pressure is responsible as the sole stress factor causing an increased level of VFA and EPS. Further experimental studies are required to understand the limitations between micro-organisms in an AHPD reactor with an increasing pCO_2 and a high shear.

2.5 Concluding remarks

We found that anaerobic micro-organisms are able to digest acetate in high pressure reactors and can build up a pressure of to 9.0 MPa through biogas production. In addition, the produced biogas was of very high quality, consisting of over 90% CH_4 and below 6% CO_2. It was also observed that less CH_4 was produced than was expected based on reaction stoichiometry. Whether this was the result of leakage, CH_4 dissolution due to Henry's law or because of biological changes, could not be determined. The measured rate of COD-conversion (SMA) decreased from 0.6 gCOD-CH_4 g^{-1} VSS d^{-1} to 0.4 gCOD g^{-1} VSS d^{-1} at 0.3 and 3.1 MPa. After decompression, propionate, butyrate and valerate were found in significant concentrations. It could not be determined if it was caused by the compression, decompression, the high stirring speed or the exposure to elevated free sodium concentrations, because all parameters changed while operating the reactor at higher pressure. Literature about piezophilic micro-organisms showed that operating pressures (up to 9.0 MPa) were in the range where most piezo-sensitive and piezo-tolerant species can still survive. So, even though decay of specific microbes had surely resulted from the pressure build-up, both experimental results and literature showed that pressures applied in this study are unlikely to have a detrimental effect on acetotrophic conversions in general. Therefore, it is concluded that AHPD has great potential for making external gas upgrading equipment obsolete.

Chapter 3

Biogas-speciation

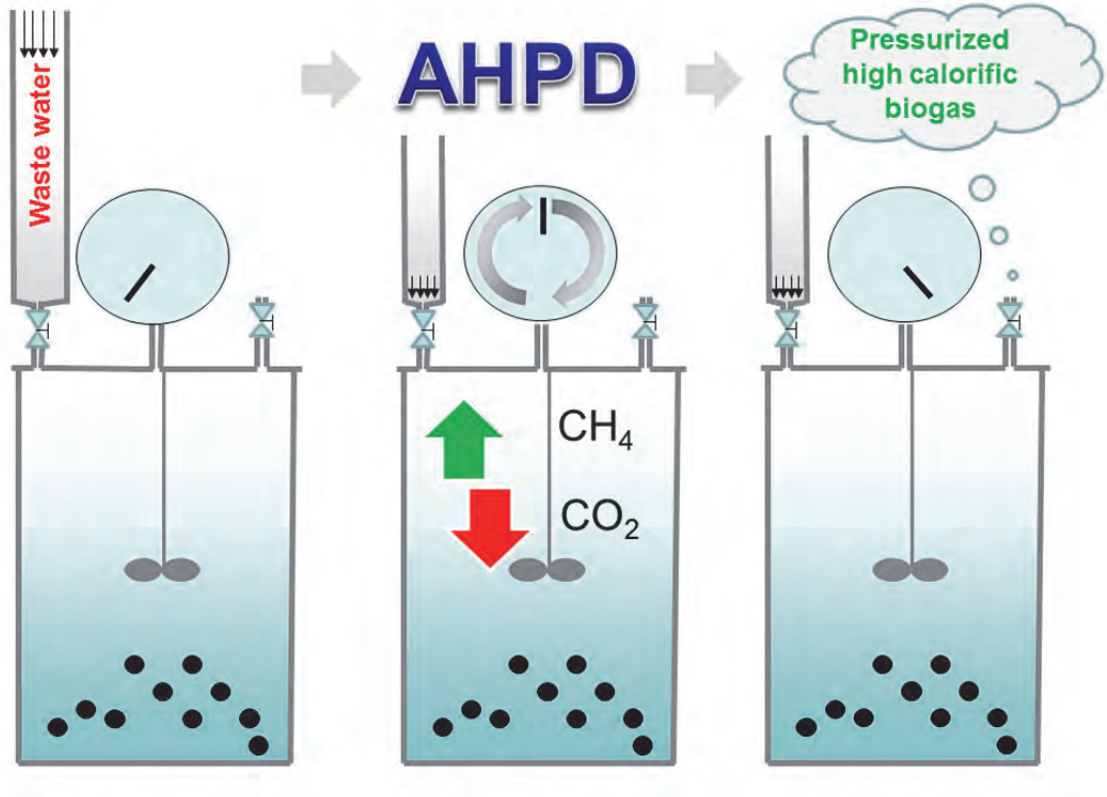

3 Biogas-speciation in a pressure digester up to 2.0 MPa

Abstract

In the experiments presented in chapter 2 micro-organisms autogenerated biogas pressures up to 9.0 MPa with >90% CH_4-content in a single reactor. The less than 10% CO_2-content was thought to be the result from proportionally more CO_2 dissolution relative to CH_4 at increasing pressure, according to Henry's law. However, at 9.0 MPa of total pressure Henry's law also predicted the dissolution of 81% of produced CH_4, which is a potential loss. Therefore, in the present research it was studied whether CO_2 could be selectively retained in solution at moderately high pressures up to 2.0 MPa, aiming to minimise methane dissolution. Experiments were performed in an 8L closed fed-batch pressure digester fed with acetate as the substrate. CH_4 distribution over gas and liquid phase behaved according to Henry's law, but the CO_2-content of the biogas was lower than expected with only 1-2 % at pH 7. By varying the ratio Acid Neutralising Capacity (ANC) over Total Inorganic Carbon ($TIC_{produced}$) of the substrate between 0 and 1 the biogas CO_2-content could be controlled independently of pressure. However, by decreasing the ANC relative to the $TIC_{produced}$ CO_2 accumulation in the aqueous medium caused acidification to pH 5. Remarkably, acetic acid was still converted into CH_4 at a rate comparable to neutral conditions.

Keywords

Autogenerative High Pressure Digestion; CO_2-sorbing effect, carbonate-equilibrium, 2.0 MPa, gas partitioning

This chapter is based on

Lindeboom, R.E.F., Weijma, J. & Van Lier, J.B. High-calorific biogas production by selective CO_2 retention at autogenerated biogas pressures up to 20 bar. Environmental Science and Technology **46**, 1895-1902 (2012).

3.1 Introduction

Biogas upgrading is generally performed outside the anaerobic reactor system and requires investments in external compressors, pumps, membranes and gas treatment equipment [4]. Nevertheless, an in-situ CH_4-enrichment method was described by Hayes [17] in which CH_4-rich biogas was produced by integrating a CO_2-air stripper and a deoxygenation reactor into a liquid recycle loop. Based on this principle the CH_4 content rose from 82 % at atmospheric pressure to over 93% at an overpressure of 0.22 MPa. Similar experimental results have been obtained by Richards, Herndon, Jewell, Cummings and White [61] and O'Keefe, Brigmon and Chynoweth [62], but the system was difficult to operate (Table 1-2).

Conventionally, anaerobic digestion is performed close to atmospheric pressure resulting in an equilibrium CO_2 content of the biogas of typically 30-40%, depending on reactor alkalinity. In chapter 2 it was however demonstrated that unadapted methanogenic biomass can autogenerate 9.0 MPa biogas pressure with >95% CH_4 by the conversion of acetate into CH_4 and CO_2 which is far above the level required for local grid injection. CO_2 is 20 times more soluble than CH_4, with Henry's constants for CO_2 and CH_4 of 0.31 and 0.016 mol L^{-1} MPa^{-1} at 30 °C, respectively [15]. Thus, at increasing biogas pressure the equilibrium CO_2 content of the biogas was expected to decrease and this was confirmed.

In practice however CO_2 and CH_4 partial pressures may deviate from equilibrium due to mass transfer limitations [63]. In addition, at increasing pCO_2 carbonic acid will be formed, possibly resulting in a pH drop to below pH 7 which would inhibit the anaerobic digestion process. The apparent dissociation constant of carbonic acid 6.36 is generally used, but it should be realised that this constant also comprises the K-values for the hydration and the dehydration reactions of carbon dioxide [64]. Aim of this chapter is therefore to study CO_2-speciation in more detail.

Furthermore, it should be realised that at 9.0 MPa and a liquid/gas ratio of 167:1 the theoretical dissolution of CH_4 is over 80% of $CH_{4produced}$,. Therefore, this chapter focussed on more moderate pressures not exceeding 2.0 MPa overpressure in a single-

stage bioreactor fed with acetate-rich synthetic waste water. Additional experiments were carried out to elucidate the role of CO_2 mass transfer on pH-stability. Results from 4 experimental series were compared with model-based predictions using Henry's law and the carbonate equilibrium.

3.2 Materials and Methods

3.2.1 Reactor setup

One pressure reactor of 8L of total volume was used (Parr Instruments, model 910908, The Netherlands). The gas phase was manually controlled at ~1.5L. This gas phase volume was chosen to ensure foaming due to degassing would not clog gas valves.

Figure 3-1: Photo of the used reactor

The reactors depicted in Figure 3-1 have been designed for operation up to 6.80 MPa in a temperature range of -10°C to 350°C. Schematically, the set-up was identical to the set-up presented in Figure 2-1b. To seal the reactors, bolts in the head were

tightened with a torque wrench supplying a torque of 33.86 Nm according to the supplier's specifications. On top of the reactor a stainless steel liquid charging pipette (250 mL) was placed vertically for forcing substrate into the reactor with N_2-pressure against the pressure gradient. The temperature in the reactor was controlled at 30°C for all experiments by a water bath (Julabo MP). Online monitoring was used to obtain data on total pressure (Ashcroft A-series 1000 PSI), temperature (PT100) and pH (Bűchi Labortechnick AG, Flawil, Switzerland high pressure pH probes) Compact field point modules (cFP1804 and cFP-CB1) functioned as data receivers to log and store data via Labview 7.1 (National Instruments Corporation, USA) on the PC. Magnetic stirring was performed by two six bladed impellers attached to a central stirrer shaft (Parr Instruments, type A709HC, The Netherlands) operating at 150 rpm for all experiments.

3.2.2 Start up and operation

Experiments I-1 to I-4 were used to assess mass transfer of CO_2 from gas to demineralised water. For experiment I-1 the reactor was pressurised with 50% CH_4 and 50% CO_2 at an initial pressure of 0.5 MPa, and demineralised water was used as liquid medium. The added CO_2 corresponds to 0.15 mol total inorganic carbon. Dissolution of both gases was monitored online by registering pressure decrease and pH. Once pressure had stabilised, the gas composition was determined by GC. From these data, the measured pressure decrease was used as an approximation of the expected dissolution flux based on Fick's law. Afterwards, proceeding to experiment I-2, 0.05 mol NaOH was added, in order to neutralise 1/3 of the added CO_2. Hereafter, in experiment I-3 and I-4, the procedure was repeated, meanwhile increasing total added NaOH to 0.1 mol and 0.15 mol, respectively.

For experiments II, III and IV, the reactor was inoculated with a mixture of 6.25L of basal medium and 256 g wet anaerobic granular sludge (6.1 gVSS L^{-1}), with a diameter of 1-4 mm from a full-scale UASB reactor treating paper mill waste water (pH 7.0, 30°C) at Industriewater Eerbeek (Eerbeek, The Netherlands). Endogenic activity of fresh inoculum was determined at an average of 0.1 mmol CH_4 g^{-1}VSS d^{-1} or 64 mg CH_4-COD g^{-1}VSS d^{-1}. Alkalinity of the sludge was determined at 2.3 meq g^{-}

[1] VSS. The basal medium consisted of demineralised water to which macronutrient and trace element stock solution were added according Table 2-1.

A week before it was used for inoculation, the sludge was reactivated with 8 mM acetate. The reactors were flushed with N_2 gas (100 % N_2) prior to the start of each experiment to remove oxygen.

Experiments II-1 to II-4 were performed to assess mass transfer of CO_2 from gas to liquid medium that also contained biomass. Experiments II-1, II-2, II-3 and II-4 were performed in a similar manner as experiments I-1 to I-4.

Experiments III-1 to III-3 aimed to assess the effect of elevated autogenerated pressure on methanogenic activity and gas composition. In each of the experiments III-1, III-2 and III-3, 0.33 mol sodium acetate trihydrate was dissolved in 67 mL demineralised water and added via the liquid charging pipette. Inside the inoculated reactor the highly concentrated substrate solution was diluted in the medium solution to 0.05 mol L^{-1}. Prior to experiment III-2 and III-3 67 mL of liquid volume was removed to maintain a total liquid volume 6.5 L, meanwhile retaining N_2, CH_4 and CO_2 in the gas phase of the reactor. In the first 48 hours of experiment III-1 the stirring speed was unintendedly set at 60 rpm, afterwards it was set to 150 rpm.

Experiment IV was performed to demonstrate the effect of feeding non-buffered substrate. Prior to the start of experiment IV, 0.33 mol of sodium acetate trihydrate was digested, but all pressure exceeding 0.20 MPa was released directly. By depressurising to atmospheric conditions CO_2 was removed and after equilibrium was reached the medium contained a 0.05 mol $NaHCO_3$ L^{-1} buffer. Afterwards, in each of the experiments IV-1, IV-2 and IV-3 0.16 mol non-buffered acetic acid was added in a similar way as described for experiments III-1 to III-3. An overview of all experiments is given in Table 3-1.

Table 3-1: Overview of CO_2-speciation experiments

Exp. nr.	Inoculum (gVSS L^{-1})	Substrate	ANC (eq)	TIC (eq)	P_{range} (MPa)*	pH
I-1	0		0	0.15	0.50-0.28	4.7
I-2			0.05	0.15	0.28-0.26	6.3
I-3			0.10	0.15	0.26-0.23	7.2
I-4			0.15	0.15	0.23-0.22	9.2
II-1	6.1		0	0.15	0.50-0.28	5.4
II-2			0.05	0.15	0.28-0.26	5.9
II-3			0.10	0.15	0.26-0.25	6.1
II-4			0.15	0.15	0.25-0.23	7.0
III-1	6.1	Sodium acetate	0.33	0.33	0.10-0.68	7.0
III-2			0.66	0.66	0.68-1.44	6.8
III-3			0.99	0.99	1.44-2.10	6.9
IV-1	6.1	Acetic acid	0.33	0.49	0.10-0.57	5.7
IV-2			0.33	0.65	0.57-1.00	4.7
IV-3**			0.33	0.81	1.00-1.34	4.5

***absolute range; not corrected for N_2 and sampling**

****steady-state not reached due to observed leakage**

3.2.3 Analyses

Total Suspended Solids (TSS) and Volatile Suspended Solids (VSS) were determined according to [57].

Biogas composition. A stainless steel tube, connected to the high pressure reactor, with valves at both ends, was used to take biogas samples, as shown in Figure 3-1. Samples were taken in duplicate as described in chapter 2. Biogas composition was analysed at atmospheric pressure by means of gas chromatography (Fisons Instruments GC 8430) like shown in chapter 2.

The specific methanogenic activity (SMA) was calculated from the pressure increase and the biogas composition following the protocol of [60]. By using the ideal gas law, the total molar production of CH_4 was calculated.

Liquid samples from the reactor were immediately injected into N_2-flushed closed 100 mL bottles, for determination of dissolved CO_2 and CH_4 in the liquid broth. Before use the pressure in the bottles was lowered to 0.05 MPa. The amount of liquid sample was determined by weighing. Gas composition was determined by GC after adjustment to atmospheric pressure with N_2. Measured values were corrected for the dissolved CO_2 and CH_4 in the sample bottle by calculating the gas partitioning based on Henry's law.

Thereafter, bottles were opened and the total liquid content of the bottle were titrated with 0.1 M HCl in an automatic titrator (Schott, Mainz, Germany) for assessing the acid neutralising capacity (ANC) or alkalinity in meq L^{-1}. The $[HCO_3^-]$ was calculated by subtracting $NaKHPO_4$ present in the medium and measured VFA concentration. This method was validated by injecting 2 ml 37% HCl into the closed sample bottle followed by measuring pressure and gas composition. The ANC present in the inoculum- was determined by titrating 0.1 M HCl to 5 g of wet sludge dissolved in 10 mL of demi-water.

Calculation of gas/liquid distribution of CO_2 and CH_4 was calculated using the carbonate equilibrium equations and Henry's law[65]. For CO_2, Henry's constant (K_{HCO2}) at 25^{o}C is 0.318 mol L^{-1} MPa^{-1} and for CH_4 (K_{HCH4}) this is 0.016 mol L^{-1} MPa^{-1} [15]. These values are applicable in the whole pressure range used in our experiments and are valid for the ionic strength of the solution, according to the experimental data provided by [66] and [67]. Henry's constants and the dissociation constants were corrected for temperature with van 't Hoff's equation [37]. The pK_a of H_2CO_3 was corrected in non-iterative manner for ion activity using the Davies equation, based on added substrate, and ranged over the experiments between 6.08-6.35.

Charge balance.

The acid neutralising capacity of the liquid reactor content is now modified from equation 1-14:

$$[ANC^-] + [H^+] = [OA^-]+[HCO_3^-]+2[CO_3^{2-}]+[OH^-] \quad \textbf{(Eq. 3-1)}$$

In which $[OA^-]$ represents the concentration of dissociated organic acids

In the expected pH range (6-8) $[CO_3^{2-}]$, $[OH^-]$ and $[H^+]$ are negligible compared to the molar substrate concentration. Therefore, equation 3-1 can be simplified to:

$$[ANC^-] = [OA^-]+[HCO_3^-] \quad \textbf{(Eq. 3-2)}$$

Now, the charge balance for the most common ions in solution should be adapted from equation 1-13:

$$2[Ca^{2+}]+2[Mg^{2+}]+[Na^+]+[K^+]+[NH_4^+]$$

$$-[Cl^-]-2[SO_4^{2-}]-3[PO_4^{3-}]-[ANC^-] + .. = 0 \quad \textbf{(Eq. 3-3)}$$

However, in these specific experiments the charge due to ions in the basal medium was negligible compared to charge of the added substrate. Also, the basal medium contained a negligible amount of $[ANC^-]$. Therefore, the charge balance was simplified by combining equation 3-2 and 3-3:

$$[Na^+] = [ANC^-] \quad \textbf{(Eq. 3-4)}$$

Combination of Equation 3-2 and 3-4 with acetate as the only present organic acid gives:

$$[Na^+] = [Acetate^-] + [HCO_3^-] \quad \textbf{(Eq. 3-5)}$$

After full conversion of sodium acetate (equation 1-1) the ANC equals $[HCO_3^-]$. To verify full acetate conversion, separate liquid samples were centrifuged, volatile fatty

acids (VFA) were analysed by a gas chromatograph (Hewlett Packard 5890 series II) equipped with a flame ionisation detector as described in detail in chapter 2.

The total inorganic carbon (TIC) balance, as a function of ANC and pH, was formed by combining equation 3-5 with the carbonate equilibrium (equations 1-8 to 1-12) and ideal gas law (equation 1-7).

$$TIC = HCO_3^- + CO_2(diss) + CO_2(gas) \quad \textbf{(Eq. 3-6)}$$

or

$$TIC = (ANC) + \frac{(ANC) * 10^{-pH}}{K_1} + \frac{(ANC) * 10^{-pH} V_g}{K_1 K_{HCO_2} V_l * R * T}$$

In which ANC is given in meq L^{-1}, $K_1 = 10^{-pKa}$, $K_{Hco2} = 10^{-6.55}$ mol L^{-1} Pa^{-1}, Vl = liquid volume in L, Vg = gas volume in L, T = 303 K and R = 8.3145 10^3 L Pa K^{-1} mol^{-1}.

Likewise, the CH_4-balance was constructed (equation 3-7) and used to calculate biogas composition and pressure.

$$TCH_4 = pCH_4 * \left(\frac{V_g}{R*T} + K_{H\,CH_4} * V_l\right) \quad \textbf{(Eq. 3-7)}$$

In which $K_{Hch4}=10^{-7.84}$ mol L^{-1} Pa^{-1}

3.3 Results

3.3.1 Experiment I and II: Mass transfer experiments

Figure 3-2 shows the pressure decrease in time for experiments I-1, I-3, II-1 and II-3. Experiment I-1 and II-1 showed an identical pressure pattern, indicating that the presence of inoculum did not affect the mass transfer rate from gas to liquid. Results of Experiments I-3 and II-3 also showed an identical pressure pattern. Both experiments I-1 and II-1 revealed that after a 4 hr, the calculated equilibrium pressure was reached.

In experiment I-3 and II-3 CH_4 and >80% CO_2 already were in equilibrium at the start of the experiment and only a relatively small pressure drop was expected due to pH increase and additional formation of HCO_3^-. In both experiments calculated equilibrium pressure was reached within 4 hr.

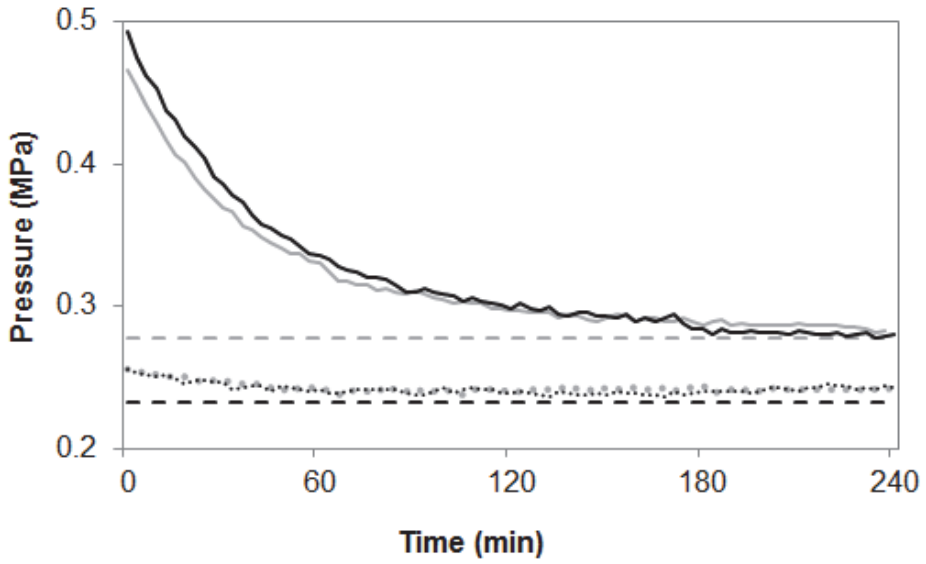

Figure 3-2: Pressure drop resulting from mass transfer of biogas into demineralised water without inoculum and ANC in Exp I-1 (grey line), with inoculum without ANC in Exp II-1 (black line), without inoculum after 2nd ANC addition in Exp I-3 (grey dotted line) and with inoculum after 2nd ANC addition in Exp II-3 (black dotted line). Theoretical equilibrium values of Exp I-1 & II-1, and Exp I-3 and II-3 are indicated by grey and black intermittent line, respectively.

As soon as a stable pressure was obtained, gas samples were taken to study the composition of the gas phase. After recalculation, measured gaseous CH_4 values for both sets of experiments (I-1 to I-4 and II-1 to II-4) were 0.22 MPa, or 0.13 mol. These values are in accordance with model predictions using Equation 8 and confirmed that Henry's law applied for CH_4 under experimental conditions. As demonstrated in Figure 3-3a, biogas composition, assuming a 1:1 CH_4:CO_2 production, showed a linear relationship with the ANC/TIC ratio for all mass transfer experiments. This indicated that the ANC/TIC ratio can be used to predict CO_2-content of the biogas when acetate is the sole substrate. When looking at these results more closely it was noticed (data not shown) that pH required a similar time lapse to reach a stable phase, with a change of less than 0.01 pH unit/hour. And therefore from Figure 3-3b it can be observed that the pH and CO_2-speciation of the inoculum-free experiments matched the model equilibrium predictions, but that this was not the case for the inoculated experiment series II. Since measured CO_2-speciation corresponded to a higher theoretical pH than the experimentally measured pH, we describe this as an apparent "CO_2-sorbing" effect.

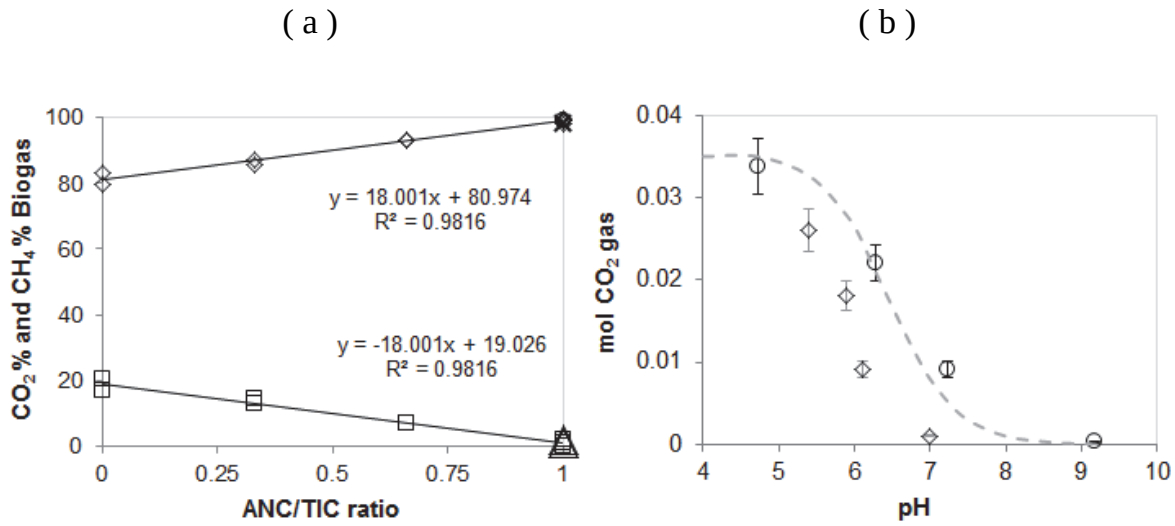

Figure 3-3: (a) produced CH_4-content exp I and II (◊) and III (x), CO_2-content exp I and II (□) and III (Δ) as a function of ANC/TIC ratio using a total molar CH_4:CO_2 ratio of 1:1 (stoichiometric ratio for acetate) and (b) experiment I (○), II (◊) and theoretical CO_2 gas-content (- - -) versus pH

3.3.2 Experiment III: Acetate conversion at a ANC/TIC ratio of 1

Figure 3-4 presents the total pressure, pH and %CO_2 for experiments III-1, III-2 and III-3. The subsequent additions of 0.33 mol of sodium acetate trihydrate led to an observed pH-drop to 6.5, which is attributed to the increase of ion activity, resulting from the highly concentrated sodium acetate addition. At the end of the experiment series II, the total overpressure was 2.0 MPa of which 0.54 MPa was due to N_2 injected together with the 3 substrate additions. After full digestion of acetate, partial CH_4 pressures were 0.49, 0.97 and 1.45 MPa or 0.29, 0.58 and 0.86 mol CH_4 for experiments III-1, III-2 and III-3, respectively. These values were close to the calculated molar CH_4-values of 0.29, 0.59 and 0.88 mol. At the end of phase III, 17 mmol $CH_{4dissolved}$ L^{-1} was expected based on equation 3-7 for the total liquid content. Because 16 mmol L^{-1} was measured, these results showed that distribution of methane behaved according to Henry's law. It should be noticed that these values correspond to a dissolution of 11% of $CH_{4produced}$ at a pCH_4 of 1.48 MPa.

In percentage, CO_2 amounted to only 1.8, 1.0 and 1.0% in the produced biogas with values corresponding to 6, 6 and 7 mmol gaseous CO_2 for III-1, III-2 and III-3,

respectively. At the respective measured pH-values, 6.95, 6.77 and 6.90 much higher total molar gaseous CO_2 of 17, 50 and 37 mol were expected based on Henry's law. In experiment III-3, 39 mmol H_2CO_3 and 1000 mmol HCO_3^- were measured at pH 6.9, whereas values of 240 mmol H_2CO_3 and 806 mmol HCO_3^- were expected based on the model calculations. Nevertheless, in Figure 3-3a it can also be seen that the resulting 3 biogas compositions for experimental series III all match the biogas composition and pH of experiment II-4, which also had an ANC over $TIC_{produced}$ ratio of 1. And even though the pH was lower in experiment III, the biogas composition was also similar to experiment I-4, again having the same $ANC/TIC_{produced}$.

For experiment III-1 and III-2, average SMA was estimated between 0.25 and 0.4gCOD-CH_4 $gVSS^{-1}$ d^{-1} or 4-7 mmol gaseous CH_4 $gVSS^{-1}$ d^{-1}. In experiment III-3 the SMA was estimated between 2-5 mmol gaseous CH_4 $gVSS^{-1}$ d^{-1}. The production rate of gaseous carbon dioxide in these three experiments was estimated to be less than 0.2 mmol $gVSS^{-1}$ d^{-1}.

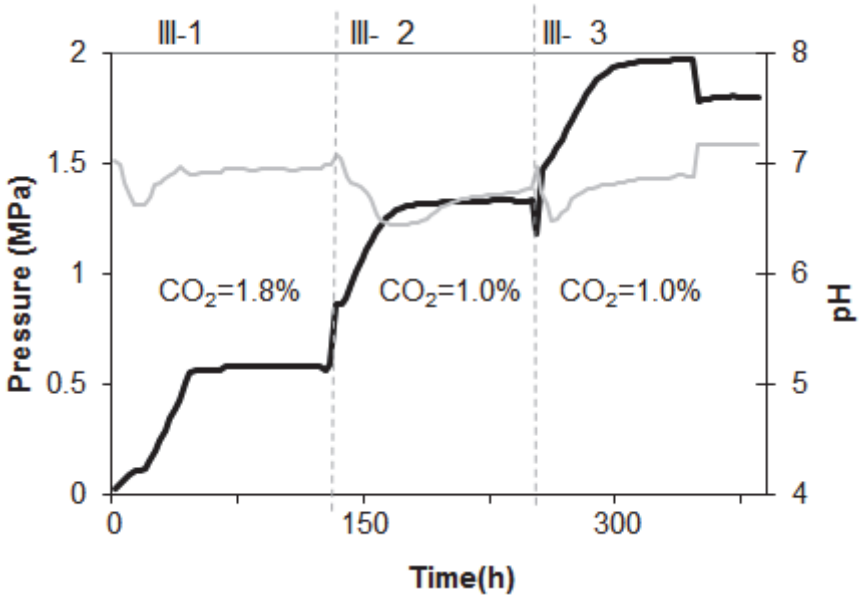

Figure 3-4: Autogenerated pressure in MPa (black) and pH development (grey) of experiment III-1, III-2 and III-3 at ANC/TIC = 1. The sharp increase in pressure at the start is caused by nitrogen used for the pressurised feeds of sodium acetate solution.

3.3.3 Experiment IV: Acetate conversion at low ANC/TIC-ratios

Figure 3-5 shows the biological pressure generation at low ANC/TIC ratio. The initial ANC was provided by converting 0.33 mol sodium acetate to sodium bicarbonate prior to experiment IV-1 after which the reactor was flushed with N_2 to remove gaseous CH_4 and CO_2. In experiment IV-1, 0.16 mol acetic acid was added due to which the reactor pH dropped from 6.7 to 5.7. This pH drop shifted the bicarbonate/Henry equilibrium to CO_2(gas) resulting in a total pressure increase to 0.24 MPa after 2 hours. Then, a gradual total pressure increase was observed up to 0.45 MPa over the next 22 hours, while pH initially dropped further to 5.5 and gradually recovered to 5.7 and biogas consisted of 16% CO_2 and 84% CH_4. As a consequence of the presence of HCO_3^- at the beginning of experiment IV, the CH_4:TIC ratio in the reactor was 1:2.

Then experiment IV-2 started with an additional substrate addition of 0.16 mol acetic acid which caused a pH drop to 4.7. Despite this low pH, substrate conversion continued and all acetate was converted, resulting in a total pressure of 0.9MPa, whereas the pH remained at 4.7. The final pCH_4 and pCO_2 were 0.56 and 0.13 MPa respectively, corresponding to 81% CH_4 and 19% CO_2 with correction for N_2.

Afterwards, experiment IV-3 was started with again an additional feeding of 0.16 mol acetic acid. At a pressure of 124 kPa a leakage was detected due to which the experiment ended before final samples could be taken. Nonetheless, pCH_4 in experiment IV had further increased to 0.68 MPa.

Experiment IV showed that the pH-drop caused by the decreasing $ANC/TIC_{produced}$ ratio was not as detrimental to the process as expected, since in three consecutive additions of acetic acid CH_4-production continued with pH between 5.5 and 4.5. For experiments IV-1 and IV-2 average rates were estimated between 2.5-3.5 mmol CH_4 $VSS^{-1}d^{-1}$. Nonetheless, the combined pH drop and the change in molar ratio in the total reactor between CH_4 and CO_2 showed that under these conditions the CO_2 in the biogas will increase to values above 6%, the maximum level for grid injection.

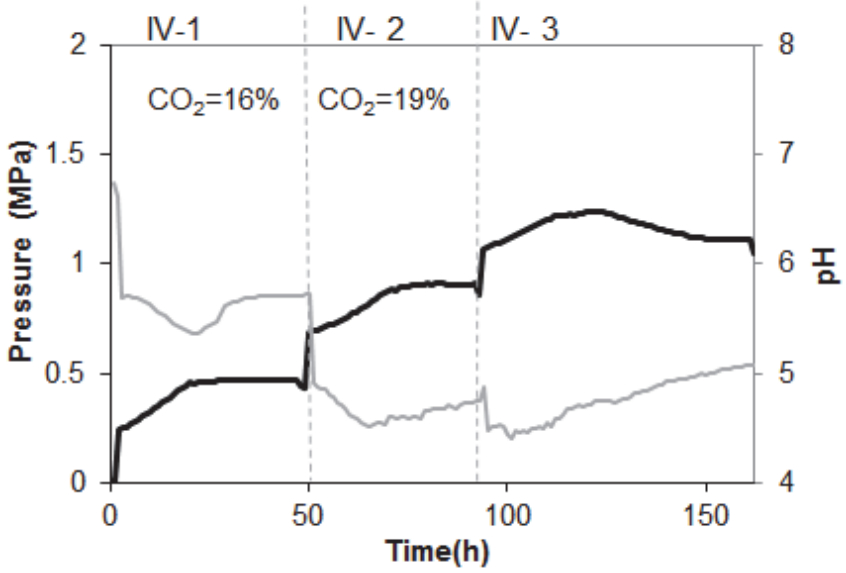

Figure 3-5: Autogenerated pressure (MPa = black) and pH development (grey) from acetic acid digestion starting with an ANC of 0.33 eq and a TIC increasing from 0.33 with 0.16 in each of the experiments IV-1, IV-2 and IV-3.

3.4 Discussion

Our results show that methane distribution over gas and liquid phase in AHPD reactors follows Henry's law. We expect that increasing operating pressures will result in proportionally more CH_4-dissolution. CH_4 dissolution in general is undesired, because it reduces the quantity of easily recoverable high quality biogas and requires additional CH_4 collection when decompressing the effluent. This should be considered in the design of an AHPD process.

However, experiments also showed that increasing the $ANC/TIC_{produced}$ ratio resulted in increased formation of $[HCO_3^-]$ in the liquid phase and thereby a decreased CO_2-content in the gas phase from 20% to below 2% at $ANC/TIC_{produced}$ of 0 and 1 for acetate, respectively. Our findings have important implications for further development of the AHPD technology, since it means that the CO_2 content of biogas can be controlled at relatively low to moderate pressures by ANC addition, while keeping pH circumneutral. Thus, methane dissolution can be reduced and reactor costs can be diminished. This opens perspectives for developing low-cost reactor systems

that can be used for producing high-quality biogas for grid injection from waste streams in decentralised settings, provided low-cost ANC is available.

In this work it has been assessed how the conversion of synthetic acetate waste water could influence biogas composition under AHPD conditions. This is of course an idealised setting and for real waste waters it should be taken into account that (a) the conversion of more complex organic matter will influence the stoichiometric production of CH_4 and CO_2 as dictated by the COD/TOC-ratio, following $CH_4\%$ = 18.75 x COD/TOC (assuming all CO_2 and CH_4 in the biogas), as described by Van Lier, Mahmoud and Zeeman [24]. On top of that (b), the actual CH_4/CO_2 ratio will be determined by the presence of alternative electron acceptors [24]. And (c) as is demonstrated in this work the ratio $ANC/TIC_{produced}$ determines the chemical CO_2 binding to the reactor broth, and this ratio is also substrate/waste water dependent. For neutralised propionate and butyrate for example, the ratio $ANC/TIC_{produced}$ equals 0.8 and 0.67 respectively. For glucose and triglycerides this ratio is 0. Anaerobic conversion of N-containing compounds like proteins and amino acids will generate NH_4^+ cations, thus increasing ANC. So, for N-containing compounds, the $ANC/TIC_{produced}$ ratio will also be determined by the ratio of N/C_{total} [68].

The importance of the $ANC/TIC_{produced}$ ratio is further stressed by the fact that the carbonate speciation predicted a substrate ANC requirement of 0.82 eq per mol $TIC_{produced}$ to maintain pH 7. At lower $ANC/TIC_{produced}$ ratios, pH was theoretically expected to decrease to values below 5 and this was confirmed by experiments I, II and IV. In general, pH-values below 6 are reported to have an inhibiting effect on methanogenesis, often due to the accumulation of volatile fatty acids [24]. Remarkably, experiment IV showed continued methane production, between 2.5 and 3.5 mmol g^{-1} VSS d^{-1}, at an estimated ANC ratio between 0.40 and 0.67 with pH dropping below 5. Fukuzaki, Nishio and Nagai [69] reported for example a 50% inhibitory value of undissociated acetic acid of 4 mM at pH 6, whereas values in experiment IV corresponded to 7.8, 16.5 and 17.8 mM undissociated acetic acid. Taconi, Zappi, Todd French and Brown [70] reported acetate-based methanogenic activity at an initial pH of 4.5, but during their experiment pH increased to pH 7. Low

pH methanogenesis has also been reported for acidic peat bog environments, but is attributed to hydrogenotrophic methane formation [71-73]. Furthermore, striking low reactor pH values of 4.2 were reported when digesting non-VFA substrates, such as methanol [74], provided that VFA/acetate was not produced as intermediate. The observed acetate conversion at low pH offers opportunities to operate AHPD at a lower pH, reducing or perhaps eliminating the need for investments for ANC recovery, recycling, and/or addition.

On top of the unexpected methane formation at low pH, inoculated experiments II and III showed an apparent "CO_2-sorbing" effect, due to which pH 6.9 was measured, whereas actual CO_2-speciation corresponded to a theoretical pH 8.1 at $ANC/TIC_{produced}$ ratio of 1. Apparently, the presence of active inoculum resulted in a deviation from pH-based predictions on CO_2-speciation. On one hand, the exact mechanisms underlying the low pH digestion of acetate and the observed disagreement between CO_2-speciation and pH in inoculated experiments are not yet elucidated. On the other hand, it is obvious that a simple modelling approach without having a detailed knowledge on the presence of unknown precipitates, proteins and organic acids in complex biological systems can result in under- or overestimation of CO_2-speciation and its dissociation constant based on pH and temperature [63]. In the below section we have identified three possible mechanisms which could give direction for further experimental work and incorporation of biological complexity into the modelling of CO_2-speciation. These are (a) monovalent and divalent free cations naturally present in the methanogenic biomass (b) mass transfer and reaction limitations resulting from the biochemical matrix and (c) enzymatic catalysis.

Titration of the used inoculum rendered 2.3 meq g^{-1} VSS of inoculum-associated ANC. For the total reactor this would contribute 94 meq, which is 9.4% of added ANC via the substrate. ANC in close association with the micro-organisms could also provide a locally elevated pH, due to which acetic acid could be converted even at low bulk pH, as is also proposed by Williams and Crawford [73]. The inoculum used in our experiments was known to be rich in Ca^{2+} [75], possibly explaining the inoculum bound ANC. The divalent cations in the inoculum, could also exchange with

monovalent cations in the liquid phase [75] and thereby increase the effect of ion pairing, especially under pressurised conditions. Due to ion pairing of carbonate and calcium ions, the apparent pKa of carbonic acid could be lowered according to Whitfield [76] and result in relatively more HCO_3^- formation at lower pH. Also, digestion of N-containing compounds generates NH_4^+, contributing to ANC build-up. Even though in our system ammonia was not present in the added substrate, Batstone and Keller [77] analysed 4 anaerobic sludges for protein content and found a minimum content of 0.14 g protein g^{-1} VSS. Therefore, endogenic respiration of the sludge mass will likely result in a further build-up of NH_4^+ linked ANC. Additionally, the presence of proteins and pressurised CO_2 could also provide an apparent "CO_2-sorbing" effect, by forming carbamate ions onto the amine groups of proteins in the presence of cations, this compound having a lower pKa than carbon dioxide [64]. Carbamate is also investigated as alternative method for CO_2-sequestration by for example McCann, Phan, Fernandes and Maeder [78] and is described as the first step of carbon fixation via the Rubisco-enzyme in many autotrophic organisms [79].

Secondly, Farajzadeh, Barati, Delil, Bruining and Zitha [80] concluded, based on their study with the surfactant sodium dodecyl sulphate, that the physical properties of the liquid can limit CO_2 mass transfer substantially, likely leading to pH gradients in the liquid. Such pH-gradients also occur due to limitations in proton transfer in granular agglomerates and biofilms of anaerobic micro-organisms of mixed reactor systems [81]. Initially granular sludge was added and after the experiments we visually observed an increased liquid viscosity in the inoculated experiments and because pH was measured in the upper part of the reactor, local pH gradients could not be excluded. Also, if gaseous micro CO_2 bubbles are trapped in remaining granules and cannot migrate upwards to the head space the pH would be influenced directly, but this CO_2 would not have to be measured until after decompression and titration. Therefore, the influence of 'biologically initiated' mass transfer limitations, even at a stirring speed of 150 rpm, cannot be excluded even though mass transfer results indicate that equilibrium had been reached.

Thirdly, the enzyme carbonic anhydrase is known to regulate the hydration and dehydration of CO_2 or HCO_3^- in many methanogenic microbes [82]. Because CO_2 is not only an end product, but also an essential compound for autotrophic growth of micro-organisms, it can be speculated that micro-organisms can actively influence the CO_2-speciation in and around their cells, possibly resulting in significant changes and retardation of the physical-chemical equilibrium of the bulk solution in AHPD systems. Ongoing experiments are focussing on elucidating these phenomena and are researching the biological consequences of elevated pCO_2 in anaerobic digestion technology.

Chapter 4

VFA-conversion

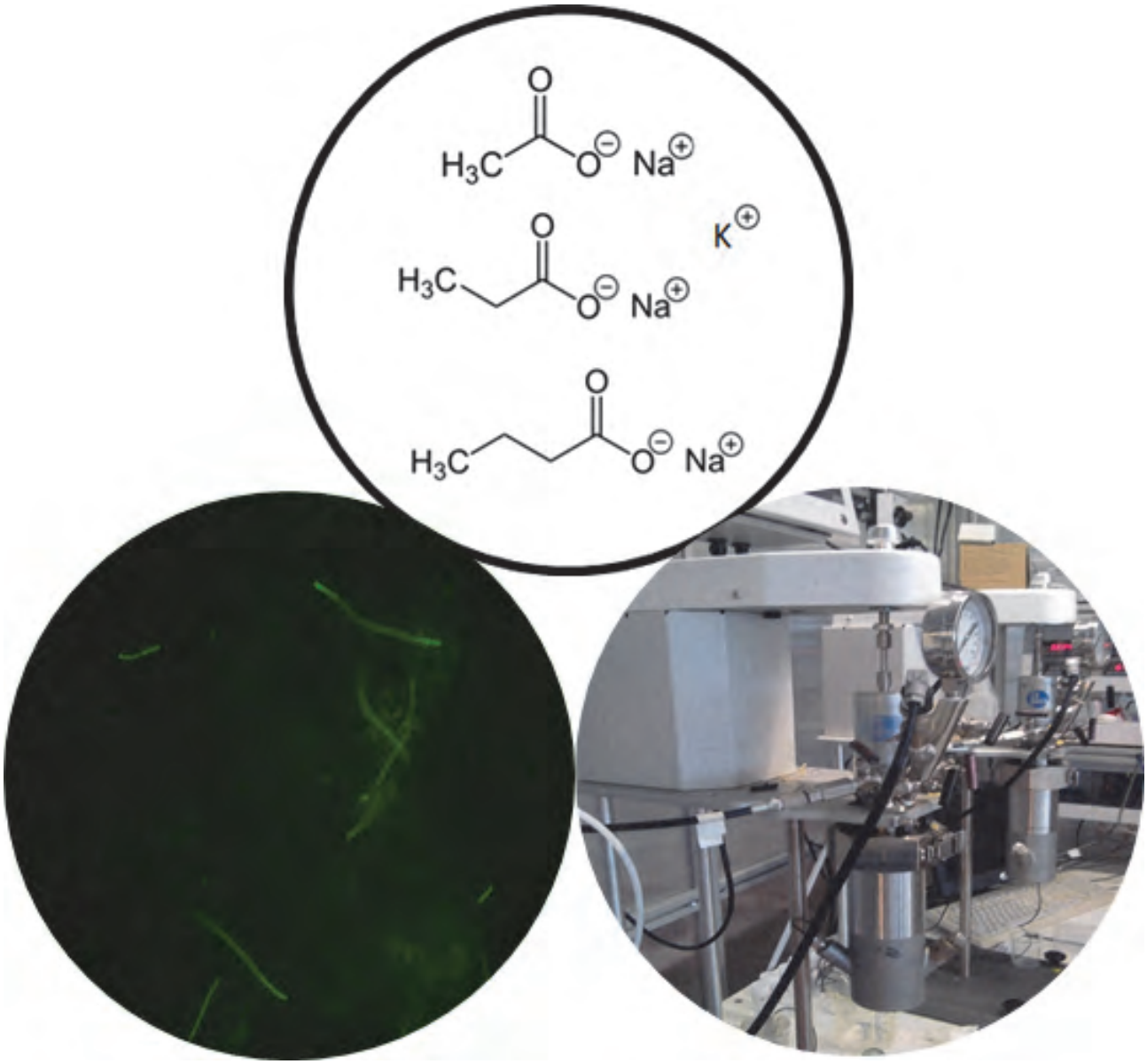

4 The effect of cation requirement on Volatile Fatty Acid conversion at elevated biogas pressures

Abstract

This work studied the anaerobic conversion of neutralised volatile fatty acids (VFA) into biogas under Autogenerative High Pressure Digestion (AHPD) conditions. The effects of the operating conditions on the biogas quality, and the substrate utilisation rates were evaluated using 3 AHPD reactors (0.6 L); feeding a concentration of acetate and VFA (1-10 g COD L^{-1}) corresponding to an expected pressure increase of 0.10-2.00 MPa. The biogas composition improved with pressure up to 0.45 MPa (>93% CH4), and stabilised at 1.0 and 2.0 MPa. Both, acetotrophic and hydrogenotrophic methanogenic activity was observed. Substrate utilisation rates of 0.2, 0.1 and 0.1 gCOD CH_4 g^{-1} VSS d^{-1} for acetate, propionate and butyrate were found to decrease by up to 50% with increasing final pressure. Most likely increased Na^+-requirement to achieve CO_2 sequestration at higher pressure rather than end-product inhibition was responsible.

Keywords

Anaerobic digestion; Biogas upgrading; Pressure; Substrate inhibition; ANC-requirement

This chapter is based on

Lindeboom, R.E.F.[1], Ferrer, I.[1], Weijma, J. & van Lier, J.B. Effect of substrate and cation requirement on anaerobic volatile fatty acid conversion rates at elevated biogas pressure. Bioresource Technology **150**, 60-66 (2013).

[1]Both first author

4.1 Introduction

Hansson [16] described the influence of end product limitation by CH_4 and CO_2 at relatively low partial pressures up to 0.1 MPa for aceticlastic methanogenesis (Table 1-2). Inhibition due to pCO_2 exceeding 10 kPa was considered significant and resulted in 30 % reduction in CH_4 yield at a pressure of 0.1 MPa pCO_2; but no data was presented at higher pCO_2. The impact of elevated CH_4 partial pressure was considered negligible. Kapp [18] reported a biogas composition of 61 % CH_4 from sludge at thermophilic pressurised conditions (0.2-0.3 MPa), while operation at mesophilic temperature was unstable (Table 1-2). Decreased NH_3 inhibition at 0.3 MPa was confirmed by modelling pressure effects on anaerobic digestion [20].

From these studies, it becomes clear that improved biogas composition can be obtained, but might come at the cost of end product inhibition and process instabilities at pressures not exceeding 0.4 MPa. However, the results presented in chapter 2 indicated a drop in the specific methanogenic activity (SMA) of only 30 % at pressures up to 9.0 MPa. It should be noticed that pCH_4 increased up to 8.8 MPa, but pCO_2 remained fairly constant with a maximum of 0.2 MPa.

These results are in accordance with the study on end product inhibition by Hansson [16]. Unlike CH_4, CO_2 should be considered both an intermediate and end product in anaerobic digestion, since it is both produced and consumed in various relevant reactions. Therefore, the aim of this study was to evaluate the effect of autogenerated biogas pressure (0.1-2.0 MPa) on the kinetics of volatile fatty acids (VFA) conversion into CH_4 and CO_2. To do so, 10 high pressure experiments were performed in 3 AHPD reactors from which the effect of autogeneration of biogas pressure (0.1-2.0 MPa) was evaluated.

4.2 Material and methods

4.2.1 Biomass

The granular sludge used as inoculum was obtained from a full-scale mesophilic Expanded Granular Sludge Bed (EGSB) treating fruit processing waste water (pH 7.0,

30°C) at FrieslandCampina Riedel B.V. (Ede, The Netherlands). Wet sludge was obtained through a 0.5 mm sieve. After sieving, average total suspended solids (TSS) and volatile suspended solids (VSS) contents were 96 and 90 g L^{-1}, respectively. The pH was 6.5 and alkalinity measured 5 meq kg^{-1} VSS.

4.2.2 Experimental set-up

All experiments were conducted in 3 batch-fed AHPD pressure reactors, with a similar setup as shown in Figure 2-1B (Parr 910908, Moline, USA). These were closed stainless steel vessels with a total volume of 0.6 L. The impeller velocity was set at 60 rpm. The temperature (30 ºC) was controlled with a water bath (Julabo, Seelbach, Germany). All reactors were equipped with temperature, pH and pressure sensors connected to a field point module for data acquisition; on-line measurements were displayed in a computer with the software Labview 7.1 (National Instruments, Austin, USA).

4.2.3 Batch experiments

The effect of pressure was evaluated in 10 batch experiments in the AHPD vessels, which are summarised in Table 4-1. The experiments were carried out with either acetate (C2) as substrate or with a mixture of volatile fatty acids (VFA) in the following proportions (expressed as chemical oxygen demand (COD): acetate (50%), propionate (25 %) and butyrate (25 %). These substrates were fed as sodium acetate trihydrate ($CH_3COONa \cdot 3H_2O$) or as solutions of propionic acid and butyric acid neutralised to pH 7 with NaOH. In all cases, the liquid and gas volumes were 0.5 L and 0.1 L, respectively. Initial substrate concentrations ranged between 1 and 10 g COD L^{-1} (1, 2.5, 5 and 10 in Table 4-1). Assuming 100 % COD conversion, these values correspond to expected pressure (90 % CH_4 / 10 % CO_2) increases ranging from 0.1 to 2.0 MPa (P1, P5, P10 and P20 in Table 4-1). One of the experiments (P10) was repeated, to assess the variability of the results between experimental runs. To compare the results, 2 ambient pressure batch experiments were performed having the same liquid composition, but operated with a larger head space.

Each experiment was started by filling the reactors with 0.5 L of solution containing the substrate VFA (1-10 g COD L^{-1}), the corresponding amount of granular sludge to get a substrate/biomass ratio of 0.5 g COD g^{-1} VSS , macronutrients, trace elements

and yeast (Table 2-1).The reactors were then flushed with nitrogen gas (99.9 % N_2) and sealed. Process evolution was followed by on-line monitoring of pressure, pH and temperature, and daily measurement of gas composition. Liquid samples were periodically taken to analyse VFA contents in the liquid phase.

Endogenic sludge respiration in absence of added substrate was measured at atmospheric pressure in the AHPD vessels during 5 days. Methane production in all experiments was corrected for this endogenic respiration.

Table 4-1: Overview of volatile fatty acid experiments

Experiment	Trial	Substrate (g COD L^{-1})	Substrate/incoculum (g VSS L^{-1})
High Pressure Acetate (C2):	P1	1	2
100 % Acetate ($NaCH_3COO \cdot 3\ H_2O$)	P5	2.5	5
	P10	5	10
	P20	10	20
Reference Pressure Acetate	P0	1	2
High Pressure VFA (C2-C4):	P1	1	2
50 % COD Acetate ($NaCH_3COO \cdot 3\ H_2O$)	P5	2.5	5
25 % COD Propionate	P10	5	10
25 % COD Butyrate	P20	10	20
Reference Pressure VFA	P0	1	2

The specific methanogenic activity (SMA) was determined by pressure increase following the method of calculation of Zandvoort, Osuna, Geerts, Lettinga and Lens [58]. The online pressure sensor in the high pressure reactor allowed us to follow pressure increase every minute. Based on the total pressure and the gas composition, the partial pressures for CH_4 and CO_2 were derived. Sufficient sample to measure dissolved CH_4 without influencing an experiment could only be retrieved from the liquid phase after decompression at the end of each experiment. By using the ideal gas law, the total molar production of CH_4 was calculated based on the method described

in chapter 3 values were corrected for proportionally higher solubility at increasing pressures during the experiment.

4.2.4 Analytical methods

TSS, VSS, pH and alkalinity were determined according to Standard Methods [57]. Gas composition (CH_4, CO_2, N_2, O_2) was determined by gas chromatography (Shimadzu GC-2010, Kyoto, Japan). The gas sample was directed over the same two columns described in chapter 2.

Hydrogen was measured with a HP 5890A gas Chromatograph (Hewlett Packard 5890A, Palo Alto, USA). 100 mL of gas-sample was directed over a molsieve column (30m x 0.53mm x 0.25mm), using argon as carrier gas. The oven temperature, injection port and TCD were 40˚C, 110˚C and 150˚C, respectively.

Volatile Fatty Acids samples were prepared and analysed as described in chapter 2.

4.3 Results and discussion

4.3.1 Autogeneration of biogas pressure

Pressure build-up resulting from biogas generation during batch experiments with acetate and VFA mixtures is shown in Figure 4-1 a and b. The rate of pressure build-up increased from experiment P1 to P20. However, the time for complete COD_{VFA} conversion into COD_{CH4} increased for P1 to P20 from 2 to 7 days, indicating lower overall conversion rates had been obtained at higher loading rates.

With acetate, the COD-balance based on recoveries from the gas phase were only between 66 and 74 % for P1, P5, P10 and P20. With VFA, the recoveries from the gas phase were between 67 - 82 %. For all P5-P20 experiments, 3 ± 1 mmol COD more CH_4 was present in the liquid phase than theoretically expected. Visual comparison between pressurised (up to 0.5 MPa) and atmospheric pressure glass bottles learnt that a part of the formed gas bubbles were attached to the partially disrupted granules, neither being part of the gas phase nor being dissolved in the liquid phase. After

including the end-measurement of the dissolved CH_4, retrieved COD-values increased to 85-95 % for all experiments.

(a)

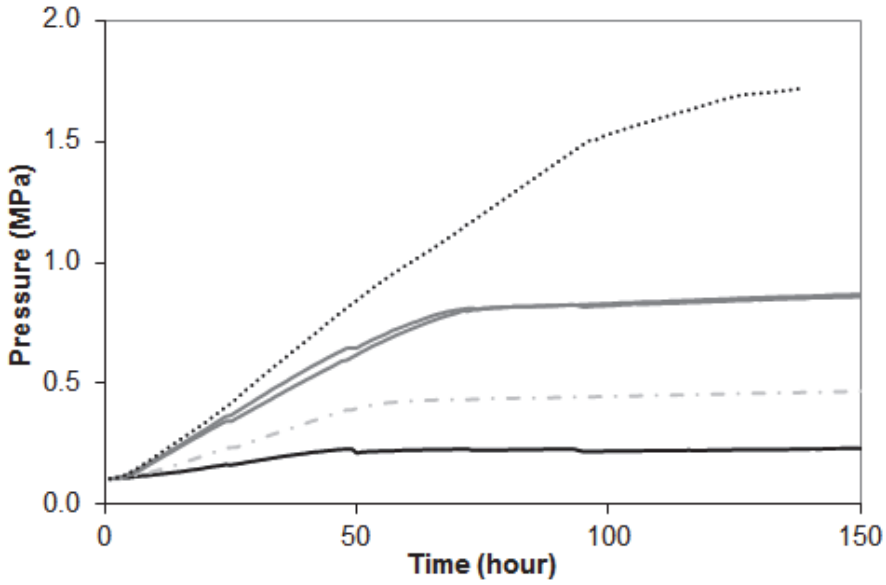

(b)

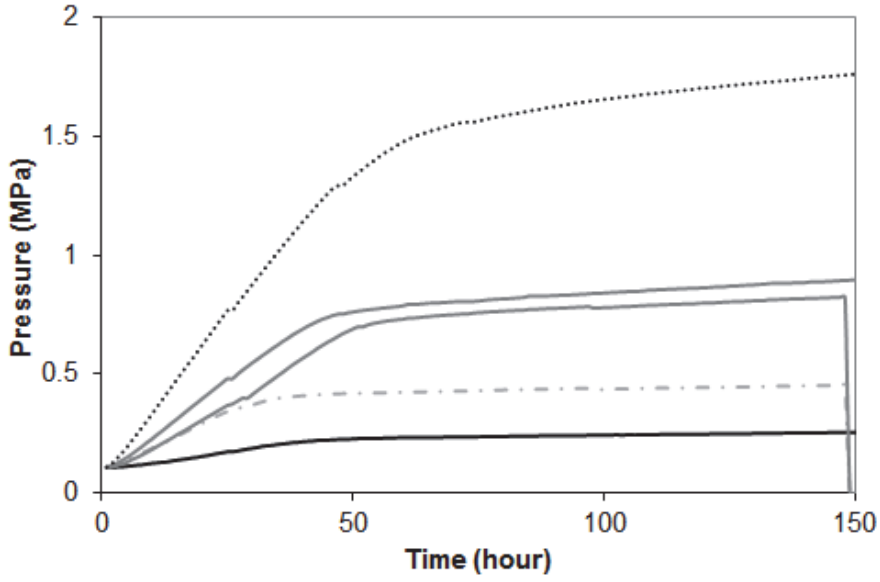

Figure 4-1: Pressure build-up in batch experiments with a concentration of (a) acetate and (b) VFA (acetate, propionate and butyrate) for experiments P1 (black line), P5 (- - -), P10 and P10rep (grey line) and P20 (black dotted line). Notice that P10 was replicated to assess the variability between experiments.

The highest pressure (1.72 MPa) using acetate was obtained in the P20 experiment, followed by P10 (0.87 MPa), P5 (0.47 MPa) and P1 (0.24 MPa). With VFA, the highest pressure was obtained with P20 (1.78 MPa), followed by P10 (0.90 MPa), P5 (0.45 MPa) and P1 (0.26 MPa). The pressure build-up in this study is the highest ever reported in the literature [17-19], except for, the results presented in chapter 2 and 3 (Table1-2).

4.3.2 Biogas composition

A main goal of the AHPD concept is to produce and upgrade biogas to the quality of highly demanding applications in a single step reactor system. In this study the CH_4 content of the gas phase always exceeded 91 % (Figure 4-2) and the CO_2 content varied between 5 - 9 %. This showed that direct injection into the Dutch natural gas grid, based on the regulation for CH_4 and CO_2, is theoretically feasible [83]. The acetate digestions had an average content of 94 ± 1% CH_4; and the VFA digestions 93 ± 1% CH_4. The remainder gas consisted of CO_2. Ambient pressure experiments gave biogas compositions of on average 90 and 88 % CH_4 content at an end pH~8 when using acetate and VFA as substrate, respectively. From Figure 4-2 it can be seen that biogas composition is initially improving up till 0.5 MPa, whereas between 1.0 and 2.0 MPa biogas composition seems no longer affected by pressure.

(a)

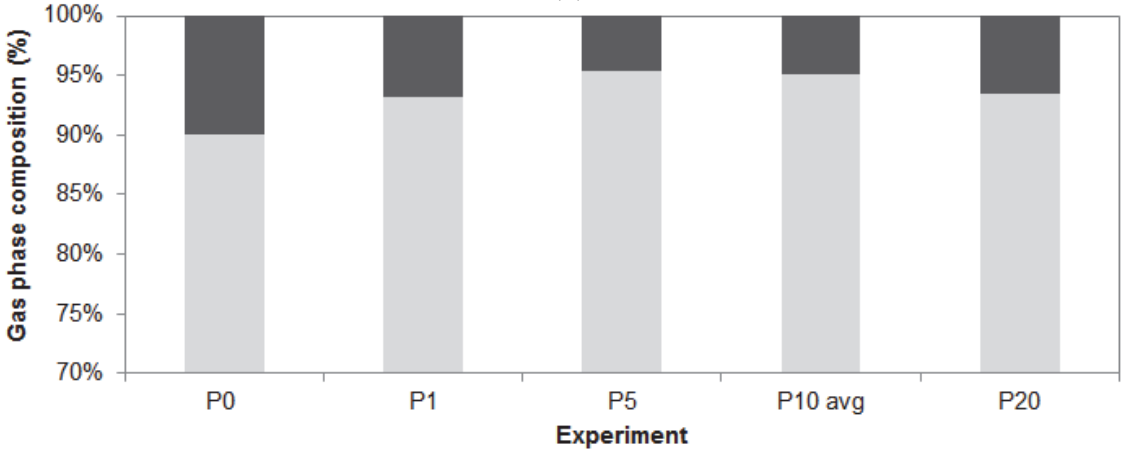

(b)

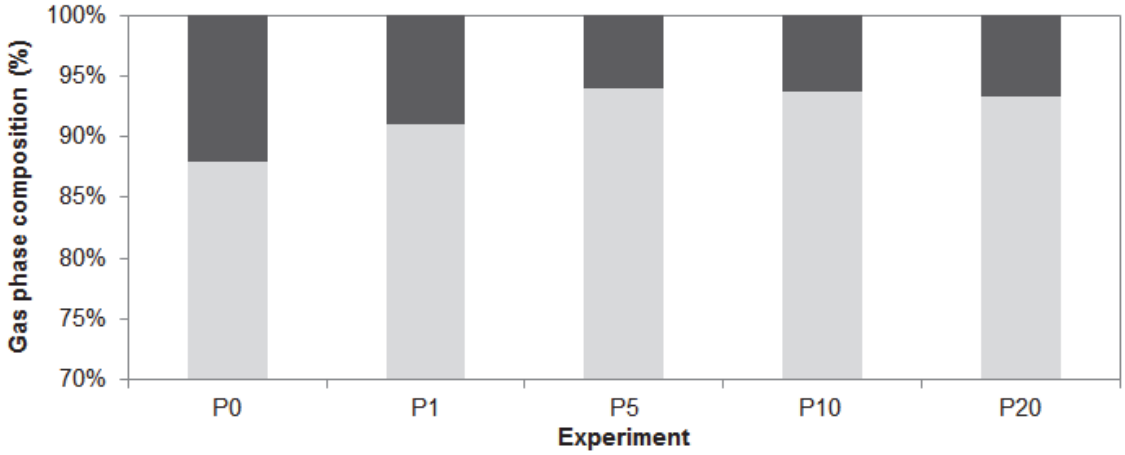

(c)

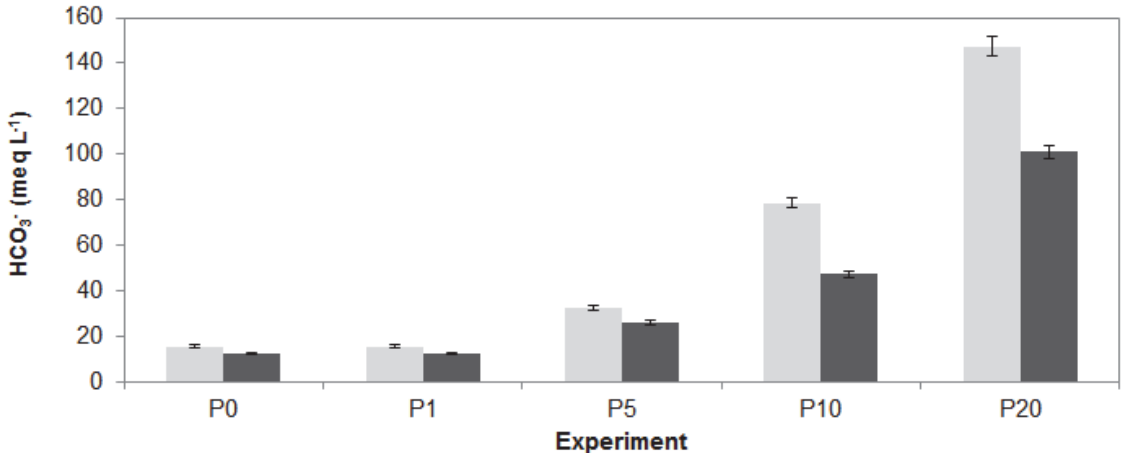

Figure 4-2: Overview of CH_4 (grey) and CO_2 (black) composition for different experiments (a) acetate (b) VFA (acetate, propionate and butyrate) and (c) HCO_3^- concentration of acetate (grey) and mix VFA (black) experiments.

The CH_4 content in biogas is in accordance with the findings in chapter 2 and 3 with 89-96 % CH_4. Hayes [17] obtained 93 % CH_4 in a fixed-film reactor with CO_2 stripping at 0.3 MPa when VFA were used as substrate and 59 % CH_4 when glucose was used instead. With complex substrates like activated sludge and swine slurry, 58-65 % CH_4 was observed at 0.1-0.4 MPa [18, 19].

From the Buswell equation the molar ratio of CH_4 to CO_2 was calculated for both substrates (acetate and VFA). The ratio CH_4: CO_2 is 1:1 for acetate, 1.625:1.375 for propionate and 2.5:1.5 for butyrate. From the final biogas composition the original stoichiometry is no longer visible due to the higher solubility of CO_2. Figure 4-2c

shows that lower concentrations of HCO_3^- were formed in the liquid phase to sequester CO_2 in the VFA experiments than in the acetate experiments. This clearly indicated that Henry's law and the carbonate equilibrium can be used to control the biogas quality dependent on quantity and oxidation state of the added substrate.

These findings correspond to our earlier findings in which we showed that CO_2-content of the biogas is dependent on the ratio between Acid Neutralising Capacity (ANC) and Total Inorganic Carbon ratio. Thus, by using more reduced substrates than acetate the ANC requirement can be significantly reduced, without compromising on the biogas quality.

4.3.3 Acetate, propionate and butyrate conversion

Within the range of 0.2 to 1.8 MPa almost complete conversion of the substrate COD_{VFA} into COD_{CH4} was obtained, as indicated by COD mass balances between 85-95 % without taking biological growth into account. The SMA decreased from atmospheric pressure by 18 % for P5 and by 56 % for P20 in the acetate experiment; while it was not reduced P5 and by 46 % for P20 in the VFA experiment. When comparing Figure 4-3a and b, the actual SMA of the elevated pressure experiments was significantly underestimated when using only gas phase measurements, according to standard SMA procedures [84]. By correcting the SMA for the rate of increase of dissolved CH_4 observed maximum SMA values increased by ~10-20 %. The values could not be corrected properly for the underestimation of CH_4-production based on the retrieved liquid CH_4 bubbles in the end measurement. It is worth mentioning that the SMA decrease may also be attributed to another required modification of the SMA protocol [84], since increased concentrations of substrate and inoculum with respect to the standard conditions were needed to increase the pressure build-up in treatments P5-P20.

Likewise, for both propionate and butyrate, a decreasing specific substrate utilisation rate with final pressure was measured from the liquid concentrations. Propionate rates were 0.10, 0.10, 0.06, 0.05, 0.05 $gCOD_{CH4}\ g^{-1}$ VSS d^{-1} and butyrate rates were 0.10, 0.09, 0.06, 0.05 and 0.05 for experiments P0, P1, P5, P10 and P20, respectively. This

is a maximum reduction in rates of about ~50 %. For comparison, overall acetate degradation rates were found to be 0.23, 0.23, 0.19, 0.17 and 0.11 gCOD g^{-1} VSS d^{-1} for P0. P1, P5, P10 and P20. Estimated K_s and K_i parameters for propionate inhibition from continuous flow reactors show wide variation, but generally are in the order of 20 mg L^{-1} and 20 mg HPr L^{-1} [85]. Given the fact that the inoculum was taken from a continuous-flow reactor, with very low bulk VFA concentrations, 250 mg COD L^{-1} could already have been sufficient to exceed the bulk concentration for which the maximum substrate utilisation rate can be found. Another possibility, is that the inoculum contained a relatively large inactive fraction of inactive volatile suspended solids and a minor fraction of active micro-organisms.

Generally, butyrate is converted into acetate (and hydrogen) and then via acetotrophic methanogenesis into CH_4 and CO_2. Propionate is generally converted into acetate, H_2 and HCO_3^- [86, 87]. Latter intermediates act as substrate for either hydrogenotrophic methanogens or homoacetogenic bacteria, impacting the pathway towards CH_4 via competition on hydrogen and bicarbonate [88]. Figure 4-4 shows that independent of the desired end pressure, the CH_4 production rate in the experiment with VFA always exceeded the CH_4-production rate of the acetate experiments. Like CH_4 and CO_2, also hydrogen may accumulate in a AHPD reactor. However, hydrogen partial pressure could not be detected above the detection limit of 60 Pa. Clearly a hydrogen consuming population was present and interspecies hydrogen transfer took place [28]. Based on thermodynamic and kinetic parameters reported by Kotsyurbenko [51] and Conrad and Wetter [87], it is considered unlikely that homoacetogens can outcompete hydrogenotrophic methanogens below a pH_2 of 60 Pa. Moreover, if hydrogen would have been used for the production of acetate, all CH_4 should have been produced by acetotrophic methanogens. Since it is assumed that the initial population was of equal size, equal CH_4 -production rates as observed for the acetate experiments were expected. Thus, it can be concluded that hydrogenotrophic methanogens are capable of increasing the overall methanogenic activity for VFA conversion under AHPD conditions.

(a)

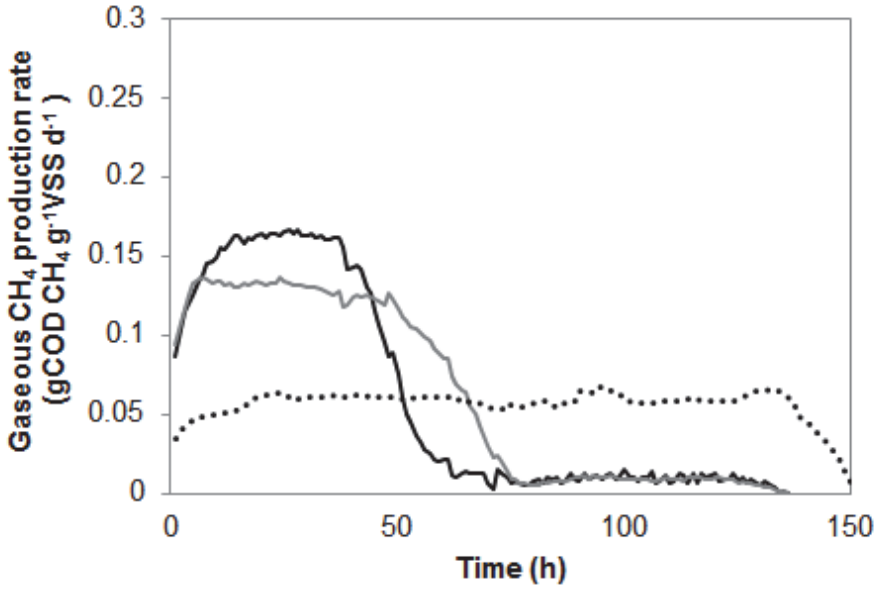

(b)

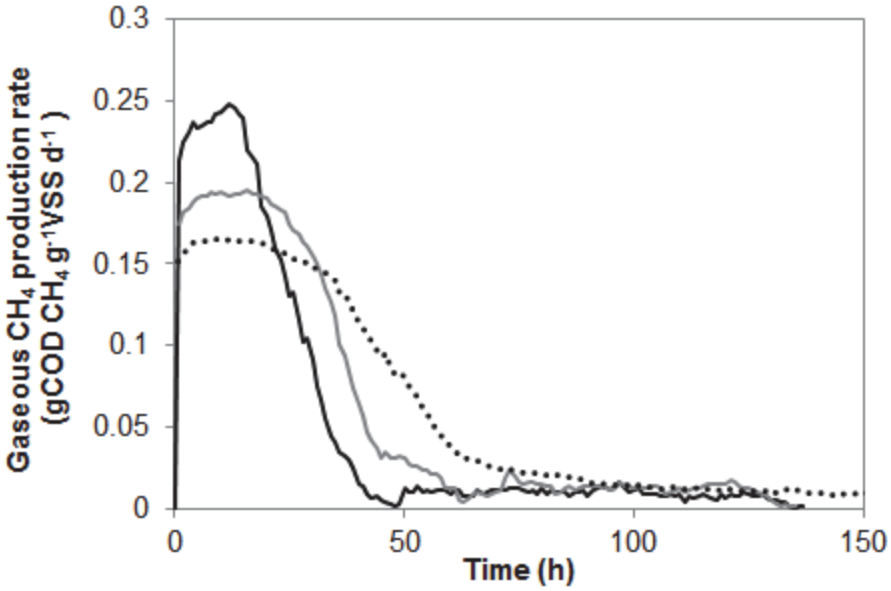

Figure 4-3: Gaseous CH_4 production rate (excluding dissolved CH_4) for experiments P5 (black line), P10 (grey line) and P20 (black dotted line) for (a) the acetate experiments and (b) the VFA-mixture experiments.

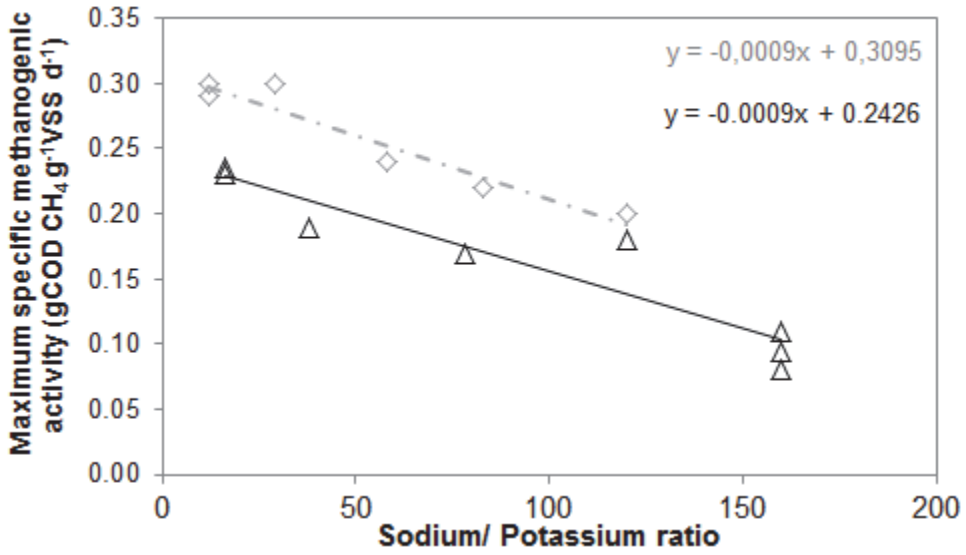

Figure 4-4: Maximum measured specific methanogenic activity (SMA) during batch experiments against the Sodium: Potassium ratio with VFA (◊) and acetate (Δ)

4.3.4 Inhibitory effects

Acetate, propionate and butyrate all showed decreased substrate utilisation rates with increasing final pressure. For propionate and butyrate, hydrogen accumulation would be a logical explanation for decreased conversion rates at higher pressures. Because H_2 was not detected above the detection limit of 30 ppm or 60 Pa at a total pressure of 2.0 MPa, inhibition by H_2 is unlikely. Especially, because both butyrate and propionate showed an equal reduction in conversion rates, and according to the thermodynamics butyrate conversion is significantly less sensitive to hydrogen accumulation. On the other hand, 60 Pa is well over the inhibiting values reported for the syntrophic conversion of propionate[28]. And thus the role of hydrogen accumulation in the observed reduced rates of propionate and butyrate can not be excluded completely.

Based on Hansson [16] it can also be speculated that accumulating pCO_2 could cause an end-product inhibition in the conversion of acetate and propionate. But since CO_2 is not involved in the butyrate pathway, end-product inhibition cannot explain the decreased butyrate conversion rates. Furthermore, in all the experiments the gas phase was flushed with pN_2 and thus initial pCO_2 was 0.00 MPa and then increased to a maximum of 0.10 MPa in the P20 experiment. Also, as can be observed from the SMA

over time in Figure 4-3b, the very constant nature of the inhibition from the beginning until the end of the experiment makes it more plausible that the lower rates were caused by inhibition from the liquid phase. Although an inhibitory effect of the VFA-concentration is likely at the chosen concentrations, an increase of SMA was expected to be clearly visible because of substrate and VFA depletion. Likewise, the very stable rate in the acetate experiment is difficult to explain if inhibition would have been solely caused by VFA (Figure 4-3). However, concomittant with the substrate concentrations also the sodium concentrations increased with increasing final pressure with maximum values of 2.7 and 3.5 g L^{-1} in the P20 experiment for VFA and acetate, respectively. In various researches these values are close to the reported 50 % inhibition value due to toxicity of Na^+ [89-91]. However, other studies showed much higher tolerance for Na^+ [90, 92, 93]. It should be realised that our inoculum was not used to high sodium levels in the full-scale treatment plant; it was mainly selected because it was naturally poor in mineral precipitates. Furthermore, potassium phosphate was minimised to a relatively low concentration of 1 mmol $NaKHPO_4^-$ L^{-1} to prevent phosphate from influencing the carbonate equilibrium. Because it was the only source of potassium, and by keeping the medium constant, the ratio between Na^+ :K^+ was increased substantially with estimated final pressure by Na-acetate, propionate and butyrate additions. With an increasing Na^+ :K^+ -ratio of 16, 38, 78 and 160 for respectively P1, P5, P10 and P20 dissapearance of the antagonistic effect as seems plausible [89, 90]. By plotting the maximum SMA versus the Na:K ratio this hypothesis is further supported with a R^2 >0.95 (Figure 4-3). The rates in the VFA experiments were affected less compared to acetate as sole substrate, which could be related to the lower Na^+/K^+ ratio i.e. 12, 29, 58 and 120, for P1, P5, P10 and P20, respectively,. Therefore, we postulate that the substrate and especially the required cations have influenced AHPD conversion rates in batch more than end-product inhibition.

4.3.5 Practical applicability

Obviously, in practice AHPD would have to be used to treat more complex organic waste streams than synthetic VFA-based (waste-)water. Based on complex substrates

however, an initial hydrogen fermentation in a two-stage approach[94] might provide a practical opportunity to control VFA and hydrogen input into a second “high pressure” methanogenic phase. Likewise, major cations, NH_4^+, K^+, Mg^{2+}, Ca^{2+}, Na^+, will be naturally present in real waste waters. If present in insufficient quantity, selecting a cation mixture that takes the synergistic and antagonistic effects of individual cations into account is advised. One could choose mafic silicate minerals as is decribed in chapter 5, but the work of Michalska, Miazek, Krzystek and Ledakowicz [95] shows furthermore that addition of Fe^{2+}/Fe^{3+} could not only serve as an alternative cation source, but could improve the hydrolysis of more complex lignocellulosic material like Sorghum, Sida or Miscanthus in the presence of hydrogen peroxide. Therefore, in order to increase the overall biogas production or quality, combinations of different novel anaerobic digestion approaches are required [96].

4.4 Concluding remarks

Under Autogenerative High Pressure Digestion conditions, both acetotrophic and hydrogenotrophic activity was observed. Maximum conversion rates up to a pressure of 2.0 MPa decreased by approximately 50% for acetate, propionate and butyrate. Because the observed inhibition occurred already from the beginning of each experiment at relatively low pressures with increasing substrate concentrations, end product inhibition in this early stage of the batch is considered unlikely. Owing to substrate neutralisation, Na^+/K^+ ratios also strongly increased with increasing pressure. Reduced SMA values are therefore attributed to substrate inhibition and cation requirement rather than to accumulated pressure and end-product inhibition.

Chapter 5

CO_2-scavenging Minerals

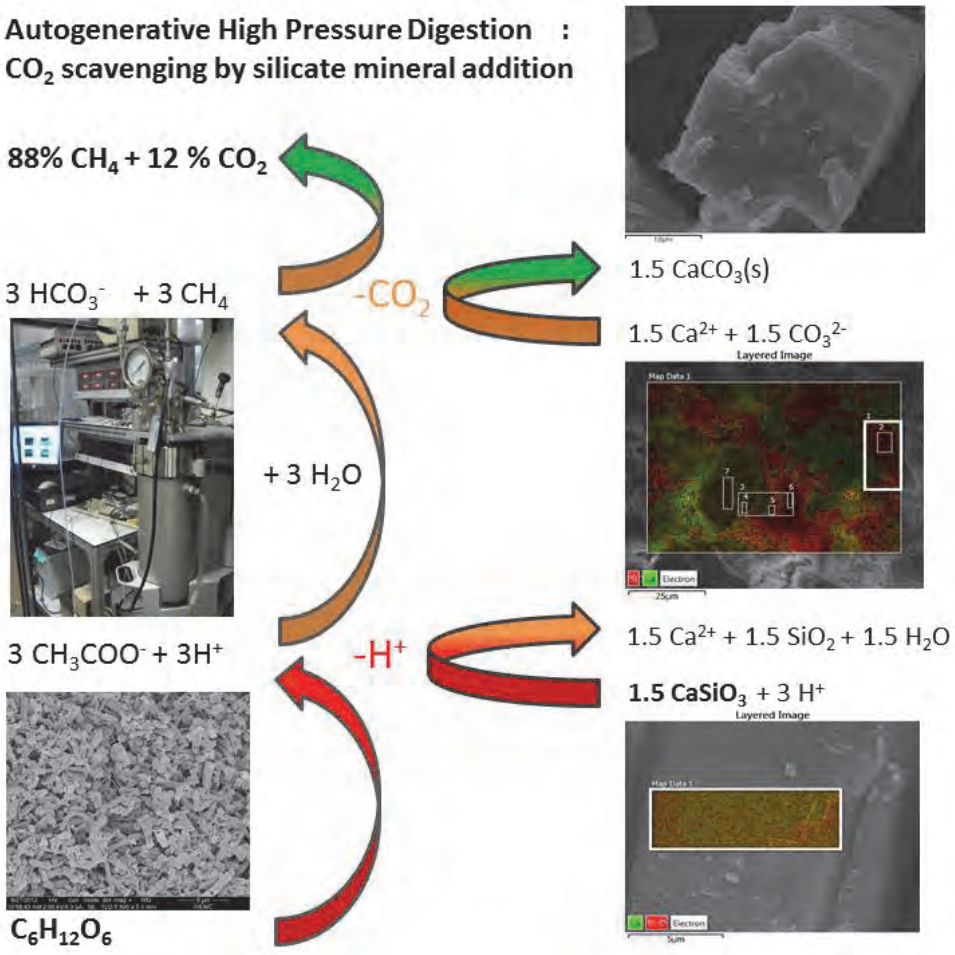

5 Silicate minerals for CO_2 scavenging in pressure digesters

Abstract

Accumulation of CO_2 and fatty acids resulting from digestion of glucose under Autogenerative High Pressure conditions may result in pH 3-5, which is unsuitable for high-rate methanogenic processes. Therefore, the use of wollastonite, olivine and anorthosite, with measured composition of $CaSi_{1.05}O_{3.4}$, $Mg_2Fe_{0.2}Ni_{0.01}Si_{1.2}O_{5.3}$ and $Na_{0.7}Ca_1K_{0.1}Mg_{0.1}Fe_{0.15}$ $Al_{3.1}Si_4O_{24}$, was studied to scavenge CO_2 during batch AHPD of glucose. Depending on the glucose to mineral ratio the pH increased to 6.0-7.5. Experiments with wollastonite showed that Ca^{2+}-leaching was caused by volatile fatty acid (VFA) production during glucose digestion. At 0.10, 0.30 and 0.90 MPa, the CH_4-content reached 74 %, 86 % and 88 %, respectively, which indicated CO_2 scavenging. Fixation of produced CO_2 by $CaCO_3$ precipitation in the sludge was confirmed by Fourier Transferred-InfraRed, Combined Field-emission Scanning Electron Microscopy-Energy-dispersive X-ray spectroscopy and Thermo-gravimetric Analysis-Mass Spectroscopy.

Keywords

acid neutralising capacity, anaerobic digestion, biogas upgrading, mineral carbonation, high pressure, weathering.

This chapter is based on

Lindeboom, R.E.F., Ferrer I., Weijma, J. & van Lier J.B., Silicate minerals for CO_2 scavenging from biogas in Autogenerative High Pressure Digestion, Water Research **47**, 3742-3751 (2013).

5.1 Introduction

As reported by the International Energy Agency [4], corrosion, condensation of water and reduced calorific value are main reasons why H_2S, NH_3, CO_2 and H_2O should be removed in order to use biogas as a substitute for natural gas. The biogas composition depends on the average oxidation state of the carbonaceous substrate, as well as the degree of substrate pre-acidification and the presence of alternative electron acceptors, such as SO_4^{2-} and NO_3^- [24, 97]. Due to fluctuations in waste water composition, biogas composition can strongly vary over time and robust upgrading systems are required, adjusted to these quality fluctuations. Conventional methods such as pressure swing adsorption or gas-selective membranes can be used, but these are only cost-effective at biogas flows above 100 $m^3 h^{-1}$ [9].

In previous chapters, autogenerative high pressure digestion (AHPD) was studied to produce high quality pressurised biogas in a single reactor system by integrating biogas upgrading and storage into an anaerobic digester. By sealing the gas phase the produced biogas auto generated biogas pressures up to 9.0 MPa and can be used directly (1) to separate CO_2 and CH_4 based on Henry's constants of 0.31 mol L^{-1} MPa^{-1} and 0.016 mol L^{-1} MPa^{-1},(2) to dry the biogas based on the Clausius Clapeyron equation and (3) to exclude membrane pumps in AnMBR setups (chapter 3). In practice, CH_4 losses up to 20 % have been reported for external upgrading, transport and storage of biogas altogether [98]. Therefore, on top of offering the above mentioned advantages, AHPD could also reduce potential losses during transport, storage and upgrading of biogas, because production, upgrading and storage are performed in a single step bioreactor.

Although 9.0 MPa biogas pressure can be produced, reactor costs and CH_4-dissolution would offset all potential benefits. However, experiments performed at moderate pressures (~0.5-1.0 MPa), thereby reducing reactor costs and CH_4-dissolution to a minimum, showed that the potential benefits could be maintained (chapters 3, 4 and 5) . However, under these economically more attractive conditions control of the carbonate equilibrium and acid neutralising capacity (ANC) is a prerequisite to

maintain a proper pH for digestion (chapter 3). Conventional industrially produced bulk-chemicals like sodium hydroxide (NaOH), sodium carbonate (Na_2CO_3) or quicklime (CaO) could provide the required ANC. However, these are produced by the energy-intensive chloralkali, solvay and $CaCO_3$ thermal decomposition processes, respectively. Combined with the required transport, and safety requirements, this potentially offsets the environmental benefits of local biogas upgrading in remote areas. Lackner, Wendt, Butt, Joyce and Sharp [99] and Schuiling and Krijgsman [100] explored natural minerals for their potential for CO_2 sequestration in industrial processes. Moreover, for minerals such as wollastonite ($CaSiO_3$) and olivine ($Mg_{1.8}Fe_{0.2}SiO_4$) and large alkaline waste streams such as steel slags, cost estimates for the total mineral carbonation process are 50-100€/ ton avoided CO_2 [101, 102]. Based on the current market price and assuming 100% reactivity however, one could expect 400-700€/ton CO_2 avoided for NaOH and Na_2CO_3 and 50 – 150 € / ton avoided for CaO [103]. Although quicklime, has a comparable current market price to silicate minerals, the thermal decomposition of $CaCO_3$ intrinsically emits 1 mol of CO_2 per mol of CaO on top of the heat demand of > 850^oC [104] .

So, assuming reactions rates are compatible with anaerobic digestion rates, a wide range of alternatives can be selected for adding ANC in AHPD, but also in conventional anaerobic digestion, nitrogen removal, desulfurisation and bioelectrochemical systems [105]. The rate and degree to which silicate minerals react is dependent on the mineral stability[65]. This is a function of, amongst others, the cation to silicate ratio and the mineral structure (mainly characterised by the Si:O ratio). Wollastonite carbonation is an exothermic process with ΔHr of -87 kJ/mol [106, 107], not requiring external heat input. Silicate minerals (like wollastonite, $CaSiO_3$) that are exposed to acid react according to the reaction equations described earlier:

$$CaSiO_3\,(s) + 2\,H^+\,(aq) \rightarrow Ca^{2+}\,(aq) + SiO_2\,(s) + H_2O \qquad \textbf{(Eq. 1-15)}$$

The required H^+ in this reaction could be provided by undissociated fatty acids, produced for example during typical anaerobic glucose digestion [27].

$$C_6H_{12}O_6\ (s) + 2H_2O \rightarrow 2\ CH_3COO^- + 2H^+ + 4H_2 + 2CO_2 \quad \textbf{(Eq. 1-5)}$$

Due to the H^+ consuming reaction, accumulating fatty acids may dissociate, meanwhile maintaining an optimal pH (6-8) for methanogens in AHPD reactors. Besides, an increasing pH also shifts the carbonate equilibrium towards HCO_3^- and CO_3^{2-}, possibly resulting in the precipitation of secondary carbonates.

$$Ca^{2+}\ (aq) + CO_3^{2-}\ (aq) \rightarrow CaCO_3\ (s) \quad \textbf{(Eq. 1-16)}$$

So, on top of HCO_3^- formation a mechanism to store produced CO_2 as solids is introduced. In AHPD, this is particularly relevant at lower ratios between ANC and produced CO_2 when the calorific value of the produced biogas is becoming diluted as was shown in chapter 3.

From a perspective of CO_2-valorisation, it is noteworthy that calcium carbonate can precipitate in 6 different forms, all having different characteristics. Amorphous calcium carbonate (ACC), hexahydrate calcium carbonate (HCC), monohydrate calcium carbonate (MCC) and the polymorphs vaterite, aragonite and calcite have respective pK_{sp} values at 25°C of 6.28, 6.59, 7.15, 7.91 ± 0.02, 8.34 ± 0.02 and 8.48 ± 0.02 [108]. It is therefore essential to realise, that bacteria and archaea induce precipitation by altering intra- and extracellular conditions and can thus influence the type of calcium carbonate formation.

The influence of anaerobic digestion conditions on $CaCO_3$ precipitation at atmospheric pressure is already widely studied [75, 109-111]. Deviations from pK_{sp} of calcite and aragonite in water have been reported as a consequence of the complex biological liquid composition [111, 112]. The sole presence of PO_4^{3-} is reported to alter the pK_{sp} from 8.4 to 6.5 due to inhibition of calcite formation from amorphous calcium carbonate [111].

The aim of this chapter is to demonstrate the feasibility of using various silicate minerals, wollastonite (W), olivine (O) and anorthosite (A) for buffering the reactor pH in autogenerative high pressure digestion. Additionally, dissolution of wollastonite

under AHPD conditions was studied, thereby focussing on the secondary precipitation of $CaCO_3$, the role of fatty acid intermediates and the CO_2 content of the biogas.

5.2 Materials and methods

5.2.1 Reactors

For AHPD experiments three pressure vessels with a total volume of 0.6 L were used (Parr 910908, Moline, USA). The volume of the liquid phase was manually controlled at 0.5 L. The reactors were equipped with a heating cylinder (Julabo MP, Seelbach, Germany), an online pressure sensor (Ashcroft A-series 1000 PSI, Stratford USA), a high-pressure pH probe (Prosense serial nr. 34002/002, Oosterhout, The Netherlands), a PT-100 temperature sensor, similar to the set-up as described in chapter 3. Compact field point modules (cFP1804 and cFP-CB1, National Instruments, Austin, USA) functioned as receivers of data. Data was logged in Labview 7.1 (National Instruments, Austin, USA). Mixing was provided at 60 rpm by two three-bladed impellors attached to a central shaft. Temperature was maintained at 30 ºC. Glass bottles were used as batch reactors for atmospheric reference experiments to acquire insights in the end pH with and without minerals. The liquid volume was set at 0.05 L. pH was monitored by taking liquid samples followed by measurement with a pH electrode. Batch experiments were carried out in a 30^{o}C controlled room and centrally shaken.

5.2.2 Operation

The reactors were inoculated with various concentrations of anaerobic granular sludge from a full-scale expanded granular sludge bed reactor treating waste water from a fruit-juice processing industry (FrieslandCampina Riedel B.V., Ede, The Netherlands). Liquid medium with trace elements and macronutrient solution was provided in concentrations as described in Table 2-1. An overview of the experiments including substrate concentration, mineral type and concentration, sludge concentration and targeted final pressure is presented in Table 5-1.

Table 5-1: Overview of silicate mineral experiments.

Exp. nr.		Mineral type*	Weight ($g\ L^{-1}$)	Glucose ($gCOD\ L^{-1}$)	Sludge ($gVSS\ L^{-1}$)	Liquid Volume (L)	Gas Volume (L)	Target pressure (MPa)
1	**A**	**W**	5.0	0.0	0.5	0.05	-	None
	B			2.5				
	C			5.0				
	D			10.0				
2	**A**	**O**	5.0	0.0	0.5	0.05	-	None
	B			2.5				
	C			5.0				
	D			10.0				
3	**A**	**A**	5.0	0.0	0.5	0.05	-	None
	B			2.5				
	C			5.0				
	D			10.0				
	E		4.0	1.0	20.0	0.5		
4	**A**		-	0.0	0.5	0.25	-	None
	B			1.0	2.0			
	C			2.5	0.5			
	D			5.0	0.5			
5		**W**	0.92	1.0	2	0.50	0.67	~0.1
6[#]		**W**	0.92	1.0	2	0.50	0.10	0.2-0.4
7[#]		**W**	4.56	5.0	10	0.50	0.10	0.9-1.1

*** W=wollastonite, O=olivine and A=anorthosite # wide target pressure range due to uncertainty on CO_2 sequestration**

Experiments 1 to 3 aimed to clarify the effect of the cation to silicate ratio of different minerals (W, O, A) on the pH under increasing biological acidifying conditions. Thus, experiments 1-3 A, B, C and D were fed with 0, 2.5, 5.0 and 10.0 g COD glucose L^{-1}, respectively. In experiments 1-3 only low amounts of sludge (0.5 g VSS L^{-1}) were used in order to minimize the impact of the sludge on the pH. Equal amounts of the minerals wollastonite (Casiflux G20 Ankerpoort BV, The Netherlands), olivine (Greensand, B.V., The Netherlands) and anorthosite (crude rock, Nordic Mining, Norway) were added (5 g L^{-1}). Anorthosite ($Na_xCa_yAl_2Si_2O_8$) was grinded and sieved to acquire powder with a particle size (volume based mean ~20 μm) like the particle size of wollastonite ($CaSiO_3$) and olivine ($Mg_{1.8}Fe_{0.2}SiO_4$). However, based on the

relatively low Ca^{2+} or Mg^{2+} to silicate ratio in anorthosite, and the observed lower reactivity, it was decided to perform experiment 3E using 4.0 g anorthosite L^{-1} and 1.0 g COD glucose L^{-1}. Experiments 4 (A, B, C and D) were performed as a reference without mineral addition, using concentrations of 0.0, 1.0, 2.5 and 5.0 g COD glucose L^{-1}.

Experiments 5 to 7 aimed to acquire more detailed insights into the leaching and secondary calcium carbonate precipitation mechanisms. The initial amount of wollastonite was stoichiometrically sufficient to neutralise (according to equation 1-15) 3 eq H^+ per mol of glucose. Experiments 5 and 6 were operated at equal conditions, but to alter the pressure increase a gas volume of 0.67 and 0.1 L were used, respectively. Experiment 7 was supplemented with 5.0 g COD glucose L^{-1}, 10 g VSS L^{-1} and 4.56 g $CaSiO_3$ L^{-1} to reach a pressure around 1.0 MPa.

5.2.3 Analyses

Total Suspended Solids (TSS) and Volatile Suspended Solids (VSS) were determined according to Standard Methods 2540 [57].

Gas sampling and CH_4 and CO_2 analysis was done as described previously. The biogas composition was corrected for flush gas (N_2) and water vapour and showed a standard deviation of less than 2%. Hydrogen was measured with a HP 5890A gas Chromatograph (Hewlett Packard 5890A, Palo Alto, USA). 100 mL of gas-sample was directed over a Molsieve column (30m x 0.53mm x 0.25mm), using argon as carrier gas. The oven temperature, injection port and TCD were 40˚C, 110˚C and 150˚C, respectively.

The specific methanogenic activity (SMA) was determined by the pressure increase following the calculation method described in chapter 2. From online total pressure measurements and the gas composition, the partial pressures for CH_4 and CO_2 were derived. Afterwards, by using the ideal gas law, the total molar production of CH_4 was calculated.

VFA samples were taken from the reactor daily. VFA were determined by means of a gas chromotograph (Hewlett Packard 5890 series II, Palo Alto, USA) with a flame ionisation detector. Sample preparation and the GC method were the same as described in chapter 3.

Dissolved Calcium was analysed with a Varian Vista-MPX (Varian, Australia) simultaneous inductively coupled plasma atomic emission spectroscopy (ICP-AES) system based on Standard Method 3120-B [57].

Particle size distribution was measured by laser diffraction analysis (Coulter LS230, Beckham Coulter, USA).

Samples for Field Emission Scanning Electron Microscopy analysis were centrifuged for 10 minutes at 5,000 rpm. Hereafter, supernatant was replaced by a 2.5 % glutaraldehyde solution for fixation during 1 hour. Afterwards samples were dried in a series of ethanol 50-75-90-95-100 % and then transferred to 100 % acetone. The samples were fixed to a brass sample holder with carbon adhesive tabs. Samples were coated by graphite sputtering. The Field Emission Scanning Electron Microscope (FESEM) (Fei Magellan, Hillsboro, USA) was connected to an Oxford INCA EDX (Oxford Instruments, Abingdon, UK) and operated between 10 and 20 kV. Scattered electrons and back scattered electrons were detected both in-lens and “under” lens at a distance of 15 mm.

For Thermogravimetric-Mass Spectroscopy analysis (TGA-MS) and Fourier Transformed-Infra Red scans (FTIR) solid samples from bioreactors were prepared by centrifugation for 5 min at 10,000 rpm. The supernatant was removed and the pellet was dried for 2 days in a desiccator. TGA-MS analyses were performed as described by Huijgen, Witkamp and Comans [34] using a thermal gravimetrical analysis system (Mettler-Toledo TGA/DTA 851e) coupled with a mass spectrometer (Pfeiffer, Thermostar). Around 20 mg of solid sample was put in aluminum oxide ceramic cups and heated under an air atmosphere at 40 $^{o}C\ min^{-1}$ from 25 to 1000 ^{o}C, while the evolved gas was analysed for CO_2 and H_2O by the MS. Two samples were prepared and analysed according to the above mentioned protocol: inoculum biomass (sludge

without added mineral) and a sample taken from the bioreactor at the end of experiment 7 (after 300 hours). An additional wollastonite sample was analysed as a reference; after drying in a desiccator centrifugation was not required.

For obtaining FT-IR spectra of the solid samples a Varian Scimitar 1000 FT-IR spectrometer (Varian, Australia) equipped with a DTSG-detector was used. The measurement resolution was set at 4−650 cm^{-1} for attenuated total reflectance (ATR). In total 64 scans were made. ATR was performed on a PIKE MIRacle ATR (Pike Technologies, Madison, USA) equipped with a diamond w/ZnSe lens single reflection plate. The sample chamber was purged by N_2 gas for 10 min before scanning was started. In the infrared spectrum, different bonds give peaks at specific wavelengths [113, 114]. A reference biological sample and a calcite sample were analysed. The attenuated infrared spectrum of wollastonite was obtained from RRUFF [115]. In the sample of experiment 4 the normalised peaks for the biological sample and wollastonite were deducted from the total sample profile. This processed profile was compared with the obtained calcium carbonate profile.

Particle surface area was measured by means of BET-analyses. Prior to the analysis samples were degassed for 2 hours with helium at 300^{o}C in a Smartprep 065 (Micromeritics, Norcross, USA). The BET-analysis was afterwards performed on a TriStar 3000 (Micromeritics, Norcross, USA) using nitrogen at a temperature of -196^{o}C. Data was acquired and analysed using TriStar software v 6.04. A linear fit to the BET-model had to have a correlation-coefficient of 0.9999. Samples were measured in triplicate.

5.3 Results

5.3.1 Characterisation of wollastonite, anorthosite and olivine

Table 5-2 shows the average elemental composition and particle morphology of the silicate minerals as determined by FESEM EDX mapping, and the mean particle size based on volume (%). It can be observed that wollastonite (W) samples only contained calcium and silicates, while olivine (O) and anorthosite (A) samples additionally contained magnesium, iron, nickel, potassium and aluminum.

Table 5-2: Overview of used mineral samples.

Mineral Name	EDX mean measured composition*	Mean Particle Size (µm)	Particle Morphology	Particle surface area (m^2 /g)
Wollastonite	$CaSi_{1.05}O_{3.4}$	18	Needle, well defined	1.8009 ± 0.0062
Olivine	$Mg_2Fe_{0.2}Ni_{0.01}Si_{1.2}O_{5.3}$	23	Rough undefined	6.2859 ± 0.0255
Anorthosite	$Na_{0.7}Ca_1K_{0.1}Mg_{0.1}$ $Fe_{0.15}Al_{3.1}Si_4O_{24}$	21	Rough undefined	1.0413 ± 0.0027

5.3.2 Buffering potential of silicates during digestion of glucose

The silicates wollastonite, anorthosite and olivine were tested for their buffering potential during glucose based biological acidification in experiments 1-4 (Table 5-3).

Table 5-3: Overview of final pH for the digestion of glucose in the presence of various minerals

Substrate (gCOD L^{-1})	Experiment 1 Wollastonite	Experiment 2 Olivine	Experiment 3 Anorthosite	Experiment 4 No mineral
0.0	8.5	8.1	7.9	7.7
1.0			6.4	4.6
2.5	7.8	7.3	4.3	4.2
5.0	7.2	5.0	3.9	3.8
10.0	5.5	4.8	3.4	

The initial pH (7.6) in the liquid remained stable in the blank experiment without any glucose and mineral addition (experiment 4 A). Upon the addition of 1.0, 2.5 and 5.0 g COD glucose L^{-1}, the pH dropped to 4.6, 4.4 and 3.8 ± 0.15 at the end of experiments 4 B, 4 C and 4 D, respectively. For addition of 5.0 g wollastonite L^{-1} (experiments 1 A, B, C and D), pH values of 8.5, 7.8, 7.2 and 5.5 ± 0.15 were found for 0.0, 2.5, 5.0 and 10.0 g COD glucose L^{-1}, respectively. For addition of 5.0 g olivine L^{-1} (experiments 2 A, B, C and D), these values were 8.1, 7.3, 5.0 and 4.8 ± 0.15. With 5.0 g anorthosite

L^{-1} (experiments 3 A, B, C and D), pH showed values of 7.9, 4.3, 3.9 and 3.4 ± 0.15. However, upon the addition of 4.0 g anorthosite L^{-1} and 1.0 g COD glucose L^{-1} (experiment 3 E), the pH stabilised at 6.4 ± 0.15.

5.3.3 Reactivity of wollastonite during AHPD of glucose

In order to elucidate the role and fate of added calcium silicates during AHPD of glucose, wollastonite (with calcium as only earth alkaline metal) was selected as model compound for further experiments (Table 5-1, experiments 5-7). Figure 5-1a shows the dissolved Ca^{2+} concentration during AHPD-experiments on glucose, with wollastonite reaching final pressures of 0.10 MPa (experiment 5), 0.30 MPa (experiment 6) and 1.00 MPa (experiment 7). Calcium contributed maximally 5, 7, and 32 meq L^{-1} to the charge balance of the reactor medium for experiments 5, 6 and 7, respectively. This corresponded to the dissolution of at least 68 %, 50 % and 42 % of the calcium in the added wollastonite. The standard deviation was 10% of the total value in meq L^{-1}. The pH reached minimum values of 5.5, 5.2 and 5.1 between 24 and 48 hours and an equilibrium pH at 6.8, 6.4, and 6.4, respectively (Figure 5-1b).

Furthermore, at atmospheric digestion (experiment 5) and at AHPD up to 0.3 MPa (experiment 6) the VFA concentrations remained below 2 meq L^{-1} (Figure 5-1b), whereas in experiment 7 acetate and propionate measured a maximum concentration of 4 and 25 meq L^{-1}, respectively (Figure 5-1 e and f). Butyrate, valerate and caproate were near or below detection limit for all experiments.

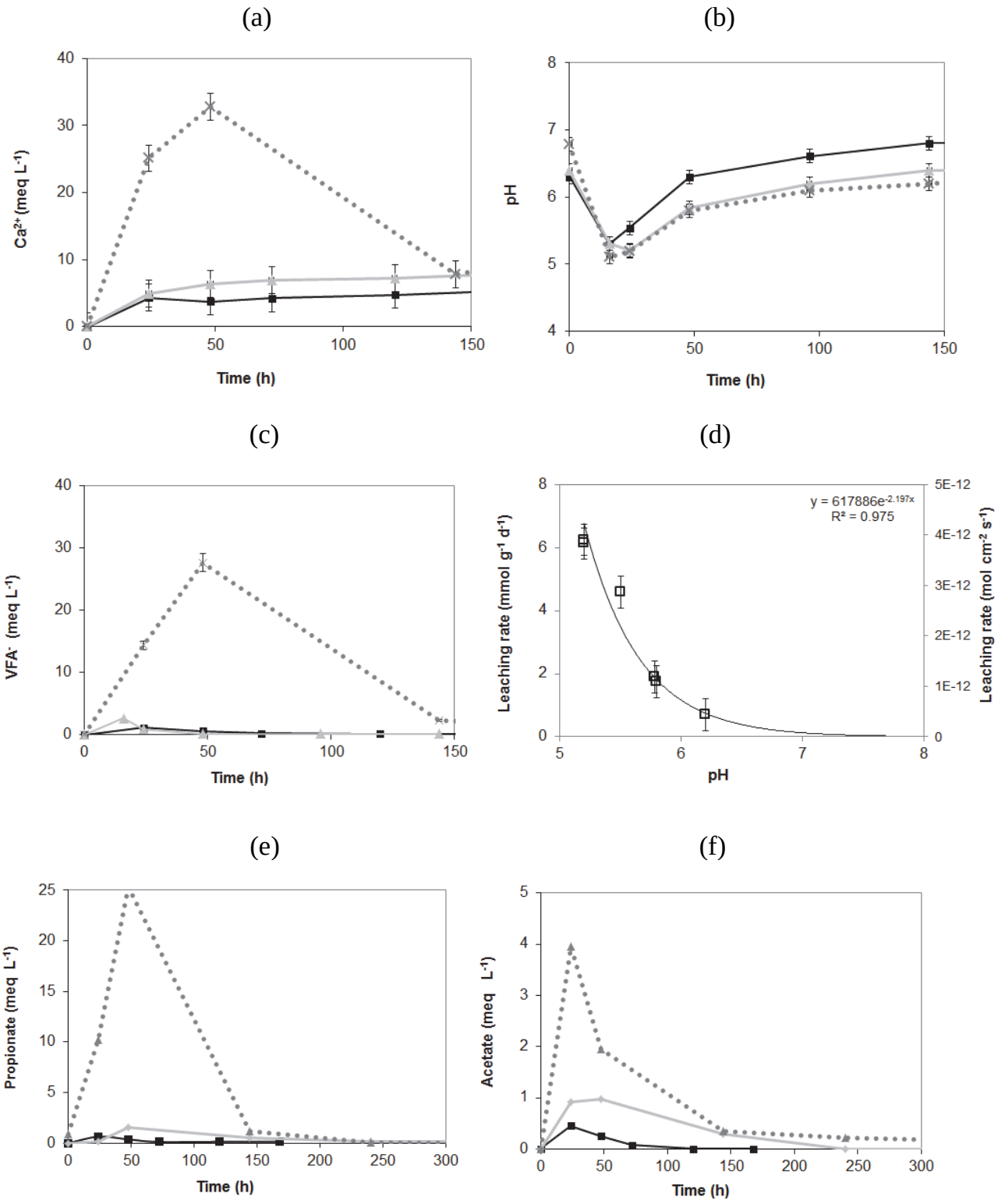

Figure 5-1: Dissolved calcium (a), pH (b), total VFA (c) against time for experiments 5 (black line), 6 (grey line) and 7 (grey dotted line), leaching rate (d) plotted against pH (□), profile of propionate (e) and acetate (f) concentrations for experiments 5, 6 and 7.

The decrease in pH in experiment 7 and the fatty acids formation peaks (Figure 5-1b and c) appear as expected simultaneously. But more importantly the fatty acid peak coincides with the Ca^{2+} leaching or acid consumption peak of wollastonite (Figure 5-1a). It must be realised that the increase of specific surface area and the pH are important parameters for increasing the reaction rate [106, 116]. As described in Table 5-2, the average wollastonite surface area was 1.8 m^2 g^{-1}. Based on this surface area maximum dissolution rates of $3.4*10^{-12}$, $3.9*10^{-12}$, $4.0*10^{-12}$ mol cm^{-2} s^{-1} were calculated for day 1. On day 2 average rates dropped to $5.0* 10^{-13}$, $1.1*10^{-12}$ and $1.2 *^{-12}$ mol cm^{-2} s^{-1} in experiments 5, 6 and 7, respectively. By plotting these against pH an exponential curve is obtained (Figure 5-1d). For the purpose of anaerobic reactor design and the comparison with existing literature mineral leaching rates have been expressed in mmol g^{-1} d^{-1} and in mol cm^{-2} s^{-1}.

5.3.4 Effect of wollastonite on biogas production and quality

Figure 5-2 shows the results on pressure autogeneration, CO_2 content in biogas and cumulative methane production for experiments 5 to 7. Figure 5-2a shows that the total pressure increase was 0.02, 0.20, and 0.88 MPa for experiments 5, 6, and 7, respectively.

The cumulative CH_4 production based on gas phase measurements, after correcting for dissolved CH_4 and sampling losses is then shown in Figure 5-2c. 85, 85 and 90 % of COD could be retrieved as CH_4 in experiments 5, 6 and 7, respectively. In all cases, produced acetate and propionate were consumed completely at the end of the experiment; indicating full conversion of glucose (Figure 5-1 e and f).

After 30 hours, the biogas contained 55, 53 and 36 % of CO_2 for experiments 5, 6 and 7, respectively. Over time, the CO_2 content of the biogas (Figure 5-2c) decreased and stabilised around 26, 14 and 13 ± 2 % for experiments 5, 6 and 7, respectively. The remainder produced biogas consisted of 74, 86 and 88± 2 % CH_4. Hydrogen was not detected in the biogas (detection limit of 30 ppm). The highest measured specific methanogenic activity (Figure 5-2d) was 0.13, 0.12 and 0.08 g COD CH_4 g^{-1}VSS d^{-1} for experiment 5, 6, and 7 respectively.

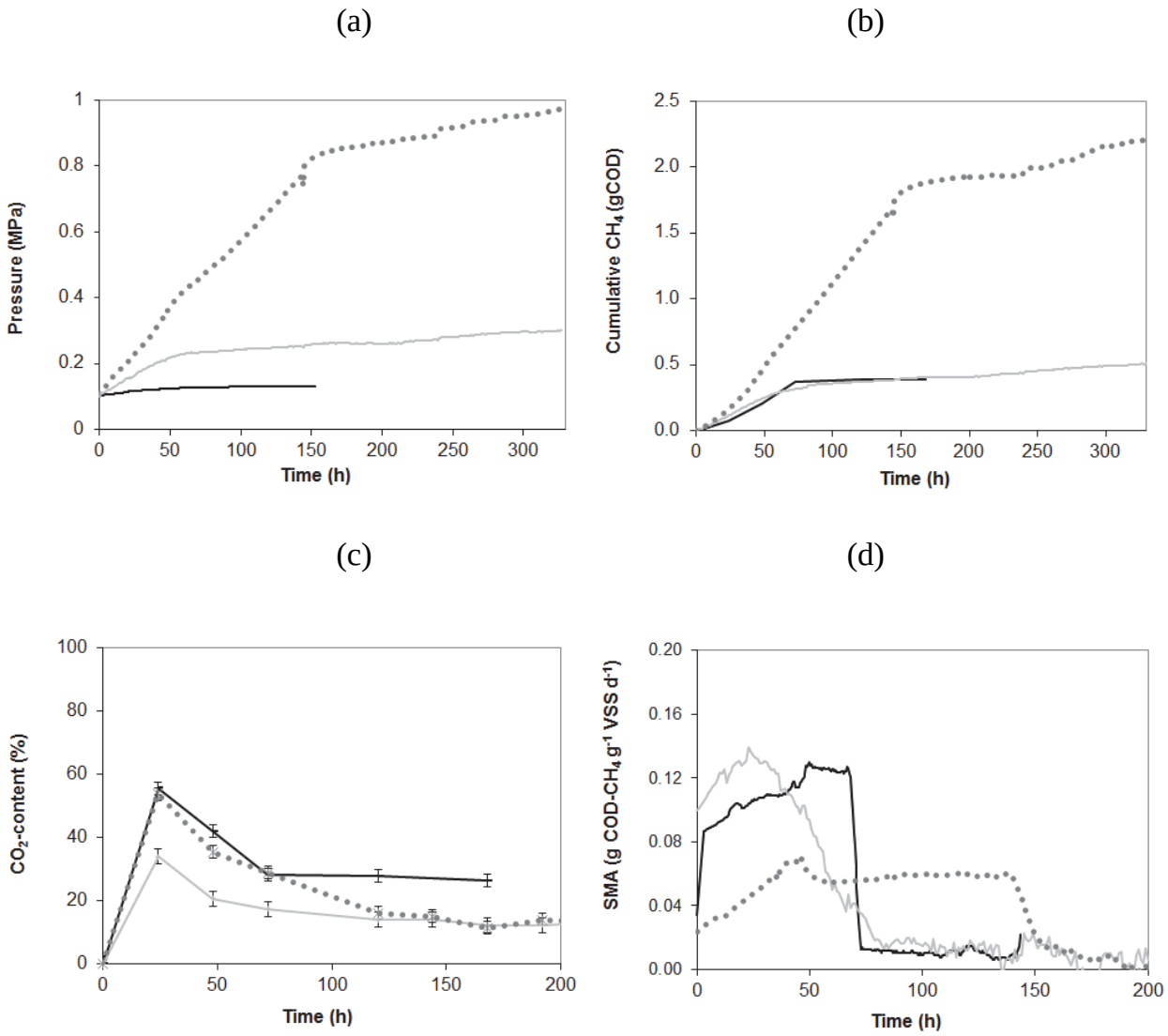

Figure 5-2: Pressure (a), cumulative CH_4 (b) CO_2-content (c) and measured specific methanogenic activity corrected for theoretical dissolution (d) for experiments 5 (black), 6 (grey) and 7 (grey dotted)

5.3.5 Precipitation products

FESEM-EDX, FT-IR and TGA-MS analysis were used to identify secondary calcium precipitates in the remaining solids after AHPD on glucose in the presence of wollastonite. Figure 5-3 shows an electron image of unreacted wollastonite, together with a layered image of a wollastonite control sample (Figure 5-3b) and reacted wollastonite from experiment 7 (Figure 5-3c). In the reacted sample, many particles with silicon but without calcium were present, in contrast to the control sample.

(a) (b) (c)

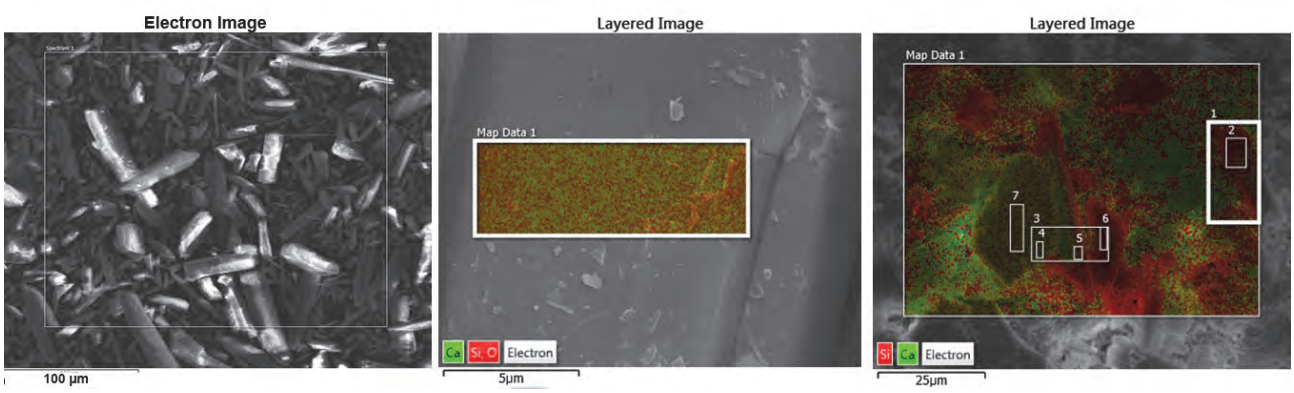

Figure 5-3: Electron image of unreacted wollastonite sample (a) and colored mapping of unreacted wollastonite sample (b) and reacted wollastonite sample from experiment 7 (c), with presence of calcium depicted in green and silicon in red.

The weight ratio (Table 5-4) based on various chosen spectrum areas, like shown in Figure 5-3a, further supports this conclusion. It was in average 0.59 for unreacted sample, similar to the theoretical molar weight distribution, and decreased to an average of 0.28 for the reacted sample. This indicated dissolution of calcium from wollastonite. No separate crystals with calcium but without silicate were found. Nonetheless, the presence of $CaCO_3$ was detected by TGA-MS analysis (Figure 5-4).

Table 5-4: Weight ratios of samples shown in Figure 5-3 combined with theoretical weight distribution of $CaSiO_3$

Unreacted $CaSiO_3$		**Reacted CaSiO3 (Figure 5-3c)**	
Theoretical weight distribution	0.59		
Sample 1 (Figure 5-3a)	0.60	Total map	0.28
Sample 2 (not shown)	0.59	Area 1	0.16
Area 1 (Figure 5-3b)	0.60	Area 2	0.11
		Area 3	0.31
		Area 4	0.37
		Area 5	0.46
		Area 6	0.12
		Area 7	0.37

Calcium carbonate and other metal carbonates decompose in the temperature range between 600°C and 900°C to CaO and CO_2 [104]. For the inoculum biomass (sludge) sample no CO_2 was liberated above 600°C (Figure 5-4c), thus it contained no calcium carbonate. Although, the wollastonite control sample released traces of CO_2 above 600°C, we assume that all initially present carbonates would have been dissolved at the beginning of experiment 7; the acidic non-saturated conditions with regard to Ca^{2+} CO_3^-. Thus, the CO_2 liberation in the area between 600-650°C indicated the presence of newly formed carbonate minerals (Figure 5-4c).

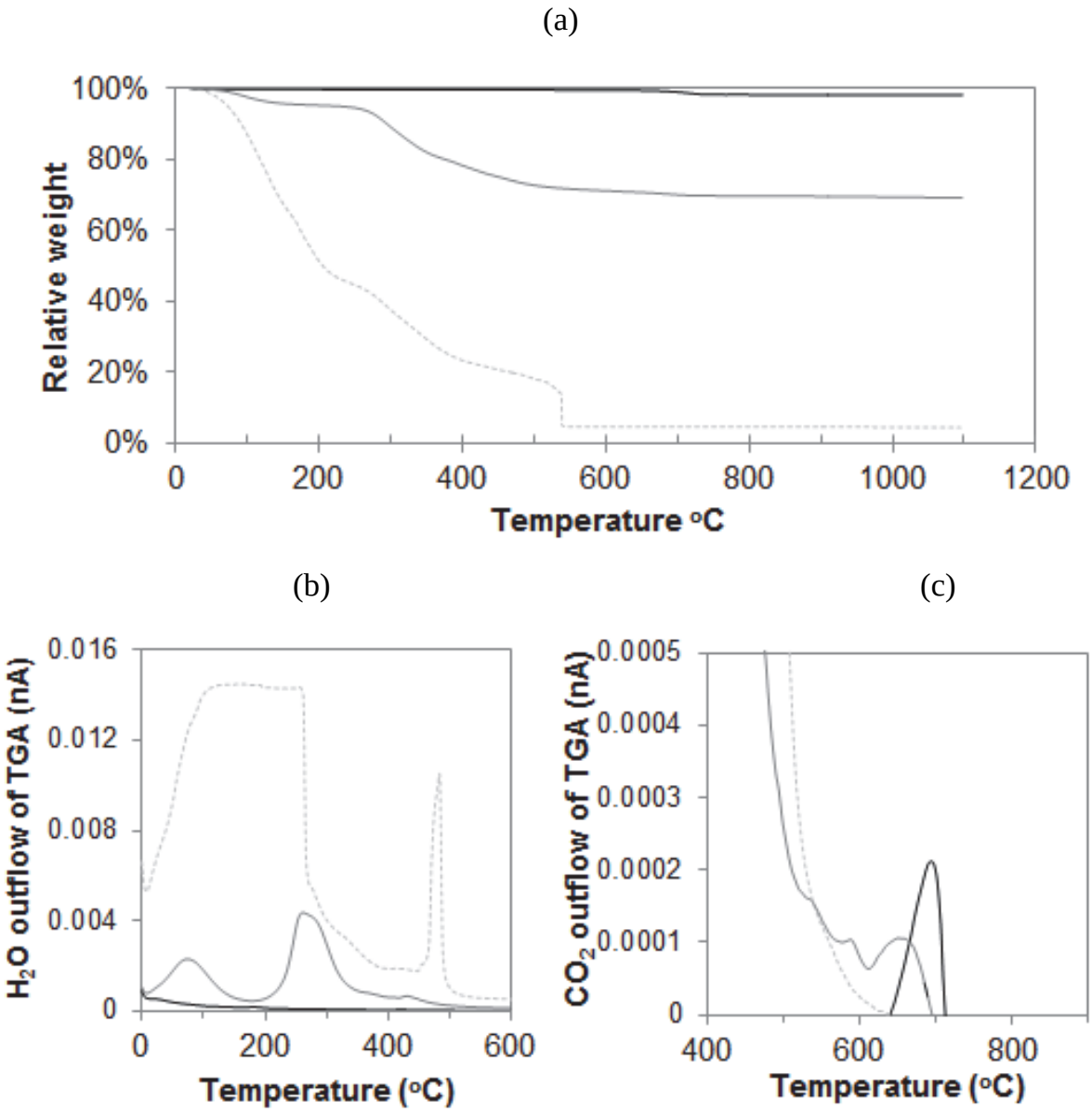

Figure 5-4: Relative weight loss against temperature (a), temperature related H_2O detection in outflow to mass spectrometer (b) and temperature related CO_2 detection in outflow to mass spectrometer (7) from a sample of experiment 7 (grey), inoculum (dotted grey line) and control wollastonite sample (black)

Furthermore, FT-IR spectra of experiment 7 showed distinct peaks at 711, 872, 1070 and 1405 cm^{-1}, a pattern comparable to the reference profiles of aragonite and calcite (Figure 5-5). Thus, FT-IR measurements verified that secondary carbonate precipitation (Equation 1-16) indeed functioned as a solid CO_2 sink.

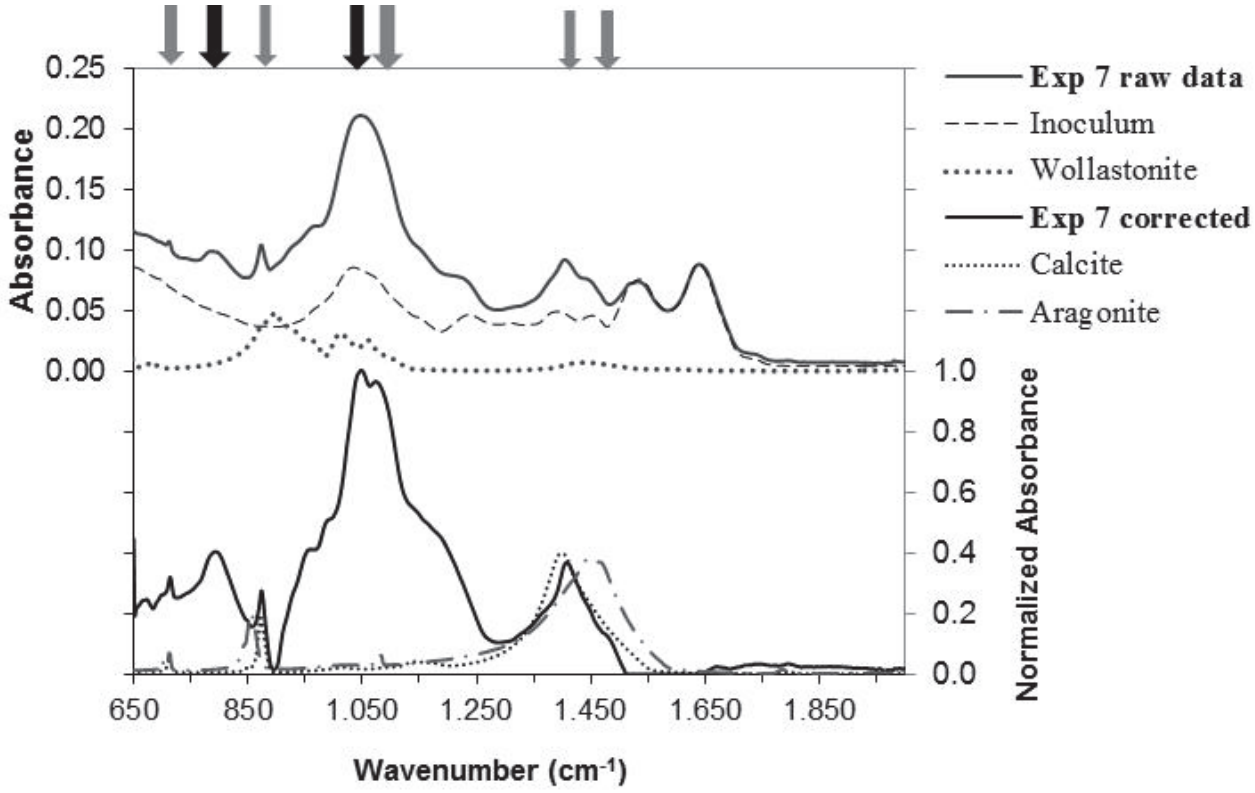

Figure 5-5: Absorbance of Infrared wavelengths of reactor sludge from experiment 7 (upper part of graph) and normalised absorbance of infrared wavelengths of reactor sludge after correction for wollastonite and inoculum spectrum. Calcium carbonate related peaks are indicated by grey arrows and amorphous silica related peaks are indicated by black arrows.

5.4 Discussion

5.4.1 Effect on biogas composition

Stoichiometrically, 1 mole of CH_4 is expected per mol of produced CO_2 for anaerobic glucose conversion. Therefore, glucose or other carbohydrates digestion generally result in a 50-60% CH_4 content taking the higher solubility of CO_2 compared to CH_4 in water into account [24]. The CH_4 content of the biogas was about 60 % CH_4 in pressurised experiments on glucose and operated at pH 7 up till 0.3 MPa [17]. Due the addition of silicate minerals, like wollastonite, olivine and anorthosite, biogas

contained already above 70 % CH_4 at atmospheric pressure (data for olivine and anorthosite are not shown). Under AHPD conditions, biogas quality improved to 86 ± 2 % CH_4 at 3 and 88 ± 2 % CH_4 at 1.0 MPa of biogas pressure. Thus, the H^+ consuming mechanism of silicate minerals (Equation 1-15) is an effective alternative to NaOH and sequesters CO_2 as HCO_3^- and $CaCO_3$ by keeping the pH above 6.3, and enabled full conversion of non-buffered glucose into CH_4.

5.4.2 Reaction rates

The estimated Ca^{2+} leaching rates in mmol g^{-1} d^{-1} observed for wollastonite in this work are in the same order of magnitude as the aerobic biological leaching rates described by Pokrovsky, Shirokova, Bénézeth, Schott and Golubev [116] in mol cm^{-2} s^{-1}. Still, these biological rates are 15-30 times slower than the physicochemical CO_2 sequestration rates presented in the literature [106, 117-119]. It is noteworthy, that in physicochemical CO_2 sequestration, high temperatures (usually >150 ^oC) are used to increase the leaching rate to match with large scale CO_2 production from combustion processes. Therefore, it may be speculated that under thermophilic conditions (55-70 °C) also higher leaching and sequestration rates could be obtained. Despite the moderate Ca^{2+} leaching, it was observed that also the VFA production at 1.0 MPa and 30^{o}C occurred at a relatively slow rate of 15 meq L^{-1} d^{-1} during the first 2 days. So, although much slower than physicochemical leaching, a maximum leaching rate of 7 mmol Ca^{2+} g^{-1} d^{-1} from needle shaped wollastonite would still be sufficient to buffer anaerobic glucose acidification at the applied slug doses. Continuous methanogenic reactor systems generally will be operated at neutral pH and low and constant fatty acid concentrations. Based on the relationship between leaching rate and pH retrieved in Figure 5-1d it can also be anticipated that under these conditions leaching rates would be significantly lower than the rates observed in this study. So, the mineral would remain intact inside the reactor for long periods of time and will only react in case of a pH drop. VFA accumulation is a general operational problem observed in anaerobic digestion and fast responses are required to prevent pH upsets. Due to the rate of increase of the leaching rate at lower pH observed in this study, dosing silicate

minerals would also provide a self-regulating low maintenance pH safeguard against fatty acid accumulation for conventional digesters.

However, compared to the 0.1 and 0.3 MPa AHPD experiments on glucose with wollastonite, the 1.0 MPa experiment showed a 50 % reduction in SMA value reaching 0.05 g COD g-1 VSS d^{-1} and a peak value of 2.8 g COD or 25 meq-propionate L^{-1} (Figure 5-1e). In the other experiments the propionate concentration never exceeded 0.15 g COD-propionate L^{-1}. The SMA drop might partially be ascribed to inhibition, since at pH 6.5 and a concentration of 0.241 g COD L^{-1}, propionate causes 50 % inhibition of the SMA [120]. Propionate accumulation could be caused by the relatively low pH as it is reported that propionate oxidizers require a pH above 6.8 to perform optimally [121]. Therefore, although acidification below pH 6 is prevented by silicate mineral addition, the possible inhibitory impact of accumulating VFA inhibition and inhibition of syntrophic propionate conversion under these conditions still poses a great challenge.

5.4.3 Effect of precipitation on digestate

The required addition of at least 1 g of mineral per g of COD-substrate will result in a larger solids fraction in the digestate streams if this concept is applied in practice. To prevent extra discharge costs, creation of added value products by mineral weathering is important. Therefore, three main research topics are identified, that could exhibit influence on the additionally produced solids: 1) type of calcium carbonate precipitation, 2) the role of silica and 3) the presence of additional trace- and macro elements.

By comparing the specific solubility products found in the bioreactor medium with the pK_{sp} of the polymorphs, the type of carbonate precipitation can be predicted [108]. Based on measured pH, VFA, HCO_3^- and Ca^{2+} concentrations, the solubility products (K) were 8.8 and 8.9 and calcium carbonate precipitation was not expected for experiments 5 and 6. In experiment 7, Ca^{2+} dissolution showed a maximum after 48 hours and dropped afterwards simultaneously with VFA converted into HCO_3^- and CH_4 (Figure 5-1 and 5-2).

Based on the Ca^{2+} concentration, biogas composition, pH and pressure measurements, the estimated pK_{sp} ranged from 7.8 to 8.3 between 48 and 144 hours. The pK_{sp} based on titration and measured evading CO_2 that reached 14.5 ± 1 mmol CO_2 L^{-1} after 200 hours was around 8.1, between the pK_{sp} of vaterite and aragonite. On the other hand, the peak at 711 cm^{-1} in the FT-IR spectrum refers to the presence of the crystalline polymorphs like calcite or aragonite [122]. The absence of a peak at 744 cm^{-1} excludes the presence of significant quantities of vaterite [123]. Likewise, the peak at 1405 cm^{-1} indicates calcite, but the shoulder at 1480 cm^{-1} indicates aragonite or ACC. So, based on the pK_{sp} 7.8 after 48 hours, just below the pK_{sp} 7.9, it can be postulated initially vaterite precipitated. Gradually, by ripening it transformed into aragonite and calcite, measured in the final sample by FT-IR.

The role of silica influencing the nature of the produced digestate is rather unknown. Kellermeier, Melero-García, Glaab, Klein, Drechsler, Rachel, García-Ruiz and Kunz [124] studied how dissolved silica concentrations of 0-2000 ppm could be used to stabilise ACC nanoparticles in physicochemical systems by sheathing them with SiO_2. With distinct peaks at 780 and 1038 cm^{-1}, we also expect amorphous silica in our samples [113, 114, 124]. This, combined with our FESEM EDX results, makes the formation of a composite of calcium carbonate and an amorphous silica-matrix, likely. Because this could have major implications for the type of by-product produced, further research into the role of silica in AHPD secondary carbonate precipitation is required.

Finally, the quantified chemical composition of olivine and anorthosite showed significant concentrations of different metals like iron, nickel, aluminum in olivine and anorthosite. From a scientific point of view, these additional elements could introduce unknown side-effects, making it more difficult to interpret the results. Aluminum could for example by metal hydrolysis produce additional H^+[65]. Likewise, iron could also give rise to metal hydrolysis, but also to a changed oxidation state in the liquid resulting in increased iron metabolism [24]. Furthermore, release of nickel could also influence the reactor conditions. Nickel is reported to chemically catalyze hydrogen evolution in geothermal vents [125]. Besides nickel is known to form the reactive core

of many metallo-enzymes present in anaerobic micro-organisms [126-128]. Despite the potential benefits, nickel and aluminum have also been reported toxic to methanogens [129, 130]. Furthermore, the reference anorthosite showed relatively higher oxygen content. This could be an indication of weathering prior to the experiment. On the one hand, this obviously introduces scientific uncertainty. But on the other hand, natural weathering of anorthosite results in the formation of kaolinite, gibbsite and ca-montmorillonite [131]. These are known constituents of alluvial fertile soil, and therefore possibly creating the desired added value from a practical point of view for the enrichment of the digestate with silicate minerals.

5.5 Concluding remarks

As a result of the weathering reaction wollastonite, olivine and anorthosite provided a self-regulating pH buffer, due to higher leaching rates at lower pH, to avoid pH drop caused by fatty acid and CO_2 production during high pressure anaerobic digestion of glucose. In this way, the methane content of the biogas could be increased to levels as high as 88 ± 2 %. Because of the required ratio of approximately 1 g $CaSiO_3$: 1 g COD-glucose, pH buffering by means of silicate minerals could result in a an accumulation of inactive solids in the digestate streams and the sludge. This could result in a lower volumetric biomass concentration and reduced overall biological conversion rates when the solid retention time is larger than the hydraulic retention time. Future research should therefore focus on the separation of the mineral fraction and the active sludge and address the secondary precipitation mechanisms of calcium carbonate polymorphs, the binding role of silica and the addition of other elements via the use of olivine or anorthosite.

It goes beyond the purpose of this work to include a full cost evaluation for the AHPD technology, but our work did show that a leaching degree of at least 68%, comparable to the values of chemical mineral carbonation [101, 102], was achieved at 30^{o}C and a biologically produced pCO_2 of 0.1-0.2 MPa and ~ 1.0 MPa of total pressure. Furthermore, produced CO_2 could partially be stored as HCO_3^- instead of CO_3^{2-} thereby reducing the required amount of mineral. These findings therefore further

support that the estimated biotechnological sequestration costs could decrease from € 102/ton CO_2 avoided to € 40/ ton CO_2 avoided [105]. Conventional waste water treatment systems however do not require investment in a high pressure reactor system and this could increase the sequestration costs significantly. It is therefore highly important that this work showed that only 0.3- 1.0 MPa of autogenerated pressure were sufficient to achieve high biogas quality without the need of conventional industrial ANC sources.

Chapter 6

Piezo-tolerant Microbes

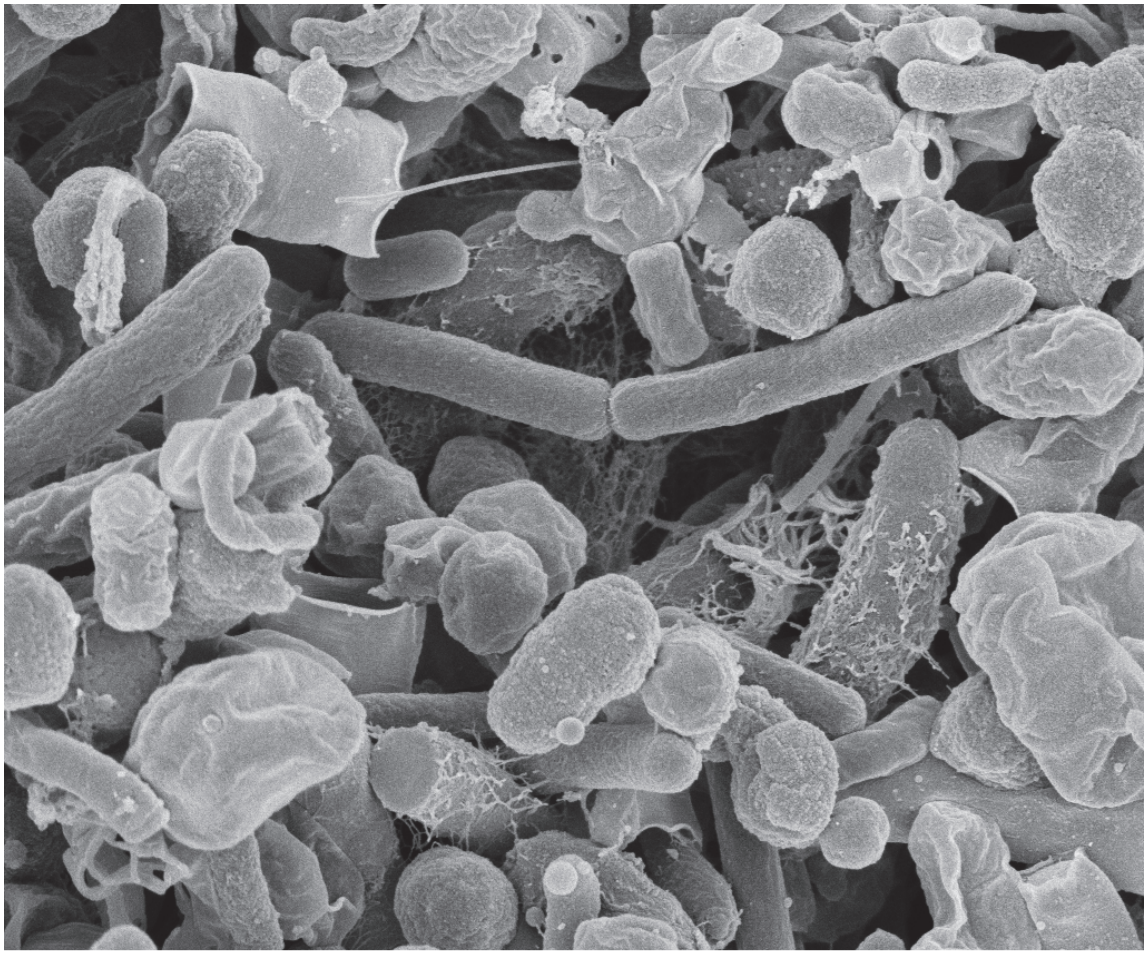

6 Piezo-tolerant natural gas-producing microbes under accumulating pCO_2

Abstract

Autogeneration of biogas pressure was previously shown to improve biogas composition to biogenic natural gas (BNG) quality. In this study, biogas pressure (<2.0 MPa) was batch-wise autogenerated over a year at 303K, resulting in a population dominated by *Methanosaeta concilii, Methanobacterium formicicum* and *Mb. beijingense* and *Kosmotoga-like (31%), Propioniferax-like (25%) and Treponema-like (12%)* micro-organisms. Remarkably, related micro-organisms have also been isolated from gas, oil or abandoned coal bed reservoirs. After prolonged pressure operation, pCO_2 was found to play a key role in the balance between propionate accumulation and CH_4 production. Alongside the *Propioniferax-like* organism, a putative propionate producer increased its dominance. Complementary experiments showed that propionate utilisation rates decreased linearly by over 90% to 2.2 mg gVS_{added}^{-1} d^{-1} as a consequence of elevating pCO_2 from 0.1 to 0.5 MPa. Neither Gibbs free energy and pH_2, nor pH could sufficiently explain this, but the effects could be attributed to reversible CO_2-toxicity.

Keywords

Population dynamics; propionate accumulation; CO_2-toxicity; Gibbs free energy; archaea and bacteria; autogenerative high pressure digestion

This chapter is based on

Lindeboom, R.E.F.[1], Shin, S.G.[1], Weijma, J., van Lier J.B., & Plugge, C., Piezo-tolerant natural gas-producing microbes under accumulating pCO_2, in preparation

[1] Both first author.

6.1 Introduction

Natural gas is a non-renewable fossil fuel formed over thousands of years. Currently, shale, coal bed, biogas and clathrates are highlighted to replace the declining resources in traditional natural gas fields[9, 132-134]. It is confirmed by isotope measurements that natural gas was partially produced by thermogenic cracking or from biogenic degradation of organic matter by micro-organisms [135, 136], but the microbial pathways involved and the time scale in which these gas fields were formed are more demanding to study. Biogas from anaerobic digesters consists of the same key components CH_4, CO_2, H_2S and H_2O and is produced from organic matter by mixed culture microbial fermentation. Moreover, autogenerated biogas pressures up to 9.0 MPa were produced in chapter 2 and the combination of substrate, the water charge balance composition and presence of alkaline earth metal precipitates were shown to directly correlate with biogas quality (chapter 5). This indicates that the microbial communities, active in anaerobic digesters today could have been responsible for the formation of ancient biogenic natural gas fields. Various researchers have isolated methanogenic archaea, such as *Methanobacterium formicicum* and *Methanosaeta concilli* from high pressure subsurface gas and oil reservoirs[137, 138]. From this perspective, actual insights in the microbial pathways and population dynamics under autogenerated pressurised biogenic gas conditions are fascinating, not only from a technological point of view, but additionally offer us insight into the origin of the biogenic natural gas which is estimated to contribute for about 20% to the total natural gas resources available today[135].

In order to produce biogas with natural gas quality directly in a bioreactor, CO_2 and H_2S have to remain dissolved in the water phase. Especially, the accumulation of CO_2 in the water matrix water is critical because its inhibitory effect at elevated concentrations that is known from food preservation [139, 140]. CO_2 also delays growth of pathogens and interferes in the intracellular metabolic pathways[141]. CO_2 can serve as electron acceptor in microbial metabolism (both anabolism and catabolism), but is also an intermediate or an end-product in fermentations. The tolerance and (adaptive) responses of micro-organisms towards increased CO_2 will

thus be different. Although the effect of pCO_2 on individual anaerobic micro-organisms has not been quantified, a 30% end-product inhibition on anaerobic digestion of sodium acetate was found under a pCO_2 of 0.1 MPa by Hansson and Molin [16] and 9.0 MPa biogas pressure (described in chapter 2). As far as the authors are aware of, the fundamental mechanism underlying these discoveries were not studied before.

6.2 Materials and Methods

6.2.1 Experimental setup 8L and 0.6L reactor

The 8 L AHPD reactor setup (Parr Instruments, model 910908, The Netherlands) as described in chapter 3 was used for this study. All experiments were kept at 30°C using a water bath (Julabo MP). Total pressure (Ashcroft A-series 1000 PSI), temperature (PT100) and pH (Bűchi Labortechnick AG, Flawil, Switzerland high pressure pH probes) were measured online and data were logged with Compact field point modules (cFP1804 and cFP-CB1) and stored with Labview 7.1 (National Instruments Corporation, USA) in the PC. The 0.6 L reactor contained Prosense high pressure pH probes (Prosense serial nr. 34002/002). Two six-bladed impellers attached to a central stirrer shaft (Parr Instruments, type A709HC, The Netherlands) were used to stir the reactors continuously at 150 rpm for the 8L reactor and 60 rpm for the 0.6L reactor.

6.2.2 Experiment I: Pressure cultivation of the micro-organisms

To examine the full anaerobic conversion of glucose, the 8L reactor was filled with 6.5 L of liquid, leaving a 1.5 L gas phase. Mesophilic anaerobic granular sludge of a fruit juice waste water processing EGSB (FrieslandCampina, Riedel, Ede, The Netherlands) was used as inoculum at a starting concentration of 2 g VSS L^{-1}. Liquid medium with trace elements and macro-nutrient solution was provided in concentrations as previously described (Table 2-1). The feed solution was then prepared by dissolving substrate, either solid sodium acetate or glucose, into 50 ml of liquid medium and fed as soon as substrate was depleted. This volume was chosen to maintain a constant liquid volume inside the pressure reactor, because 50 ml of reactor fluid was removed

during each phase for sampling . Additionally, a Schott titrator (end pH 4.1) was used to determine the quantity of solid $NaHCO_3$ that had to be dissolved in the feed solution in order to keep the Acid Neutralising Capacity (ANC) of the reactor constant at 150 meq L^{-1}. Liquid and gas samples were taken regularly.

6.2.3 Experiment II and III: Propionate degradation in small reactors

Propionate degradation kinetics under different pCO_2 conditions (0.0, 0.1, 0.3, and 0.5 MPa) was determined using batch cultures (experimental series II) at a temperature of 30 ± 1^oC (table 6-1). The batch incubation at elevated pCO_2 (0.3 and 0.5 MPa) was conducted in 0.6 L pressure-resistant bioreactors with 0.2 L liquid volume (chapter 4) and the unpressurised incubation in 0.125 L serum bottles with 0.05 L liquid volume. The seed sludge, 10.8 ± 0.3 g VS L^{-1}, was taken from the pressurised digester (1.0 MPa) fed with glucose. The synthetic medium was prepared (Table 2-1) and stoichiometric amounts of propionate (250 mg L^{-1} at time 0) were added. pH was adjusted to 7.0 with 15% HCl. The batch incubation started after mixing 20% (v/v) seed sludge and 80% (v/v) medium and replacing headspace with 0.10 +/- 0.01 MPa (pN_2), 0.10 +/-0.1, 0.30 +/-0.01, and 0.50 +/-0.02 MPa pCO_2 for experiments II-1, II-2, II-3 and II-4, respectively. Additional CO_2 was injected when necessary in the initial period of CO_2 dissolution.

Liquid samples were periodically taken from the cultures to measure VFA concentrations. When propionate was depleted, gas composition was measured with GC to calculate stoichiometric conversion to CH_4. Propionate concentrations were plotted to calculate the lag periods and propionate degradation rates using the modified Gompertz model (Eq. 6-1) [142].

$$y = A \exp\left\{-\exp\left[\frac{r_{smax}\cdot\exp(1)}{A}(\lambda - t) + 1\right]\right\} \qquad \textbf{(Eq. 6-1)}$$

where A is the maximum value of propionate (near to the initial concentration), r_{smax} maximum substrate utilisation rate (mg L^{-1} d^{-1}), and λ lag time.

Additional duplicate experiments (experiment III) with 1g VS L^{-1} pressure cultivated sludge, the same inoculum as used in experimental series II, were performed to

determine whether observed effects were pH or pCO_2 related (Table 6-1). 1.2 g propionate L^{-1} was fed to observe the overall conversion rates under different conditions. Experiment III-1 was operated at pH 8 and flushed with N_2 and controlled at 0.1 MPa. Experiment III-2 was operated at pH 8 with 50% CH_4 and 50% CO_2 at 0.1 MPa. The headspace of experiment III-3 was flushed with N_2 (0.1 MPa) and a pH was lowered to 6.3 by titrating the sludge with 0.1M HCl prior to the start of the experiment. Experiment III-4 was kept at pH 6.3 by pressurising the headspace of the reactor with 50% CH_4 / 50% CO_2 to a maximum of 1.2 MPa.

6.2.4 Analytical methods

A limited amount of biogas samples were taken in order to minimize the biogas losses for each substrate addition. Therefore, biogas samples were taken during the experiments, but at least as soon as pressure stabilised and analysed at atmospheric pressure by means of GC (chapter 4). All reported biogas compositions in this work were corrected for flush gas (N_2) and water vapour and showed a standard deviation of less than 2%. VFA were determined by gas chromatography (Hewlett Packard 5890 series II, Palo Alto, USA) with a flame ionisation detector. The protocol as described in chapter 2 was used for preparation and analysis of the samples.

In order to determine a large spectrum of liquid intermediates (i.e. fatty acids, organic acids and alcohols), liquid samples were centrifuged at 10000 rcf and the supernatant of the sample was 1.1-4.0 times diluted with concentrated H_2SO_4 solution to a vial concentration of 0.2 M, a value chosen to exceed the sample buffering capacity of 150 mM HCO_3^-. Samples were via an autosampler eluted with 1.25 mM H_2SO_4, injected and pumped at a flow rate of 0.6 ml min^{-1} with a HPLC pump (Dionex High Precision model 480) separated on an Alltech OA-1000 column (length=300 mm, internal diameter =6.5 mm) at 60^oC and 6.0-6.5 MPa and detected by means of refractive index.

Total Suspended Solids (TSS) and Volatile Suspended Solids (VSS) of the inoculum were determined using standard methods [57]. Due to the suspended nature of the

sludge, reactor samples were determined without first filtrating them and should therefore be interpreted as Total Solids (TS) and Volatile Solids (VS).

Samples for Field Emission Scanning Electron Microscopy (FeSEM) were centrifuged for 10 minutes at 4,300 rcf. Hereafter, supernatant was replaced by a 2.5% glutaraldehyde solution for fixation during 1 hour at 4^{o}C. Afterwards samples were dehydrated in a series of ethanol 50-75-90-95-100% and then transferred to acetone. To prevent the samples from shrinking due to removing the acetone in air, supercritical carbon freeze drying procedure as described in [92] was used. Afterwards the samples were glued to a brass sample holder by using iridium glue. Then samples were sputter-coated with iridium. The Field Emission Scanning Electron Microscope (Fei Magellan FESEM) was connected to an Oxford Aztec EDX and operated between 2 kV and 6.3 pA current. Scattered Electrons were detected by Through Lens Detection (TLD) at a Working Distance of 1.9 and 5.1 mm.

6.2.5 DNA extraction and amplification

Samples withdrawn from the reactor were centrifuged at 10,000 relative centrifugal force (rcf) for 5 min and stored at –20 °C before extraction. Total genomic DNA was extracted using FastDNA Spin kit for soil (MP Biomedicals, Santa Ana, CA). The extracted DNA was quantified and checked for purity with a Nanodrop spectrophotometer (Nanodrop Technologies, Wilmington, DE). The 16S rRNA genes were amplified using Phire Hot Start DNA polymerase (Thermo Fisher Scientific, Vantaa, Finland). Primer pairs GC-ARC344f/519r [143] and GC-968f /1401r [144] were used to specifically amplify the archaeal and bacterial 16S rRNA genes, respectively. The PCR mixture of 50 μL contained 400 nM of each primer, 200 μM of each dNTP, and 50 ng of template DNA. PCR was performed according to the following thermocycling protocol: pre-denaturation at 98 ^{o}C for 2 min; 35 cycles of denaturation at 98 ^{o}C for 10s, annealing at 56 ^{o}C for 10s, and elongation at 72 ^{o}C for 20s (archaea) or 30s (bacteria); post-elongation at 72 ^{o}C for 10 min. PCR product size was confirmed by electrophoresis in 1% (w/v) agarose gels stained with SYBR Safe (Invitrogen, Carlsbad, CA).

For cloning, nearly full-length 16S rRNA gene fragments, amplified with primers 109f and 1492r (Archaea) or 4f and 1492r (Bacteria) were obtained using , the same PCR protocol as described above.

6.2.6 DGGE

DGGE analysis of the amplicons was conducted on 8% (w/v) polyacrylamide gels with denaturant gradients of 40–60% and 30–60% for archaeal and bacterial communities, respectively, where 100% was defined as 7 M urea with 40% (*v*/*v*) formamide. Electrophoresis was performed using a D-Code system (Bio-Rad, Hercules, CA) in 0.5× TAE buffer at 60 ^{o}C and 85 V for 16 h. During the first 10 min of the electrophoresis, a voltage of 200 V was applied. The band patterns of the resulting gels were visualised by silver staining [145].

6.2.7 Clone library and phylogenetic analysis

Clone libraries of 16S rRNA genes were constructed to identify dominant microbial species. Two (A, L) and three (F, L, and U) DNA samples were chosen for archaeal and bacterial analyses, respectively, to maximize likelihood of including clones related to prominent DGGE bands. Nearly full-length 16S rRNA gene fragments were cloned into pGEM-T easy vector (Promega, Madison, WI) and transformed into Escherichia coli DH5α. White colonies were sent for sequencing with the primers SP6 and T7 to GATC Biotech (Konstanz, Germany). All overlapping reads were trimmed of vector sequence and bad quality sequences and were assembled into contiguous reads using DNAMAN software (Lynnon Biosoft, Quebec, Canada). Possible chimeras were removed using the Greengenes Bellerophon Chimera check [146]. All sequences were grouped into operational taxonomic units (OTUs) by constructing a similarity matrix with ClustalX 2.1 [147]. Phylogenetic trees were constructed using neighbor-joining method using MEGA software [148]. Hierarchical classification of the 16S rRNA gene sequences was assisted by Classifier from the Ribosomal Database Project [149]. The nucleotide sequences reported in this study have been deposited under GenBank accession numbers KJ206630-KJ206896. Additional DGGE analyses were conducted to crosslink band patterns with identified clones. At least one clone from each OTU

was used as template for amplification using above mentioned method. For bacterial clones, a nested PCR approach with SP6 and T7 primers was employed to exclude the amplification of the host 16S rRNA gene. The migration of clonal amplicons was directly compared to that of different bands on denaturing gradient gels.

6.2.8 Thermodynamic calculations

Both pCO_2 and HCO_3^- are commonly used for Gibbs free energy calculations[87, 150]. Because of the changes in CO_2-speciation due to reactor operation, $\Delta G_r''$ values for $CO_2(g)$, $CO_2(aq)$ and HCO_3^- were calculated for each relevant reaction at the specific conditions according to Thauer, Jungermann and Decker [27], which is explained in chapter 1.

6.3 Results

6.3.1 Reactor operational profile

During one year, mesophilic anaerobic granular sludge from an expanded granular sludge bed (EGSB) reactor processing fruit juice waste water (Friesland Campina, Riedel, Ede, The Netherlands) was cultivated under autogenerated pressure in an 8 L autoclave. The overall cultivation has been divided into 6 separate periods: 1) adaptation to a sodium concentration of 3.5 g Na^+ L^{-1} 2) adaptation to autogenerated pressure conditions on glucose, 3) pressure operation A on glucose, 4) pressure operation B on glucose, 5) reactor recovery and 6) pressure operation C, on glucose (table 6-1).

In previous experiments (chapter 4) it was found that methanogenic activity from acetate of the inoculum sludge was particularly sensitive to elevated sodium levels. Therefore sodium acetate was fed in 10 portions to allow adaptation of the slow growing, acetotrophic population to increasing sodium concentrations (experiment 0-1 to 0-10, Table 6-1). Although this procedure surely had an effect on population dynamics, glucose was deliberately not fed in this non-pressurised stage of the experiment. A relatively low number of the fast growing hydrogen, fatty acid and glucose metabolising organisms at the start of period 2, would then decrease the

required time for significant changes to occur in the population dynamics, when glucose was fed.

Table 6-1: overview of fed-batch pressure cultivation experiments

Exp.	Period	Days*	P_{start} (MPa)	VS (g L^{-1})	Substrate Type (gCOD $reactor^{-1}$)		DNA sample
Experiment I							
	Inoculum						A
0-1	1) Sodium adaptation	-110	0.10	2.0	NaAc	6.4	B
Till				-	-	-	till
0-10		-14	0.10	2.9	NaAc	6.4	H
I-1	2) Glucose and	0-7	0.10	2.9	Glucose	7.2	I
I-2	pressure adaptation	7-14	0.27		Glucose	7.2	
I-3		14-21	0.60	4.0	Glucose	7.2	J
I-4		21-56	0.10		Glucose	14.4	
I-5		56-63	0.65	3.8	Glucose	7.2	K
I-6	3) High pressure	63-70	0.10	4.0	Glucose	14.4	L
I-7	operation- A	70-77	0.60	4.7	Glucose	14.4	N
I-8		77-84	0.90	5.5	Glucose	14.4	O
I-9		84-93	1.22	6.3	Glucose	14.5	P
I-10		93-107	1.68	7.1	Glucose	14.4	Q
I-11	4) High pressure	107-114	0.10	2.0	Glucose	14.4	R
I-12	operation- B	114-128	0.62	4.0	Glucose	14.4	S
I-13		128-135	0.88	5.0	Glucose	7.2	T
I-14[#]		135-149	1.06	3.6	gluc + HAc	14.4	U
I-15[#]	5) Reactor Recovery	149-157	0.10		gluc + HAc	7.2	V
I-16[#]		157-169	0.10		HAc + H_2[**]	3.6 +1	
I-17	6) High pressure	169-176	0.10		Glucose	7.2	
I-18	operation- C	176-183	0.35		Glucose	7.2	W
I-19		183-192	0.64		Glucose	14.4	X
I-20	7) Hydrogen	248-257	0.10		Glucose	14.4	
I-21	Addition	257-261	0.30		H_2	2.7**	Y
I-22		261- 268	0.36		H_2	4.0 **	Z

Experiment II and III		Type of pressure					pH
II-1	Propionate degradation using pressure cultivated sludge under manually added pCO_2****	pCO_2	0.00	2.2	Propionate	0.25	
II-2		pCO_2	0.10	2.2	Propionate	0.25	
II-3		pCO_2	0.30	2.2	Propionate	0.25	
II-4		pCO_2	0.50	2.2	Propionate	0.25	
III-1	Propionate degradation pH and pCO_2 using pressure cultivated sludge****	pN_2	0.10	1.0	Propionate	1.8	8.0
III-2		pCO_2	0.05	1.0	Propionate	1.8	8.0
III-3		pN_2	0.10	1.0	Propionate	1.8	6.3
III-4		pCO_2	<0.60	1.0	Propionate	1.8	6.3

*medium addition and total sampling liquid were equal to keep 1.5 L gas phase constant ** in MPa # HAc = undissociated acetic acid was added to keep ANC constant, but directly dissociated due to excess HCO_3^-

During the experiment CH_4-content fluctuated between 70-90% (Figure 6-1) and showed a pattern similar to pH. After 100 days however, when the propionate started accumulating, CH_4-content dropped to <70%. The most important reactor parameters, pressure, pH, pCH_4, CO_2-speciation and fatty acid composition have been depicted in Figure 6-2, a, b, c and d.

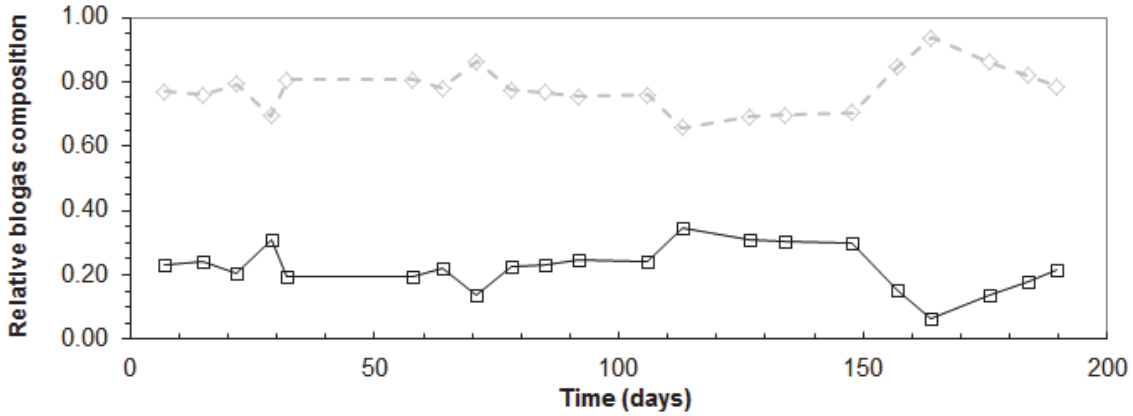

Figure 6-1: Biogas CH_4 (◊) and CO_2 (□)composition and pH (Δ) over time

During period 2 (Day 0-56), acetate and propionate were produced from glucose at concentrations below 300 mg COD L^{-1} (Figure 6-2b) and converted instantaneously, resulting in a maximum volumetric CH_4 production of 400 mgCOD L^{-1} d^{-1} (data not shown).

In period 3 (Day 63-93) average volumetric CH_4 production rates increased to 600-700 mgCOD L^{-1} d^{-1}. However, after the autogenerated pressure reached 1,8 MPa with a pCO_2 of 0.44MPa (Figure 6-2c), CH_4 production rates decreased to 400-500 mgCOD L^{-1} d^{-1}, until the final pressure of 2 MPa was succesfully obtained, while propionate concentrations remained below 100 mgCOD L^{-1}. Nevertheless, feeding of experiment I-11 was postponed until day 107, due to an observed reduction in methanogenic activity.

After decreasing to atmospheric pressure (day 107), pressure autogeneration was repeated in period 4 (Day 107-135)). From day 107 to day 115 CH_4 production rates were 400-500 mgCOD L^{-1} d^{-1}. From day 115 however, at a respective pCO_2 of 0.10 MPa, CH_4-production rates dropped further to 100-200 mgCOD L^{-1} d^{-1} and stabilised while pCO_2 increased to 0.25 MPa. Concomitantly, propionate accumulated to 1300 mg COD L^{-1} and calculated pCO_2 no longer corresponded to measured pCO_2.

Period 5 (Day 149-157) started at day 149, pressure was released to facilitate conversion of accumulated propionate, while adding 550 and 550 mgCOD L^{-1} of acetate and glucose, respectively. This initially led to an increase in propionate up to 800 mgCOD L^{-1} and then from Day 154 on, a decline of propionate with an estimated conversion rate of 120 ± 10 mgCOD L^{-1} d^{-1} occured. On day 157, 550 mgCOD L^{-1} of acetate was fed and the headspace was flushed with hydrogen (resulting in 0.10 MPa pH_2). While acetate and H_2 were converted into biogas by the acetotrophic and hydrogenotrophic methanogens, propionate degradation was inhibited initially at a concentration of 330 mgCOD L^{-1}, but subsequently decreased to 40 mgCOD L^{-1}.

Then, in period 6 (Day 169- 192) on day 169 a third autogeneration of biogas pressure was started. Glucose was provided in 2 subsequent loads of 1100 mgCOD L^{-1}, producing a pressure of 0.59 MPa (on day 182). Propionate was again the dominant

VFA, but concentrations never exceeded 300 mgCOD L^{-1}. However, upon bringing the COD to the original level of 2200 mgCOD glucose L^{-1}, propionate accumulated to 800 mgCOD L^{-1}. At a pressure of 0.84 MPa (on day 192) the experiment was terminated. From that point onwards the reactor was fed as soon as substrate and propionate was fully converted in order to facilitate recovery, but total pressure was not allowed to accumulate over 0.50 MPa.

(a)

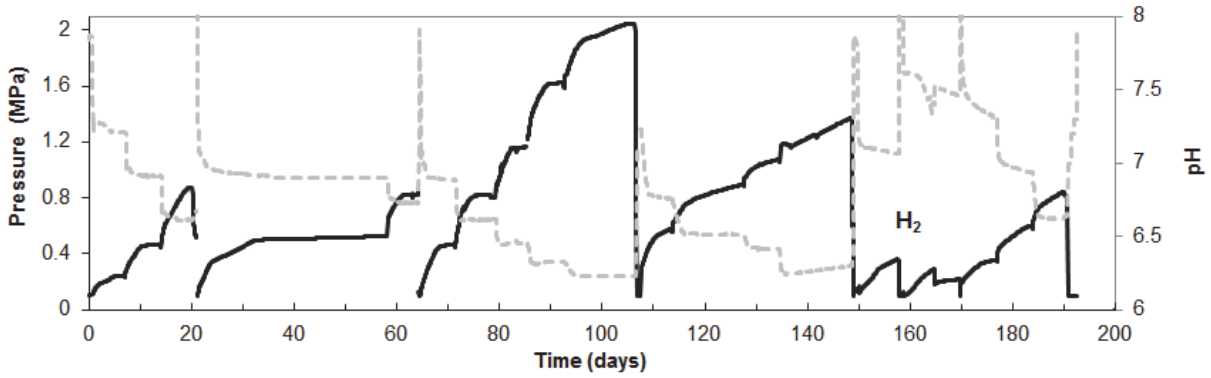

(b)

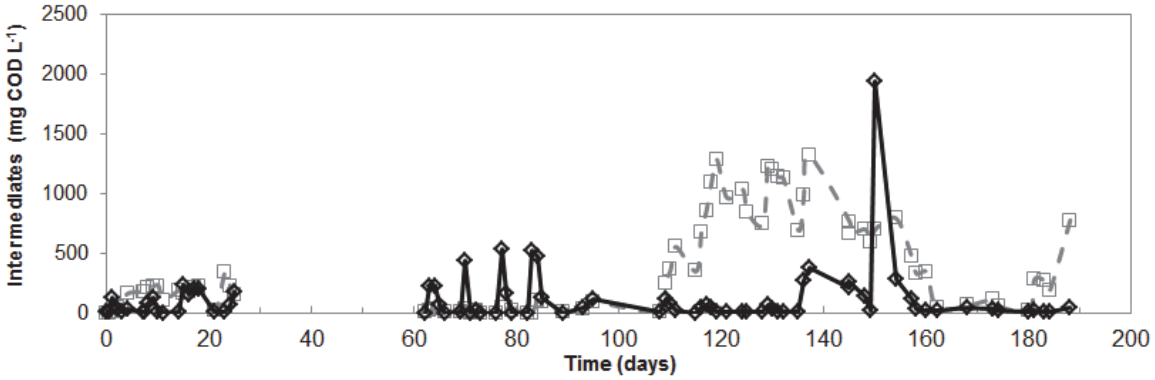

(c)

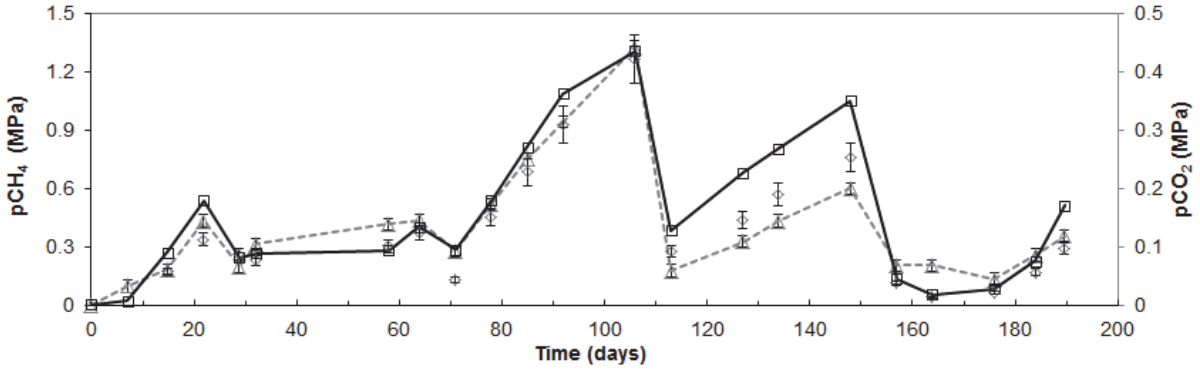

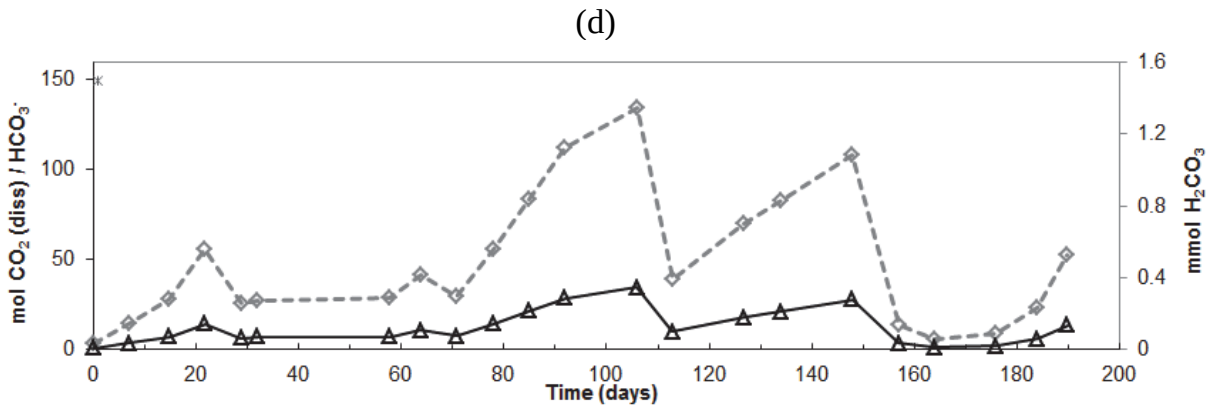

Figure 6-2: Results of fed-batch reactor operation; (a) Pressure (—) and pH (- -), (b) acetate (◊) and propionate (□), (c) pCH_4 (Δ), calculated pCO_2 (□) and measured pCO_2 (○)and (d) HCO_3^- (*) and calculated dissolved CO_2 (◊) and H_2CO_3 (Δ) profiles

In period 7 (day I-20, 21 and 22) the growth and activity of the hydrogenotrophic methanogens was stimulated. These methanogens can act as syntrophic partner of the propionate oxidising bacteria, thereby enhancing propionate conversion. After initially adding glucose (2200 gCOD L^{-1}), which resulted in propionate accumulation, the hydrogen partial pressure in the reactor was increased in two subsequent stages to 0.27 and 0.40 MPa, (Figure 6-3a). This caused a slight increase in pH, due to CO_2-consumption (Figure 6-3a). Although the system remained pressurised with pH_2, propionate conversion resumed (Figure 6-3b) and was converted into acetate (800 mgCOD L^{-1}) and biogas (0.15 MPa). This indicated that despite the earlier observed propionate accumulation, the presence of an active homoacetogenic and/or hydrogenotrophic population was confirmed.

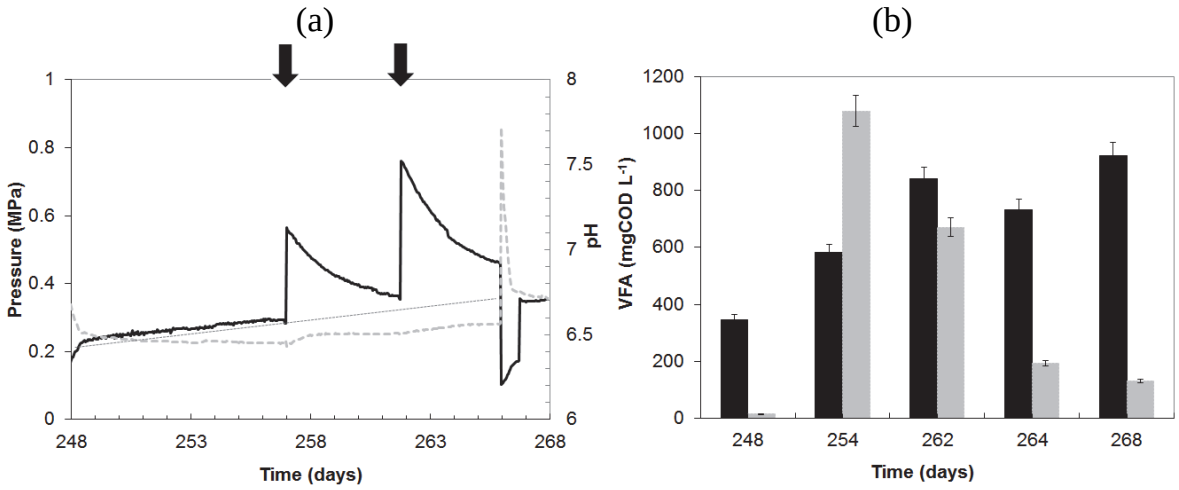

Figure 6-3:(a) Pressure (black) and pH (grey) profile for experiments I-20, 21 and 22 with hydrogen additions (arrows) and (b) related propionate (grey) and acetate (black) concentrations

6.3.2 Thermodynamic feasibility

During the experiment the involved biological conversions (Table 6-2) had to be performed under accumulating gaseous end-products and or intermediates. Therefore, Gibbs free energy calculations were used to acquire more insight in the thermodynamic feasibility associated to end-product inhibition. It should however be emphasised that Figure 6-2 c and d showed that HCO_3^- remained practically constant at 150 mmol L^{-1}, but pCO_2 and CO_2 (aq) fluctuated depending on the converted amount of substrate up to 0.50 MPa and up to 135 mmol L^{-1}, respectively. Therefore, Table 6-2 shows standard and actual conditions for the 3 main speciated forms of CO_2.

The feasibility of aceticlastic methanogenesis can simply be analysed by including pressurised CH_4 up to 2.00 MPa, because due to the charge balance requirements HCO_3^- should be produced. In line with previous results (chapter 2 and 3) accumulation from 0.07 (atmospheric) up to 2.00 Pa CH_4 decreases the ΔG_r of aceticlastic methanogenesis from -27.3 to -16.9 kJ $reaction^{-1}$. Therefore this is not expected to significantly inhibit CH_4 formation under the actual reactor conditions.

Likewise, hydrogenotrophic methanogenesis (Table 6-2 reaction 2) is unlikely to be affected by pCH_4 up to 2.00 MPa, since even at 1 Pa pH_2 ΔG_r only decreases from – 21.3 to – 13.8 kJ $reaction^{-1}$ using HCO_3^- (ΔG_r^b and ΔG_r^c). It is noteworthy that values become slightly less favourable (reaction 2 a and b) when using elevated values for CO_2(g) or CO_2 (aq). At atmospheric digester conditions (30 kPa pCO_2 and 1 Pa pH_2) ΔG_r^b would only be +18.2 kJ $reaction^{-1}$ whereas at 0.50 MPa pCO_2 and 1 Pa pH_2, ΔG_r of homoacetogenesis becomes +4.2 kJ $reaction^{-1}$. So, although increased pCO_2 has a positive effect on the thermodynamic favourability of homoacetogenesis, a slight elevation of pH_2 is required to make significant differences.

The ΔG_r of propionate degradation changes from -16.9 to -9.9 kJ mol^{-1}, by elevating pCO_2 from 0.03 to 0.50 MPa at an assumed pH_2 of 1 Pa. This value is slightly higher than the 9.3 kJ mol^{-1} calculated by using a HCO_3^- based reaction equation (4c). By elevating pH_2 to 60 Pa, the propionate oxidation certainly becomes unfavourable. In terms of the overall glucose reaction, it can be seen that although elevation of CO_2 in

any form makes the reactions less favourable. The largest effect should however only be expected when changing the pH_2 (ΔG_r^d).

Table 6-2: Gibbs free energy calculations of relevant reactions combined with CO_2-speciation. Based on ΔG_f^0 [27]

Eq.	Reaction Equation	$\Delta G_r^{0'a}$	ΔG_r^c	ΔG_r^d	ΔG_r^b
		kJ reaction^{-1}			
1*	$acetate^- + H_2O$ ==> CH_4 + $\mathbf{HCO_3^-}$	-31.0	-27.3	-18.6	-16.9
2a**	$4H_2$ + $\mathbf{CO_2\ (g)}$ ==> $CH_4 + 2H_2O$	-130.8	-14.5	-13.2	-53.8
2b**	$4H_2$ + $\mathbf{CO_2(aq)}$ ==> $CH_4 + 2H_2O$	-139.2	-14.3	-12.9	-53.5
2c**	$4H_2$ + $\mathbf{HCO_3^- + H^+}$ ==> $CH_4 + 3H_2O$	-135.6	-21.3	-13.8	-54.4
3a	$4H_2$ + $\mathbf{2CO_2\ (g)}$ ==> $acetate^- + H^+ + 2H_2$	-95.1	+18.2	+4.2	-36.3
3b	$4H_2$ + $\mathbf{2CO_2\ (aq)}$ ==> $acetate^- + H^+ + 2H_2O$	-111.8	+18.8	+4.8	-35.8
3c	$4H_2$ + $\mathbf{2HCO_3^- + H^+}$ ==> $acetate^- + 4H_2O$	-104.6	+3.0	+3.0	-37.5
4a	$propionate^- + 2H_2O$ ==> $acetate^- + 3H_2$ + $\mathbf{CO_2(g)}$	+71.8	-16.9	-9.9	+20.5
4b	$propionate^- + 2H_2O$ ==> $acetate^- + 3H_2$ + $\mathbf{CO_2(aq)}$	+80.1	-17.2	-10.2	+20.2
4c	$propionate^- + 3H_2O$ ==> $acetate^- + 3H_2$ + $\mathbf{HCO_3^- + H^+}$	+76.5	-9.3	-9.3	+21.1
5a	$C_6H_{12}O_6 + 2H_2O$ ==> $2\ acetate^- + 2H^+ + 4H_2$ + $\mathbf{2CO_2(g)}$	-215.9	-338.4	-324.4	-283.8
5b	$C_6H_{12}O_6 + 2H_2O$ ==> $2acetate^- + 2H^+ + 4H_2$ + $\mathbf{2CO_2(aq)}$	-199.3	-338.9	-325.0	-284.4
5c	$C_6H_{12}O_6 + 4H_2O$ ==> $2\ acetate^- + 4H^+ + 4H_2$ + $\mathbf{2HCO_3^-}$	-206.5	-323.2	-323.2	-282.6

$\Delta G_r^{0'a}$ at 25^0C, pH 7 and 0.10 MPa pressure and 1 molar of all aquatic species; ΔG_r^b at 25^0C 0.01 M aquatic species, 0.15M HCO_3^-, pH= 6.2 and a pCO_2=30 kPa and pH_2= 1 Pa ; [c] ΔG_r at 25^0C 0.01 M aquatic species, 0.15M HCO_3^-, pH= pKa = 6.2 and a pCO_2= 0.50 MPa and pH_2 =1 Pa; ΔG_r^d at 25^0C 0.01 M aquatic species, 0.15M HCO_3^-, pH= pKa = 6.2 and a pCO_2= 0.50 MPa and pH_2 =60 Pa; *pCH_4 in $\Delta G_r^{0'a}$, ΔGr^b, ΔGr^c and ΔGr^d is 0.10, 0.07, 1.00 and 2.00 MPa respectively, **pCH_4 in $\Delta G_r^{0'a}$, ΔGr^b, ΔGr^c and ΔGr^d is 0.10, 0.07, 1.00 and 1.00 MPa respectively.

6.3.3 Population dynamics

Figure 6-4 shows FESEM micrographs of coccus-(A) and rod-shaped (C), filamentous (B), and spiral (D) micro-organisms in a representative sample from the reactor

biomass after completing the experiment. The sizes varied between 0.5-1.0 µm diameter for the coccus-shaped organisms, up to a width x length of 0.5 x 6 µm and 80 nm x 30 µm for the rod-shaped organisms and filamentous organisms, respectively. The spiral organism had a width of 150 nm and a length of 8-10 µm. Furthermore, organisms with different cell surface characteristics were present, from apparently smooth (B) to the presence of tubular pores (E).

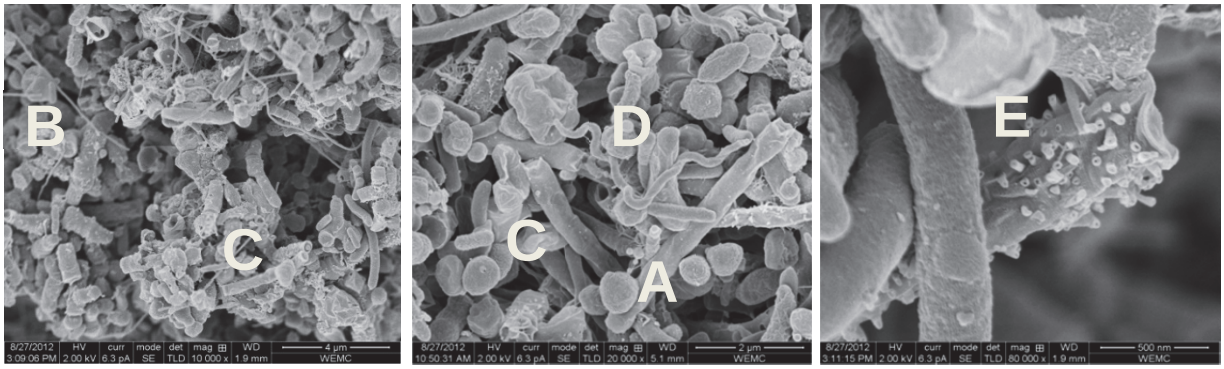

Figure 6-4: FESEM micrographs from representative reactor samples of coccus (A), filamentous (B), and rod (C)-shaped (left) and spiral (D) organisms (middle). Smooth and tubular pore (E) cell-surfaces are magnified on the right.

DGGE was performed to characterize the microbial community structure in the pressurised bioreactor (Figure 6-5 and Figure 6-6). Both archaeal and bacterial DGGE profiles showed continuous shifts according to temporal changes; bacteria exhibited more diverse and dynamic shifts than archaea. Neighbour-joining trees showing the phylogenetic identities of the representative clones from archaeal and bacterial OTUs were constructed (Figure 6-6 and 6-8). In order to construct phylogenetic trees, clone libraries were constructed to provide sequence information of major microbial species. Two archaeal clone libraries, sample A, the inoculum (26 clones) and sample L (27), and three bacterial clone libraries, sample F (53 clones), sample L (42), and sample U (59), were generated. The archaeal clones were grouped into 5 original taxonomic units (OTUs), whereas the bacterial clones were classified into 30 OTUs. The five archaeal OTUs were closely (>98%) related to *Methanosaeta concilii*, *Methanosarcina acetivorans*, *Methanoregula boonei*, *Methanobacterium beijingense*, and *Methanobacterium formicicum*, respectively (Figure 6-6).

The *Msa. concilii*-like clones constituted the major population in both inoculum (16/26, 62%) and R4.6 (22/27, 81%) libraries. These putative acetate-utilising clones appeared at the same positions as bands 1–3 (Figure 6-5); accordingly, bands 1 and 2 were the most prominent bands in all lanes. The two OTUs related to *Msr. acetivorans* and *Mr. boonei* were only present in the inoculum library. The OTU related to *Mtb. beijingense* was present in both methanogenic clone libraries. Clones related to these OTUs migrated to the same positions as bands 5 and 6, indicating that the relative abundance of these species decreased with time. The *Mtb. formicicum*-like clones, in contrast, were only detected in sample L (3/27, 11%) and not in the inoculum sample (A). Still, band 4 was visible from the inoculum DGGE profile (Figure 6-5), which faded and became prominent from sample F onwards, implying that the *Mtb. formicicum*-related archaeon was one of the dominant hydrogen-utilising methanogens under pressure.

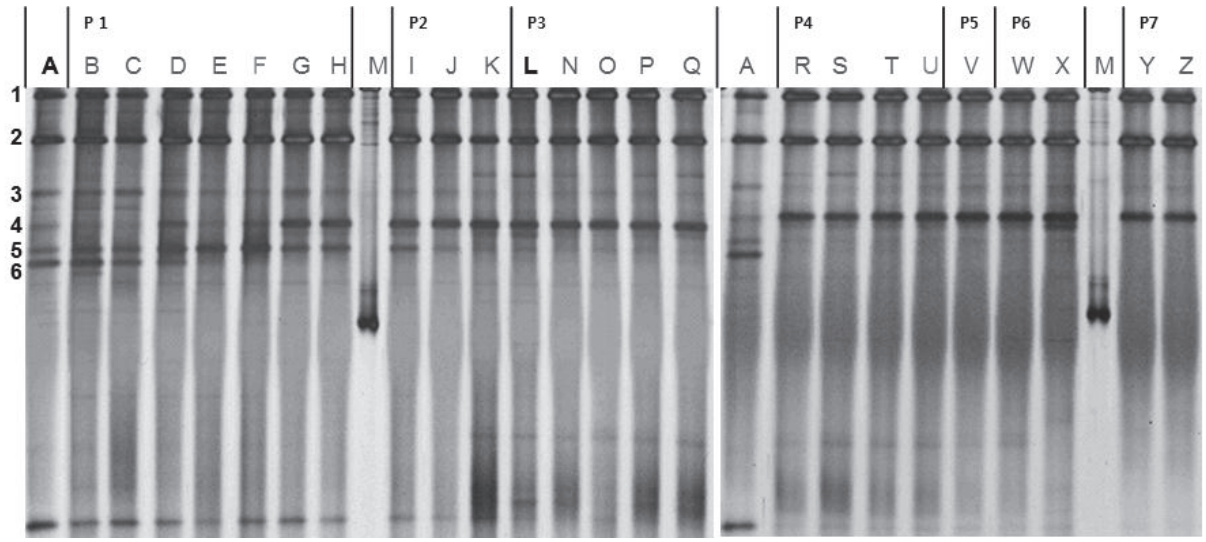

Figure 6-5: Archaeal DGGE profiles of the 16S rRNA gene fragments. Numbered bands indicate the positions identical to the migration of clone samples closely related to (1–3) *Methanosaeta concilii,* (4) *Methanobacterium formicicum,* (5) *Methanoregula boonei* and/or *Methanosarcina acetivorans,* and (6) *Methanoregula boonei* and/or *Methanobacterium formicicum*.

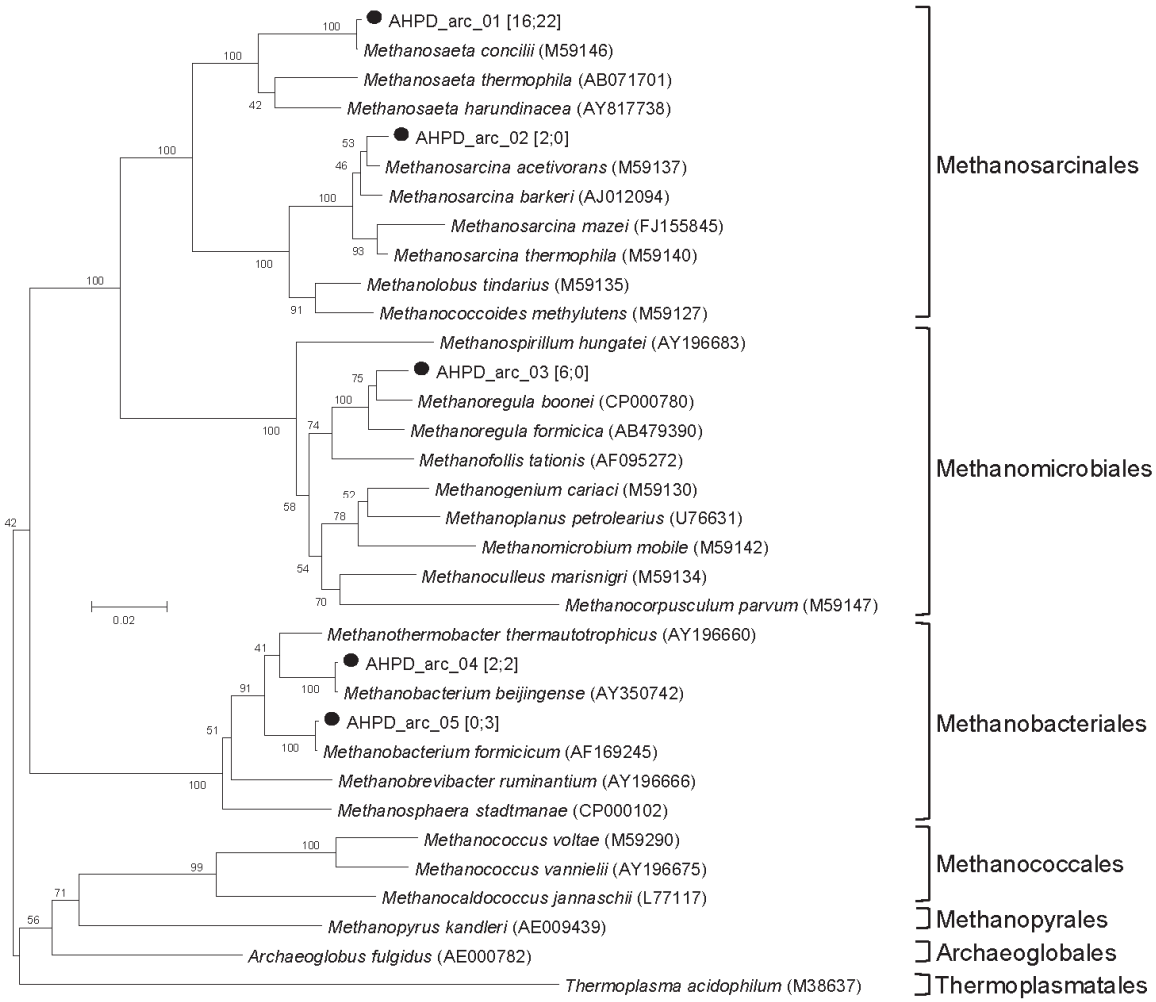

Figure 6-6: Neighbour-joining tree illustrating the phylogenetic identities of the archaeal 16S rRNA gene fragments obtained from clone samples. Clone counts of each OTU are given in brackets; the first and the second numbers indicate the counts derived from inoculum and R4.6, respectively. Numbers at nodes are bootstrap values derived from 100 analyses.

The thirty bacterial OTUs were affiliated to nine phyla: *Firmicutes*, *Thermotogae*, *Synergistetes*, *Actinobacteria*, *Spirochaetes*, *Lentisphaerae*, *Verrucomicrobia*, *Proteobacteria*, and *Bacteroidetes* (Figure 6-8). Among these, 15 OTUs matched to 12 bands with identical mobility on DGGE (Figure 6-7).

Band 1, the matching clone of which was deeply related within Synergistaceae, appeared at the point when the substrate was changed from acetate to glucose (Figure 6-7). This emphasised that this switch in substrate had influenced the microbial community and should be taken into account when analysing the data.

Bands 2, 3, and 4, whose intensities increased and decreased with time, showed the same migration on DGGE to clones closely related to *Bacteroidales and/or Victivallis*, *Clostridium quinii and/or Clostridia*. For band 3, in the DGGE profile no distinction could be made between the *Bacteroidales* and *Victivallis*, belonging to the phylum *Lentisphaerae*, because both appeared at the same position.

The position of band 5 on DGGE was identical to that of *Syntrophobacter fumaroxidans*-like clone (99% sequence identity), a propionate oxidizer. The fact that this band was relatively weak and appeared during period 2, matched the results of the clone library, because only one related clone was counted in sample U. However, this band was also observed in later samples in P3, and P4.

Band 6 was linked to a *Treponema*-like OTU; this genus consists of many member species including the homo-acetogenic *T. primitia* [151]. It appeared at the end of P1 and remained relatively stable throughout the later periods. In accordance with the emergence of band 6 which was absent in the inoculum, the related clones were only detected from sample F (5/42, 12%) and sample U (7/59, 12%) libraries. A *Kosmotoga*-affiliated clone constituted 7% (3/42) and 31% (18/59) of the clone counts of sample L and sample U libraries, respectively. Considered together with the visualisation of band 7 from the end of period 2, this *Kosmotoga*-related phylotype seems to have developed as one of the dominant bacterial species.

Band 8, identified as a *Propionibacteriaceae*-like organism, was present from the reactor start up, but decreased its intensity from period 3 onwards.

Band 9 was prominent in the inoculum and the acetate-fed lanes, but gradually lost its intensity afterwards (Figure 6-7). This band is linked to a group of clones closely related to *Brachymonas denitrificans*, a denitrifying bacterium[152]. This OTU accounted for 36% (19/53) population of the sample F library but none of the other two libraries, supporting the observation from band patterns.

The propionate producing *Propioniferax*-like species (band 10) was only retrieved in the clone library of sample U with 25% of the total counts (15 of 59 clones). This fact, together with the high intensity of band 10 shown from sample S (day 112) onwards

showed that this organisms had a significant role in the observed propionate accumulation.

It is also noteworthy that band 11, which was identified as a *Petrimonas*-related clone, increased in intensity during the period of pressure operation (P2), but showed diminished intensity after pressures decreased to below 1.0 MPa.

Band 12, related to *Succiniclasticum*, appeared at the end of P2, but decreased in intensity from P4 onwards (Figure 6-7).

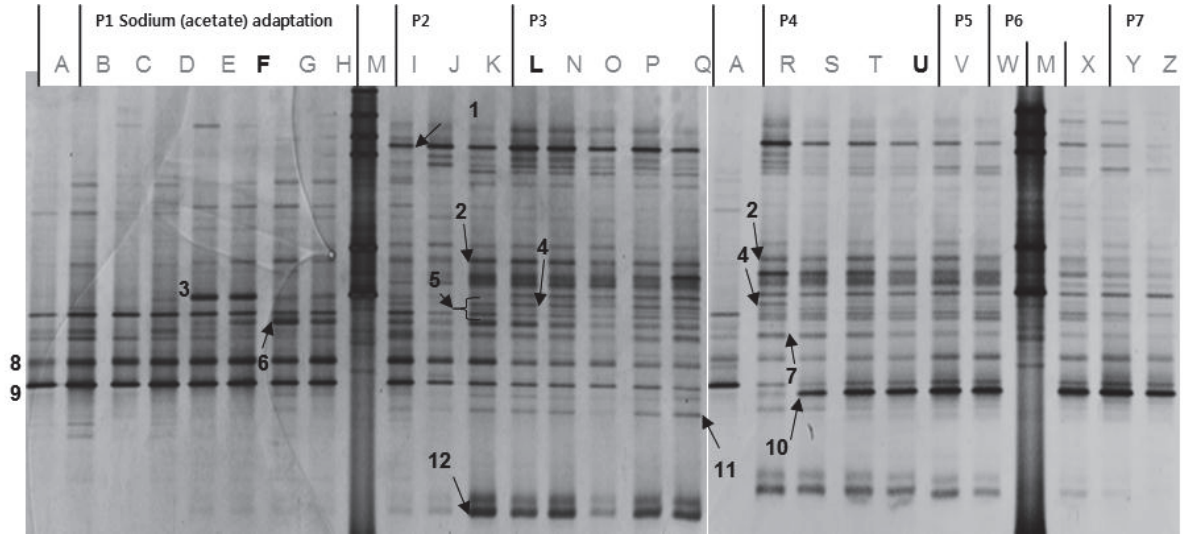

Figure 6-7: Bacterial DGGE profiles of the 16S rRNA gene fragments. Numbered bands indicate the positions identical to the migration of clone samples closely related to (1) *Synergistaceae*, (2) *Bacteroidales*, (3) *Bacteroidales* and/or *Victivallis*, (4) *Clostridium quinii* and/or *Clostridia*, (5) *Syntrophobacter fumaroxidans*, (6) *Treponema*, (7) *Kosmotoga*, (8) *Propionibacteriaceae*, (9) *Brachymonas denitrificans* and/or *Tessaracoccus*, (10) *Propioniferax*, (11) *Petrimonas*, and (12) *Succiniclasticum*.

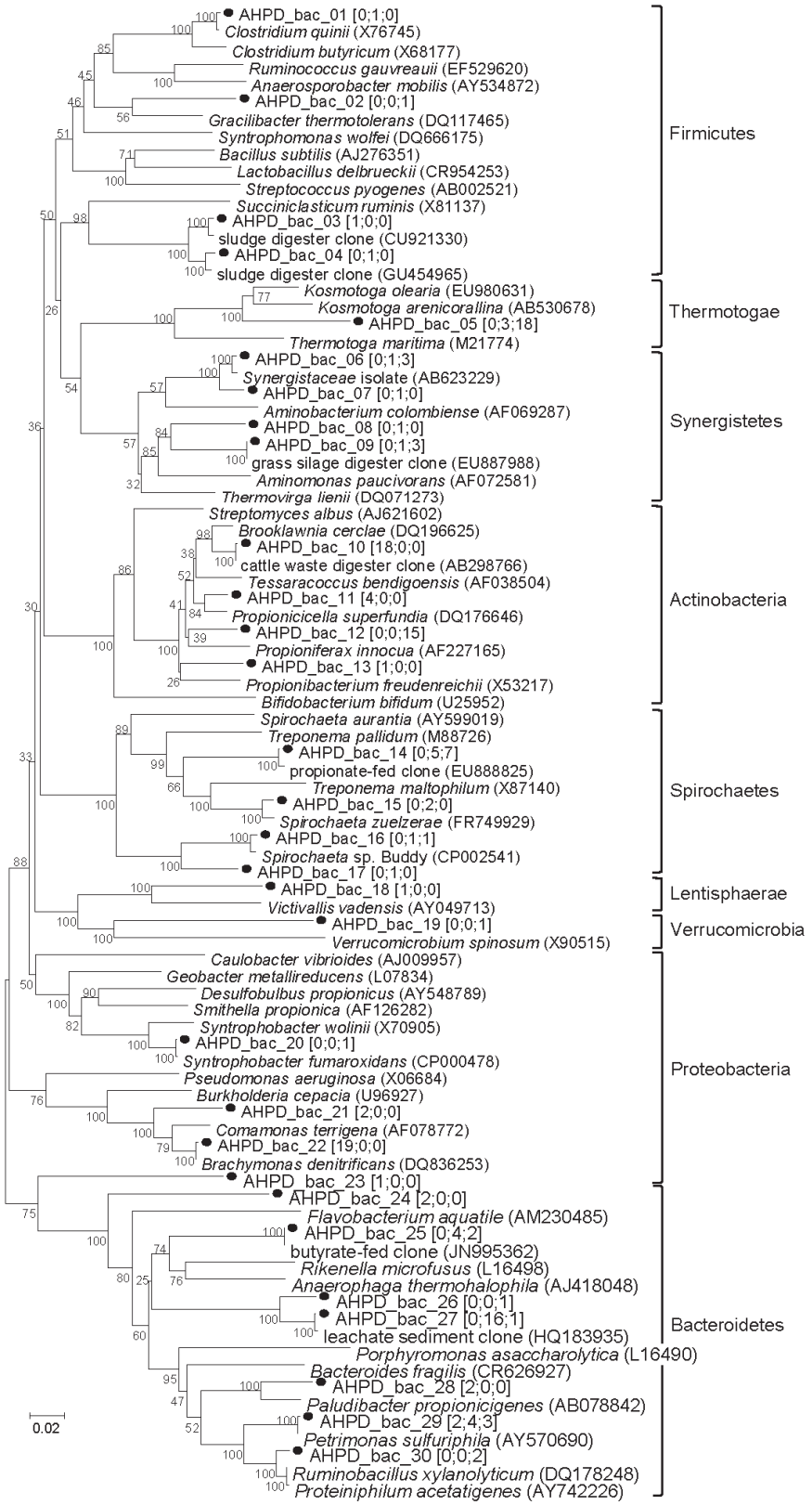

Figure 6-8: Neighbour-joining tree illustrating the phylogenetic identities of the bacterial 16S rRNA gene fragments obtained from clone samples. Clone counts of each OTU are given in brackets; numbers in series indicate the counts derived from SR46, R4.6, and R4.14, respectively. Numbers at nodes are bootstrap values derived from 100 analyses.

6.3.4 Propionate kinetics

The combined reactor operation and population dynamics study revealed important changes in the propionate degradation kinetics with concomitant dissolved CO_2 concentrations. Therefore, propionate conversion was examined under 0.0, 0.1, 0.3, and 0.5 MPa pCO_2 conditions (figure 6-9a and b). The initial propionate dose was completely utilised during the batch test. Kinetic parameters derived from modified Gompertz model[153, 154] are listed in table 6-3. The maximum degradation rate (r_{smax}) decreased and the lag period (λ) increased with higher pCO_2, indicating that an elevated CO_2 exhibits detrimental effects on anaerobic propionate catabolism. Especially, the 0.5 MPa trial showed significant reduction (93.4%) of the maximum utilisation rate compared to the 0.0 MPa trial. Besides propionate, acetate was the only VFA detected in this experiment. Acetate profiles of the 0.5 MPa trial are represented in figure 6-9b. Acetate levelled up to 68 mgCOD L^{-1} during the lag period, and maintained at low levels during the entire active propionate degradation period. The average molar ratio of CH_4 produced to the propionate dose fed was 2.0. Since this is only 12% higher than the theoretically expected CH_4, it is expected to be from endogenic respiration. By plotting the calculated substrate conversion rates against the substrate concentration, Monod curves have been estimated, showing the strong pressure related effect (figure 6-9c). Maximum relative growth rates showed a linear relationship with both pCO_2 and $[H^+]$ (figure 6-9d).

Table 6-3: Kinetic parameters derived from the propionate oxidation experiment. All p values are < 10^{-4}.

Parameter	pCO_2 (MPa) pH	0.00 7.8	0.10 7.1	0.30 6.3	0.50 6.1
A (mg L^{-1})		283	283	266	258
λ (d)		2.8	3.4	3.8	16.8
r_{smax} (mg L^{-1} d^{-1})		72.8	58.5	35.5	4.8
reactor r_{smax} (mg COD L^{-1} d^{-1})$^{\lozenge}$		546	441.5	268	36
specific r_{smax} (mg g VS_{added}^{-1} d^{-1})		30.3	24.4	16.5	2.2
Relative μ_{max} (%)*		100	80.5	54.5	7.3

A = initial substrate concentration in mg L^{-1}; λ = lag phase in days *calculated by assuming constant Yield-coefficient in different experiments $^{\lozenge}$ given 5 times dilution of reactor sludge concentration

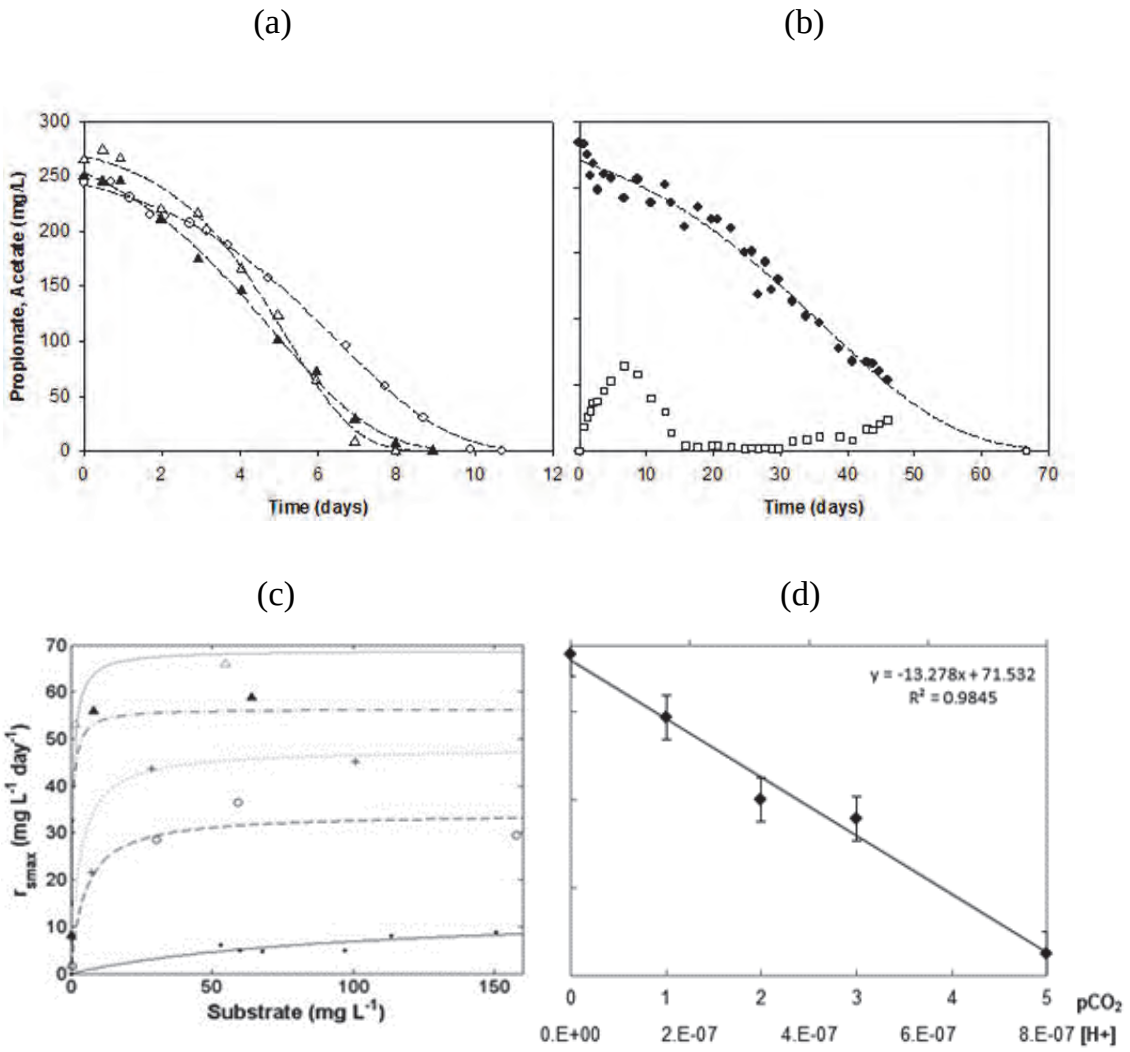

Figure 6-9: (a) Propionate degradation profiles under different pCO_2 conditions with 0.00 MPa (△); 0.10 MPa (▲); 0.20 MPa (+) and 0.30 MPa (○). Acetate (□) and propionate (♦) profiles in mg L^{-1} (b) of 0.50 MPa trial are shown for representation. Dashed lines represent curve fittings using modified Gompertz model. (c) Estimated Monod curves for propionate degradation based on low substrate concentrations derived from the experimental data (d) linear retrieved relationship between $[H^+]/pCO_2$ and r_{smax}.

From Figure 6-10, it can be observed that independent of pH 1200 mg L^{-1} propionate was degraded in all experiments within 6 days. Yet, the elevated pCO_2 experiment (III-4) still had 600 mg L^{-1} propionate left after 7 days. Although these results require further elaboration, the decreasing propionate conversion cannot be explained by decreasing pH alone (Table 6-3).

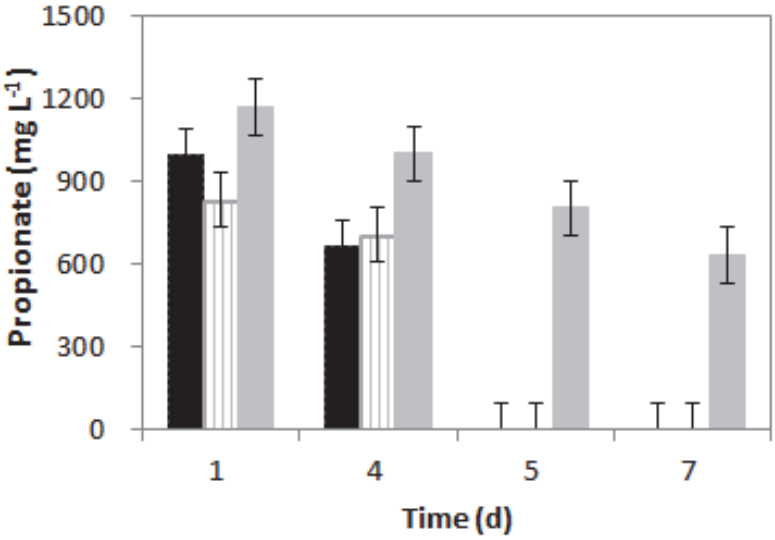

Figure 6-10: **Degradation of propionate in time at 0.10 MPa pN_2, and pH ~8 (Δ) 0.10 MPa pN_2 and pH 6.3 (□), 50 kPa pCO_2 and pH ~8 (◊) and, 0.60 MPa pCO_2 and pH 6.2 (x)**

6.4 Discussion

6.4.1 Shifts in population dynamics

It was found that over time and concomitantly with increasing pCO_2 a shift occurred from acetate to propionate as main accumulating intermediate from glucose degradation. A *Kosmotoga*-affiliated clone constituted 7% (3/42) and 31% (18/59) of the clone counts of the L and U libraries, respectively. Considered together with the first visualisation of band 7 near the end of period 2, this *Kosmotoga*-related organism seems to have developed as one of the dominant bacterial species under the pressure conditions of period 3, where acetate was the main intermediate. However, its relative band intensity decreased from day 112 onwards, when more propionate was found as intermediate. The only mesophilic member of this genus, *K. olearia*, was isolated from oil production fluid produced at an oil platform in the North Sea and is characterised by an outer sheath-like structure or 'toga' and is a known acetate and hydrogen producer [155]. *Clostridium quinii* and *Petrimonas sulfuriphila*, the only characterised species of the genus *Petrimonas*, are both sugar-utilising organisms producing acetate and hydrogen as common products[156, 157]. The genus *Victivallis* includes only one isolated species, *V. vadensis*, which could convert glucose to acetate and H_2 in a syntrophic co-culture with hydrogen-utilising methanogens [158].

Besides acetate producers also propionate producers were found in the clone libraries. The genus *Succiniclasticum* includes its sole member, S. *ruminis*, which is known to convert succinate to propionate[159]. *Propionibacteriaceae* are well recognised for a sub-lineage *Propionibacteria spp.* which produces propionate via the Wood-Werkmann cycle in anaerobic digesters[160]. However, conditions showed to be unfavourable for these organisms, since band 8 (Figure 6-7) faded from day 64 onwards (P3). Besides, no clones were counted in samples L and U. In contrast, conditions favoured the growth of a propionate producing *Propioniferax*-like organism (band 10; Figure 6-7). The abundance of these organisms, as evidenced by the clone counts and band prominence from day 112, suggests that the presence of this organism was strongly related to the accumulation of propionate under the tested conditions. Strikingly, the increase in band intensity (Figure 6-7) of the *Propioniferax*-like organism is accompanied by the decrease in band intensity of the *Kosmotoga*- like organism (band 7: Figure 6-7). Apparently, both organisms compete for glucose under the given conditions. Before drawing any conclusions however, both acetate and propionate oxidation should be discussed.

With regard to acetate degradation, it can be observed that under the initial acetate feeding, a *Msr. acetivorans*-like organism became prominent. However, after switching to glucose digestion it progressively disappeared until the highest pressures of this study were obtained. The *Msa. concilii*-like species appeared to be the most abundant archaeon throughout the further operation. The kinetic competition for acetate utilisation between *Methanosaeta* and *Methanosarcina spp.* is well documented in the literature[161, 162]. In an acetate-fed batch incubation harboring the two genera, the r-strategist[3] *Methanosarcina* typically outcompetes the K-strategist3 *Methanosaeta* given that the initial acetate concentration is high (> 120 mgCOD L^{-1}). In period 2 onwards, intermediate acetate concentrations maintained below 120 mgCOD L^{-1}, except within 1-3 days after feeding glucose. From the end of

[3] Commonly used definitions in population dynamics; K-strategists invest relatively a lot in maintenance and reproduction of fewer off-spring, whereas r-strategist invest mainly in producing as much off-spring as possible to deal with changing environments

period 3 (sample L), intermediate acetate concentrations never exceeded 100 mgCOD L^{-1} when excluding the peaks caused by acetate addition between days 150-170. Because clone counts of the *Kosmotoga*-like organism increased from 7 to 31 % in samples L and U respectively, it is expected that both acetate production and consumption were well balanced.

Like acetate, propionate is a significant intermediate in the anaerobic food chain comprising 6–35% of the carbon balance under atmospheric conditions[163]. Elevated levels of propionate, are often regarded as a sign of digester instability due to its toxicity[164] and thermodynamically unfavourable reaction nature[120, 165]. Although propionate oxidation seemed to occur readily up till a pressure of 2.0 MPa and pH 6.1 (P3) with concentrations below 400 mgCOD L^{-1}, detrimental accumulation of propionate, coinciding with significantly decreased CH_4-production rates, occurred in P4 and P6 experiments. The *Syntrophobacter fumaroxidans*-like clone (99% sequence identity) was counted only once in sample U and its related band 5 was weak in intensity. Nevertheless, it should be realised that these culture-independent methods, DGGE and clone library analyses, do not support direct evidence on the population size or activity, and are subject to PCR bias[166]. So, employment of additional techniques, such as fluorescence in situ hybridisation, radiography, and polyomics approaches, would provide multi-dimensional insights to further elucidate population dynamics. Another possibility is that another organism was responsible for propionate oxidation. Clone AHPD_bac_14 for example, may have been involved in propionate oxidation, because it showed highest similarity (99%) to a clone (EU888825) retrieved from a propionate fed anaerobic reactor [167].

Data from reactor operation in P4, P5 and P6 showed stable or increasing propionate concentrations directly after glucose feeding and could, besides increased propionate production, indicate decreased propionate consumption. However, propionate degradation rates at least up to 250-300 mgCOD L^{-1} d^{-1} were also observed in P4 and P5 about four days after glucose was fed. It was therefore confirmed that an active propionate degrading community was still present, although it could not prevent propionate accumulation. In addition, the microbial diversity analysis confirmed the

continued presence of a stable hydrogen consuming population. Next to the hydrogenotrophic methanogens, *Mtb. formicicum* and *Mtb. beijingense*, the presence of a *Treponema*-like bacterium was shown. This genus consists of many member species including the hydrogen consuming homo-acetogenic *T. primitia* [151]. Furthermore, H_2 was never detected above the detection limit of 60 Pa in the gas phase, but as calculations (Table 6-2) show this pH_2 could already inhibit propionate oxidation. Nevertheless, propionate was oxidised in P7 (exp I-21, 22) under elevated pH_2 of 0.27 and 0.40 MPa (Figure 6-3). Under the even higher pH_2, this is only feasible with an active syntrophic community keeping pH_2 in the proximity of propionate oxidising organisms low and is comparable to the thermophilic propionate conversion kinetics observed by Van Lier, Grolle, Frijters, Stams and Lettinga [165]. This allows us to exclude the possibility that the mixing profile had disturbed the granular structure providing the required proximity for interspecies hydrogen transfer. It can however not be excluded that temporary increases in pH_2 as small as 1 Pa resulting from rapid glucose degradation could have reduced the thermodynamic favourability of syntrophic propionate oxidation, temporarily resulting in lower propionate oxidation rates.

6.4.2 Thermodynamics and CO_2- toxicity

Despite the fact that the inoculum for experiment II was taken from the 8L reactor at a pCO_2 exceeding 0.30 MPa, experiment II showed that the specific propionate oxidation rate had linearly reduced with increasing pCO_2 from 30.3 to 2.2 mg g^{-1} VS d^{-1} (Table 6-3). Both values are within the 0.9 to 500 mg g^{-1} VSS d^{-1} range for specific propionate degradation activity described in previous studies [168-172]. The 2.2 mg g^{-1} VS d^{-1} at 0.50 MPa pCO_2 is similar to the values obtained from extremely high solids digestion (65% or 75% moisture content)[170]. Likewise, in experiments I-14 propionate degraded (after glucose was consumed) at an estimated rate of ~ 60 mg COD L^{-1} d^{-1} at a pCO_2 of 0.25 MPa and estimated CO_2(aq) of 110 mmol L^{-1}. Afterwards, in experiment I-15 and 16 when pCO_2 was below 0.1 MPa, propionate degraded at an estimated rate of 120 mg COD L^{-1} d^{-1}. Although, this suggest a reversible inhibition caused by CO_2 accumulation, Figure 6-9b leaves no doubt that it

also concerns a pH-related effect, especially because it is also known from literature that pH drops from 6.8 to 6.2 can inhibit propionate degradation significantly [121]. It is however remarkable that the HCl induced pH drop did not inhibit the conversions significantly and therefore results suggest that the observed reversible inhibition should be related to the pH-based speciation of CO_2.

On one hand (Table 6-2 reaction 4a and Figure 6-3) actual autogenerated pCO_2 (of 0.03 up to 0.50 MPa) is unfavourable for the thermodynamic feasibility of propionate oxidation ΔG_r from -16.9 to -9.9 kJ mol^{-1}. On the other hand it also provides excess electron acceptor, thereby increasing the ΔG_r of the hydrogenotrophic and homoacetogenic pathway at 1 10^{-5} pH_2 from -14.5 and +18.2 to -21.5 and +4.3 kJ $reaction^{-1}$, respectively. This slightly improves the conditions for interspecies hydrogen transfer and thereby enhances propionate degradation again. Generally, an energy quotum of -20kJ mol^{-1}, corresponding to 1/3 ATP, is needed to sustain life [27], but the continuous production of CH_4 up to 9.0 MPa (chapter 2) would thermodynamically not have been possible with a ΔG_r of -13.1 kJ mol^{-1}. Changes in free energy could theoretically also affect kinetics and thereby cause the observed phenomena [173, 174], but we consider it unlikely that these minor changes with a positive feedback-loop could have caused a >90% decrease in observed propionate oxidation rates, in a linear manner. Actually, many sources in literature [139-141, 150, 175, 176] show clear evidence that CO_2 rather than only being an substrate, intermediate and end-product in free energy calculations, results in a pH effect. Becker [176] even reported stronger effects of carbonic acid than could be explained from $[H^+]$ alone. From the data in Figure 6-10, it can indeed be observed that correction of pH to 6.3 by HCl compared to reaching this pH by pCO_2, resulted in only limited inhibition, giving rise to speculate on a combined pH-pCO_2 inhibition mechanism. At increasing pCO_2 and decreasing pH, CO_2 potentially binds to the amine groups of proteins, forming carbamino-proteins, thereby potentially deactivating an enzyme. This would then require investment in maintenance to prevent their inactivation, especially, at reducing pH closer to the pKa (~5.5) of some known carbamino-proteins, other than hemoglobin [177]. The formation of carbamino-proteins, was also

reported to cause reversible sol-gel interactions in the protoplasm of single cell organisms of for example *Nitella clavata*[175]. However, rapid or excessive increase in pCO_2, caused irreversible damage to the cell structure [140]. Rajagopal, Werner and Hotchkiss [139] concluded that gram-positive bacteria are more resistant towards elevated pCO_2, than gram-negative bacteria. A thick peptidoglycan cell wall, offers a better barrier to prevent CO_2 diffusion into the protoplasma, than an open lipopolysaccharide membrane combined with a thin peptidoglycan inner membrane. Additionally, the gram-positive *Propioniferax*-like organism was renamed from *Propionibacterium innocuum* to *Propioniferax innocua*, because of the exceptional cell wall structure.[178]

Likewise, the *Kosmotoga*-like organism sets itself aside from other putative acetate producers, by being closely related to the only mesophilic member of the *Thermotogales*, characterised by an additional protective outer envelope[179]. Although being different in composition, the thicker cell wall of archaea probably also offers more protection. It seems that the micro-organisms in the AHPD reactor have structural adaptations to survive high pressure and high CO_2 conditions. More fundamental research is needed to further study this phenomenon.

6.5 Concluding remarks

This study showed that the methanogens *Msa. concilii* and *Mtb. formicicum,* were proven to thrive on autogenerative conditions and capable of generating 2.0 MPa of biogas pressure (with 80% CH_4) from glucose. The DGGE and clone library results also indicated that a *Propioniferax*-like organism, a *Kosmotoga*-like organism, and a *Treponema*-like organism became the dominant bacterial species under AHPD conditions. Although the organism responsible for propionate oxidation could not be identified, propionate conversion rates, and thus overall CH_4-production rates, were inhibited by 0-90% by the accumulated pCO_2 and could not be explained by the relatively small changes in $\Delta G_{r.}$ So, the piezo-tolerant organisms were strongly influenced by the operating conditions. This allows us to speculate that pCO_2 can also

be actively used to steer population dynamics and conversion kinetics by using its reversible toxicity.

Additionally, similar to the autogeneration found in AHPD reactors, the microbial community responsible for the production of biogenic natural gas from gas, oil or coal bed reservoirs at a pressure of 10.0-30.0 MPa with an average CO_2-content of 0-8% [8] is also exposed to elevated pCO_2. Additionally, the closest neighbours to the identified archaea and bacteria include piezo-tolerant and piezophilic organisms sourced from deep-sea, gas, oil and coalbed reservoirs[137, 138, 180]. Therefore, the increased understanding on the effect of pCO_2 on the population dynamics and conversion rates in AHPD obtained in this study, also provide valuable insight into the origin and population dynamics of the biogenic natural gas our society relies on today.

Chapter 7

Pressure hydrolysis

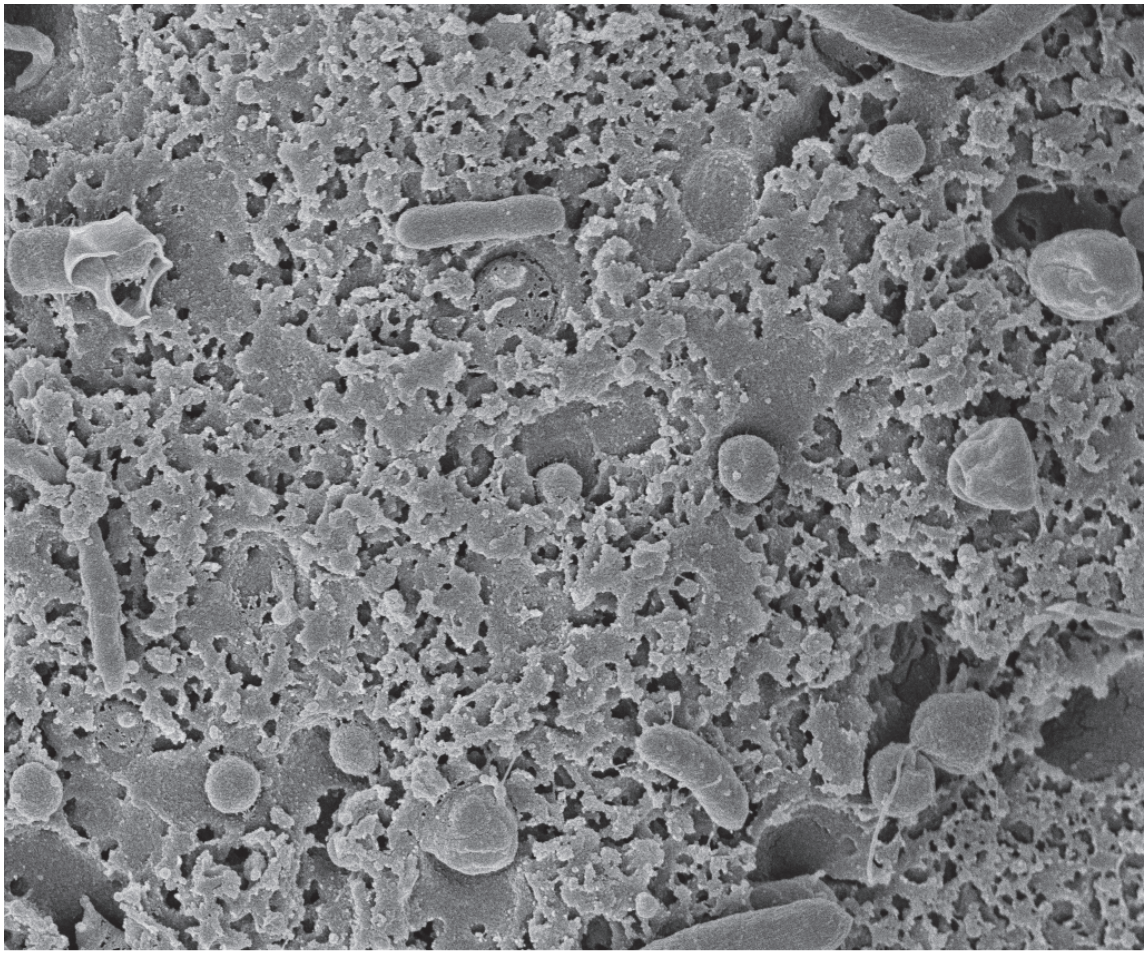

7 Gelatinisation and saccharification as rate limiting steps in autogenerative high pressure starch hydrolysis.

Abstract

Hydrolysis is generally regarded as the rate-limiting step in the anaerobic digestion of complex organic matter, governing the VFA production rate for subsequent conversion to methane. In this chapter starch hydrolysis rates in AHPD systems are studied in order to assess potential risks for VFA accumulation when digesting non-hydrolysed matter under pressure conditions. Under the anticipated practical moderate pressure conditions at 30^{o}C, experimental CH_4-content of the biogas improved from 49 to 73 ± 2 % at atmospheric and elevated pressure, respectively. Furthermore, no significant effect of pressure on the hydrolysis was found. Like under atmospheric pressure, gelatinisation was the rate-limiting step for particulate starch (0.05 d^{-1}) and saccharification for gelatinised starch (0.1 d^{-1}). Because no effect was observed on starch, an effect on the hydrolysis rate of more complex organic matter like (ligno-)cellulose is also not anticipated. When digesting complex organic matter in general it is therefore also expected that higher biogas qualities can be achieved in AHPD systems with overall methane production rates similar to conventional digestion.

Keywords

CO_2 accumulation; 2.0 MPa; particulate and gelatinised starch; hydrolysis rate constants; particle size; maltose conversion

This chapter is based on

Lindeboom, R.E.F., Ding, L., Weijma, J., Plugge, C.M. & van Lier J.B., Starch hydrolysis in autogenerative high pressure digestion: gelatinisation and saccharification as rate limiting steps, submitted to Biomass and Bioenergy

7.1 Introduction

Using acetate as the substrate autogenerated biogas pressures, between 0.5 and 9.0 MPa, containing > 95 % methane, were attained in chapters 2, 3 and 4. Owing to increased CO_2 solubility however, increased operational pressures may result in VFA accumulation, low reactor pH and deterioration of the digestion process. This was particularly relevant for experiments presented in chapters 5 and 6 with easily degradable substrates, such as monomeric sugars. Most anaerobic digestion processes for wastes and slurries are however fed with complex particulate organic matter consisting of (ligno-) cellulose, lipids and proteins. The aim of this chapter is to define the rate-limiting steps under anticipated practical AHPD conditions and thereby assess the risk of VFA accumulation for more complex substrates.

The first-order empirical hydrolysis model[29], shows that hydrolysis of complex particulate organic matter is the rate-limiting step at atmospheric pressure and ambient temperature [181, 182] and therefore reduces the risk of VFA accumulation. Carbohydrate hydrolysis typically only results in the formation of monomeric sugars[183], for which the subsequent conversion in AHPD reactors could result in a pH drop as shown in chapter 3 and 5. Within the group of carbohydrates, first-order empirical hydrolysis constants observed for starch generally are significantly higher than for (ligno-)cellulose [182]. Therefore, it is postulated that if fatty acid accumulation can be prevented with starch as a model compound, it should certainly be possible to prevent fatty acid accumulation with (ligno-) cellulose.

Multiple authors demonstrated that the particle surface area available for enzyme binding is generally determining the overall hydrolysis rate[181, 184, 185]. Gelatinisation, i.e. the conversion of crystalline starch into amorphous starch by inclusion of water molecules in the crystal lattice, is the mechanism that enlarges the physical contact area and subsequently increases the hydrolysis rates of starch and cellulose[181, 182, 186-188]. Amorphous starch is then dissolved in a much faster enzymatic step, in which dextrin and oligosaccharides are formed, i.e. the liquefaction.

In the last step of the hydrolysis, saccharification, dissolved oligosaccharides are then converted into monosaccharides by an also relatively fast enzymatic reaction [186].

Pressure treated starches were found more susceptible to α-amylase degradation than non-pressure treated starches and therefore pressure can theoretically be used, besides temperature, to increase the enzyme binding capacity of the starch [189]. Nevertheless, pressures between 100.0 and 600.0 MPa at 29 ^{o}C with a 15 minute exposure time were required to significantly enhance the gelatinisation degree of particulate starch [190]. These pressures are however way above the operational pressure of an AHPD system. Likewise, structural changes in enzymes resulting from compression or decompression of intermolecular cavities are theoretically possible [30, 191], but in order to increase the α-amylase activity of *B. licheniformis* significantly a pressure of over 10.0 MPa was required [192, 193]. Nevertheless, Francisco and Sivik [194] found that chemical effects of dissolved CO_2 improved the degree of gelatinisation by 10-15% after 20 minutes exposure by using a relatively low pressure of 8.0 MPa pCO_2 at 46^{o}C. A pCO_2 of 0.1-1.0 MPa can already significantly decrease pH depending on the buffering capacity (chapter 3 and 5). So, this may influence the gelatinisation, enzyme-substrate binding, and enzyme denaturation by strong interdependent relations between ionic strength, salt effect, pH, temperature and substrate characteristics according to the theory described by Morild [30]. Consequently, despite the fact that operational pressure and temperatures in AHPD systems can be characterised as still moderate, some impact of dissolved CO_2 concentrations up to 150 mmol L^{-1} (at 0.5 MPa) combined with a hydraulic retention time in the order of days, instead of minutes, may be anticipated.

This work describes two series of duplicate experiments. The first series of experiments aims to clarify the influence of physical pressures up to 2.0 MPa on enzyme-based hydrolysis rates of gelatinised starch using a non-adapted mixed anaerobic culture.

The second experimental series aims to determine whether particulate starch hydrolysis remains the rate-limiting step under AHPD conditions (up to 2.0 MPa and 30 ^{o}C), with little risk of VFA accumulation.

7.2 Materials & Methods

7.2.1 Experimental setups

The 1st set of experiments was performed in three 0.6 L AHPD reactors as described in more detail in chapter 4. For the 2nd set of experiments, an 8 L AHPD reactor setup (Parr Instruments, model 910908, Moline, USA) was used as described in chapter 3.

All setups were controlled at 30°C by a water bath (Julabo MP, Seelbach, Germany). Total pressure (Ashcroft A-series 1000 PSI, Stratford, USA), temperature (PT100) and pH were measured online and data was logged with Compact field point modules (cFP1804 and cFP-CB1) and stored with Labview 7.1 (National Instruments Corporation, Austin, USA) on the PC. The 0.6 L setups contained Prosense high pressure pH probes (Prosense serial nr. 34002/002, Oosterhout, The Netherlands) and the 8 L setup contained Bűchi high pressure probes (Bűchi Labortechnick AG, Flawil, Switzerland). Two six bladed impellers with a 9.8 cm diameter attached to a central stirrer shaft (Parr Instruments, type A709HC, Moline, USA) were used to stir the reactors continuously at 150 rpm for the 8 L reactor. Two 4 bladed impellers with a 3.5 cm diameter were used to stir the 0.6 L reactor at 60 rpm (Parr Instruments, type A837HC, Moline, USA) . Additionally, a calibrated milligascounter (Ritter, MGC-1 V3.0, Bochum, Germany) was connected to the gas phase of the pressure vessel to monitor volumetric gas production for experiment 8. In experiments 1, 5 and 7 a glass water lock was filled with water to allow produced gas to escape.

7.2.2 Start up and operation of AHPD reactors

7.2.2.1 Experimental I: the physical role of pressure

Liquefaction and saccharification were performed under elevated N_2 pressures to provide reference experiments (experiment 1-6) for the 2nd experimental series. To do so, 0.6 L reactors were inoculated with 75 g wet anaerobic granular sludge (~13.5 g VSS L^{-1}) in exp. 1-4, and 25 g of fresh inoculum (~4.5 g VSS L^{-1}) in exp. 5 and 6 from a full-scale expanded granular sludge bed (EGSB) reactor treating waste water from a

fruit-juice processing factory (Riedel Friesland Campina, Ede, The Netherlands). This sludge is referred to as Riedel sludge. Granular starch was gelatinised in boiling water, cooled down to 30 ^{o}C and then added to the reactors at a final concentration of 3.64 g L^{-1} or 4.3 g COD L^{-1}. Experiments 1-4 were fed on 3 consecutive days at a N_2-pressure of 0.1, 0.5, 1.0 and 2.0 MPa, respectively. 24 hours after each substrate addition, the sludge was settled and the supernatant was removed in order to reduce the VFA concentration and possible pH decrease. The sludge was then fed with fresh substrate and liquid medium. Due to reusing the inoculum in subsequent experiments 1-4, potentially the sludge adapted or increased in concentration over time, introducing uncertainty when comparing between experiments 1-4. In order to reduce this uncertainty in sludge effects over time experiments 5 and 6 were operated simultaneously at atmospheric pressure and 2.0 MPa of nitrogen pressure, respectively. Furthermore, the experimental period for intermediate measurements was prolonged by inoculating experiments 5 and 6, with three times less sludge. As a result the increased substrate-inoculum ratio gave additional insights in the sludge specific conversion rates.

7.2.2.2 Experiment II: Starch conversion under actual AHPD conditions

In order to study starch hydrolysis under actual AHPD conditions, the 8L-reactor was fed with 3.2 g L^{-1} particulate starch (Merck amylodextrin 9005-84-9) for experiment 7, 8 and 9. The starch granules had a median particle size of 35 µm as determined by particle size distribution measurement using laser diffraction analysis (Coulter LS230, Beckham Coulter, USA) using a method described elsewhere [195]. For experiment 10 starch granules were gelatinised in 50 mL boiling water, which was left to cool to 30 ^{o}C, before it was added to the reactor. The inoculum consisted of 6 L (~ 4 g VSS L^{-1}) of suspended AHPD adapted biomass cultivated on fed batch glucose feedings for over 1 year. The reactor was then filled to a total liquid volume of 6.5 L by adding 0.5 L concentrated nutrient medium (Table 2-1).

.

Table 7-1: overview of starch hydrolysis experiments

Name*	Substrate (mmol L^{-1})	Pressure range (MPa)	Gas type	Substrate type	Inoculum Type	Concentration (gVSS L^{-1})
Exp. 1	22.5	0.1	N_2	Gelatinised	EGSB granular inoculum	13.5
Exp. 2	22.5	0.5	N_2	Gelatinised	From Exp. 1	13.5
Exp. 3	22.5	1.0	N_2	Gelatinised	From Exp. 2	13.5
Exp. 4	22.5	2.0	N_2	Gelatinised	From Exp. 3	13.5
Exp. 5	22.5	0.1	N_2	Gelatinised	EGSB granular inoculum	4.5
Exp. 6	22.5	2.0	N_2	Gelatinised	EGSB granular inoculum	4.5
Exp. 7	20	0.1	CH_4/CO_2	Particulate	Glucose grown, Pressure adapted **	4.0
Exp. 8	20	0.1-0.5	CH_4/CO_2	Particulate	**	4.0
Exp. 9	20	1.0-1.5	CH_4/CO_2	Particulate	**	4.0
Exp. 10	20	1.0-1.5	CH_4/CO_2	Gelatinised	From granular experiments	4.0

*All experiments were performed in duplicate ** order of duplicate experiments 7, 8 and 9 was 0.1, 0.1-0.5, 1.0-1.5, 0.1-0.5, 0.1, 1.0-1.5 MPa.

To study starch degradation at elevated pressure in experiments 9 and 10, the reactor was started at atmospheric pressure and then manually pressurised by using a mixture of 50% CO_2 and 50% CH_4 to 1.6 MPa. Afterwards during 6 hours, additional gas samples were taken to correct the CH_4 production for dissolution of the manually added CH_4 and CO_2.

7.2.3 Analytical methods

Total Suspended Solids (TSS) and Volatile Suspended Solids (VSS) were determined according to Standard Methods [57].

Gas composition was determined by taking biogas samples at the end of each run and analysing them by gas chromatography as previously described (chapter 4). Biogas composition was corrected for flush gas (N_2) and water vapour. To calculate the hydrolysis rate constants for experiments 7-10, it was assumed that 180 g of starch could produce 3 moles of CH_4 and by this a maximum CH_4 production for each experiment was calculated. Subsequently, the cumulative CH_4 in time was subtracted from the maximum CH_4-production for each data point in time. Then the remaining CH_4 production potential was assumed to represent the remaining starch, because methane production was limited by starch hydrolysis and data showed intermediate glucose and VFA conversion were much faster. Finally, an exponential function was plotted through the calculated data points to determine the first order hydrolysis constant. Differences in first order hydrolysis constants resulting from minor temperature fluctuations of ± 1^oC for experiments 7, 8, 9 and 10 and ± 3^oC for the duplicate of experiment 8 were corrected with Arrhenius to 30^oC experiments using an E_a= 64 kJ mol^{-1} as described in Veeken, Kalyuzhnyi, Scharff and Hamelers [185].

VFA were determined by gas chromatography (Hewlett Packard 5890 series II, Palo Alto, USA) as described in chapter 2 and 3. Additionally, maltotriose, maltose, glucose, succinic acid, lactic acid, formic acid and ethanol were measured by High Performance Liquid Chromatography (HPLC). Samples were prepared by centrifugation at 9,300 rcf. Supernatant was diluted and acidified with concentrated H_2SO_4 solution to pH < 3. Acidified samples were pumped, using 1.25 mM H_2SO_4 as eluent at a flow rate of 0.6 mL min^{-1} with a HPLC pump (Dionex High Precision model 480) through an Alltech OA-1000 column (length=300 mm, internal diameter =6.5 mm, partnr. 9064) at 60^oC and 6.0-6.5 MPa and measured by means of an refractive index (RI) detector (Shodex RI, Showa Denko KK, Kawasaki, Japan).

Gelatinised starch was measured by a photometric cuvet test (Dr. Lange LCK 357) using the manufacturer protocol.

The molecular weight distribution of hydrolyzed starch samples was measured by high-performance size-exclusion chromatography (HPSEC) on a Dionex Ultimate 3000 system (Dionex, Sunnyvale, CA) equipped with a set of four TSK-Gel super AW

columns (Tosoh Bioscience, Tokyo, Japan) in series, guard column (6 x 40 mm), and separation columns 4000, 3000, and 2500 (6 x 150 mm). Elution took place at 40^0C with filtered aqueous 0.2 M sodium nitrate at a flow rate of 0.6 mL min^{-1} followed by refractive index detection (Shodex RI, Showa Denko K.K., Kawasaki, Japan).

The oligosaccharides composition, i.e. maltose to maltohexaose, was determined in more detail by High Performance Anion Exchange Chromatography (HPAEC) using an ICS-3000 Ion Chromatography HPLC system equipped with a CarboPac PA-1 column (2 × 250 mm) in combination with a CarboPac PA guard column (2 × 25 mm) and a pulsed electrochemical detector in pulsed amperometric detection mode (Dionex, Sunnyvale, USA). Dextrins, higher oligosaccharides and CH_4 were not quantified in exp.1- 4 and therefore the mass balance could not be closed entirely in these experiments. A flow rate of 0.3 mL min^{-1} was used and the column was equilibrated with 100 mM NaOH. The following gradient of sodium acetate in 100 mM NaOH was used: 0-0.5 min at 0 M; 0.5–40 min at 0–0.1 M; 40–60 min at 0.1–0.4 M; 60–75 min at 0.4–1.0 M; 75–80 min at 1 M. Samples were taken from the liquid sampling port of the reactor and centrifuged at 9,300 rcf for 5 minutes, then the supernatant was pipetted into a HPLC vials and diluted 5 times with demi-water. Glucose, malto-oligosaccharides, and dextrin (Sigma Aldrich) were used as standards for identification.

Light microscope images of starch particles were made with a Nikon eclipse E400 (Nikon, Japan), using different Nikon lenses, CFI plan fluor DLL 40x with phase condenser annulus 2 or CFI plan fluor DLL 100x with a phase condenser annulus 3. A Nikon C-SP 754535 polarisation filter was used to obtain the polarised light images, using the same lenses with bright field annulus. Photographs were recorded with a Nikon Digital Sight Camera DS 5M connected to Nikon eclipse software in a PC.

Samples for Field Emission Scanning Electron Microscopy (FESEM) were centrifuged for 10 minutes at 4,651 rcf. Hereafter, supernatant was replaced by a 2.5% glutaraldehyde solution for fixation during 1 hour (at 4^oC). Afterwards samples were dried in a series of ethanol 50-75-90-95-100% and then transferred to acetone. To

prevent the samples from shrinking due to removing the acetone in air, supercritical carbon freeze drying procedure as described in [92] was used. Afterwards samples were glued to a brass sample holder using iridium glue. Then samples were sputter-coated with iridium. The Field Emission Scanning Electron Microscope (Fei Magellan FESEM) was connected to an Oxford Aztec EDX and operated at 2 kV and a 6.3 pA current. Scattered Electrons were detected by Through Lens Detection (TLD) at a Working Distance of 1.9 and 5.1 mm.

7.3 Results

7.3.1 The physical effect of pressure on enzyme-based kinetics

Experiments 1-4 were performed to acquire insight in the potential roles of physical pressure on the enzyme-based liquefaction and saccharification with unadapted Riedel inoculum using gelatinised starch. Figure 7-1 and table 7-2 reveal that the estimated 1st-order liquefaction constants for experiment 1, 2, 3 and 4 were 7.2, 8.8, 10.4 and 9.2 h^{-1}, respectively. So, the physical effect of pressure up to 2.0 MPa was marginal.

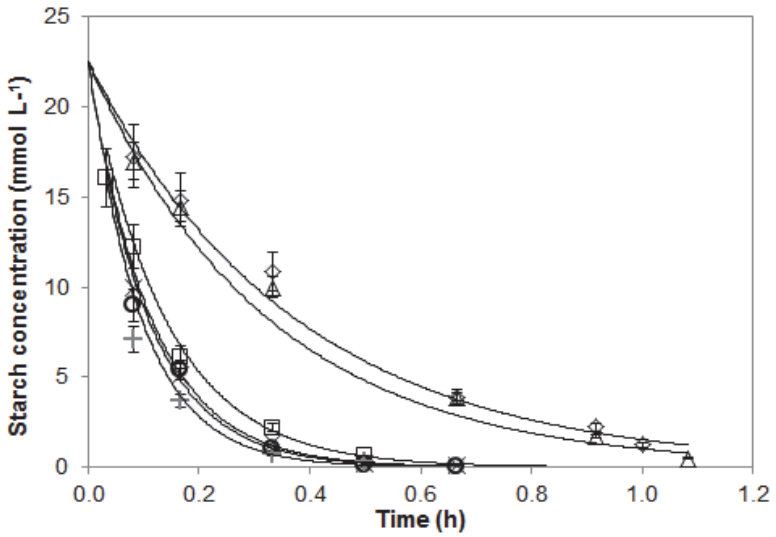

Figure 7-1: Overview of starch degradation rates for exp. 1 under 0.1 MPa pN_2 (□), exp. 2 under 0.5 MPa pN_2 (o), exp. 3 under 1.0 MPa pN_2 (x) and exp. 4 under 2.0 MPa pN_2 (+) using 13.5 g VSS L^{-1} and exp. 5 under 0.1 MPa pN_2 (◊) and exp. 6 under 2.0 MPa pN_2 (Δ) using 4.5 g VSS L^{-1}

Experiments 5 and 6 showed an average liquefaction rate constant of 2.7 and 3.0 h^{-1}. It is noteworthy, that the threefold decrease in inoculum concentration from 75 g wet

sludge L^{-1} to 25 g wet sludge L^{-1} also resulted in a threefold decrease in rate constant. So, despite the physical pressure up to 2.0 MPa the enzyme and biomass concentration were rate-limiting for gelatinised starch, similar to conventional digestion processes [183].

Table 7-2: Overview of experimental results for starch degradation under AHPD conditions

Name	Estimated rate equation	R^2	Rate-limiting step	pH	Biogas composition	
					CH_4 %	pCO_2 (MPa)
Exp. 1	$22.5e^{-7.2t}$	0.9966	Saccharification	7.0 ± 0.2	-	-
Exp. 2	$22.5e^{-8.8t}$	0.9905	Saccharification	7.0 ± 0.2	-	-
Exp. 3	$22.5e^{-10.4t}$	0.9832	Saccharification	7.0 ± 0.2	-	-
Exp. 4	$22.5e^{-9.2t}$	0.9228	Saccharification	7.0 ± 0.2	-	-
Exp. 5	$22.5e^{-2.7t}$	0.9818	Biomass concentration	7.0 ± 0.2	-	-
Exp. 6	$22.5e^{-3.1t}$	0.9519	Biomass concentration	7.0 ± 0.2	-	-
Exp. 7	$20e^{-0.002t}$	0.9848	Gelatinisation	7.3 ± 0.1	49	0.05
Exp. 8	$20e^{-0.002t}$	0.9967	Gelatinisation	6.6 ± 0.1	73	0.10-0.20
Exp. 9	$20e^{-0.002t}$	0.9963	Gelatinisation	6.3 ± 0.1	73	0.40-0.80
Exp. 10	$20e^{-0.004t}$	0.999	Saccharification	6.2 ± 0.1	72	0.40-0.80

[t] is expressed in hours

Profiles of the liquefaction products, i.e. maltose up to maltohexaose, and the saccharification product glucose for experiments 1, 2, 3 and 4 are shown in Figure 7-2. Results indicated that the effect of pressure on type of intermediates formed was limited, despite the slightly elevated maltose concentrations at 2.0 MPa. Glucose concentrations remained stable and were comparable for pressurised and atmospheric experiments i.e. 0.5 ± 0.05 mmol L^{-1} over the first 6 hours. For higher oligosaccharides, i.e. maltopentaose and maltohexaose, a typical first order hydrolysis rate equation fitted the data points at concentrations below 0.5 and 0.3 mmol L^{-1}. Besides, concentrations of maltopentaose and maltohexaose in experiments 3 and 4,

i.e. 1.0 and 2.0 MPa, respectively, were significantly lower than in experiment 1 which was performed under atmospheric pressure.

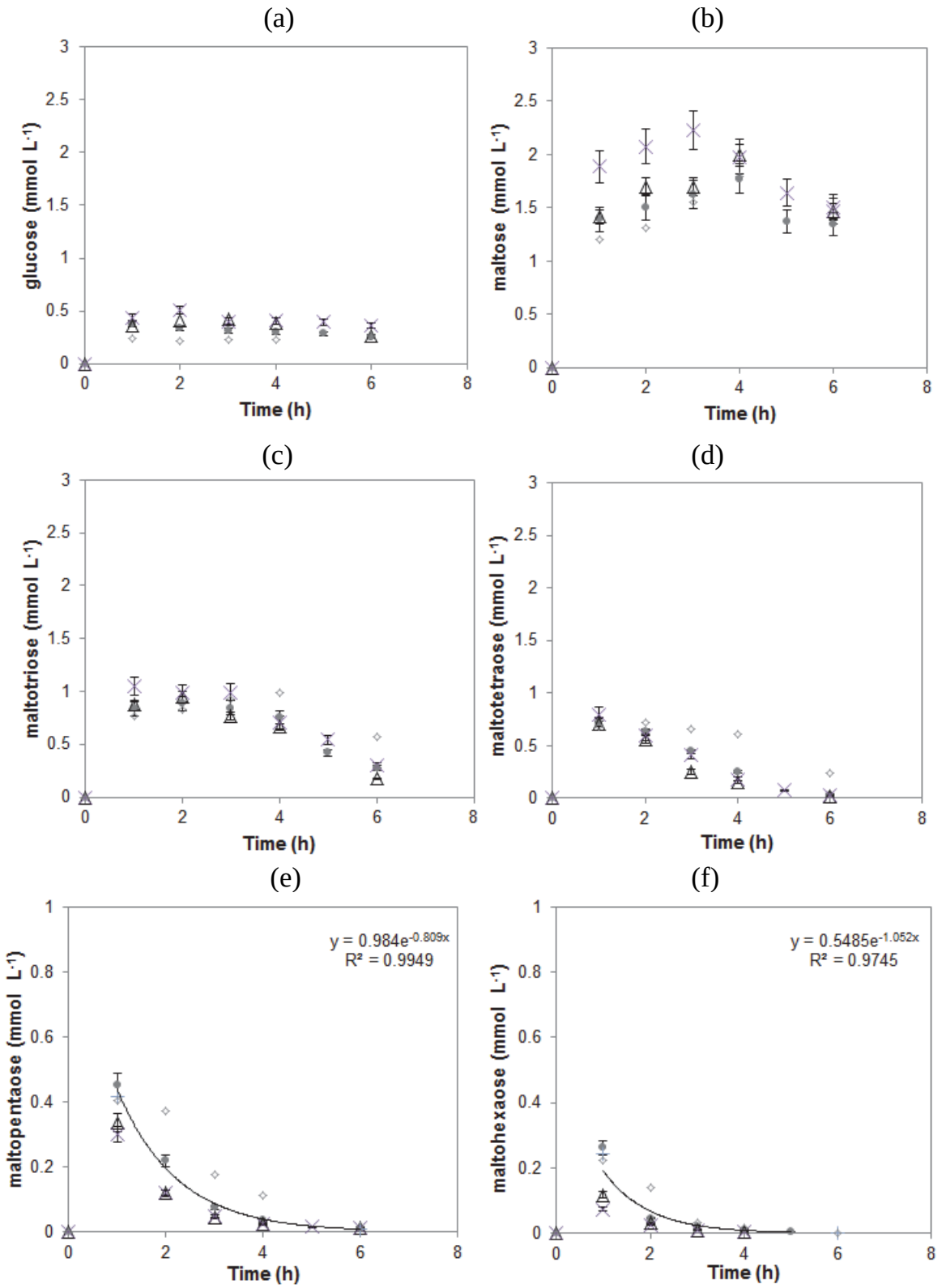

Figure 7-2: Liquefaction and saccharification product profile of experiments 1 (●), 2(◊) 3 (Δ) and 4 (x) over time (a) glucose, (b) maltose (c) maltotriose, (d) maltotetraose, (e) maltopentaose and (f) maltohexaose

However, because experiments 2, 3 and 4 were performed with the sludge from experiment 1, observed differences could not solely be attributed to differences in pressure. Maltotetraose showed an initial peak concentration of 0.8 ± 0.05 mmol L^{-1} and a gradual decline in concentration afterwards. Maltotriose was present in a constant concentration of 1.0 ± 0.05 mmol L^{-1} and started decreasing in concentration after 4 hours. Maltose, in contrast to the other measured oligosaccharides, reached a significantly higher maximum concentration of 1.5 to 2.2 ± 0.05 mmol L^{-1} after 3 hours and afterwards declined in concentration. The elevated molar concentration of maltose, maltotriose and maltotetraose compared to the molar concentration profile of glucose and especially the presence of a distinct concentration peak in the maltose profile showed that saccharification was the overall rate-limiting step.

The molecular size distribution as measured by high performance size exclusion chromatography for experiments 1-4 showed relatively low concentrations of 180 Da compounds compared to molecules of 360 and 540 Da and further supported these findings(figure 7-3).

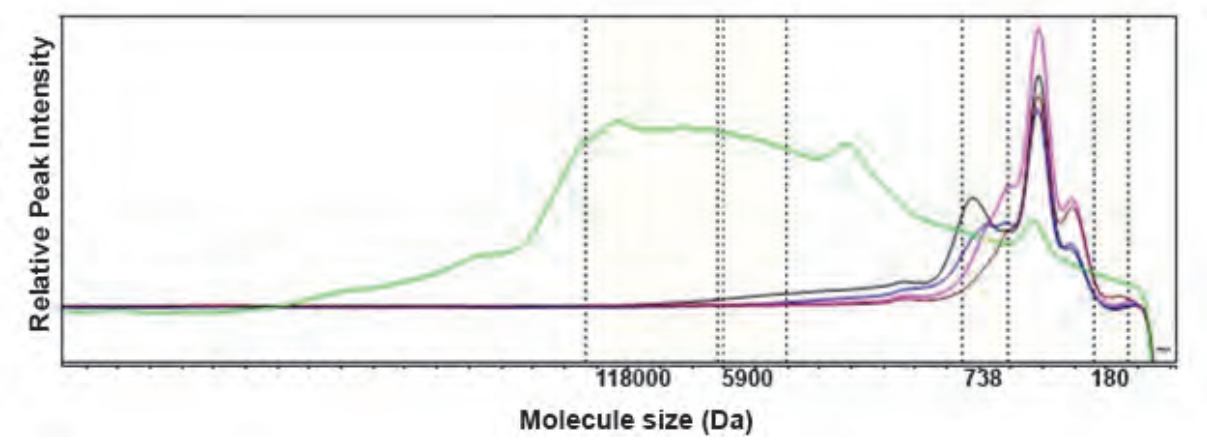

Figure 7-3: Overview of molecular size division of reference starch (green) and after 1 hour hydrolysis under a pN_2 head space of 0.1 MPa (black), 0.5 MPa (blue), 1.0 MPa (pink) and 2.0 MPa (brown) of experiments 1, 2, 3 and 4, respectively.

7.3.2 Starch conversion under actual AHPD conditions

With increasing pressure, the final pH decreased from 7.3 at atmospheric pressure to 6.6 at 0.5 MPa, 6.3 and 6.2 at 1.5 MPa (Table 7-2) for experiments 7, 8, 9 and 10, respectively. Despite the lower pH, the biogas composition significantly improved

from experiment 7 to experiment 8, 9 and 10, with a maximum CH_4-content of 49, 73, 73 and 72 ± 2 %, respectively (Table 7-2). Therefore, it can be concluded that from the perspective of biogas quality AHPD operation was beneficial. However, the cumulative methane production and the methane production rate were similar for all pressures applied (Figure 7-4a exp.7, 8 and 9).

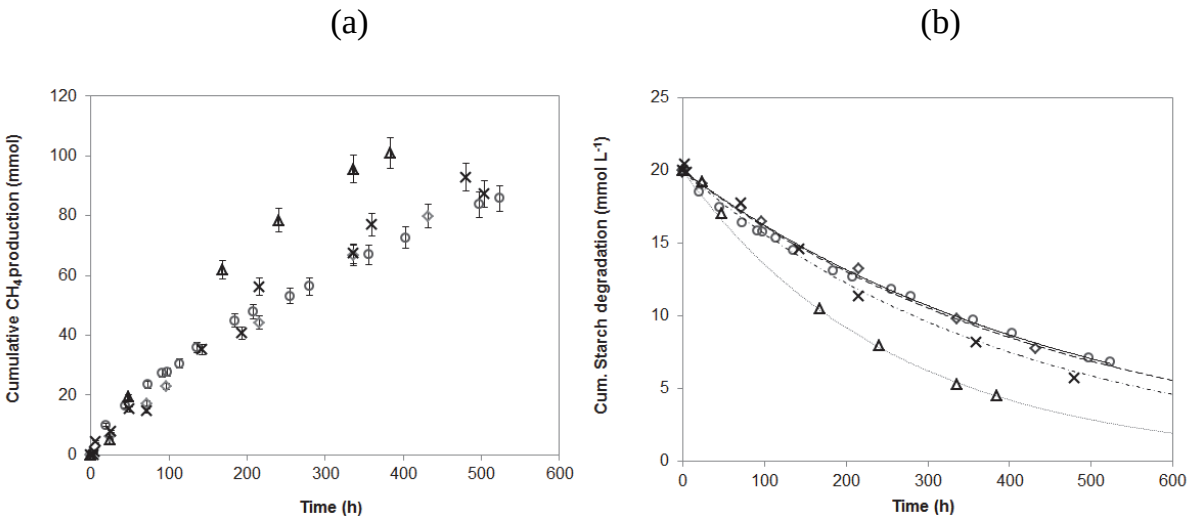

Figure 7-4: Overview of (a) cumulative CH_4 production and (b) converted into cumulative starch degradation with (□) experiment 7, (◊) experiment 8, (x) experiment 9 and (Δ) experiment 10.

Both the CH_4 production rate and cumulative amount were significantly higher with gelatinised starch compared to granular starch. Although CH_4 production potential was assumed equal for gelatinised and particulate starch, it was later confirmed that crystalline starch was present after 8 days of pressure operation (Figure 7-6). This strongly indicated a poor biodegradability of at least a part of the dosed particulate starch. Figure 7-4b shows the estimated starch concentration against time and in Table 7-2 the estimated hydrolysis rate constants for experiments 7, 8 and 9 showed a practically equal value of 0.002 ± 0.0005 h^{-1}, or 0.05 d^{-1}. This coincided with a maximum measured methanogenic activity of 0.13 g COD-CH_4 g^{-1} VSS d^{-1}, based on the original inoculum concentration. Overall these values are also comparable to reported cellulose degradation rates [182]. However, for experiment 10 the overall CH_4-production rate had doubled to 0.1 d^{-1} by using gelatinised instead of particulate starch. Consequently also the maximum measured methanogenic activity had doubled to 0.27 g COD-CH_4 g^{-1} VSS d^{-1}.

The time-profile of intermediate compounds also showed a clear distinction between particulate (Figure 7-5a and c) and gelatinised starch (Figure 7-5b and d).

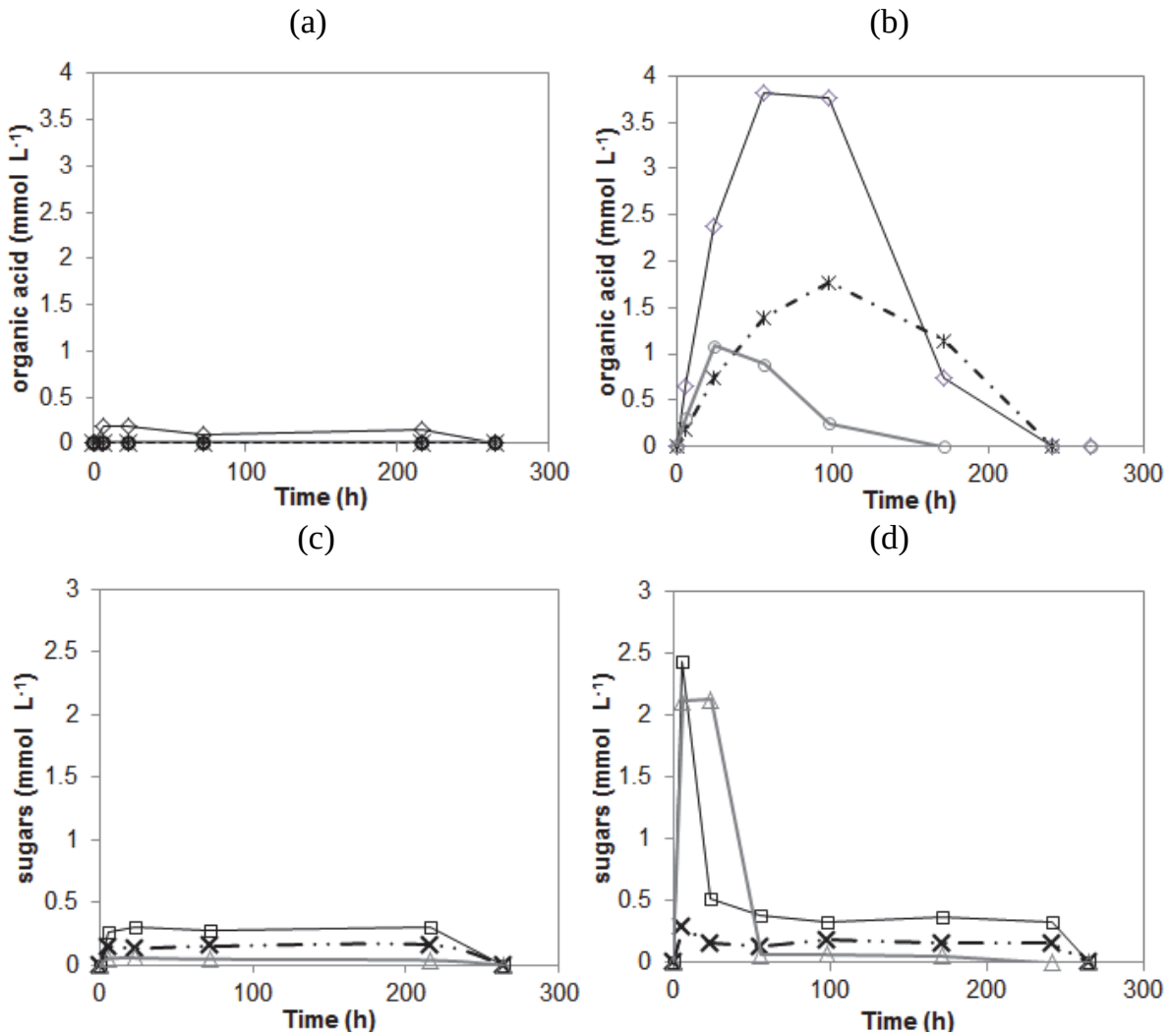

Figure 7-5: Maximum observed acetate (◊), propionate (*), succinate (o) (a and b), glucose (Δ), maltose (□) and maltotriose (x) (c and d) concentrations between 1.0-1.5 MPa and pH~6.3 when feeding 20 mmol L^{-1} of particulate starch in experiment 9 (a and c) and gelatinised starch in experiment 10 (b and d).

In experiment 9 intermediate VFA remained < 0.25 mmol L^{-1}, whereas for the gelatinised starch (experiment 10), acetate, propionate and succinate concentrations all exceeded 1 mmol L^{-1} within 96 hours after starting the experiment. Glucose concentrations were below 0.1 mmol L^{-1} in experiment 9, but showed accumulation up to 2 mmol L^{-1} in experiment 10. Maltose and maltotriose were present in average concentrations below 0.5 mmol L^{-1} in both experiments, but maltose showed a peak value at the start of the experiment 10 of 2.5 mmol L^{-1}, respectively. Thus, similar to the results presented for gelatinised starch under a pN_2-atmopshere, saccharification

was the rate-limiting step. Despite of intermediate organic acid concentrations being higher, these were readily metabolised, overall resulting in a doubled CH_4-production rate. However, although additions of 20 mmol L^{-1} of gelatinised starch did not result in VFA accumulation, higher slug additions will generate more oligosaccharides and thus glucose per unit of time, assuming the biomass concentration is not rate-limiting like in experiments 5 and 6. This could depending on the maximum rate of saccharification and methanogenic activity potentially result in similar VFA accumulation as described in chapter 6.

In Figure 7-6 it was found by light microscopy that the crystalline nature of starch particles did not disappear over a period of 8 days. The Maltese cross, the typical sign of crystalline starch [196] can be observed in the polarised light images. It was also noticed that similar size and crystalline structure of particles was found after 0, 4 (not shown) and 8 days. For samples present for longer term inside the reactor visually significantly fewer particles with the Maltese cross could be found. Additionally, the surfaces of unreacted and reacted starch granule are shown in Figure 7-6e and f. The particle diameter was similar, whereas the initially smooth surface of the starch granule became porous and micro-organisms can be seen penetrating into the granules after 4 days of exposure to the reactor environment.

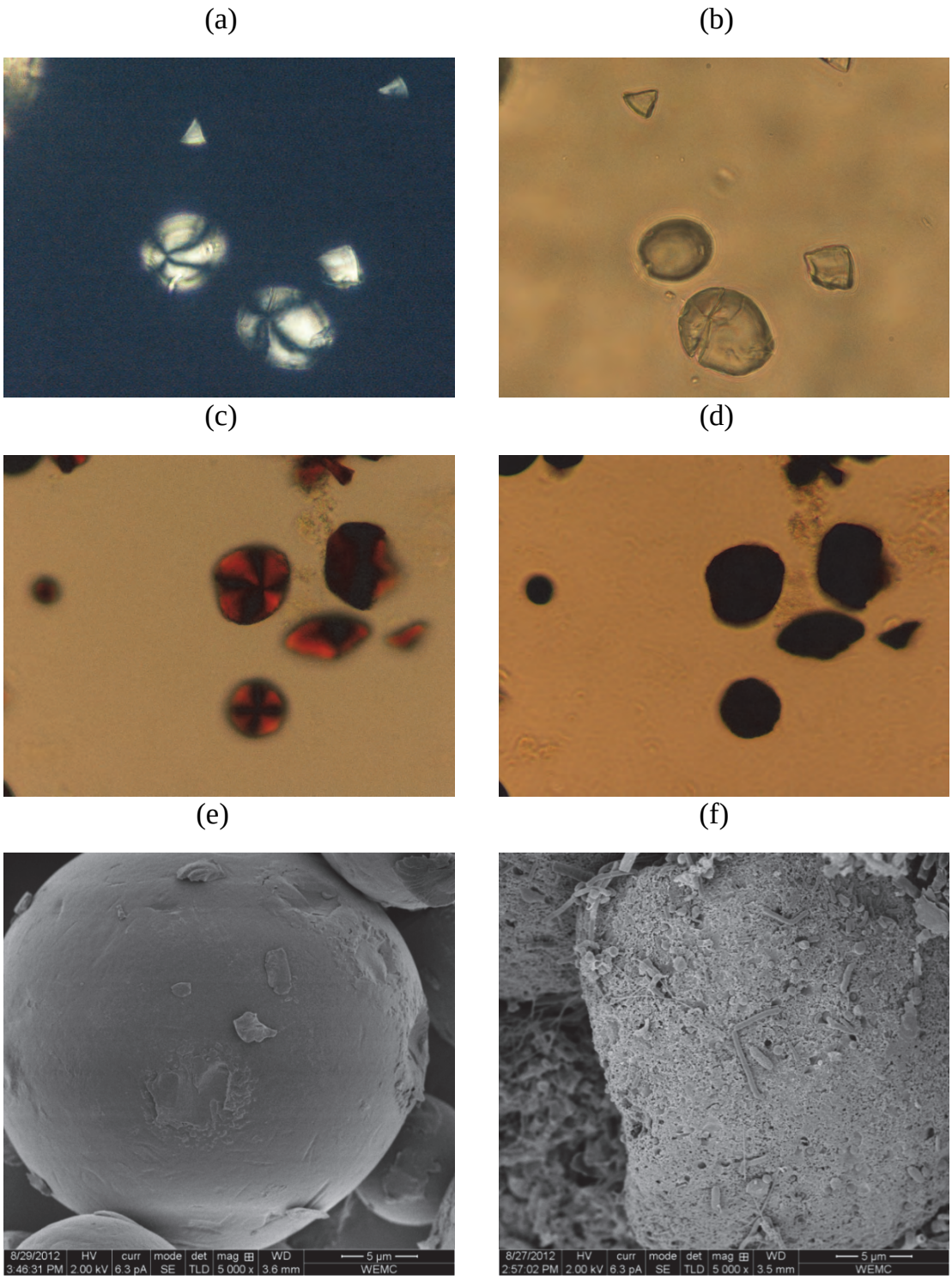

Figure 7-6: Representative starch microscope images after (a, b) 0, (c, d) 8 days (reacted with I_2) with (a and c) polarised light (b, d) phase contrast light. Starch Granule surface structure (e) reference and (f) exposed to reactor conditions for 4 days

7.4 Discussion

In the current work it was found that pressure up to 2.0 MPa and mesophilic conditions had at most only a marginal influence on starch conversion rates. Conversion rates were apparently determined by the particle structure for particulate starch and by biomass concentration for gelatinised starch. Both were similar to atmospheric conditions.

Consequently, it can be concluded that the overall starch hydrolysis rates in an AHPD process might well be comparable to conventional anaerobic digestion. Based on our results the biogas quality significantly improved from atmospheric 49 ± 2% CH_4 and 51 ± 2% CO_2 up to maximum of 73 ± 2% CH_4 and 27 ± 2% CO_2 at 0.5 MPa. At pressures exceeding 0.5 MPa, no further improvement of biogas composition was obtained. Furthermore, due to the rate-limitations posed by hydrolysis results showed that fatty acids did not accumulate and did not reduce $[HCO_3^-]/CO_2$ ratio, keeping the pH stable. Under similar conditions using glucose as substrate, propionate accumulation was observed due to elevated pCO_2 in chapter 6. This means that acid neutralising capacity based pH-control strategies in chapter 3 are of less importance with particulate substrates. No direct effect of pressure up to 2.0 MPa was observed in this work and based on literature pressure does have the potential to influence the three main steps, gelatinisation, liquefaction and saccharification required for starch hydrolysis [30, 194, 197, 198].

7.4.1 Gelatinisation

Our results show that physical pressures up to 1.6 MPa are insufficient to physically enhance gelatinisation and also no indirect effect of CO_2 was observed. This is in line with other work, in which significant physical effects of pressure were not found below 100 MPa [30, 190, 194, 198, 199]. From our results however, gelatinisation of particulate starch was the slowest step of the overall CH_4 production under the imposed conditions, with an overall conversion rate of 0.05 d^{-1}.

In line with the hydrolysis mechanisms described by Oates [200] Figure 7-6 visually showed that starch particles digested in the reactor for several days increased in

surface area, by becoming porous. Further increase in particle surface area could then be obtained by using moderate pCO_2 to force dissolved CO_2 into porous starch granules [201]. Once inside the granule, due to a change in the carbonate equilibrium by decompression, temperature or pH change, conditions similar to CO_2 or steam explosion [202] could be obtained, disrupting the particle structure. As a consequence, the increased particle surface area could then result in higher overall CH_4 production. It should be noticed however, that this may be harmful for the micro-organisms and could affect subsequent digestion stages.

7.4.2 Enzyme-based hydrolysis

Our results show that with gelatinised substrates, saccharification, i.e. the conversion of maltose and maltotriose to glucose was the rate-limiting step with pressures up to 2 MPa. Physical pressure was therefore not found to have significant influence in this pressure range, which is in line with literature [193]. Although it was only the aim of the experiments to define the rate-limiting steps under anticipated AHPD conditions, it is noteworthy that different (thermophilic) archaeal and bacterial enzymes involved in starch hydrolysis have different pH optima, ranging from pH 2.0 - 9.0 [203-205]. Moreover, the α-amylase and pullulanase isolated from a single organism, *Thermotoga maritima* (MSB8), had pH optima of 7.0 and 6.0, respectively [206]. In this perspective it is highly interesting that in the used pressure-adapted inoculum (chapter 6) a *Kosmotoga*-like organism dominated the bacterial population and the genome of the versatile bacterium *Kosmotoga olearia* contains both α-amylase and pullulanase coding genes [207]. Furthermore, pullulanase is required for converting side-branched chains (amylopectin) into amylose, making it available for the relatively faster α-amylase enzyme [208]. Operating an AHPD reactor at pH 6, near the pKa of HCO_3^-, may thus optimize pullulanase activity, thereby converting more amylopectin into amylose. Additionally, increase of 22% and 43% in alpha-amylase and protease excretion was reported for a mixed culture cultivated under increased pCO_2 [209]. Therefore, it would be interesting to study the effect of pCO_2 on organisms cultivated in AHPD to determine whether enzyme-based hydrolysis rates can be optimised.

It should however be emphasised that addition of 20 mmol gelatinised starch L^{-1} resulted in a short period in which elevated VFA concentrations were present. As a consequence, enhancing the liquefaction or saccharification rate in AHPD without simultaneously enhancing methanogenic activity may result in acidification and reactor upsets, especially at more concentrated periodical substrate additions.

7.4.3 Outlook: pressurised hydrolysis of different complex organic material

This study was carried out with specific model substrates, i.e. particulate starch and gelatinised starch. Extrapolation of these results to more complex organic material is desirable, but not straightforward due to the different nature of proteins, lipids and carbohydrates. The most straightforward extrapolation can be made for carbohydrates. For cellulose in particular, literature showed that cellulose degradation in the deep sea also required a gelatinisation step to dissolve the substrate [197]. In line with the more complex molecular structure however, even higher pressures than reported for starch were required to enhance gelatinisation. So, based on the even more complex molecular structure of lignocellulose, we consider it unlikely that degradation can be enhanced by applying moderate AHPD conditions. Despite the fact that, lipids and proteins also require a physicochemical dissolution step to make the substrate accessible for hydrolytic enzymes, the liquid surface interaction is too different to make a good extrapolation based on the results obtained with starch. Therefore, additional studies are required. With regard to the effect of pressure on enzyme based hydrolysis we found that, like in atmospheric digestion, biomass concentration is determining the slowest step, i.e. the saccharification rate. No evidence was found under the imposed AHPD conditions that the hydrolytic activity of the biomass was affected on the short term. This study therefore shows no indication that this will be different for lipid or protein hydrolysis.

7.5 Concluding remarks

Under the anticipated moderate pressure conditions at 30^{o}C no effect of pressure on the hydrolysis was found. Like under atmospheric pressure, gelatinisation was the rate-limiting step for particulate starch and saccharification for gelatinised starch and thus the overall methane production rates in AHPD are expected to be similar to conventional digestion. Additionally, it was found that the rate-limitation set by the hydrolysis, reduced the risk of acidification in AHPD by keeping intermediate VFA concentrations relatively low. Because the biogas quality was improved significantly from 49 to 73 % CH_4 at 0.5 MPa and remained stable at higher pressures, AHPD operation is considered beneficial for the overall digestion of starch and potentially for more complex organic material in general.

Chapter 8

Summary and General discussion

8 Summary, general discussion and outlook

8.1 Summary and general discussion

8.1.1 Anaerobic treatment for waste stabilisation and energy recovery

The widespread use of household digesters in India and China proofs that the potential of biogas production from organic matter has been applied for centuries. With the development of high rate anaerobic reactor systems in the 70's and 80's, anaerobic digestion (AD) became an alternative to aerobic waste water treatment for stabilising organically polluted waste waters. Under temperate climate conditions, such as in the Netherlands, full scale high rate anaerobic waste water treatment is generally only applied for industrial waste water streams that are rich in organic matter. With regard to domestic or municipal waste water AD is, thus far, restricted to warm climates[210]. In addition, anaerobic treatment is largely applied for the digestion of primary and secondary sludge, stabilisation of pig and cow manure, and digestion of agricultural and agro-industrial wastes [211]. In the Netherlands, direct anaerobic sewage treatment is not applied, because the organic fraction in municipal waste water is too diluted and temperatures are too low for effective treatment. Moreover, considering the C/N ratio in our domestic sewage, anaerobic pre-treatment would also impact the biological nutrient removal capacity of our sewage treatment plants, which are designed on conventional nitrogen removal, using nitrification-denitrification. Provided alternative approaches for N removal or N recovery are available, anaerobic stabilisation of sanitary waste waters under Dutch conditions is only possible when sewage waters are up-concentrated or when the produced black waters, i.e. human excreta and urine, are separately collected by e.g. applying vacuum sewer systems for slurry conveyance [12]. Digestion experiments performed with concentrated black water indicated that conversion of all produced biogas in combined heat and power (CHP) systems could result in a total energy production of 140 MJ p^{-1} y^{-1} of which 56 MJ p^{-1} y^{-1} as electricity and 84 MJ p^{-1} y^{-1} as additional heat. Furthermore, it is estimated that by addition of solid kitchen refuse, this amount could be doubled[212]. However, the relatively low quality of the produced biogas limits the use of biogas in

particularly the decentralised applications, where generated biogas flows are below 100 m^3 h^{-1}. In fact, existing external biogas upgrading technologies are only economically feasible at larger scale [8, 9]. This thesis focusses on in-situ biogas upgrading by making use of the differences in gas solubility between CH_4 and CO_2 as described by Henry's law, resulting in higher CH_4 concentrations in the produced biogas at high pressures compared to atmospheric digestion systems. The digestion process is denominated as Autogenerative High Pressure Digestion (AHPD).

8.1.2 Anaerobic digestion at elevated pressure

Conventional atmospheric anaerobic digestion is studied worldwide, but there is limited and only scattered literature available on pressurised digestion [18, 21, 41, 62]. Based on the available literature and the work performed in this thesis, the graphical presentation used in the introduction was adjusted (Figure 8-1).

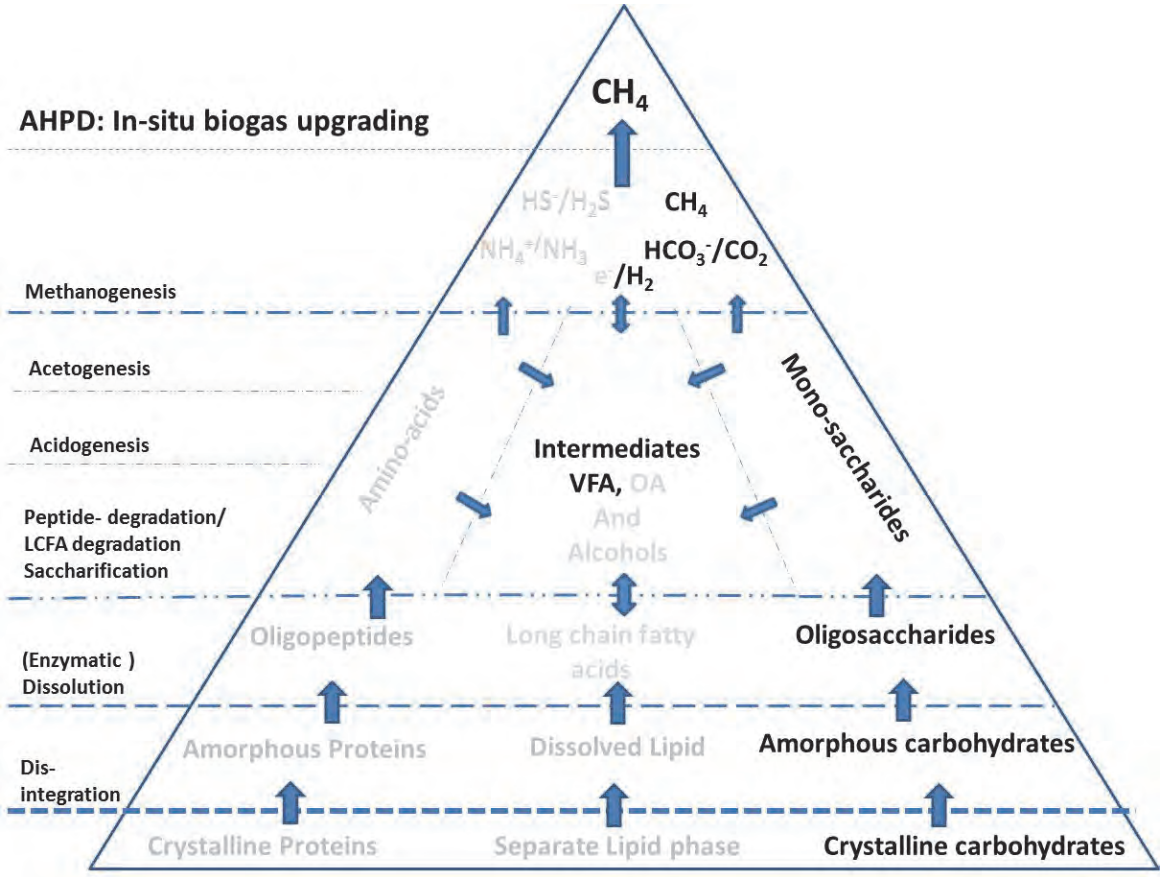

Figure 8-1: Overview of anaerobic digestion updated with topics discussed in this thesis on autogenerative high pressure digestion (in bold). Other features of the figure are explained in Fig. 1.1 (chapter 1)

Figure 8-1 also includes in-situ biogas upgrading as a separate stage. Furthermore, the topics that have been studied in this thesis and that were all related to the carbohydrate and volatile fatty acid digestion are depicted in black.

Experimental results showing a total pressure in the digester of 9.0 MPa and a CH_4-content exceeding 95%, illustrate the bio-technical feasibility of the AHPD process. In addition, the very low H_2O content of the in-situ compressed biogas, as calculated from the Clausius Clapeyron equation (Eq. 1-17) [36], is a big advantage when gas grid injection is considered.

As discussed in chapter 3 however, it must be realised that also CH_4 follows Henry's law and will dissolve to a large extent in the pressurised liquid. Figure 8-2 therefore shows the autogenerated pCH_4 potential at various COD concentrations and the relative CH_4 dissolution (as % of total production) versus the liquid to total volume ratio during batch digestion of the substrate.

(a) (b)

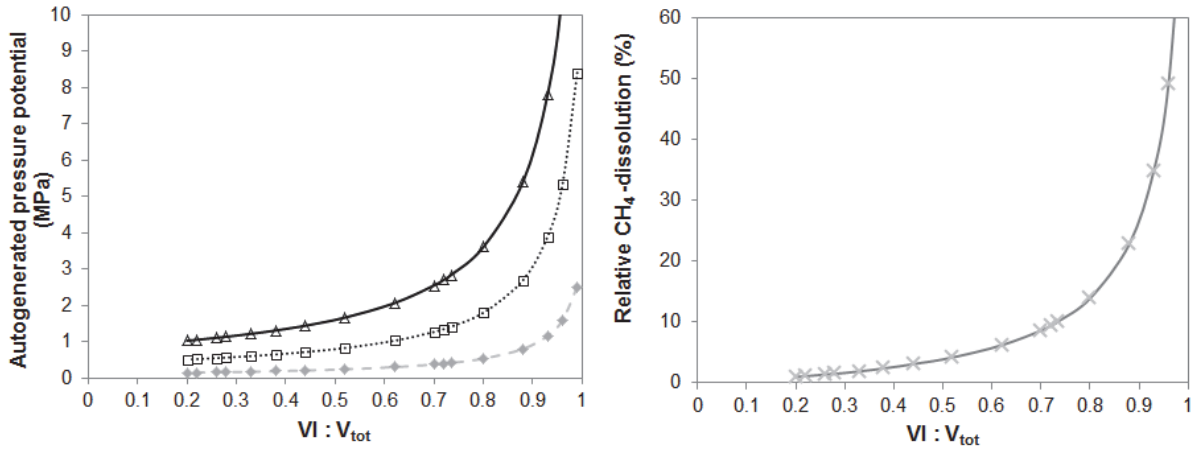

Figure 8-2: (a) theoretical autogenerated pCH_4 potential (MPa) for 3 g COD L^{-1} (♦), 10 g COD L^{-1} (□), 20g COD L^{-1} (Δ) and (b) % dissolved CH_4 of total (x), against liquid :total volume- ratio, assuming a 1 L batch reactor.

To reach a pCH_4 of 2.0 MPa using 3 g COD L^{-1}, a V_l:V_{tot} ratio of 0.97 is required and because the dissolved CH_4 is dependent on the V_l:V_{tot} ratio it can be found in Figure 8-2b that dissolved CH_4 amounts 58% of total produced CH_4. However, if this pressure is obtained with 10 or 20 g COD L^{-1} the required V_l:V_{tot} ratio decreases to

0.81 and 0.60 and as a consequence the relative CH_4-dissolution decreases to ~14 and 6% of total produced CH_4 in a batch digestion, respectively. If overpressure valves in batch setups would be set below the autogenerated pressure potential, CH_4-dissolution would follow the operational pressure and not the V_l:V_{tot} ratio and could therefore be reduced significantly.

Obviously, in continuous flow systems the biodegradable COD concentration determines the maximum pCH_4 that can be reached in an AHPD system.

The chemical energy potential of CH_4 under standard conditions is 890 kJ mol^{-1} [37], but additionally the autogenerated biogas contains a mechanical energy potential that is dependent on prevailing pressure and can be harvested by allowing the biogas to decompress. In batch digestion, by increasing the V_l:V_{tot} ratio different end pressures can be obtained upon digestion of a specific amount of substrate (Figure 8-2a). However, the potential decompression energy that can be converted into actual work by isothermally decompressing biogas from 0.50 and 10.0 MPa to atmospheric pressure increases only from 4 to 12 kJ per mol biogas according to Equation 1-22**.**

Given the increasing dissolution and potential CH_4–losses via the effluent at elevated pressure, the benefits of operating at high pressure from an overall energy efficiency point of view should be considered carefully. Moreover, the extent to which the chemical energy of the dissolved CH_4 can be utilised without further upgrading will depend on the CH_4 –content of the biogas released by decompressing the effluent. It is however noteworthy that during decompression only CO_2 and CH_4 are released and $NaHCO_3$ is kept in solution due to the charge balance. So, assume one would produce 3 mol CH_4 and 3 mol Total Inorganic Carbon by digestion of glucose. If initially 2 out of 3 mol of Total Inorganic Carbon (TIC) would be captured as $NaHCO_3$/$CaCO_3$ by ANC addition the remaining biogas that obeys Henry's law would consist of 3 mol CH_4 and 1 mol CO_2. When by autogeneration of biogas pressure 50% of CH_4, 1.5 mol, would dissolve, one could still produce at least an atmospheric quality biogas (60% CH_4 and 40% CO_2) from the decompressed effluent. Additionally, chapters 2, 3, and 4, showed that a CH_4-content exceeding 90% could be obtained at pressures of about only 0.5 MPa when feeding neutralised VFA, thereby minimising the dissolved CH_4.

As described above, the dissolved CH_4 can be easily quantified in the AHPD process. And because the whole process occurs in a single step reactor, CH_4-losses can be easily prevented, whereas for conventional digesters using external gas upgrading, CH_4-losses are often not reported and may add up to 20% of produced CH_4 [98].

8.1.3 Managing liquid acidity in AHPD processes

Given the difference in Henry's constants of 0.016 and 0.31 mol L^{-1} MPa^{-1} [15] for CH_4 and CO_2, respectively, it should be emphasized that high quality biogas at low pressure is only feasible by controlling CO_2-speciation via the total Acid Neutralising Capacity (ANC) of the digester liquid. The ANC or alkalinity can be defined as the excess charge of all cations minus the charge of all anions, e.g. Na^+, K^+ , Ca^{2+} , Mg^{2+} and/or NH_4^+ minus Cl^-, SO_4^{2-}, NO_3^{2-} and dissociated organic acids [68]. The remaining gap in charge is then balanced by the formation of HCO_3^-. Theoretically, this means that for waste water in which the ANC to TIC production-ratio is 1:1, all CO_2 will dissociate to HCO_3^-. Our experimental results in chapter 3 show that with an ANC to TIC-ratio of 1:3 the pCO_2 will increase, resulting in lower CH_4 concentrations in the biogas and a drop in pH to 5 or lower. The remarkable continuation of CH_4-production, at the low bulk pH caused by CO_2-induced acidification in chapter 3, was attributed to the presence of alkaline precipitates in the inoculum, which were speculated to cause a pH-gradient around and in the bacterial aggregates. The observed phenomenon would however, deserve further attention in future studies, because the reactor was well mixed and aggregates' sizes were low.

On one hand, increased ANC is beneficial for the biogas quality and pH, and elevated substrate concentrations have a higher pressure potential. On the other hand, literature shows that elevated cation concentrations and high volatile fatty acid concentrations could also inhibit CH_4-production rates [91]. Chapter 4 therefore focussed on the conversion of COD concentrations between 1 and 10 g L^{-1} of sodium-neutralised acetate and a mixture of acetate, propionate and butyrate. By working at a constant V_l:V_{tot} ratio this resulted in final pressures of 0.1, 0.3, 0.5, 1.0, and 2.0 MPa at 30 ^oC in the batch digester. A maximum CH_4-content of the produced biogas of 95% and 94% was achieved at 0.5 MPa in experiments using sodium acetate and mixture of VFAs as

the substrate, respectively. No further increase in the biogas CH_4 content was observed with increasing final pressure. Following Buswell's equation [24], the cation requirement was decreased from 0.36 g Na^+ per g COD L^{-1} for acetate to 0.28 g Na^+ per g COD L^{-1} for mixed VFA as a consequence of the higher COD/TOC ratio of propionate and butyrate.

In many practical situations however, the ANC in the waste water will most likely be insufficient to sequester CO_2 inside the reactor as HCO_3^- and will therefore lead to a reduced pH, rendering in-situ CO_2 removal difficult. Although in chapter 3 we showed that granular inoculum could also provide ANC "to bind CO_2 or buffer H^+ " in the form of precipitates, carboxylic groups or amine groups of proteins, this CO_2-sink is highly dependent on the type and quantity of suspended solids inside a waste stream and requires further research. In case of a consistent ANC shortage during a continuously fed AHPD process, continuous dosage of caustic (NaOH), is regarded as a technically feasible solution, but both energy-intensive and costly. In chapter 5, in-situ mineral weathering and secondary carbonation of naturally occurring mafic silicate minerals is proposed as a low-cost energy-efficient alternative to conventional caustic dosage. The envisaged natural mineral weathering and secondary carbonation is based on reaction equations 1-5, 1-15 and 1-16 [34].

It was experimentally verified that wollastonite, olivine and anorthosite could substitute caustic dosage during glucose digestion under non-pressurised conditions. A more detailed study on the CO_2-sequestration mechanism showed that 1 g wollastonite per 1 g glucose-COD provided sufficient ANC to prevent a pH drop to 4 and produce 76, 86 and 88 ±2% CH_4 at a pressure of 1, 0.3 and 1.0 MPa, respectively. Furthermore, the leaching rate of Ca^{2+} correlated with the pH and fatty acid formation. Secondary precipitation in the form of $CaCO_3$ provided the desired long term CO_2-storage mechanism. Results indicated that at least 1 g mineral per gram of converted non-acidified COD should be added to the digester. The addition of minerals is considered advantageous if the sludge or digestate can be used as soil enhancer. However, these additions are a disadvantage when the sludge has to be deposited in a landfill or burnt.

Although the CH_4 content in the biogas reached 88 ± 2% in the 1.0 MPa experiment, the specific methanogenic activity was fairly low, i.e. about 0.15 g COD.g^{-1} VSS.d^{-1} and was associated with temporary propionate accumulation. It was speculated that this propionate accumulation was related to increasing pCO_2 and relatively low pH in the early stages of the batch experiment.

8.1.4 AHPD reactor conditions impacting bioconversions of acidified substrates

In the feasibility study (chapter 2) it was found that methanogenic conversion rates of sodium acetate were affected by a maximum of 30% up to a total pressure of 9.0 MPa when using inoculum from a UASB treating paper factory waste water (Industriewater Eerbeek, The Netherlands). In chapter 4, the methanogenic conversion rates on acetate decreased from 0.23 g COD.g^{-1} VSS.d^{-1} to 0.11 g COD.g^{-1} VSS.d^{-1} and on mixed VFA from 0.29 g COD.g^{-1} VSS.d^{-1} to 0.16 g COD.g^{-1} VSS.d^{-1} for experiments designed to reach final pressures of 0.1 and 2.0 MPa, respectively. Counter intuitively, this reduction in conversion rates showed not to be related to end product inhibition and pressure, but to the increasing sodium and substrate concentrations required to reach the high pressures at a constant V_l:V_{tot} ratio. Although initial VFA concentrations were exceeding reported inhibition values at pH 7 [69, 84, 91, 213], a decreased inhibition and thus increased methane production rates were expected towards the end of each experiment, due the biomass yield linked to the conversion of fatty acids to HCO_3^-. Against expectation however, the conversion rates remained relatively constant over time. Sodium concentrations increased with final pressure, but remained constant throughout each substrate conversion experiment. The maximum concentrations of 2.8 and 3.5 g Na^+ L^{-1} can be considered low compared to the sodium concentrations used in high salinity studies [75, 214]. Nevertheless, the used inoculum (FrieslandCampina Riedel Ede, The Netherlands) was retrieved from a saline-poor environment, and was selected for its low inorganic solids content and was not given time to adapt. Moreover, the Na^+/K^+ ratio increased due to substrate addition from 12 to 160 and from 16 to 120 in the acetate and mixed VFA experiment, respectively. These results are in line with the results obtained by [75, 90], showing a 50% activity

inhibition between 3-16 g Na^+ L^{-1}, depending on possible occurrence of the antagonistic effects of the nutrients in the medium. Consequently, it was concluded that, although the reduction in methane production rates could have concerned a short-term effect, cation requirement and substrate inhibition are as important or more important than end product inhibition for AHPD batch reactors using acidified substrates.

8.1.5 AHPD reactor conditions impacting bioconversions of glucose

During operation of the AHPD reactors on sodium acetate, propionate and butyrate (chapters 2,3 and 4) the ANC/TIC ratio was kept such that practically all produced CO_2 could be chemically bound as HCO_3^- and pCO_2 remained relatively low, keeping pH circumneutral. For example, even in the 9.0 MPa experiment the pCO_2 in the gas phase did not exceed 0.1 MPa. According to the carbonate equilibrium and the prevailing CO_2 solubility, significant quantities of dissolved CO_2 will be stored in the liquid especially when the pCO_2 increases and the pH subsequently decreases. In practice, this situation occurs when feeding non-acidified substrates, like glucose, under limited ANC-conditions. Because in the same pH range $H_2CO_3^*$ can diffuse through charged membranes and can donate H^+, whereas HCO_3^- cannot, it was expected that pressurised biogas conditions would impact the bioconversions significantly, due to the presence of significant amounts of $H_2CO_3^*$.

Therefore, to study the effect of gradually increasing the pCO_2 on reactor kinetics and population dynamics, a long-term fed-batch pressurised glucose digestion experiment was commenced, in which ANC and thus HCO_3^- was controlled at 150 ± 10 meq L^{-1}. In the first 100 days of the experiment, glucose conversion resulted in a modest VFA accumulation and a pH drop to 6.1 at an autogenerated pressure of 2.0 MPa. The CH_4/CO_2 ratio in the biogas changed from the theoretical stoichiometric production of 50% CH_4 and 50% CO_2 to about 80% CH_4 and 20% CO_2. Bacterial community analyses showed that at this moment, the bacterial population was dominated by a putative acetate-producing *Kosmotoga*-like organism. However, from this point onward a putative propionate-producing *Propioniferax*-like organism increased in dominance. With the increasing dominance of this organism, reaching 25% of the

bacterial populations, propionate concomitantly started to accumulate inside the reactor and significantly reduced the biogas production rate, but also decreased the CH_4-content of the biogas by over 10%. Meanwhile, the DGGE and clone library profiles suggested that a stable methanogenic population was present, dominated by *Methanosaeta concilii*-, *Methanobacterium formicicum*- and *Methanobacterium beijingense*-like organisms. Therefore, the decreased methanogenic rates were attributed to a shift in the bacterial population and a shift in the produced intermediate substrates from mainly acetate, a methanogenic substrate, to relatively more propionate, a bacterial acetogenic substrate. By accumulation of propionate, which generally is converted into acetate, the methanogenic substrate availability is decreased and this will therefore indirectly influence the methanogenic community.

Propionate accumulation is often attributed to end-product inhibition by pH_2 formation [28]. For instantaneous propionate oxidation adequate interspecies electron transfer is considered essential [28]. A close proximity of hydrogen consuming organisms is a prerequisite for decreasing the local pH_2 (below 1 Pa) and improving the thermodynamic feasibility of the conversion, allowing the thermodynamic energy gain to be shared by transport of reducing equivalents [28]. Strikingly, propionate and H_2 were readily converted under a manually added pH_2 up to 0.40 MPa , whereas H_2 was not detected above the detection limit of 60 Pa throughout the earlier experiments. Additionally, the constructed archaeal clone library consisted of 19 % hydrogenotrophic methanogenic clones after pressure operation and an excess of electron acceptors was present in the form of accumulating CO_2. Therefore, it is hypothesised that not hydrogen but accumulating CO_2 caused the decrease in propionate oxidation rates. In literature [215] pCO_2 is described to cause end-product inhibition in the anaerobic digestion of glucose, butyrate, propionate and acetate. In order to verify this hypothesis, propionate degradation was tested up to 0.5 MPa pCO_2 using the same cultivated sludge. A linear reciprocal relation between pCO_2 and estimated relative growth rate was found. At pCO_2= 0.5 MPa, a reduction over 90% in propionate conversion rates was observed compared to the 0.1 MPa pCO_2-experiment. The Gibbs free energy change (ΔG_r) however, only improved marginally from -9.9 to -

13.9 kJ per mol propionate converted when decreasing the pCO_2 from 0.5 MPa to 0.1 MPa bar and assuming a pH_2 of 1 Pa. Interestingly, other authors found that pCO_2 under the examined pressure range is reversibly toxic and can be used to induce narcosis by the ability to diffuse into the protoplasm of many different organisms and bind to enzymes and proteins [139, 140, 176]. For anaerobic digestion specifically no references on this topic were found. Interestingly, it would also offer a plausible explanation for the observed dominance of bacterial species with highly developed outer cell-membrane structures, i.e. *Kosmotoga*- and *Propioniferax*-like organisms and the fact that the methanogenic Archaea seemed relatively unaffected.

8.1.6 AHPD reactor conditions impacting bioconversions of starch

Generally, when using complex substrates instead of glucose at ambient temperature and atmospheric pressure, hydrolysis is the rate-limiting step and retarded hydrolysis reduces the risk of fatty acid accumulation [97, 181]. Although pCO_2 enhanced hydrolysis at pressures of 7.0-8.0 MPa[199], total pressures exceeding 100.0 MPa are required to enhance the hydrolysis under mesophilic conditions[30, 190, 193]. Therefore it was postulated and tested in chapter 7 that under AHPD conditions hydrolysis would remain the rate-limiting step using particulate and gelatinised starch as model compounds.

Like under atmospheric mesophilic conditions, saccharification of gelatinised starch showed to be the rate-limiting step. The concentration of added inoculum determined the saccharification rate [183] and was not significantly affected by pressures up to 2.0 MPa N_2. Likewise, gelatinisation remained the rate-limiting step under AHPD conditions for particulate starch. Moreover, limited VFA accumulation was observed and glucose concentrations remained below 100 mg L^{-1}. Additionally, the biogas composition was significantly improved, from 49% CH_4 under atmospheric conditions to a maximum of 73% CH_4 under AHPD conditions.

8.1.7 Short summary

The most important results have been summarised in Table 8-1.

Table 8-1: Summary of most important results per thesis chapter

Chapter / Stage	Substrate	Aim	Result (at 303 K)
2 Methanogenesis	**Na-acetate**	Autogeneration potential	Exceeding 9.0 MPa
		Biogas quality	Exceeding 99% CH_4
		Methanogenic activity	30% reduction in SMA
3 Methanogenesis (up to 2.0 MPa)	**Na-acetate**	Mass transfer reactor	Gas liquid equilibrium within 4 h
		CH_4 dissolution	Follows Henry's law
		CO_2 dissolution	ANC to TIC ratio determines CO_2 speciation
	Acetic acid	<1 ANC to TIC ratios	CH_4 content decreases to 80%
		SMA at low pH	Marginally decreased below pH 5
4 Acetogenesis (up to 2.0 MPa)	**Na-acetate**	Acetate-conversion & CH_4 production rate	0.11 to 0.23 g COD g^{-1} VSS. d^{-1}
		Cation requirement & biogas quality	0.36 g Na^+ g COD L^{-1} for ~95% CH_4
	MixVFA (Acetate, propionate & butyrate)	Max. CH_4 production rate	0.30 g COD g^{-1} VSS. d^{-1}
		Propionate & Butyrate conversion rate	0.05 to 0.10 g COD g^{-1} VSS. d^{-1}
		Cation requirement & biogas quality	0.28 g Na^+ g COD L^{-1} for ~94% CH_4
	General	Methanogenic activity	Substrate induced 10-50% inhibition
5 Acidogenesis (up to 1.0 MPa)	**Glucose**	Buffering pH by silicate minerals	Wollastonite (Most effective) Olivine (Effective) Anorthosite (Suitable)
		Ca^{2+} leaching rates wollastonite	Dependent on pH and particle size
		CO_2 Sequestration wollastonite	As H_2CO_3, $Ca(HCO_3^-)_2$ and some $CaCO_3$
		CH_4-content biogas	86 and 88% CH_4 at 0.3 and 1.0 MPa

6	**Acidogenesis (up to 2.0 MPa)**	**Glucose**	Autogeneration at 150 meq L^{-1} ANC	Feasible up to 2.0 MPa with 75-80% CH_4
			Operational problems	Recurring propionate accumulation
			Dominant archaea	*Methanosaeta concilii-*, *Mtb. formicicum-* & *Mtb. beijingense-*like organisms
			Dominant bacteria	*Kosmotoga-*, *Propioniferax*-like and *Treponema*-like organisms
		Propionate	H_2 (max 0.4 MPa)	Improving propionate conversion indirectly
			CO_2 (max 0.5 MPa)	Inhibiting propionate conversion by toxicity
7	**Hydrolysis (up to 2.0 MPa)**	**Dissolved starch**	Pressure effect	No effects <1.0 MPa pCO_2 or 2.0 MPa p_{Total}
			Rate-limitation	Saccharification (maltose)
		Particulate starch	Pressure effect	Not significant, effects at pressures >100 MPa
			Rate-limitation	Gelatinisation (particle surface)
		General	Biogas quality	50% CH_4 (atmospheric) >70% CH_4 at 0.5, 1.0 and 1.5 MPa
			Operation	Reduced risk VFA accumulation

8.2 Outlook

8.2.1 Mesophilic high-quality biogas production and use

AHPD was introduced as a potentially feasible alternative for decentralised biogas upgrading. Flaring of biogas, because it has a too low quality or too low quantity to use and/or it is too complex or too expensive to upgrade the quality by external equipment, is the second worst option after releasing the biogas directly into the atmosphere. This thesis shows that low volume flows of biogas can be upgraded for further use by in-situ methane enrichment in AHPD reactor systems without having to invest in external biogas upgrading equipment. Although this work shows that it is theoretically and technically feasible to produce natural gas-like biogas, it also shows that for achieving the desired biogas quality, the digestion process is associated with more complex operation than for atmospheric digestion and it is expected that pressurised reactor systems will be more costly in terms of required investment. Therefore, biogas upgrading by AHPD or any other technique should be carefully assessed on overall energy balances for different situations that include all potential applications to ensure biogas is used in the most energy-efficient way. To highlight this, a decision making tree has been incorporated in that could be used as a guideline for further studying the benefits of AHPD in different scenarios.

When deciding on implementing AHPD technology, it is important to consider whether the theoretical biogas production exceeds your private gas (heating) demand. If it does exceed your private heating demand, upgrading the biogas allows for many high quality applications. Nevertheless, it could occur that the substrate is too diluted, or too oxidised, and/or the ANC is too low to increase the AHPD-biogas to a quality suitable for direct injection into the gas grid. Especially the requirement of costly caustic dosage could increase operational costs significantly, if no local alkaline resources are present to sequester CO_2, or no cheap electron donors are available that could reduce CO_2. It should, however, be noticed that digestion of concentrated sludges and slurries, i.e. >20 gTS L^{-1}, will consume much less caustic owing to their relatively high ammonium production upon digestion [26]. Despite the relatively dry

nature of the AHPD biogas, it is essential to ensure that the dew point is sufficiently low to ensure that water vapour will not condensate and damage expensive machinery or gas pipelines. Likewise, the equipment or grid injection specifications for H_2S, halogenated compounds and siloxanes and other trace pollutant should be compared to the actual acquired biogas quality to decide on the benefits of additional upgrading [9]. However, these compounds have not been studied in this thesis, and further studies to determine the effect of AHPD on trace gas pollutants, like H_2S, NH_3, siloxanes and halogenated compounds are still required.

In many situations, the local (bio-) gas demand for low quality applications, such as cooking, gas heaters and stationary engines, may exceed the potential biogas supply by decentralised digestion of local resources, like black water and kitchen waste [2]. In these situations, using biogas directly on-site for low quality applications seems most logical, to reduce the dependence on external energy sources [3-10]. Nevertheless, the low quality applications would likely still benefit from increasing the calorific value and lowering the water vapour inside the biogas at moderate pressures (<1.0 MPa).

In the mentioned decentralised applications, maximised COD concentrations will generate biogas flows of interest. The COD-concentration of black water without kitchen waste, for example, varies between 2 and 8 g COD L^{-1} depending on the type of sanitation [212]. Although operation up to 2.0 MPa is feasible (1.9 MPa pCH_4 and 0.1 MPa pCO_2) for all these concentrations, relative CH_4-dissolution would reduce from 97% of total produced CH_4 at 2g COD L^{-1} to 25% of total produced CH_4 at 8 gCOD L^{-1}. At an operational pressure of 1.0 MPa these values would reduce to 52 and 13 % respectively. Furthermore, based on [216, 217] it is estimated that black water for example contains about 0.18 g Na^+-equivalents per g COD (including NH_4^+).

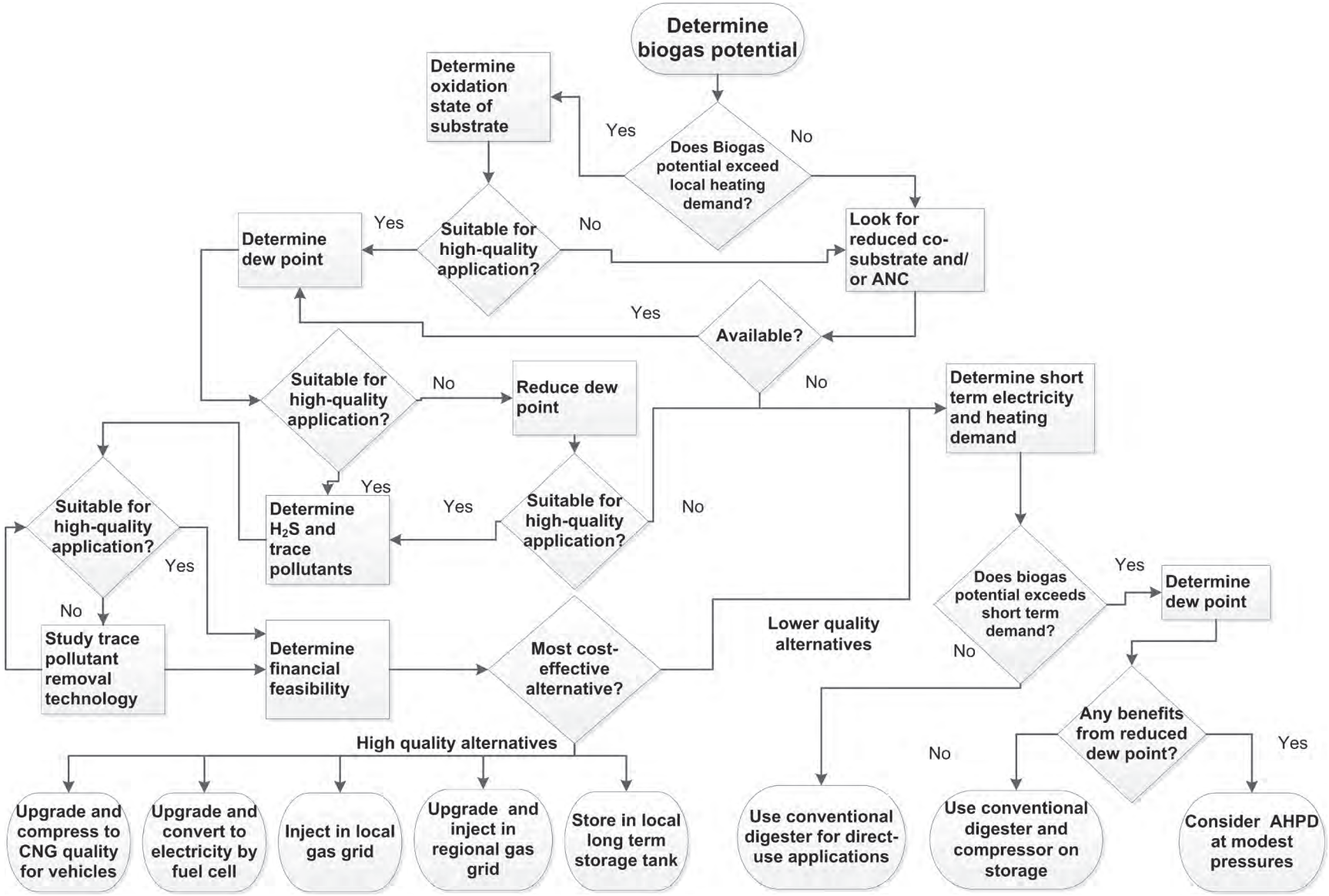

Figure 8- 3: Decision tree diagram on the required degree of upgrading in AHPD (this thesis and[9])

Given the values for cation requirement of 0.36 g Na^+-equivalents per g COD (chapter 4) an additional amount of 0.18 g Na^+-equivalents would be required to sequestrate all CO_2 as HCO_3^-, when assuming an average carbon oxidation state of '0', equal to acetate or glucose. With a more reduced carbon oxidation state, like the acetate propionate and butyrate mixture (2:1:1) only 0.1 g Na^+ per g COD would be needed and with co-digestion of lipids, ethanol, or hydrogen, cation requirement can be reduced to a minimum. However, when neither ANC nor reduced co-substrates are locally available, a CO_2 content of 20% could already be achieved by applying modest pressures of 0.3-1.0 MPa if the substrate contains 0.17 g Na^+ per g COD. Additionally, this would reduce water vapour content, and therefore, increase the lower heating value further. This could then improve CHP performance or enhance short-term storage possibilities without any additional biogas upgrading step.

8.2.2 Operating AHPD at different temperature

This work shows the effect of pressure in the mesophilic temperature range. AHPD applications in a different temperature range (psychrophilic or thermophilic) may give different results. Under thermophilic conditions for example, the effect of pressure on gelatinisation and enzyme activity becomes stronger with increasing temperature, potentially enhancing the dissolution of particulate matter [30]. With regard to CO_2, thermophilic conditions (55^oC) will result in a lower solubility due to a reduced Henry's constant, as can be calculated with van 't Hoffs equation [37]. However, the lower CO_2 solubility will not immediately result in a poorer biogas quality, because also the CH_4 and calcium carbonate solubility are decreasing with increasing temperature [65]. Furthermore, due to the relatively low solubility of CO_2 at increased temperatures, the observed CO_2-induced inhibition might be less pronounced. Based on the results of Huijgen and Comans [106], leaching of cations from silicate minerals is a process which is also known to accelerate with increasing temperature, and additionally, temperature enhances $CaCO_3$ precipitation rates. And finally, *Kosmotoga*-like bacteria, active and dominant in our reactors, are reported to have an extraordinarily wide temperature range in which growth is sustained, including both mesophilic and thermophilic conditions [179]. For the *Propioniferax*-like organisms

and for the observed methanogenic population this cannot a priori be predicted, because like in the work of van Lier [218] a shift towards a thermophilic methanogenic community is expected. Although this can be associated with temporary VFA accumulation [60], Kapp [18] reported a more stable thermophilic pressurised operation due to reduced pH and therefore reduced ammonia toxicity. In contrast, operation at 4^{o}C would decrease the conversion rates, but maximize CO_2 and CH_4 solubility. Altogether a very interesting part of research that still remains completely unexplored.

8.2.3 Towards continuous reactor setups

All the experiments in this thesis were performed in batch or fed-batch reactors systems. The observed overall conversion rates were relatively low, possibly resulting in large pressurised reactors that would be required for full scale operation. From this perspective, development of high rate biomass retention systems like UASB-type AHPD systems with high specific volumetric conversion rates, could be of interest. Compact AHPD systems could significantly reduce capital investment costs. Potentially, biomass retention in AHPD could for example be achieved by operating a pressurised AnMBR or a pressurised granulation process. It should however be stressed that for continuous AHPD reactors especially valves and pumps and an automated process control require attention, since the reactor pressurizes both gas and liquid flow by itself.

8.2.4 Application of AHPD reactors for non-methane fermentations

Methane is often regarded as the final electron deposit for the anaerobic digestion of organic waste streams, because it is relatively inert and migrates to the gas phase. Alternatively, anaerobic fermentation could be applied to produce intermediate dissolved products like VFA [219] The results presented in chapter 6 showed that pressure could affect the kinetics of mixed culture fermentations and may result in selective production of propionate due to CO_2-induced inhibition. Interestingly, literature showed that diffusion of CO_2 into the cell protoplasm could pause cell metabolism completely by reversibly deactivating different amine groups of enzymes

by formation of carbamino-proteins [140, 176]. Moreover, the toxicity effect depends on type of cell wall structure, on type of enzymes and proteins and on the CO_2-transport and utilisation mechanisms inside the cell and therefore each organism should theoretically respond differently to different pCO_2-levels [140]. Summarising, it is interesting to investigate whether CO_2 narcosis can be used as an additional environmental parameter, besides for example, pH, oxygen, temperature and salinity to increase the selectivity of undefined mixed culture fermentations.

Another interesting feature of AHPD reactors is that high concentrations of methane can be achieved in the liquid phase. By doing so, CH_4 might become an intermediate for anaerobic methane oxidising bacteria, thereby opening up possibilities to store electrons in CH_4 and reusing them for other purposes [220]. Furthermore, despite the toxicity of CO, elevated solubility of gases in AHPD reactor systems could also be an advantage for synthesis gas fermentations, since these are generally limited by gas-liquid mass transfer [221, 222]. Altogether, these examples of non-methane fermentations clearly demonstrate that application of AHPD could offer many advantages for a much broader range of biotechnological applications.

Hoofdstuk 9

Nederlandse Samenvatting

9 Nederlandse Samenvatting en algemene discussie

9.1.1 Anaerobe behandeling voor stabilisatie van afval en bio-energie

De miljoenen huishoudvergisters in India en China bewijzen dat de productie van biogas uit organisch afval al eeuwen toegepast wordt. Pas met de ontwikkeling van de high-rate vergistingssystemen in de jaren 70 en 80 werd anaerobe vergisting een serieus alternatief voor aerobe waterzuivering. In gematigde klimaatzones, zoals in Nederland, worden 'high-rate' systemen vrijwel alleen toegepast voor geconcentreerd industrieel afvalwater. Voor huishoudelijk en municipaal afvalwater is dit beperkt tot warmere klimaatzones [210]. Anaerobe zuivering is echter een gangbare technologie voor het behandelen primair en secundair zuiveringsslib, stabilisatie van koeien en varkensmest en vergisting van organisch huishoudelijk, agrarisch en industrieel afval [211]. In Nederland wordt directe anaerobe behandeling van het afvalwater niet toegepast, omdat de concentratie van het organisch afval in het afvalwater en de temperatuur te laag zijn voor effectieve behandeling. Bovendien, met het oog op de C/N ratio in het municipale afvalwater, zou anaerobe behandeling teveel invloed uitoefenen op de conventionele nutriëntenverwijdering van de huidige waterzuiveringen. Als alternatieve N-verwijdering beschikbaar is, zal anaerobe behandeling van rioolwater in Nederland, alleen een serieuze optie zijn als het water geconcentreerd of gescheiden wordt ingezameld met vacuümsystemen[12].

De anaerobe omzetting van het organisch afval van zwart water in decentrale sanitatie-concepten in combinatie met een biogas aangedreven warmte-kracht koppeling kan circa 140 MJ p^{-1} j^{-1} op leveren, waarvan circa 56 MJ p^{-1} j^{-1} en 84 p^{-1} j^{-1} als respectievelijk elektriciteit en warmte [212]. Bij toevoeging van organisch keukenafval kan deze opbrengst mogelijk verdubbeld worden [212]. Daarbovenop beperkt de lage kwaliteit van het biogas het gebruik op decentrale schaal, kleiner dan 100 m^3 u^{-1}, vanwege de kosten voor externe opwaardering[9]. Dit proefschrift richt zich op het in-situ opwaarderen van biogas door gebruik te maken van de verbeterde oplosbaarheid van CO_2 ten opzichte van CH_4, volgens de wet van Henry. De hier onderzochte technologie is bekend onder de noemer “Autogeneratieve hogedruk vergisting”.

9.1.2 Anaerobe vergisting bij verhoogde druk

Conventionele atmosferische vergisting wordt wereldwijd bestudeerd, maar omtrent drukvergisting is slechts zeer beperkte literatuur te vinden[17, 18, 61, 62]. Op basis van de beschikbare literatuur en het onderzoek beschreven in dit proefschrift is de schematische figuur uit de introductie aangepast in figuur 8.1. Deze figuur bevat de in-situ biogasopwaardering als een extra fase. Verder zijn de onderwerpen gerelateerd aan koolhydraten en vetzuurvergisting, die in deze thesis onderzocht zijn, vetgedrukt.

Experimentele resultaten laten zien dat het biologisch en technisch haalbaar is om een biogas druk van 90 bar met een methaangehalte van meer dan 95% op te bouwen. Bovendien is onder druk geproduceerd biogas relatief droog, zoals uit de Clausius Clapeyron vergelijking (1-17) berekend kan worden en dit is een groot voordeel voor gasnetinjectie. Zoals besproken in hoofdstuk 3, volgt CH_4 de wet van Henry en lost dus ook op onder druk. Figuur 8.2 laat zien welke druk er opgebouwd kan worden met verschillende substraat concentraties en de relatieve hoeveelheid CH_4 die er onder de gegeven condities oplost (als % van de totale CH_4 productie) bij gegeven verhoudingen tussen het totaal, het gas en het vloeistofvolume.

Om met een CZV concentratie van 3g CZV L^{-1} een p CH_4 van 20 bar op te bouwen moet het de verhouding tussen vloeistof en totaal volume 0,97 zijn zoals uit figuur 8-2a afgelezen kan worden. Uit figuur 8-2b blijkt dan dat er onder deze condities 58% van de totaal geproduceerde CH_4 dan opgelost is. Als deze druk bereikt moet worden met 10 of 20 gCZV L^{-1}, daalt de benodigde volume verhouding naar respectievelijk 0,81 en 0,60 en daarmee de opgeloste hoeveelheid CH_4 naar 14 en 6% in batchvergisting. Door gebruik te maken van overdrukventielen kan de opgeloste hoeveelheid methaan gestuurd worden op basis van de ingestelde operationele druk in batch systemen. In continue systemen wordt de maximale biogas druk vooral bepaald door de toegevoerde substraat concentratie.

De chemische potentiaal van CH_4 bedraagt 890 kJ mol^{-1} onder standaard condities (37), maar het biogas bevat additionele mechanische energie, die afhankelijk is van de heersende druk. Deze energie kan geoogst worden doormiddel van decompressie van het biogas. In batch vergisting kan met verschillende Vl:Vtot verhoudingen bij verschillende substraat-concentraties een verschillende druk opgebouwd worden. Hierdoor kan er bij een druk van 5 tot 100 bar, 4 tot 12 kJ mol^{-1} aan additionele energie worden teruggewonnen als het biogas bij gelijkblijvende temperatuur tot atmosferische druk kan expanderen. Omdat het opereren bij verhoogde druk ook leidt tot meer opgelost CH_4, moet er een weloverwogen worden op welke druk er gewerkt wordt vanuit energetisch perspectief. Het is daarbij belangrijk om te overwegen dat de bruikbaarheid van de opgeloste CH_4 en dus de chemische energie afhankelijk is van het CH_4-gehalte van het biogas. Tijdens het ontspannen van het biogas zullen CO_2 en CH_4 vrijkomen, maar blijft de HCO_3^- vrijwel geheel in oplossing als gevolg van de ladingsbalans. Als we aannemen dat er 3 mol CO_2 en 3 mol CH_4 uit 1 mol glucose geproduceerd worden bij vergisting en 2 mol CO_2 als bicarbonaat opgeslagen kan worden door toevoeging van base, bestaat het gas dat de wet van Henry volgt uit 3 mol CH_4 en 1 mol CO_2. Als we dan druk opbouwen totdat er 50% van de geproduceerde CH_4 opgelost (1,5 mol) is, zal het biogas dat na ontspanning vrijkomt minimaal gelijk zijn aan atmosferische biogas kwaliteit (60% CH_4 en 40% CO2). Omdat uit de resultaten in hoofdstuk 2, 3 en 4 blijkt dat er slechts 5 bar nodig is om een CH_4-gehalte van boven de 90% te bereiken als er gebufferde vetzuur-oplossing wordt vergist. Op deze wijze kunnen potentiele verliezen door oplossing van CH_4 makkelijk in kaart worden gebracht en voorkomen worden, omdat het hele proces in 1 gesloten reactor omgeving gebeurd. In tegenstelling, worden de CH_4 verliezen voor atmosferische vergisters vaak uberhaupt niet in kaart gebracht terwijl de verliezen op kunnen lopen tot 20% van de geproduceerde CH_4 [98].

9.1.3 Controleren van verzuring in AHPD processen

Gegeven de verschillen in de constants van Henry van 0.016 en 0.31 mol L^{-1} MPa^{-1} [15] voor CH_4 en CO_2 moet het benadrukt worden dat hoge kwaliteit biogas bij lage druk alleen bereikt kan worden door het toevoegen van Zuur Neutraliserende

Capaciteit (ZNC) De ZNC of alkaliteit kan gedefinieerd worden als het ladingsverschil tussen alle kationen en anionen opgelost in een vloeistof zoals bijvoorbeeld Na^+, K^+ , Ca^{2+} , Mg^{2+} en NH_4^+ min Cl^-, SO_4^{2-}, NO_3^{2-} en gedissocieerde vetzuren [68]. Het ladingsverschil wordt dan opgeheven door de vorming van HCO_3^- uit water en CO_2. Theoretisch, betekent dit voor al het afvalwater waarin er evenveel ZNC als totale anorganische koolstof (TAK) aanwezig is, alle CO_2 zich in de vorm van HCO_3^- bevindt. Onze resultaten in hoofdstuk 3 geven aan dat met een ZNC tot TAK ratio van 1: 3, slechts 1/3 van de totale CO_2 in de vorm van HCO_3^- aanwezig is, waardoor er relatief meer CO_2 in de gasfase terecht komt, de partiële CO_2-druk oploopt en de pH van de vloeistof tot beneden de 5 daalt. Gezien deze lage pH in de bulk vloeistof is het opmerkelijk dat de methaan productie door ging. Het is de verwachting dat zich in het gebruikte korrelslib basische neerslag (o.a. $CaCO_3$) bevond, wat een tijdelijke veilige pH-zone rondom de micro-organismen heeft gecreëerd. Toch verdient het fenomeen verder onderzoek omdat de reactor goed geroerd en de korrels relatief klein waren.

Aan de ene kant heeft een hoge ZNC voordelen voor de biogas kwaliteit, de pH en vertalen hoge substraat concentraties zich in een hoog drukpotentiaal. Aan de andere kant, blijkt uit de literatuur dat hoge kation concentraties en hoge vluchtige vetzuur concentraties (zoals azijnzuur, propionzuur en boterzuur) tot inhibitie van de methaanproductie snelheid leiden, doordat deze componenten toxisch zijn voor micro-organismen in hogere concentraties [91]. Hoofdstuk 4 richtte zich daarom op hogere substraat concentraties van 1 tot 10 g L^{-1} natrium acetaat of een mix van natrium acetaat, propionaat en butyraat. Bij het werken met een constante V_l:V_{tot} resulteerde dit in opgebouwde biogasdrukken van 1, 3, 5, 10, en 20 bar bij 30 ^oC in de batch vergister. Het gemeten maximum CH_4-gehalte van het geproduceerde biogas was 95% en 94% bij 5 bar voor natrium acetaat en de mix van VFA's. Met toenemende druk is er geen verdere verbetering van het CH_4-gehalte gemeten. Met de Buswell vergelijking [24] is vervolgens uitgerekend dat het benodigde cation-gehalte daalde van 0.36 g Na^+-equivalenten per g CZV L^{-1} voor natrium acetaat naar 0.28 g Na^+ per g CZV L^{-1} voor de vetzuurmix als gevolg van de gunstigere chemische samenstelling voor vergisting van propion- en boterzuur.

In veel praktische situaties zal er onvoldoende ZNC in het afvalwater aanwezig zijn om alle CO_2 via de lading in de vloeistof te kunnen houden als HCO_3^-, waardoor in-situ CO_2 verwijdering moeilijk wordt. Omdat we in hoofdstuk 3 zagen dat korrelslib op basis van aanwezige anorganische precipitaten of eiwitten CO_2 kon binden of zuur kon bufferen moeten we de zwevende stof in afvalwater beter bestuderen alvorens AHPD toe te passen. Als er een consistent tekort aan ZNC optreedt bij een continu hogedruk gistingsproces is natronloog of soda dosering een technisch haalbare maar energetisch en economisch dure oplossing Daarom hebben we in hoofdstuk 5 naar goedkopere alternatieven gezocht en werd het doseren van verschillende typen natuurlijke silicaatmineralen voorgesteld. Het beoogde proces is gebaseerd op de chemische reacties beschreven in figuur 1-5, 1-15 en 1-16 [34].

Het is experimenteel geverifieerd dat wollastoniet, olivijn en anorthosiet, natronloog dosering kunnen vervangen voor glucose vergisting onder niet-druk condities. Een meer gedetailleerde studie van het CO_2-sequestratiemechanisme laat zien dat 1 g wollastoniet per 1 g glucose-CZV, voldoende ZNC bevatte om een pH val naar pH 4 te voorkomen en 76, 86 en 88 ±2% CH_4 bij een druk van 1, 3 and 10 bar . Verder, kwam de snelheid waarmee Ca^{2+} uit het mineraal loogde overeen met de pH en vetzuurvorming. Secundaire precipitatie in de vorm van $CaCO_3$ gaf het gewenste lange termijn CO_2 opslagmechanisme. Resultaten geven aan dat er minimaal 1 g mineraal per gram CZV omgezet niet-verzuurd substraat nodig is. Het toevoegen van mineralen is een voordeel als het slib gebruikt kan worden als bodemverbeteraar, maar een nadeel als het slib te vervuild is en verbrand of gestort moet worden. Alhoewel het CH_4-gehalte in het biogas 88 ± 2% was in het 10 bar experiment, was de specifieke methanogene activiteit relatief laag, circa 0.15 g CZV.g^{-1} VSS.d^{-1} en deze ging gepaard met tijdelijke propionaat ophoping. Er wordt gespeculeerd dat de propionaat ophoping gerelateerd was aan de oplopende pCO_2 en relatief lage pH.

9.1.4 Effecten AHPD reactor condities op bioconversie van verzuurd substraat

In de haalbaarheidsstudie uitgevoerd in hoofdstuk 2 hebben we gevonden dat de methanogene omzettingssnelheden van natrium acetaat afnamen met een maximum van 30% bij drukken tot 90 bar toen er gebruik werd gemaakt van het inoculum van een UASB reactor die afvalwater van de papierindustrie behandeld (Industriewater Eerbeek, Nederland). In hoofdstuk 4 daalden de methanogene omzettingssnelheden op basis van acetaat van 0.23 g CZV.g^{-1} VSS.d^{-1} naar 0.11 g CZV.g^{-1} VSS.d^{-1} en op basis van de vetzuur mix van 0.29 g CZV.g^{-1} VSS.d^{-1} tot 0.16 g CZV.g^{-1} VSS.d^{-1} voor de experimenten gericht op een einddruk van respectievelijk 1 en 20 bar. Contra-intuïtief, bleek deze verlaagde omzettingssnelheid echter niet gerelateerd aan eindproduct-inhibitie, maar aan de oplopende natrium en substraat concentraties, die benodigd waren om de hogere druk te bereiken bij de constante V_l:V_{tot} ratio. Alhoewel de initiële vetzuurconcentraties gerapporteerde inhibitiewaardes uit de literatuur overschreden bij een pH 7 [69, 84, 91, 213], verwachtten we een verlaagde inhibitie en dus verhoging van de methaanproductiesnelheid richting het einde van elk experiment door de groei van biomassa gelinked aan de omzetting van vetzuren in HCO_3^-. Tegen verwachting, bleven de omzettingsnelheden relatief constant over de tijd. De natrium concentratie nam toe met gewenste einddruk, maar bleef constant tijdens de afzonderlijke experimenten. De maximale concentraties van 2.8 en 3.5 g Na^+ L^{-1} kunnen als laag beschouwd worden in vergelijking met studies bij hoge zoutgehaltes [75, 214]. Het gebruikte inoculum was echter afkomstig uit een zoutarme omgeving (EGSB, FrieslandCampina Riedel Ede, The Netherlands), en was specifiek geselecteerd vanwege de lage concentraties anorganische precipitaten en was geen tijd gegeven om aan te passen. Bovendien steeg de Na^+/K^+ ratio door substraat additie van 12 tot 160 en van 16 tot 120 in respectievelijk het acetaat en vetzuur mix experiment. Deze resultaten liggen in lijn met resultaten in de literatuur [75, 90], die een 50% inhibitie van activiteit laten zien tussen 3-16 g Na^+ L^{-1}, afhankelijk van de verhoudingen tussen nutriënten in het gevoede medium. Mogelijk betrof de verlaagde methaanproductiessnelheid een tijdelijk effect, maar zelfs dan zijn kation

benodigdheden en substraat inhibitie net zo belangrijk of nog belangrijker dan eindproductinhibitie voor AHPD batch reactoren gevoed met verzuurde substraten.

9.1.5 Effecten AHPD reactor condities op de bioconversie van glucose

In praktische situaties zal er voor substraten zoals glucose onvoldoende HCO_3^- gevormd kunnen worden om alle CO_2 te binden, waardoor er onder druk condities opgeloste CO_2 ontstaat. $H_2CO_3^*$ kan door geladen membranen heen diffunderen en H^+ doneren, terwijl HCO_3^- dit niet kan. Het lag daarom in de lijn der verwachting dat biogasdruk de bioconversie significant zou kunnen beïnvloeden als er veel $H_2CO_3^*$ gevormd zou worden.

Om dit te kunnen bestuderen is de drukbatchreactor lange termijn als wekelijk gevoed met glucose, terwijl de HCO_3^- gecontroleerd werd via de ZNC op 150 ± 10 meq L^{-1}. Tijdens de 1^e 100 dagen werd de glucose relatief eenvoudig omgezet in CH_4, trad er beperkte vetzuuraccumulatie op in de periode na een voeding en daalde de pH tot 6.1, terwijl de druk opliep tot 20 bar. De biogassamenstelling was 80% CH_4 en 20% CO_2, terwijl de stoichiometrisch biogas productie op basis van glucose 50% CH_4 en 50% CO_2 bedraagt. De populatiedynamica analyses lieten zien dat de bacteriele populatie op dit moment gedomineerd werd door de acetaat-producerende *Kosmotoga*-achtige organismen. Vanaf dit moment verkregen de *Propioniferax*-achtige organismen ook een dominante rol, en van deze organismen wordt over het algemeen aangenomen dat zij propionaat produceren. Gelijktijdig met de toenemende dominatie begon propionaat op te hopen, nam de biogas productiesnelheid significant af en ging het CH_4-gehalte van het biogas om lag met circa 10%. De DGGE and clone library profielen gaven echter aan dat er een stabiele methanogene populatie aanwezig was, die werd gedomineerd *Methanosaeta concilii*-, *Methanobacterium formicicum*- and *Methanobacterium beijingense*-achtige organismen. Om deze reden, werden de afgenomen methaanproductiesnelheden toegeschreven aan de verschuiving van acetaat naar propionaat als belangrijkste tussenprodukt.

Propionaat accumulatie wordt vaak toegeschreven aan oplopende pH_2 [28] limitatie in de "interspecies hydrogen transfer" door bijvoorbeeld toenemende afstand tussen

micro-organismen. Verbazingwekkend genoeg werden H_2 en propionaat tegelijkertijd geconsumeerd bij een verhoogde pH_2tot circa 40 bar, terwijl H_2 eerder niet gedetecteerd was beneden de detectielimiet van 60 Pa. Bovendien bestond 19% van de archaeal clone library uit waterstofconsumerende methanogenen en was er overmaat aan elektronacceptor aanwezig in de vorm CO_2. We postuleren daarom dat niet waterstof maar CO_2, verantwoordelijk was voor de afnemende propionaat-oxidatie snelheid, zoals ook beschreven in de literatuur [215]. Om dit te toetsen werd propionaat-degradatie in afzonderlijke drukexperimenten afgebroken onder oplopende pCO_2 tot 5 bar. Hier werd een lineaire relatie gevonden tussen pCO_2 en geschatte relatieve groeisnelheid. Bij een pCO_2= 5.0 bar werd een afname van 90% in de omzettingssnelheid van propionaat waargenomen in vergelijking tot de 1 bar pCO_2-experimenten. De verandering in Gibbs vrije energie (ΔG_r) was echter beperkt tot -9.9 to -13.9 kJ per mol propionaat bij afnemende pCO_2 van 5 bar tot 1 bar en een constante pH_2 of 1 Pa. Interessant genoeg vonden andere auteurs een reversibele CO_2 toxiciteit gekoppeld aan CO_2 geïnduceerde narcose door diffusie in het protoplasma en de reversibele binding van CO_2 met eiwitten en enzymen [139, 140, 176]. Specifiek voor anaerobe vergisting is dit bij ons weten nooit eerder gerapporteerd.

9.1.6 Effecten AHPD reactor condities op de bioconversie van zetmeel

Over het algemeen genomen is de omzetting van complex organisch materiaal de snelheidsbepalende stap bij omgevingstemperatuur en atmosferische druk en verlaagt dit het risico op vetzuur accumulatie [97, 181]. Alhoewel een pCO_2 van 70-80 bar de hydrolyse kan verbeteren [199], is er totaal druk nodig van over de 1000 bar om onder mesofiele condities bij gebruik van chemisch inerte gassen [30, 190, 193]. Daarom was het de verwachting dat hydrolyse in AHPD systemen nog steeds de snelheidsbepalende stap zou blijven. In hoofdstuk 7 is dit getoetst met onopgelost zetmeelpoeder en met gegelatiniseerd zetmeel. De snelheid van omzetting van opgelost zetmeel naar suikers werd niet significant beïnvloed door drukken tot 20 bar pN_2. En ook voor het oplossen/gelatiniseren van zetmeelpoeder werd geen significant drukeffect gevonden. Er werd vrijwel geen vetzuur-accumulatie waargenomen en de

glucose concentratie bleef beneden 100 mg L^{-1}. De kwaliteit van het biogas verbeterde van 49% CH_4 onder atmosferische condities naar 73% CH_4 onder druk condities.

9.1.7 Het gebruik en de mesofiele productie van hoge kwaliteit biogas

AHPD werd geïntroduceerd als een mogelijk alternatief decentrale opwaardering van biogas. Dit werk laat zien dat het opwaarderen van biogas in de bioreactor technisch haalbaar is, maar dat de bedrijfsvoering complexer zal worden. Eveneens moet er rekening gehouden worden met hogere investeringskosten in de bioreactor, waardoor er altijd een afweging gemaakt moet worden omtrent de economische haalbaarheid van AHPD in een bepaalde situatie. Het effect van drukvergisting op componenten zoals H_2S en NH_3 is nog niet bestudeerd, maar verdient gezien de potentiele effecten op verbrandingsapparatuur zeker de aandacht.

Verder zal het in decentrale systemen vaak voorkomen dat de biogasproductie kleiner is dan de lokale vraag voor laagwaardige applicaties zoals koken. In deze gevallen zal het niet direct lonen om het biogas op te waarderen tot aardgaskwaliteit om het vervolgens direct te verbranden. Dat neemt echter niet weg dat deze laagwaardige applicaties ook baat hebben bij het sturen van de gaskwaliteit (met name CH_4 en H_2O) en via de bedrijfsvoering van een drukvergister. Hierbij moet er wel in acht genomen worden dat er gezocht moet worden naar goedkope drukreactoren, om hiermee de investeringskosten te verlagen. In alle gevallen is het dan ook relevant om na te gaan in hoeverre ZNC lokaal beschikbaar is en of het mogelijk is om gereduceerde substraten zoals vetten, ethanol of waterstof co te vergisten om daarmee het methaangehalte van het biogas verhoogd kan worden bij slechts kleine drukverhoging.

10 References

1. Deublein, D., Steinhauser, A. Biogas from Waste and Renewable Resources: An Introduction. Wiley VCH Verlag Gmbh, Weinheim, Germany (2008).
2. Wempe, J. Vol gas vooruit; de rol van groen gas in de Nederlandse energiehuishouding. Senter Novem, Dutch Ministry of Economic affairs (in Dutch) (2007).
3. Electrigaz Technologies Inc. Feasibility Study – Biogas upgrading and grid injection in the Fraser Valley, British Columbia. BC Innovation Council, Canada (2008).
4. Wellinger, A. & Lindberg, A. Bioenergy Task 24: Biogas upgrading and utilisation. International Energy Agency (2001).
5. Dewil, R., Appels, L. & Baeyens, J. Energy use of biogas hampered by the presence of siloxanes. *Energy Conversion and Management* **47**, 1711-1722 (2006).
6. Polman, E.A., Brouwer, W. Kwaliteitsaspecten biogas. Kiwa Gastec N.V. (in Dutch) (2007).
7. Cimac. Information about the influence on NO_x emissions of ammonia in the fuel gas. International council on combustion engines, Frankfurt, Germany (2008).
8. Persson, M., Jönsson, O. & Wellinger, A. Bioenergy task 37: Biogas upgrading to vehicle fuel standards and grid injection. International Energy Agency (2006).
9. Petersson, A. & Wellinger, A. Bioenergy Task 37: Biogas upgrading technologies–developments and innovations. International Energy Agency (2009).
10. Papadias, D., Ahmed, S. & Kumar, R. Fuel quality issues in stationary fuel cell systems. Argonne National Laboratory (ANL) (2012).
11. Beauchamp, R., Bus, J.S., Popp, J.A., Boreiko, C.J., Andjelkovich, D.A. & Leber, P. A critical review of the literature on hydrogen sulfide toxicity. *CRC Critical Reviews in Toxicology* **13**, 25-97 (1984).
12. Zeeman, G., Kujawa, K., de Mes, T., Hernandez, L., de Graaff, M., Abu-Ghunmi, L., Mels, A., Meulman, B., Temmink, H., Buisman, C., van Lier, J. and Lettinga, G. Anaerobic treatment as a core technology for energy, nutrients and water recovery from source-separated domestic waste(water). *Water Science and Technology* **57**, 1207-1212 (2008).
13. Zagt, K., Barelds, J., Lindeboom, R.,Weijma, J.,Plugge, C., Van Lier, J. Energie uit rioolwater en keukenafval bij hoge druk. *H2O*, (in Dutch) (2010).
14. LEAF Project Bareau. Lettinga Associates Foundation, Wageningen, The Netherlands (2006).
15. Wang, L.K., Chen, G. J., Han, G. H., Guo, X. Q., Guo, T. M. Experimental study on the solubility of natural gas components in water with or without hydrate inhibitor. *Fluid Phase Equilibria* **207**, 143-154 (2003).
16. Hansson, G. Methane production from glucose and fatty acids at 55-85°C: Adaption of cultures and effects of pCO_2. *Biotechnology Letters* **4**, 789-794 (1982).
17. Hayes, T.D., Isaacson, H. R., Pfeffer, J. T. and Liu, Y. M. In situ methane enrichment in anaerobic digestion. *Biotechnology and Bioengineering* **35**, 73-86 (1990).
18. Kapp, H. The effect of higher pressures on the mesophilic and the thermophilic anaerobic sludge digestion. *Int. Symp. On Anaerobic Digestion of Solid Waste, Venice, Italy*, 85-94 (1992).

19. Lee, S.R., Cho, N.K., Maeng, W.J. Using the pressure of biogas created during anaerobic digestion as the source of mixing power. *Journal of Fermentation and Bioengineering* **80**, 415-417 (1995).
20. Vavilin, V.A., Vasiliev, V. B. and Rytov, S. V. Modelling of gas pressure effects on anaerobic digestion. *Bioresource Technology* **52**, 25-32 (1995).
21. Richards, B.K., Cummings, R. J., Jewell, W. J., Herndon, F. G. High solids anaerobic methane fermentation of sorghum and cellulose. *Biomass and Bioenergy* **1**, 47-53 (1991).
22. Miller, J.F., Almond, E.L., Shah, N.N., Ludlow, J.M., Zollweg, J.A., Streett, W.B., Zinder, S.H., Clark, D. High pressure-temperature bioreactor for studying pressure -temperature relationships in bacterial growth and productivity. *Biotechnology and Bioengineering* **31**, 407-413 (1988).
23. Batstone, D.J., Keller, J., Angelidaki, I., Kalyuzhnyi, S., Pavlostathis, S., Rozzi, A., Sanders, W., Siegrist, H. & Vavilin, V. The IWA Anaerobic Digestion Model No 1(ADM 1). *Water Science & Technology* **45**, 65-73 (2002).
24. Van Lier, J.B., Mahmoud, N. & Zeeman, G. Anaerobic Wastewater Treatment. in Biological Wastewater Treatment, Principles, Modelling and Design (ed. Henze, M., van Loosdrecht, M.C.M., Ekama, G.A., Brdjanovic, D.) IWA Publishing. 415-456 (2008).
25. Tchobanoglous, G., Burton, F. & Stensel, H. Wastewater Engineering Treatment and Reuse, 4th Edn. Metcalf and Eddy. Inc. McGraw-Hill Company (2003).
26. De Mes, T., Stams, A., Reith, J. & Zeeman, G. Methane production by anaerobic digestion of wastewater and solid wastes. in Bio-methane & Bio-hydrogen (2003).
27. Thauer, R.K., Jungermann, K. & Decker, K. Energy conservation in chemotrophic anaerobic bacteria. *Bacteriological Reviews* **41**, 100-180 (1977).
28. Stams, A.J.M. & Plugge, C.M. Electron transfer in syntrophic communities of anaerobic bacteria and archaea. *Nature Reviews Microbiology* **7**, 568-577 (2009).
29. Pavlostathis, S.G. & Giraldo-Gomez, E. Kinetics of anaerobic treatment: A critical review. *Critical Reviews in Environmental Control* **21**, 411-490 (1991).
30. Morild, E. The Theory of Pressure Effects on Enzymes. *Advances in Protein Chemistry* **34**, 93-166 (1981).
31. Cavalcanti, P.F., van Haandel, A., Lettinga, G. Effect of carbon dioxide and ammonium removal on pH changes in polishing ponds. *Water Science and Technology* **45**, 377-382 (2002).
32. Deffeyes, K.S. Carbonate equilibria: a graphic and algebraic approach. *Limnology and Oceanography* **10**, 412 (1965).
33. Huijgen, W.J.J., Ruijg, G. J., Comans, R. N. J., Witkamp, G. J. Energy consumption and net CO_2 sequestration of aqueous mineral carbonation. *Industrial and Engineering Chemistry Research* **45**, 9184-9194 (2006).
34. Huijgen, W.J.J., Witkamp, G.J. & Comans, R.N.J. Mineral CO_2 sequestration by steel slag carbonation. *Environmental Science and Technology* **39**, 9676-9682 (2005).
35. Chen, Z.Y., O'Connor, W. K., Gerdemann, S. J. Chemistry of aqueous mineral carbonation for carbon sequestration and explanation of experimental results. *Environmental Progress* **25**, 161-166 (2006).
36. Curry, J.A. & Webster, P.J. Thermodynamics of atmospheres and oceans. Academic Press (1999).
37. Jones, L. & Atkins, P. Chemistry Molecules Matter and Change: 4th edition. WHFreeman (1999).

38. Yayanos, A.A., Chastain, R.A. The influence of nutrition on the physiology of piezophilic bacteria. *8th International Symposium on Microbial Ecology, Microbial Biosystems: New Frontiers* (1999).
39. Abe, F. & Horikoshi, K. The biotechnological potential of piezophiles. *Trends in Biotechnology* **19**, 102-108 (2001).
40. Takai, K., Nakamura, K., Toki, T., Tsunogai, U., Miyazaki, M., Miyazaki, J., Hirayama, H., Nakagawa, S., Nunoura, T. & Horikoshi, K. Cell proliferation at 122°C and isotopically heavy CH_4 production by a hyperthermophilic methanogen under high-pressure cultivation. *Proceedings of the National Academy of Sciences of the United States of America* **105**, 10949-10954 (2008).
41. Kato, C., Li, L., Nogi, Y., Nakamura, Y., Tamaoka, J., Horikoshi, K. Extremely barophilic bacteria isolated from the Mariana trench, challenger deep, at a depth of 11,000 meters. *Applied and Environmental Microbiology* **64**, 1510-1513 (1998).
42. Jeanthon, C., L'Haridon, S., Pradel, N., Prieur, D. Rapid identification of hyperthermophilic methanococci isolated from deep-sea hydrothermal vents. *International Journal of Systematic Bacteriology* **49**, 591-594 (1999).
43. Zhao, H., Wood, A. G., Widdel, F., Bryant, M. P. An extremely thermophilic Methanococcus from a deep sea hydrothermal vent and its plasmid. *Archives of Microbiology* **150**, 178-183 (1988).
44. L'Haridon, S., Miroshnichenko, M.L., Hippe, H., Fardeau, M.L., Bonch-Osmolovskaya, E.A., Stackebrandt, E. & Jeanthon, C. Petrotoga olearia sp. nov., and Petrotoga sibirica sp. nov., two thermophilic bacteria isolated from a continental petroleum reservoir in Western Siberia. *International Journal of Systematic and Evolutionary Microbiology* **52**, 1715-1722 (2002).
45. Jeanthon, C., L'Haridon, S., Pradel, N., Reysenbach, A. L., Vernet, M., Messner, P., Sleytr, U. B., Prieur, D. Methanococcus infernus sp. nov., a novel hyperthermophilic lithotrophic methanogen isolated from a deep-sea hydrothermal vent. *International Journal of Systematic Bacteriology* **48**, 913-919 (1998).
46. Jones, W.J., Leigh, J. A., Mayer, F. Methanococcus jannaschii sp. nov., an extremely thermophilic methanogen from a submarine hydrothermal vent. *Archives of Microbiology* **136**, 254-261 (1983).
47. Jeanthon, C., L'Haridon, S., Reysenbach, A. L., Corre, E., Vernet, M., Messner, P., Sleytr, U. B., Prieur, D. Methanococcus vulcanius sp. nov., a novel hyperthermophilic methanogen isolated from East Pacific Rise, and identification of Methanococcus sp. DSM 4213(T) as Methanococcus fervens sp. nov. *International Journal of Systematic Bacteriology* **49**, 583-589 (1999).
48. Takai, K., Inoue, A., Horikoshi, K. Methanothermococcus okinawensis sp. nov., a thermophilic, methane-producing archaeon isolated from a Western Pacific deep-sea hydrothermal vent system. *International Journal of Systematic and Evolutionary Microbiology* **52**, 1089-1095 (2002).
49. Huber, H., Thomm, M., Konig, H. Methanococcus thermolithotrophicus, a novel thermophilic lithotrophic methanogen. *Archives of Microbiology* **132**, 47-50 (1982).
50. Burggraf, S., Fricke, H., Neuner, A., Kristjansson, J., Rouvier, P., Mandelco, L., Woese, C. R., Stetter, K. O. Methanococcus igneus sp. nov., a novel hyperthermophilic methanogen from a shallow submarine hydrothermal system. *Systematic and Applied Microbiology* **13**, 263-269 (1990).

51. Kotsyurbenko, O.R., Chin, K. J., Glagolev, M. V., Stubner, S., Simankova, M. V., Nozhevnikova, A. N., Conrad, R. Acetoclastic and hydrogenotrophic methane production and methanogenic populations in an acidic West-Siberian peat bog. *Environmental Microbiology* **6**, 1159-1173 (2004).
52. Baross, J.A., Hanus, F. J., Morita, R. Y. Survival of human enteric and other sewage microorganisms under simulated deep sea conditions. *Journal of Applied Microbiology* **30**, 309-318 (1975).
53. Vogel, R.F. & Ehrman, M.A. Effects of Pressure on Lactic acid Bacteria. in High Pressure Microbiology (ed. Michiels, C., Bartlett, D.H., Aertsen, A.) American Society for Microbiology Press (2008).
54. Michiels, C., Bartlett, D.H., Aertsen A. High Pressure Microbiology. American Society for Microbiology Press, Washington D.C. (2008).
55. Bartlett, D.H. Pressure effects on in vivo microbial processes. *Biochimica et Biophysica Acta - Protein Structure and Molecular Enzymology* **1595**, 367-381 (2002).
56. Martin, W. & Müller, M. The hydrogen hypothesis for the first eukaryote. *Nature* **392**, 37-41 (1998).
57. APHA Standard Methods for the Examination of Water and Wastewate: 20th edition. American Public Health Association/ American Water Work Association/Water Environment Federation, Washington D.C. (2005).
58. Zandvoort, M.H., Osuna, M.B., Geerts, R., Lettinga, G. & Lens, P.N.L. Effect of nickel deprivation on methanol degradation in a methanogenic granular sludge bioreactor. *Journal of Industrial Microbiology and Biotechnology* **29**, 268-274 (2002).
59. Aquino, S.F. & Stuckey, D.C. Soluble microbial products formation in anaerobic chemostats in the presence of toxic compounds. *Water Research* **38**, 255-266 (2004).
60. Van Lier, J.B., Grolle, K.C.F., Stams, A.J.M., Conway de Macario, E. & Lettinga, G. Start-up of a thermophilic upflow anaerobic sludge bed (UASB) reactor with mesophilic granular sludge. *Applied Microbiology and Biotechnology* **37**, 130-135 (1992).
61. Richards, B.K., Herndon, F.G., Jewell, W.J., Cummings, R.J. & White, T.E. In situ methane enrichment in methanogenic energy crop digesters. *Biomass and Bioenergy* **6**, 275-282 (1994).
62. O'Keefe, D.M., Brigmon, R.L. & Chynoweth, D.P. Influence of methane enrichment by aeration of recirculated supernatant on microbial activities during anaerobic digestion. *Bioresource Technology* **71**, 217-224 (2000).
63. Hafner, S.D. & Bisogni Jr, J.J. Modeling of ammonia speciation in anaerobic digesters. *Water Research* **43**, 4105-4114 (2009).
64. Edsall, J., Forster, R., Otis, A. & Roughton, F. CO_2-Chemical, Biochemical, and Physiological Aspects. *Science* **17**, 410-413 (1969).
65. Essington, M.E. Soil and Water chemistry: an integrated approach. CRC Press, Washington D.C. (2004).
66. Li, J. & Duan, Z. A thermodynamic model for the prediction of phase equilibria and speciation in the H_2O-CO_2-NaCl-$CaCO_3$-$CaSO_4$ system from 0 to 250°C, 1 to 1000 bar with NaCl concentrations up to halite saturation. *Geochimica et Cosmochimica Acta* **75**, 4351-4376 (2011).
67. Duan, Z. & Mao, S. A thermodynamic model for calculating methane solubility, density and gas phase composition of methane-bearing aqueous fluids from 273

to 523 K and from 1 to 2000 bar. *Geochimica et Cosmochimica Acta* **70**, 3369-3386 (2006).
68. Van Haandel, A.C. Influence of the digested COD concentration on the alkalinity requirement in anaerobic digesters. *Water Science and Technology* **30**, 23-34 (1994).
69. Fukuzaki, S., Nishio, N. & Nagai, S. Kinetics of the methanogenic fermentation of acetate. *Applied and Environmental Microbiology* **56**, 3158-3163 (1990).
70. Taconi, K.A., Zappi, M.E., Todd French, W. & Brown, L.R. Feasibility of methanogenic digestion applied to a low pH acetic acid solution. *Bioresource Technology* **98**, 1579-1585 (2007).
71. Bräuer, S.L., Cadillo-Quiroz, H., Ward, R.J., Yavitt, J.B. & Zinder, S.H. Methanoregula boonei gen. nov., sp. nov., an acidiphilic methanogen isolated from an acidic peat bog. *International Journal of Systematic and Evolutionary Microbiology* **61**, 45-52 (2011).
72. Goodwin, S. & Zeikus, J.G. Ecophysiological adaptations of anaerobic bacteria to low pH: analysis of anaerobic digestion in acidic bog sediments. *Applied and Environmental Microbiology* **53**, 57-64 (1987).
73. Williams, R.T. & Crawford, R.L. Methanogenic bacteria, including an acid-tolerant strain, from peatlands. *Applied and Environmental Microbiology* **50**, 1542-1544 (1985).
74. Florencio, L., Nozhevnikova, A., van Langerak, A., Stams, A.J.M., Field, J.A. & Lettinga, G. Acidophilic degradation of methanol by a methanogenic enrichment culture. *FEMS Microbiology Letters* **109**, 1-6 (1993).
75. Ismail, S.B., Gonzalez, P., Jeison, D. & Van Lier, J.B. Effects of high salinity wastewater on methanogenic sludge bed systems. *Water Science and Technology* **58**, 1963-1970 (2008).
76. Whitfield, M. The Ion-Association Model and the Buffer Capacity of the Carbon Dioxide System in Seawater at 25°C and 1 Atmosphere Total Pressure. *Limnology and Oceanography* **19**, 235-248 (1974).
77. Batstone, D.J. & Keller, J. Variation of bulk properties of anaerobic granules with wastewater type. *Water Research* **35**, 1723-1729 (2001).
78. McCann, N., Phan, D., Fernandes, D. & Maeder, M. A systematic investigation of carbamate stability constants by 1H NMR. *International Journal of Greenhouse Gas Control* **5**, 396-400 (2011).
79. Cleland, W.W., Andrews, T.J., Gutteridge, S., Hartman, F.C. & Lorimer, G.H. Mechanism of rubisco: The carbamate as general base. *Chemical Reviews* **98**, 549-561 (1998).
80. Farajzadeh, R., Barati, A., Delil, H.A., Bruining, J. & Zitha, P.L.J. Mass transfer of CO2 into water and surfactant solutions. *Petroleum Science and Technology* **25**, 1493-1511 (2007).
81. Lens, P.N.L., De Beer, D., Cronenberg, C.C.H., Houwen, F.P., Ottengraf, S.P.P. & Verstraete, W.H. Heterogeneous distribution of microbial activity in methanogenic aggregates: pH and glucose microprofiles. *Applied and Environmental Microbiology* **59**, 3803-3815 (1993).
82. Smith, K.S., Jakubzick, C., Whittam, T.S. & Ferry, J.G. Carbonic anhydrase is an ancient enzyme widespread in prokaryotes. *Proceedings of the National Academy of Sciences of the United States of America* **96**, 15184-15189 (1999).
83. Bekkering, J., Broekhuis, A.A. & van Gemert, W.J.T. Optimisation of a green gas supply chain – A review. *Bioresource Technology* **101**, 450-456 (2010).

84. Cho, Y.T., Young, J.C., Jordan, J.A. & Moon, H.M. Factors affecting measurement of specific methanogenic activity. *Water Science and Technology* **52**, 435-440 (2005).
85. Maillacheruvu, K.Y., Parkin, G.F. Kinetics of growth, substrate utilization and sulfide toxicity for propionate, acetate, and hydrogen utilizers in anaerobic systems. *Water Environment Research* **68**, 1099-1106 (1996).
86. Dong, X. & Stams, A.J.M. Evidence for H_2 and formate formation during syntrophic butyrate and propionate degradation. *Anaerobe* **1**, 35-39 (1995).
87. Conrad, R. & Wetter, B. Influence of temperature on energetics of hydrogen metabolism in homoacetogenic, methanogenic, and other anaerobic bacteria. *Archives of Microbiology* **155**, 94-98 (1990).
88. Weijma, J., Gubbels, F., Hulshoff Pol, L.W., Stams, A.J., Lens, P. & Lettinga, G. Competition for H_2 between sulfate reducers, methanogens and homoacetogens in a gas-lift reactor. *Water Science and Technology* **45**, 75-80 (2002).
89. Kugelman, I.J. & McCarty, P.L. Cation Toxicity and Stimulation in Anaerobic Waste Treatment. *Journal of Water Pollution Control Federation* **37**, 97- 116 (1965).
90. Feijoo, G., Soto, M., Méndez, R. and Lema, J. M. Sodium inhibition in the anaerobic digestion process: Antagonism and adaptation phenomena. *Enzyme and Microbial Technology* **17**, 180-188 (1995).
91. Chen, Y., Cheng, J.J. & Creamer, K.S. Inhibition of anaerobic digestion process: A review. *Bioresource Technology* **99**, 4044-4064 (2008).
92. Ismail, S.B., de La Parra, C. J., Temmink, H. and Van Lier, J. B. Extracellular polymeric substances (EPS) in upflow anaerobic sludge blanket (UASB) reactors operated under high salinity conditions. *Water Research* **44**, 1909-1917 (2010).
93. Dereli, R.K., Ersahin, M. E., Ozgun, H., Ozturk, I., Jeison, D., van der Zee, F. and van Lier, J. B. Potentials of anaerobic membrane bioreactors to overcome treatment limitations induced by industrial wastewaters. *Bioresource Technology* **122**, 160-170 (2012).
94. Massanet-Nicolau, J., Dinsdale, R., Guwy, A. & Shipley, G. Use of real time gas production data for more accurate comparison of continuous single-stage and two-stage fermentation. *Bioresource Technology* **129**, 561-567 (2013).
95. Michalska, K., Miazek, K., Krzystek, L. & Ledakowicz, S. Influence of pretreatment with Fenton's reagent on biogas production and methane yield from lignocellulosic biomass. *Bioresource Technology* **119**, 72-78 (2012).
96. Nie, Y.Q., Li, Y.X., He, H., Zhou, W.J., Pang, Z.H. & Peng, H.B. Production of High Calorific Biogas from Organic Wastewater and Enhancement of Anaerobic Digestion. *Advanced Materials Research* **550**, 522-528 (2012).
97. Vavilin, V.A., Vasiliev, V.B. & Rytov, S.V. Modelling of gas pressure effects on anaerobic digestion. *Bioresource Technology* **52**, 25-32 (1995).
98. Börjesson, P. & Berglund, M. Environmental systems analysis of biogas systems--Part I: Fuel-cycle emissions. *Biomass and Bioenergy* **30**, 469-485 (2006).
99. Lackner, K.S., Wendt, C.H., Butt, D.P., Joyce, B.L. & Sharp, D.H. Carbon dioxide disposal in carbonate minerals. *Energy* **20**, 1153-1170 (1995).
100. Schuiling, R. & Krijgsman, P. Enhanced Weathering: An Effective and Cheap Tool to Sequester CO_2. *Climatic Change* **74**, 349-354 (2006).
101. Mazzotti, M., Abanades, J.C., Allam, R., Lackner, K.S., Meunier, F., Rubin, E., Sanchez, J.C., Yogo, K. & Zevenhoven, R. Mineral carbonation and industrial uses of carbon dioxide. *IPCC special report on carbon dioxide capture and storage*, 321-338 (2005).

102. Huijgen, W.J.J., Comans, R.N.J. & Witkamp, G.-J. Cost evaluation of CO_2 sequestration by aqueous mineral carbonation. *Energy Conversion and Management* **48**, 1923-1935 (2007).
103. Alibaba. Products carbonate and alkali. http://www.alibaba.com/showroom/ (visited 03-04-2013).
104. Whitfield, P.S. & Mitchell, L.D. In situ laboratory X-ray powder diffraction study of wollastonite carbonation using a high-pressure stage. *Applied Geochemistry* **24**, 1635-1639 (2009).
105. Salek, S.S., Kleerebezem, R., Jonkers, H.M., Witkamp, G.-j. & van Loosdrecht, M.C.M. Mineral CO_2 sequestration by environmental biotechnological processes. *Trends in Biotechnology* **31**, 139-146 (2013).
106. Huijgen, W.J.J. & Comans, R.N.J. Carbonation of steel slag for CO_2 sequestration: Leaching of products and reaction mechanisms. *Environmental Science and Technology* **40**, 2790-2796 (2006).
107. Lackner, K.S. Carbonate chemistry for sequestring fossil carbon. *Annual Review of Energy and the Environment* **27**, 193-232 (2002).
108. Nehrke, G. Calcite precipitation from aqueous solution: transformation from vaterite and role of solution stoichiometry. *PhD Dissertation*, Utrecht University, Earth Sciences - Geochemistry (2007).
109. De Graaff, M.S., Temmink, H., Zeeman, G., van Loosdrecht, M.C.M. & Buisman, C.J.N. Autotrophic nitrogen removal from black water: Calcium addition as a requirement for settleability. *Water Research* **45**, 63-74 (2011).
110. Van Langerak, E.P.A., Ramaekers, H., Wiechers, J., Veeken, A.H.M., Hamelers, H.V.M. & Lettinga, G. Impact of location of $CaCO_3$ precipitation on the development of intact anaerobic sludge. *Water Research* **34**, 437-446 (2000).
111. Van Langerak, E.P.A., Beekmans, M.M.H., Beun, J.J., Hamelers, H.V.M. & Lettinga, G. Influence of phosphate and iron on the extent of calcium carbonate precipitation during anaerobic digestion. *Journal of Chemical Technology and Biotechnology* **74**, 1030-1036 (1999).
112. Dupraz, C., Reid, R.P., Braissant, O., Decho, A.W., Norman, R.S. & Visscher, P.T. Processes of carbonate precipitation in modern microbial mats. *Earth-Science Reviews* **96**, 141-162 (2009).
113. Coates, J. Interpretation of Infrared Spectra, A Practical Approach. in Encyclopedia of Analytical Chemistry, John Wiley & Sons Ltd, Chichester, UK (2000).
114. Povarennykh, A.S. The use of infrared spectra for the determination of minerals. *American Mineralogist* **63**, 956-995 (1978).
115. Downs, R.T. The RRUFF Project: an integrated study of the chemistry, crystallography, Raman and infrared spectroscopy of minerals. Wollastonite-1A R040131, International Mineralogical Association (2006).
116. Pokrovsky, O.S., Shirokova, L.S., Bénézeth, P., Schott, J. & Golubev, S.V. Effect of organic ligands and heterotrophic bacteria on wollastonite dissolution kinetics. *American Journal of Science* **309**, 731-772 (2009).
117. Teir, S., Eloneva, S. & Zevenhoven, R. Production of precipitated calcium carbonate from calcium silicates and carbon dioxide. *Energy Conversion and Management* **46**, 2954-2979 (2005).
118. Park, A.H.A. & Fan, L.S. CO_2 mineral sequestration: Physically activated dissolution of serpentine and pH swing process. *Chemical Engineering Science* **59**, 5241-5247 (2004).

119. Kodama, S., Nishimoto, T., Yamamoto, N., Yogo, K. & Yamada, K. Development of a new pH-swing CO2 mineralization process with a recyclable reaction solution. *Energy* **33**, 776-784 (2008).
120. Ma, J., Carballa, M., Van De Caveye, P. & Verstraete, W. Enhanced propionic acid degradation (EPAD) system: Proof of principle and feasibility. *Water Research* **43**, 3239-3248 (2009).
121. Boone, D.R. & Xun, L. Effects of pH, Temperature, and Nutrients on Propionate Degradation by a Methanogenic Enrichment Culture. *Applied and Environmental Microbiology* **53**, 1589-1592 (1987).
122. Addadi, L., Raz, S. & Weiner, S. Taking advantage of disorder: Amorphous calcium carbonate and its roles in biomineralization. *Advanced Materials* **15**, 959-970 (2003).
123. Wu, Q.-S., Sun, D.-M., Liu, H.-J. & Ding, Y.-P. Abnormal Polymorph Conversion of Calcium Carbonate and Nano-Self-Assembly of Vaterite by a Supported Liquid Membrane System. *Crystal Growth & Design* **4**, 717-720 (2004).
124. Kellermeier, M., Melero-García, E., Glaab, F., Klein, R., Drechsler, M., Rachel, R., García-Ruiz, J.M. & Kunz, W. Stabilization of amorphous calcium carbonate in inorganic silica-rich environments. *Journal of the American Chemical Society* **132**, 17859-17866 (2010).
125. McCollom, T.M. & Bach, W. Thermodynamic constraints on hydrogen generation during serpentinization of ultramafic rocks. *Geochimica et Cosmochimica Acta* **73**, 856-875 (2009).
126. Fermoso, F.G., Collins, G., Bartacek, J., O'Flaherty, V. & Lens, P. Role of nickel in high rate methanol degradation in anaerobic granular sludge bioreactors. *Biodegradation* **19**, 725-737 (2008).
127. Ragsdale, S.W. Nickel and the carbon cycle. *Journal of Inorganic Biochemistry* **101**, 1657-1666 (2007).
128. Drennan, C.L. & Peters, J.W. Surprising cofactors in metalloenzymes. *Current Opinion in Structural Biology* **13**, 220-226 (2003).
129. Cabirol, N., Barragán, E.J., Durán, A. & Noyola, A. Effect of aluminium and sulphate on anaerobic digestion of sludge from wastewater enhance primary treatment. *Water Science and Technology* **48**, 235-240 (2003).
130. Zayed, G. & Winter, J. Inhibition of methane production from whey by heavy metals - Protective effect of sulfide. *Applied Microbiology and Biotechnology* **53**, 726-731 (2000).
131. Oelkers, E.H. & Schott, J. The dependence of silicate dissolution rates on their structure and composition. *Water Rock Interaction*, 153-156 (1995).
132. Collett, T.S. Energy Resource Potential of Natural Gas Hydrates. *American Association of Petroleum Geologists Bulletin* **86**, 1971-1992 (2002).
133. Kinnaman, T.C. The economic impact of shale gas extraction: A review of existing studies. *Ecological Economics* **70**, 1243-1249 (2011).
134. Strąpoć, D., Mastalerz, M., Dawson, K., Macalady, J., Callaghan, A.V., Wawrik, B., Turich, C. & Ashby, M. Biogeochemistry of Microbial Coal-Bed Methane. *Annual Review of Earth and Planetary Sciences* **39**, 617-656 (2011).
135. Rice, D.D. & Claypool, G.E. Generation, accumulation, and resource potential of biogenic gas. *American Association of Petroleum Geologists Bulletin* **65**, 5-25 (1981).
136. Schoell, M. Isotope techniques for tracing migration of gases in sedimentary basins. *Journal of the Geological Society* **140**, 415-422 (1983).

137. Wu, S.Y. & Lai, M.C. Methanogenic archaea isolated from Taiwan's Chelungpu fault. *Applied and Environmental Microbiology* **77**, 830-838 (2011).
138. Jones, D.M., Head, I. M., Gray, N. D., Adams, J. J., Rowan, A. K., Aitken, C. M., Bennett, B., Huang, H., Brown, A., Bowler, B. F. J., Oldenburg, T., Erdmann, M., Larter, S. R. Crude-oil biodegradation via methanogenesis in subsurface petroleum reservoirs. *Nature* **451**, 176-180 (2008).
139. Rajagopal, M., Werner, B.G. & Hotchkiss, J.H. Low Pressure CO_2 Storage of Raw Milk: Microbiological Effects. *Journal of Dairy Science* **88**, 3130-3138 (2005).
140. Dixon, N.M. & Kell, D.B. The inhibition by CO_2 of the growth and metabolism of micro-organisms. *Journal of Applied Bacteriology* **67**, 109-136 (1989).
141. Debs-Louka, E., Louka, N., Abraham, G., Chabot, V. & Allaf, K. Effect of compressed carbon dioxide on microbial cell viability. *Applied and Environmental Microbiology* **65**, 626-631 (1999).
142. Do, H., Lim, J., Shin, S.G., Wu, Y.-J., Ahn, J.-H. & Hwang, S. Simultaneous effect of temperature, cyanide and ammonia-oxidizing bacteria concentrations on ammonia oxidation. *Journal of Industrial Microbiology and Biotechnology* **35**, 1331-1338 (2008).
143. Yu, Z., García-González, R., Schanbacher, F.L. & Morrison, M. Evaluations of different hypervariable regions of archaeal 16S rRNA genes in profiling of methanogens by archaea-specific PCR and denaturing gradient gel electrophoresis. *Applied and Environmental Microbiology* **74**, 889-893 (2008).
144. Nübel, U., Engelen, B., Felske, A., Snaidr, J., Wieshuber, A., Amann, R.I., Ludwig, W. & Backhaus, H. Sequence heterogeneities of genes encoding 16S rRNAs in Paenibacillus polymyxa detected by temperature gradient gel electrophoresis. *Journal of Bacteriology* **178**, 5636-5643 (1996).
145. Sanguinetti, C., Dias, N.E. & Simpson, A. Rapid silver staining and recovery of PCR products separated on polyacrylamide gels. *Biotechniques* **17**, 914 (1994).
146. DeSantis, T.Z., Hugenholtz, P., Larsen, N., Rojas, M., Brodie, E.L., Keller, K., Huber, T., Dalevi, D., Hu, P. & Andersen, G.L. Greengenes, a Chimera-Checked 16S rRNA Gene Database and Workbench Compatible with ARB. *Applied and Environmental Microbiology* **72**, 5069-5072 (2006).
147. Larkin, M.A., Blackshields, G., Brown, N.P., Chenna, R., McGettigan, P.A., McWilliam, H., Valentin, F., Wallace, I.M., Wilm, A., Lopez, R., Thompson, J.D., Gibson, T.J. & Higgins, D.G. Clustal W and Clustal X version 2.0. *Bioinformatics* **23**, 2947-2948 (2007).
148. Tamura, K., Dudley, J., Nei, M. & Kumar, S. MEGA4: Molecular Evolutionary Genetics Analysis (MEGA) Software Version 4.0. *Molecular Biology and Evolution* **24**, 1596-1599 (2007).
149. Cole, J.R., Wang, Q., Cardenas, E., Fish, J., Chai, B., Farris, R.J., Kulam-Syed-Mohideen, A.S., McGarrell, D.M., Marsh, T., Garrity, G.M. & Tiedje, J.M. The Ribosomal Database Project: improved alignments and new tools for rRNA analysis. *Nucleic Acids Research* **37**, D141-145 (2009).
150. Alberty, R.A. Apparent Equilibrium Constants and Standard Transformed Gibbs Energies of Biochemical Reactions Involving Carbon Dioxide. *Archives of Biochemistry and Biophysics* **348**, 116-124 (1997).
151. Graber, J.R., Leadbetter, J.R. & Breznak, J.A. Description of Treponema azotonutricium sp. nov. and Treponema primitia sp. nov., the First Spirochetes Isolated from Termite Guts. *Applied and Environmental Microbiology* **70**, 1315-1320 (2004).

152. Hiraishi, A., Shin, Y.K. & Sugiyama, J. Brachymonas denitrificans gen. nov., sp. nov., an aerobic chemoorganotrophic bacterium which contains rhodoquinones, and evolutionary relationships of rhodoquinone producers to bacterial species with various quinone classes. *Journal of General and Applied Microbiology* **41**, 99-117 (1995).
153. Do, H., Lim, J., Shin, S.G., Wu, Y.-J., Ahn, J.-H. & Hwang, S. Simultaneous effect of temperature, cyanide and ammonia-oxidizing bacteria concentrations on ammonia oxidation. *Journal of industrial microbiology & biotechnology* **35**, 1331-1338 (2008).
154. Zwietering, M., Jongenburger, I., Rombouts, F. & Van't Riet, K. Modeling of the bacterial growth curve. *Applied and Environmental Microbiology* **56**, 1875-1881 (1990).
155. DiPippo, J.L., Nesbø, C.L., Dahle, H., Doolittle, W.F., Birkland, N.-K. & Noll, K.M. Kosmotoga olearia gen. nov., sp. nov., a thermophilic, anaerobic heterotroph isolated from an oil production fluid. *International Journal of Systematic and Evolutionary Microbiology* **59**, 2991-3000 (2009).
156. Svensson, B.H., Dubourguier, H.-C., Prensier, G. & Zehnder, A.J.B. *Clostridium quinii* sp. nov., a new saccharolytic anaerobic bacterium isolated from granular sludge. *Archives of Microbiology* **157**, 97-103 (1992).
157. Grabowski, A., Tindall, B.J., Bardin, V., Blanchet, D. & Jeanthon, C. Petrimonas sulfuriphila gen. nov., sp. nov., a mesophilic fermentative bacterium isolated from a biodegraded oil reservoir. *International Journal of Systematic and Evolutionary Microbiology* **55**, 1113-1121 (2005).
158. Zoetendal, E.G., Plugge, C.M., Akkermans, A.D.L. & de Vos, W.M. Victivallis vadensis gen. nov., sp. nov., a sugar-fermenting anaerobe from human faeces. *International Journal of Systematic and Evolutionary Microbiology* **53**, 211-215 (2003).
159. van Gylswyk, N.O. Succiniclasticum ruminis gen. nov., sp. nov., a ruminal bacterium converting succinate to propionate as the sole energy-yielding mechanism. *International Journal of Systematic Bacteriology* **45**, 297-300 (1995).
160. Poonam, P., Pophaly, S., Tomar, S., De, S. & Singh, R. Multifaceted attributes of dairy propionibacteria: a review. *World Journal of Microbiology and Biotechnology* **28**, 3081-3095 (2012).
161. Yu, Y., Kim, J. & Hwang, S. Use of real-time PCR for group-specific quantification of aceticlastic methanogens in anaerobic processes: Population dynamics and community structures. *Biotechnology and Bioengineering* **93**, 424-433 (2006).
162. Conklin, A., Stensel, H.D. & Ferguson, J. Growth kinetics and competition between *Methanosarcina* and *Methanosaeta* in mesophilic anaerobic digestion. *Water Environment Research* **78**, 486-496 (2006).
163. Scholten, J.C.M. & Conrad, R. Energetics of syntrophic propionate oxidation in defined batch and chemostat cocultures. *Applied and Environmental Microbiology* **66**, 2934-2942 (2000).
164. Pind, P.F., Angelidaki, I. & Ahring, B.K. Dynamics of the anaerobic process: Effects of volatile fatty acids. *Biotechnology and Bioengineering* **82**, 791-801 (2003).
165. Van Lier, J.B., Grolle, K., Frijters, C., Stams, A. & Lettinga, G. Effects of acetate, propionate, and butyrate on the thermophilic anaerobic degradation of propionate by methanogenic sludge and defined cultures. *Applied and Environmental Microbiology* **59**, 1003-1011 (1993).

166. Polz, M.F. & Cavanaugh, C.M. Bias in Template-to-Product Ratios in Multitemplate PCR. *Applied and Environmental Microbiology* **64**, 3724-3730 (1998).
167. Worm, P., Fermoso, F.G., Stams, A.J.M., Lens, P.N.L. & Plugge, C.M. Transcription of fdh and hyd in Syntrophobacter spp. and Methanospirillum spp. as a diagnostic tool for monitoring anaerobic sludge deprived of molybdenum, tungsten and selenium. *Environmental Microbiology* **13**, 1228-1235 (2011).
168. Gavala, H., Angelidaki, I. & Ahring, B. Kinetics and modeling of anaerobic digestion process. in Biomethanation I, Springer-Verlag, Berlin (2003).
169. Worm, P., Fermoso, F.G., Lens, P.N.L. & Plugge, C.M. Decreased activity of a propionate degrading community in a UASB reactor fed with synthetic medium without molybdenum, tungsten and selenium. *Enzyme and Microbial Technology* **45**, 139-145 (2009).
170. Le Hyaric, R., Chardin, C., Benbelkacem, H., Bollon, J., Bayard, R., Escudié, R. & Buffière, P. Influence of substrate concentration and moisture content on the specific methanogenic activity of dry mesophilic municipal solid waste digestate spiked with propionate. *Bioresource Technology* **102**, 822-827 (2011).
171. Tale, V.P., Maki, J.S., Struble, C.A. & Zitomer, D.H. Methanogen community structure-activity relationship and bioaugmentation of overloaded anaerobic digesters. *Water Research* **45**, 5249-5256 (2011).
172. McKeown, R.M., Scully, C., Mahony, T.e., Collins, G. & O'Flaherty, V. Long-term (1243 days), low-temperature (4-15 ^{o}C), anaerobic biotreatment of acidified wastewaters: Bioprocess performance and physiological characteristics. *Water Research* **43**, 1611-1620 (2009).
173. McCarty, P.L. & Bae, J. Model to Couple Anaerobic Process Kinetics with Biological Growth Equilibrium Thermodynamics. *Environmental Science & Technology* **45**, 6838-6844 (2011).
174. Hoh, C.Y. & Cord-Ruwisch, R. A practical kinetic model that considers endproduct inhibition in anaerobic digestion processes by including the equilibrium constant. *Biotechnology and Bioengineering* **51**, 597-604 (1996).
175. Fox, D.L. Presumed carbaminoprotein equilibria and free energy exchanges in reversible carbon dioxide narcosis of protoplasm. *Journal of Theoretical Biology* **90**, 441-443 (1981).
176. Becker, Z.E. A comparison between the action of carbonic acid and other acids upon the living cell. *Protoplasma* **25**, 161-175 (1936).
177. Morrow, J.S., Keim, P. & Gurd, F.R.N. CO_2 Adducts of Certain Amino Acids, Peptides, and Sperm Whale Myoglobin Studied by Carbon 13 and Proton Nuclear Magnetic Resonance. *Journal of Biological Chemistry* **249**, 7484-7494 (1974).
178. Yokota, A., Tamura, T., Takeuchi, M., Weiss, N. & Stackebrandt, E. Transfer of Propionibacterium innocuum Pitcher and Collins 1991 to Propioniferax gen. nov. as Propioniferax innocua comb. nov. *International Journal of Systematic Bacteriology* **44**, 579-582 (1994).
179. DiPippo, J.L., Nesbø, C.L., Dahle, H., Doolittle, W.F., Birkland, N.K. & Noll, K.M. Kosmotoga olearia gen. nov., sp. nov., a thermophilic, anaerobic heterotroph isolated from an oil production fluid. *International Journal of Systematic and Evolutionary Microbiology* **59**, 2991-3000 (2009).
180. Jones, E.J., Voytek, M.A., Corum, M.D. & Orem, W.H. Stimulation of methane generation from nonproductive coal by addition of nutrients or a microbial consortium. *Applied and Environmental Microbiology* **76**, 7013-7022 (2010).

181. Sanders, W.T.M., Geerink, M., Zeeman, G. & Lettinga, G. Anaerobic hydrolysis kinetics of particulate substrates. *Water Science & Technology* **41**, 17-24 (2000).
182. Vavilin, V.A., Fernandez, B., Palatsi, J. & Flotats, X. Hydrolysis kinetics in anaerobic degradation of particulate organic material: An overview. *Waste Management* **28**, 939-951 (2008).
183. Sanders, W.T., Zeeman, G. & Lettinga, G. Hydrolysis kinetics of dissolved polymer substrates. *Water Science and Technology* **45**, 99-104 (2002).
184. Hills, D.J. & Nakano, K. Effects of particle size on anaerobic digestion of tomato solid wastes. *Agricultural Wastes* **10**, 285-295 (1984).
185. Veeken, A., Kalyuzhnyi, S., Scharff, H. & Hamelers, B. Effect of pH and VFA on hydrolysis of organic solid waste. *Journal of Environmental Engineering* **126**, 1076-1081 (2000).
186. Borglum, G.B. Starch hydrolysis for ethanol production. *ACS Division of Fuel Chemistry, Preprints* **25**, 264-269 (1980).
187. South, C.R., Hogsett, D.A.L. & Lynd, L.R. Modeling simultaneous saccharification and fermentation of lignocellulose to ethanol in batch and continuous reactors. *Enzyme and Microbial Technology* **17**, 797-803 (1995).
188. Pei-Ling, L., Xiao-Song, H. & Qun, S. Effect of high hydrostatic pressure on starches: A review. *Starch/Staerke* **62**, 615-628 (2010).
189. Hayashi, R. & Hayashida, A. Increased Amylase Digestibility of Pressure-treated Starch. *Agricultural and Biological Chemistry* **53**, 2543-2544 (1989).
190. Bauer, B.A. & Knorr, D. The impact of pressure, temperature and treatment time on starches: Pressure-induced starch gelatinisation as pressure time temperature indicator for high hydrostatic pressure processing. *Journal of Food Engineering* **68**, 329-334 (2005).
191. Warren, F.J., Royall, P.G., Gaisford, S., Butterworth, P.J. & Ellis, P.R. Binding interactions of α-amylase with starch granules: The influence of supramolecular structure and surface area. *Carbohydrate Polymers* **86**, 1038-1047 (2011).
192. Baks, T., Kappen, F.H.J., Janssen, A.E.M. & Boom, R.M. Towards an optimal process for gelatinisation and hydrolysis of highly concentrated starch-water mixtures with alpha-amylase from B. licheniformis. *Journal of Cereal Science* **47**, 214-225 (2008).
193. Baks, T., Bruins, M.E., Matser, A.M., Janssen, A.E.M. & Boom, R.M. Effect of Gelatinization and Hydrolysis Conditions on the Selectivity of Starch Hydrolysis with α-Amylase from Bacillus licheniformis. *Journal of Agricultural and Food Chemistry* **56**, 488-495 (2007).
194. Francisco, J.D.C. & Sivik, B. Gelatinization of cassava, potato and wheat starches in supercritical carbon dioxide. *Journal of Supercritical Fluids* **22**, 247-254 (2002).
195. Lindeboom, R., Smith, G., Jeison, D., Temmink, H. & van Lier, J.B. Application of high speed imaging as a novel tool to study particle dynamics in tubular membrane systems. *Journal of Membrane Science* **368**, 95-99 (2011).
196. Herrera-Gómez, A., Canónico-Franco, M. & Ramos, G. Aggregate formation and segregation of maize starch granules cooked at reduced moisture conditions. *Starch/Staerke* **57**, 301-309 (2005).
197. Deguchi, S., Tsudome, M., Tsujii, K., Ito, S. & Horikoshi, K. Cellulose degradation in deep-sea ecosystem. *Polymer Preprints* **55**, 2232 (2006).
198. Ahromrit, A., Ledward, D.A. & Niranjan, K. Kinetics of high pressure facilitated starch gelatinisation in Thai glutinous rice. *Journal of Food Engineering* **79**, 834-841 (2007).

199. Liu, H., Yu, L., Dean, K., Simon, G., Petinakis, E. & Chen, L. Starch gelatinization under pressure studied by high pressure DSC. *Carbohydrate Polymers* **75**, 395-400 (2009).
200. Oates, C.G. Towards an understanding of starch granule structure and hydrolysis. *Trends in Food Science & Technology* **8**, 375-382 (1997).
201. Singh, B., Rizvi, S.S.H. & Harriott, P. Measurement of Diffusivity and Solubility of Carbon Dioxide in Gelatinized Starch at Elevated Pressures. *Industrial and Engineering Chemistry Research* **35**, 4457-4463 (1996).
202. Zheng, Y., Lin, H.M. & Tsao, G.T. Pretreatment for cellulose hydrolysis by carbon dioxide explosion. *Biotechnology Progress* **14**, 890-896 (1998).
203. Bertoldo, C. & Antranikian, G. Starch-hydrolyzing enzymes from thermophilic archaea and bacteria. *Current Opinion in Chemical Biology* **6**, 151-160 (2002).
204. Lévêque, E., Janeček, S., Haye, B. & Belarbi, A. Thermophilic archaeal amylolytic enzymes. *Enzyme and Microbial Technology* **26**, 3-14 (2000).
205. Horváthová, V., Janeček, Š. & Šturdík, E. Amylolytic enzymes: Molecular aspects of their properties. *General Physiology and Biophysics* **20**, 7-32 (2001).
206. Bibel, M., Brettl, C., Gosslar, U., Kriegshäuser, G. & Liebl, W. Isolation and analysis of genes for amylolytic enzymes of the hyperthermophilic bacterium Thermotoga maritima. *FEMS Microbiology Letters* **158**, 9-15 (1998).
207. Swithers, K.S., DiPippo, J.L., Bruce, D.C., Detter, C., Tapia, R., Han, S., Goodwin, L.A., Han, J., Woyke, T. & Pitluck, S. Genome sequence of Kosmotoga olearia strain TBF 19.5. 1, a thermophilic bacterium with a wide growth temperature range, isolated from the Troll B oil platform in the North Sea. *Journal of Bacteriology* **193**, 5566-5567 (2011).
208. Hii, S.L., Tan, J.S., Ling, T.C. & Ariff, A.B. Pullulanase: Role in Starch Hydrolysis and Potential Industrial Applications. *Enzyme Research* **14** (2012).
209. Bader, J., Skelac, L., Wewetzer, S., Senz, M., Popović, M.K. & Bajpai, R. Effect of partial pressure of CO_2 on the production of thermostable alpha-amylase and neutral protease by Bacillus caldolyticus. *Prikladnaia biokhimiia i mikrobiologiia* **48**, 206-211 (2012).
210. Lettinga, G. Anaerobic digestion and wastewater treatment systems. *Antonie van Leeuwenhoek* **67**, 3-28 (1995).
211. Peene, A., Velghe, F., and Wierinck, I. Evaluatie van de vergisters in Nederland. Agentschap NL, Ministry of Economic affairs, agriculture and innovation (in Dutch) (2011).
212. De Graaff, M.S., Temmink, H., Zeeman, G. & Buisman, C.J. Anaerobic treatment of concentrated black water in a UASB reactor at a short HRT. *Water* **2**, 101-119 (2010).
213. Fukuzaki, S., Nishio, N., Shobayashi, M. & Nagai, S. Inhibition of the fermentation of propionate to methane by hydrogen, acetate, and propionate. *Applied and Environmental Microbiology* **56**, 719-723 (1990).
214. Rinzema, A., van Lier, J. & Lettinga, G. Sodium inhibition of acetoclastic methanogens in granular sludge from a UASB reactor. *Enzyme and Microbial Technology* **10**, 24-32 (1988).
215. Hansson, G. & Molin, N. End product inhibition in methane fermentations: Effects of carbon dioxide on fermentative and acetogenic bacteria. *European Journal of Applied Microbiology and Biotechnology* **13**, 242-247 (1981).

216. Kujawa-Roeleveld, K. & Zeeman, G. Anaerobic treatment in decentralised and source-separation-based sanitation concepts. *Re-views in Environmental Science and Biotechnology* **5**, 115-139 (2006).
217. Schouw, N.L., Tjell, J.C., Mosbaek, H. & Danteravanich, S. Availability and quality of solid waste and wastewater in Southern Thailand and its potential use as fertiliser. *Waste Management and Research* **20**, 332-340 (2002).
218. van Lier, J.B. Limitations of thermophilic anaerobic wastewater treatment and the consequences for process design. *Antonie van Leeuwenhoek* **69**, 1-14 (1996).
219. Temudo, M.F., Kleerebezem, R. & van Loosdrecht, M. Influence of the pH on (open) mixed culture fermentation of glucose: A chemostat study. *Biotechnology and Bioengineering* **98**, 69-79 (2007).
220. Meulepas, R.W., Stams, A.M. & Lens, P.L. Biotechnological aspects of sulfate reduction with methane as electron donor. *Reviews in Environmental Science and Bio/Technology* **9**, 59-78 (2010).
221. Klasson, K.T., Ackerson, M.D., Clausen, E.C. & Gaddy, J.L. Bioreactor design for synthesis gas fermentations. *Fuel* **70**, 605-614 (1991).
222. Henstra, A.M., Sipma, J., Rinzema, A. & Stams, A.J.M. Microbiology of synthesis gas fermentation for biofuel production. *Current Opinion in Biotechnology* **18**, 200-206 (2007).

List of Abbreviations

AD	- Anaerobic Digestion
AHPD	- Autogenerative High Pressure Digestion
GC	- GasChromatography
FID	- Flame Ionisation Detector
TCD	- Thermal Conductivity Detector
FESEM	- Field Emission Scanning Electron Microscope
XRD	- XRay Diffraction
HPLC	- High-Performance Liquid Chromatography
HPSEC	- High-Performance Size-Exclusion Chromatography
TIC	- Total Inorganic Carbon
TGA	- ThermoGravimetric Analysis
FTIR	- Fourier Transferred Infrared
RET	- Reversed Electron Transport
AMOB	- Anaerobic Methane Oxidising Bacteria
VFA	- Volatile Fatty Acids
TOC	- Total Organic Carbon
EDX	- Energy Dispersive Xray
ICPAES	- Inductively coupled plasma atomic emission spectroscopy
BNG	- Biogenic Natural Gas
SNG	- Synthetic Natural Gas
COD	- Chemical Oxygen Demand
HPAEC	- High Performance Anion Exchange Chromatography
PCR	- Polymerase Chain Reaction
DGGE	- Denaturing Gradient Gel Electrophoresis
DNA	- DesoxyriboNucleic acid
16s rRNA	- Ribosomal Ribonucleic acid
OUT	- Operational Taxonomic Unit

CHP - Combined Heat and Power

Rpm - Rounds per minute

Rcf - Relative centrifugal force

Nomenclature and definitions

V_l - Liquid volume (L)

V_g - Gas volume(L)

R - Universal gas constant , 8.3145 J $K^{-1}mol^{-1}$

P - Pressure (MPa or Pa)

W - Workload (J)

PJ - Petajoule

MJ - Megajoule

Nm^3 - Normalised cubic meter

$\Delta G^{0,}$ - Gibbs free energy under standard conditions, 298 K and 1 atm

T - Temperature (K)

n - Gas molar quantity (mol)

K_{Hco2} - Henry's constant for CO_2

K_{Hch4} - Henry's constant for CH_4

K_1 - Dissociation constant HCO_3^-

K_2 - Dissociation constant CO_3^{2-}

K_w - Dissociation constant water

K_s - Solubility product $CaCO_3$

Alk - Alkalinity

ANC - Acid neutralising capacity

e_s - The saturation water vapour pressure in hPa

e_{so} - The saturation water vapour pressure at To (6.11 hPa)

L - The latent heat of vapourisation (2.453 × 106 J kg^{-1})

R_v - The water vapour gas constant (461 J kg^{-1} K^{-1})

α_r	-Coefficient to include dissolved gas fraction (%)
μ	-Bacterial growth rate (d^{-1})
SMA	-Specific methanogenic activity (g COD g^{-1} VSS d^{-1})
VS	-Volatile solids
VSS	-Volatile suspended solids
TS	-Total solids
Ppm	-Parts per million
A	-Propionate concentrations
r_{smax}	-Maximum substrate utilisation rate (mg L^{-1} d^{-1})
λ	-Lag time

List of figures

List of tables

List of publications

Peer reviewed publications

Lindeboom, R.E.F., Fermoso, F.G., Weijma, J., Zagt, K. & Van Lier, J.B. Autogenerative high pressure digestion: Anaerobic digestion and biogas upgrading in a single step reactor system. Water Science and Technology **64**, 647-653 (2011).

Lindeboom, R.E.F., Weijma, J. & Van Lier, J.B. High-calorific biogas production by selective CO_2 retention at autogenerated biogas pressures up to 20 bar. Environmental Science and Technology **46**, 1895-1902 (2012).

Lindeboom, R.E.F., Ferrer I., Weijma, J. & van Lier J.B., Silicate minerals for CO_2 scavenging from biogas in Autogenerative High Pressure Digestion, Water Research **47**, 3742-3751 (2013).

Lindeboom, R.E.F.[1], Ferrer, I.[1], Weijma, J. & van Lier, J.B. Effect of substrate and cation requirement on anaerobic volatile fatty acid conversion rates at elevated biogas pressure. Bioresource Technology **150**, 60-66 (2013).

To be submitted publications

Lindeboom, R.E.F., Ding, L., Weijma, J., Plugge, C.M. & van Lier, J.B., Gelatinisation and saccharification as rate-limiting steps in autogenerative high pressure starch hydrolysis, submitted to Biomass & Bioenergy.

Shin, S.G.[1], Lindeboom, R.E.F.[1], , Weijma, J., van Lier, J.B., and Plugge, C.M., Piezo-tolerant natural gas-producing microbes under accumulating pCO_2, in preparation.

[1] both first author

Conference proceedings

Lindeboom, R.E.F., Weijma J. & van Lier J.B., Microbial Mineral Carbonation in Anaerobic Fermentations. *Goldschmidt Conference, Knoxville, Tennessee, USA* (2010).

Lindeboom, R.E.F., Fermoso, F.G., Weijma, J., Zagt, K. & van Lier, J.B. Autogenerative high pressure digestion: a new concept for biogas upgrading. *In: Proc. Of IWA world conference on anaerobic digestion (pp. 1-8). Guadalajara, Mexico: IWA.* (2010).

Lindeboom, R.E.F., Fermoso, F.G., Weijma, J., Zagt, K. & van Lier, J.B. Autogenerative High Pressure Digestion: anaerobic digestion and biogas upgrading in a single step reactor system. *In: Proc. Of IWA Int. Water and Energy Conference, November 10-12, Amsterdam, The Netherlands* (2010).

Lindeboom, R.E.F., Weijma, J., Zagt, K., & van Lier, J.B. 'Biogenic Natural Gas' Formation in a Pressurized Lab Scale Reactor. *Goldschmidt Conference, Prague, Czech Republic*. (2011).

Lindeboom R.E.F., Zagt, C.E., Weijma, J., & van Lier, J. B. Operational implications of Autogenerative High Pressure Digestion. *IWA-Young Water Professionals conference, Leuven, Belgium* (2011).

Lindeboom R.E.F., Zagt, C.E., Shin S.G. Weijma, J., Plugge C.M. & van Lier, J.B. Autogenerative High Pressure Digestion: Future Potentials and Constraints. *IWA world conference on anaerobic digestion, Santiago de Compostela, Spain: IWA* (2013).

Acknowledgements

At the start of my PhD in december 2008, I couldn't have imagined that my PhD would become the adventure that it turned out to be. But like in any adventure there are up's and down's, and without the down's I would certainly have experienced the up's less intensively.

Rather than being the work of just 1 person, I consider this the work of all the people I interacted with in and outside the department during the 4.5 years in which I was actively working on this thesis, with me writing results down and my supervisors steering my progress. Some persons probably don't even realise to what extent they have contributed by explaining something seemingly irrelevant or cheering me up at the right moment! Likewise, with the funding by Agentschap NL, subsidiary of the Dutch Ministry of Economic affairs, all the Dutch tax-payers have contributed to my development, and I am deeply grateful for that.

Although a Philosophers degree insinuates one mainly requires reasoning, without physical labour and fingerspitzengefühl there wouldn't have been any input to the "reasoning process". The bruises Fernando and me obtained in my first few weeks for opening and closing the high pressure reactor are the perfect example. Therefore, before thanking anyone else I would like to thank Hillion, Ardy, Gaby, Ilse, Jean, Geert, Hans, Jan, Bert and Vinnie of the environmental technology lab for making the lab a place to smile. And Katja, special thanks to you for teaching me to teach the same practicals that I was struggling with myself one day. Likewise, I performed many of the analyses outside our own laboratory because of the required expertise. So, also special thanks to Adriaan, Guus, Harry, Andre And Margaret for helping me to get useful information out of strange samples. Although I was only temporarily working in the microbiological lab, I really appreciate the help of Peer and especially Aura, to take the time to teach me the definition of "precise" from a microbiological point of view.

Then ofcourse I also want to thank Liesbeth, Gea, Anita, Romana, Frank and Tom for all the organisational, financial and legislational support that is easily forgotten, but is

also required to finalise a PhD. Liesbeth, the help you gave me with the last bits of handing in this thesis, is the perfect example of how important you are for the ETE-department.

Furthermore, I couldn't have completed my thesis in the same way without the practical and theoretical help of Fernando, Ivet, Lei, Seye and Seung Gu. Above being fruitful, I consider our co-operation very pleasant and I am confident that we will keep in touch in the future. To Seye and Seung Gu, I would have enjoyed to include our nice results on succinate production, but unfortunately the time wasn't right.

I had the pleasure of being supervised by Jan, Caroline and Jules and realise that my project was not the easiest. After Bert unfortunately resigned in a very early stage of the research, Jan took over as my daily supervisor and managed to create a stable environment, in which I could really focus on my research. Thanks a lot for that! When it became clear that the microbiological part of the research would be highly interesting, I felt lucky that Caroline wanted to supervise me as well. Without you, it would have been hard to make a credible contribution from a microbiological point of view. Then Jules, I am happy that you have showed me the beauty of a scientific career and convinced me to start my PhD with you.

Since I had to quit my job at KWRwater to start my PhD, this was an important decision. Fortunately, my decision was made much easier, because I had a good reference by being supervised by both Hardy and Jules in the department and enjoyed the nice atmosphere with my fellow students.

Jules' departure to Delft unfortunately created some situations in which both Cees and Huub had to "adopt" me, for which I am very grateful. Although, I never had the pleasure of "really working" with you, I hope that in the future new and less complicated opportunities will arise.

Another reason to work on this topic was that the practical application was ensured by an involved start-up company, Bareau B.V. I expected that our co-operation with Kirsten would ensure that the project besides being scientifically interesting, could generate societal impact directly. Although we are not there yet, I have learnt a lot

from our cooperation and I would like to thank you for that. I wish you all the best with Bareau B.V. and of course hope for rapid implementation of the AHPD-technology in full scale systems.

And then to all fellow PhD's, post-docs and colleagues (also at LEAF) Tim G., Marjolein, Jan, Mieke, Magdalena, Simon, Christel, Diego, Paula, Ruud, Nora, Kanjana, Zhubiao, Wijb, Zhang Lei, Bruna, Koen, Claudia, Tania, Alex, Tim H., Kirsten, Cees, Marc, Annemiek, David, Ingo, Harry, Tim, Grietje, Els, Iemke, Darja, Myriam, Tiemen, Kasia and Marjo. I hope I am not forgetting anyone….. Anyhow, I am happy that we always managed to find common cheerful activities, like the ETE-band, teaching, visiting conferences or courses, plenty of We-days, running, biking and buying, brewing and drinking beers or just having a coffee break. Therefore I really hope that in the future we will continue to keep in touch even though I am not around anymore!

I was, am and will always be a dreamer and because of starting my PhD, the last few years I guess sometimes I seemed to be living in my own safe cloud castle. Fortunately, my friends and family, and especially Noemí, have always been there to wake me up to the real world. I guess my alarm is ringing now, time to enter the real world!

About the author

Ralph Lindeboom was born on the 29th of June 1982 in Leidschendam, The Netherlands. After completing his secondary education (VWO) in 2000, he studied “Natuurwetenschap en Innovatiemanagement” with a special focus on renewable energy at Utrecht University, where he graduated in 2005 with a thesis on knowledge management related to water loop closure in paper industry. In the beginning of 2006 he started working at KWRwater, formerly known as Kiwa Water Research. Meanwhile he started a 2nd master at the Environmental Technology group in Wageningen. His MSc- thesis entitled “Gas slug flow characterization for optimization of external Anaerobic Membrane Bioreactors” paved the way for starting his PhD-thesis, Autogenerative High Pressure Digestion, in the same department under the supervision of Dr J. Weijma, Dr C.M. Plugge and Prof Dr J.B. van Lier. Currently, he is working as a lecturer and researcher for Saxion, University of Applied Sciences, Enschede, in the department of sustainable energy.

Netherlands Research School for the
Socio-Economic and Natural Sciences of the Environment

C E R T I F I C A T E

The Netherlands Research School for the
Socio-Economic and Natural Sciences of the Environment
(SENSE), declares that

Ralph Erwin Franciscus Lindeboom

born on 29 June 1982 in Leidschendam, The Netherlands

has successfully fulfilled all requirements of the
Educational Programme of SENSE.

Wageningen, 27 February 2014

the Chairman of the SENSE board	the SENSE Director of Education
Prof. dr. Huub Rijnaarts	Dr. Ad van Dommelen

The SENSE Research School has been accredited by the Royal Netherlands Academy of Arts and Sciences (KNAW)

KONINKLIJKE NEDERLANDSE
AKADEMIE VAN WETENSCHAPPEN

The SENSE Research School declares that **Mr. Ralph Erwin Franciscus Lindeboom** has successfully fulfilled all requirements of the Educational PhD Programme of SENSE with a work load of 47 ECTS, including the following activities:

SENSE PhD Courses

- Environmental Research in Context
- Research Context Activity: Co-organizing Study Trip to Canada for Department of Environmental Technology (June 2012)
- Advanced Course on Environmental Biotechnology
- Sustainable Bio-energy and Innovation

Other PhD Courses

- Entrepeneurial Bootcamp
- Food Fermentation
- Masterclass on Applied Biocatalysis

Management and Didactic Skills Training

- Teaching assistant course Introduction environmental technology
- Teaching assistant course Renewable energy
- MSc-thesis supervision: 'The effect of organic loading rate on biogas quantity and quality in an AHPD membrane system'
- BSc-thesis supervision: 'Increasing the methane in biogas through mineralisation'

Oral Presentations

- *Autogenerative high pressure digestion: a new concept for biogas upgrading.* IWA-AD12 Anaerobic Digestion, 31 October - 4 November 2010, Guadalajara, Mexico
- *'Biogenic Natural Gas' Formation in a Pressurized Lab Scale Reactor.* Goldschmidt Conference, 14-19 August 2011, Prague, Czech Republic
- *Operational implications of Autogenerative High Pressure Digestion.* IWA-YWP Benelux, 21-23 September 2011, Leuven, Belgium
- *Autogenerative High Pressure Digestion: Future Potentials and Constraints.* IWA-AD13 Anaerobic Digestion, 25-28 June 2013, Santiago, Spain

SENSE Coordinator PhD Education

Dr. ing. Monique Gulickx

The research described in this thesis was financially supported by Netherlands Enterprise Agency, formerly known as Agentschap NL, subsidiary of The Dutch Ministry of Economic Affairs.

Financial support from Wageningen University for printing this thesis is gratefully acknowledged.

Adriaan van Aelst is gratefully acknowledged for making the anaglyph on the front cover based on an olivine sample, provided by Olaf Schuiling, that reacted under AHPD-conditions.